Technische Universität München
TUM School of Life Sciences

BETA-D-XYLOSIDASE 4 and carbohydrate pathways modulate systemic immune signaling in *Arabidopsis thaliana*

Kornelia Bauer

Vollständiger Abdruck der von der TUM School of Life Sciences der Technischen Universität München zur Erlangung einer

Doktorin der Naturwissenschaften (Dr. rer. nat.)

genehmigten Dissertation.

Vorsitz: Prof. Dr. Brigitte Poppenberger-Sieberer

Prüfer*innen der Dissertation:

1. Prof. Dr. Jörg Durner
2. Prof. Dr. Wilfried Schwab

Die Dissertation wurde am 10.01.2023 bei der Technischen Universität München eingereicht und durch die TUM School of Life Sciences am 09.05.2023 angenommen.

Publications related to the topic of this thesis

Lenk M, Wenig M, Bauer K, Hug F, Knappe C, Lange B, Timsy, Häußler F, Mengel F, Dey S, Schäffner A, Vlot AC. Pipecolic Acid Is Induced in Barley upon Infection and Triggers Immune Responses Associated with Elevated Nitric Oxide Accumulation. Mol Plant Microbe Interact. 2019 Oct;32(10):1303-1313. doi: 10.1094/MPMI-01-19-0013-R. Epub 2019 Aug 20. PMID: 31194615.

Vlot AC, Sales JH, Lenk M, Bauer K, Brambilla A, Sommer A, Chen Y, Wenig M, Nayem S. Systemic propagation of immunity in plants. New Phytol. 2021 Feb;229(3):1234-1250. doi: 10.1111/nph.16953. Epub 2020 Oct 24. PMID: 32978988.

Wenig M, Bauer K, Lenk M, Vlot AC (2022) Analysis of Innate Immune Responses Against Pathogenic Bacteria in Arabidopsis, Tomato, and Barley. Methods Mol. Biol. pp 2494:269–289

Guzha A, McGee R, Scholz P, Hartken D, Lüdke D, Bauer K, Wenig M, Zienkiewicz K, Herrfurth C, Feussner I, et al (2022) Cell wall-localized BETA-XYLOSIDASE4 contributes to immunity of Arabidopsis against Botrytis cinerea. Plant Physiol 189: 1794–1813

Bauer K, Wenig M, Lehmann M, Nayem S, Geigenberger P, Vlot AC (2022) *β-D-xylosidase 4* modulates systemic immune signaling in *Arabidopsis thaliana*.
Manuscript submitted, currently under review.

I Table of contents

I Table of contents III

II Summary VII

III Zusammenfassung VIII

IV Abbreviations X

V List of Figures XIII

VI List of Tables XV

1. Introduction 1

1.1 Plant defense 1

1.2 Cell wall glycans and related molecules shape plant immunity 4

1.3 Phytohormones and crosstalk involved in plant defense 7

1.3.1 Salicylic acid 7

1.3.2 Jasmonic acid 10

1.3.3 Ethylene 13

1.3.4 Abscisic acid 14

1.3.5 Plant hormonal crosstalk 15

1.4 Inducible defense responses activate entrainment and priming 20

1.5 Metabolite signals promote the establishment of systemic acquired resistance 21

1.6 *EDS1*-dependent proteins are suggested to modify systemic acquired resistance and are connected to carbohydrate molecules 26

1.7 Aim of this work 29

2. Material and methods 30

2.1 Materials 30

2.1.1 Plants 30

2.1.2 Bacteria 30

2.1.3 Kits 30

2.1.4 Chemicals 31

2.1.5 Enzymes 32

2.1.6 Buffers and solutions 32

2.1.7 Media 32

2.1.8 Antibiotics 33

2.1.9 Primers 33

2.1.10 Devices and instruments 34

2.1.11 Software and web applications 35

2.2 Methods 36

2.2.1 Plant material and growth conditions 36

2.2.2 Pathogens and preparation of bacterial inoculum 37

2.2.3 Bacterial infections 37

2.2.4 Petiole exudate assays 39

2.2.5 Plant-to-plant (PTP) communication assays 40

2.2.6 Chemical treatments with xylose 41

2.2.7 RNA isolation and gene expression analysis by qRT-PCR 41

2.2.8 Metabolite analysis by Liquid-Chromatography coupled to Mass Spectrometry (LC-MS) 41

2.2.9 Metabolite analysis by Gas Chromatography coupled to Mass Spectrometry *(GC-TOF-MS)* 43

2.2.10 Comprehensive Microarray Polymer Profiling (CoMPP) for carbohydrates 44

2.2.11 Determination of electrical conductivity 45

2.2.12 Systemic response regulated by MeJA 46

2.2.13 Root growth assays 46

2.2.14 Statistics 47

3. Results 48

3.1 *XYL4* promotes ETI 48

3.2 *XYL4* is essential for SAR 53

3.3 Systemic defense regulated by *XYL4* is not affected by a treatment with MeJA 57

3.4 *XYL4* moderately affects the root growth of seedlings under abiotic stress and exposure to MeJA 58

3.5 Long-distance SAR signaling via the phloem depends on *XYL4* 61

3.6 *XYL4* putatively regulates *FMO1* during SAR 63

3.7 *XYL4* promotes communication via the airborne route 65

3.8 Cell wall composition is affected by ETI in an *EDS1*- and *XYL4*-dependent manner 66

3.9 *EDS1*- and *XYL4*-associated signals modulate carbohydrate metabolism . 70

3.10 *XYL4*-triggered defense responses are putatively linked to a xylose-dependent pathway 74

3.11 Xylose-inducible defense is putatively linked to pathways involving SA and NHP-H2 77

4. Discussion 80

4.1 *XYL4* potentially modulates ETI via wounding-associated signals 81

4.1.1 Bacterial treatments (PTI, ETI) trigger local *XYL4* expression..... 81

4.1.2 *XYL4* is associated with wounding responses rather than with stomatal defense 82

4.1.3 Crosstalk of JA/ET and SA as modulatory key of *XYL4*-related signaling during defense and plant root growth?..... 84

4.2 *XYL4*, *LLP1-3*, and *EDS1* might co-regulate SAR signaling events 86

4.2.1 Modification of systemic wound responses via *EDS1* and *XYL4* 86

4.2.2 *XYL4*-dependent immune signaling involves *FMO1* and DAMPs? 87

4.2.3 Local signals via *XYL4* and *LLP3* promote systemic defense 90

4.2.4 SA-JA crosstalk and systemic defense modified by *XYL4* and *LLP1,3* . 94

4.3 Defense-related metabolism including carbohydrates is regulated by XYL4 and networking pathways..... 96

4.3.1 *LLP1*, *EDS1, XYL4,* and xylose potentially regulate glycosylation events and SAG/NHP-H2-dependent defense 96

4.3.2 Xylosidases and AZI1 may regulate an SAR-associated pathway involving lipid-derived molecules and carbohydrates 99

4.3.3 *XYL4* and *EDS1* modify metabolites along the glycolytic pathway 100

4.4 Cell wall defense and its connection to SAR..... 104

4.4.1 Cell wall-associated defense during SAR might be regulated by SA, *EDS1*, and *XYL4* 104

4.4.2 *EDS1*-dependent cell wall remodeling needed to fine-tune SA-signaling during SAR? 106

4.4.3 Xylose-associated defense might be modulated by XYL4 and *EDS1*.. 108

4.4.4 Fucose-related signals connect different branches of the SAR-signaling network 110

4.5 Conclusion..... 113

5. Outlook 109

6. References..... 114

7. Supplemental data 165

8. Acknowledgements 187

9. Curriculum Vitae ..... **Fehler! Textmarke nicht definiert.**

10. Eidesstattliche Erklärung ..... **Fehler! Textmarke nicht definiert.**

II Summary

Cell walls constitute a "shell" outside of the plasma membrane that protects cells while providing mechanical stiffness. Pectin- and hemicellulose-associated structures of plant cell walls are known to be involved in defense responses against parasitic pathogens. In this context, immune responses incorporate hormonal signaling routes via salicylic acid (SA), ethylene, and jasmonic acid (JA). SA plays a pivotal role in systemic acquired resistance (SAR), an inducible form of innate immunity that - following a local immune stimulus - confers long-lasting, systemic protection against a broad range of biotrophic invaders.

It was formerly described that BETA-D-XYLOSIDASE 4 (XYL4) protein accumulation is enhanced in the apoplast of plants undergoing SAR. This process is regulated in dependence of *ENHANCED DISEASE SUSCEPTIBILITY 1* (*EDS1*). To date, it is unclear to what extent *XYL4*, which is also termed *AtBXL4*, contributes to plant defense. The goal of this work was to ascertain the function of *XYL4* in basal resistance and SAR. The findings suggest that *XYL4* affects innate immunity in both locally treated and distal plant tissues. Virtual grafting experiments using petiole exudates from infected plants revealed that *XYL4* modulates the generation of defense signals at the site of infection or promotes their transmission to distal plant parts. Furthermore, *XYL4* promoted systemic perception or propagation of systemically mobile molecules. In addition to this function in long-distance signaling via the vasculature, plant-to-plant communication experiments showed that *XYL4* also promotes airborne signal transmission in SAR. Metabolite analyses implied that the metabolism of compounds such as glycerol-3-phosphate - which was formerly described to promote intra- and inter-plant communication – depends on *XYL4*. The data further suggest that *XYL4* signaling controls molecules related to the glycolytic pathway including fucose, serine, and glucose-6-phosphate in a feedback loop with *EDS1*. Moreover, fucose, xylulose and erythritol, SA, pipecolic acid, and derivatives of N-hydroxy pipecolic acid appear to be regulated by a mutual, effector-triggered immunity (ETI)-inducible pathway of *EDS1* and *XYL4*. As mutants deficient in either *EDS1* or *XYL4* predominantly had an altered composition of pectin, both genes can be expected to influence components of the cell wall and their structural traits. Consequently, inducible changes in cell walls presumably contribute to basal defense and SAR. The results presented in this work provide promising features of cell walls and carbohydrates

as modulators of SAR in *Arabidopsis thaliana* and call for further studies to uncover their potential in plant protection.

III Zusammenfassung

Zellwände bilden eine „Schale" außerhalb der Plasmamembran, die Zellen schützt und gleichzeitig für mechanische Steifigkeit sorgt. Über pflanzliche Zellwandstrukturen wie Pektine und Hemicellulose ist bekannt, dass sie an Abwehrreaktionen gegen parasitäre Krankheitserreger beteiligt sind. Die Immunantworten umfassen dabei hormonelle Signalwege über Salicylsäure (SA), Ethylen (ET) und Jasmonsäure (JA). SA spielt eine zentrale Rolle bei der systemisch erworbenen Resistenz (SAR), einer induzierbaren Form der angeborenen Immunität, die – nach einem lokalen Immunreiz – einen langanhaltenden, systemischen Schutz gegen eine breite Palette biotropher Eindringlinge bietet.

Es wurde zuvor beschrieben, dass BETA-D-XYLOSIDASE 4 (XYL4) Proteine im Apoplast von SAR-induzierten Pflanzen verstärkt akkumulieren. Dieser Prozess wird in Abhängigkeit von *ENHANCED DISEASE SUSCEPTIBILITY 1* (*EDS1*) reguliert. Bisher ist unklar, inwieweit *XYL4* zur pflanzlichen Abwehr beiträgt. In dieser Arbeit wurde die Funktion von *XYL4* für die basale Resistenz und SAR ermittelt. Die Erkenntnisse deuten darauf hin, dass *XYL4* die angeborene Immunität sowohl in lokal behandelten als auch in entfernten Pflanzengeweben beeinflusst. Virtuelle Pfropfexperimente mit Blattstielexsudaten infizierter Pflanzen zeigten, dass *XYL4* die Erzeugung von Abwehrsignalen am Infektionsort moduliert oder deren Übertragung auf entfernte Pflanzenteile fördert. Darüber hinaus förderte *XYL4* die systemische Wahrnehmung oder Ausbreitung systemisch mobiler Moleküle. Zusätzlich zu dieser Funktion bei der Fernsignalisierung über das Gefäßsystem zeigten Experimente zur Kommunikation von Pflanze zu Pflanze, dass *XYL4* die Signalübertragung auch über die Luft bei SAR fördert. Metabolit Analysen implizierten, dass der Metabolismus von Verbindungen wie Glycerol-3-Phosphat – von dem früher beschrieben wurde, dass es die Kommunikation innerhalb und zwischen Pflanzen fördert – von *XYL4* abhängt. Die Daten deuten ferner darauf hin, dass die *XYL4*-Signalgebung in einer Rückkopplungsschleife mit *EDS1* Moleküle steuert, die mit dem glykolytischen Weg verwandt sind, einschließlich Fucose, Serin und Glukose-6-Phosphat. Zudem werden Fucose, Xylulose,

Erythritol, SA, Pipecolinsäure und Derivate von N-hydroxypipecolinsäure vermutlich durch *EDS1* und *XYL4* reguliert, die einen ETI-induzierbaren Signalweg bilden. Da *EDS1*- oder *XYL4*-defiziente Mutanten überwiegend einen kompositionellen Unterschied in Pektinen aufweisen, ist zu erwarten, dass beide Gene Bestandteile der Zellwand und deren strukturelle Merkmale beeinflussen. Folglich tragen vermutlich induzierbare Veränderungen in Zellwänden zur basalen Abwehr und SAR bei. Die in dieser Arbeit vorgestellten Ergebnisse liefern vielversprechende Eigenschaften von Zellwänden und Kohlenhydraten als Modulatoren von SAR in *Arabidopsis thaliana* und zeigt auf, dass es weiterer Studien bedarf, um ihr Potenzial im Pflanzenschutz aufzudecken.

IV Abbreviations

°C	Degree Celcius
ABA	Abscisic acid
AIR	Alcohol-insoluble residue(s)
A. thaliana	*Arabidopsis thaliana*
AzA	Azelaic acid
Bc	*Botrytis cinerea*
bp	Base pair(s)
cfu	Colony forming units
CK	Cytokinin
DA	Dehydroabietinal
DAMP	Damage-associated molecular patterns
DNA	Desoxyribonucleic acid
dpi	Days post infection
EDTA	Ethylenediaminetetraacetate
ET	Ethylene
ETI	Effector-triggered immunity
ETS	Effector-triggered susceptibility
eV	Electron volt
FA	Fatty acid
Fig.	Figure
G3P	Glycerol-3-phosphate
G-6-P	Glucose-6-phosphate
GC-MS	Gas Chromatography coupled to Mass Spectrometry
GC-TOF-MS	GC coupled to Time-of-Flight Mass Spectrometry
h	Hour(s)
hpi	Hours post infection
HRGP	Hydroxyproline-rich glycoprotein
HR	Hypersensitive response
INA	2,6-dichloroisonicotinic acid

JA	Jasmonic acid
JA-Ile	Jasmonoyl-L-isoleucine
L	Liter(s)
LB	Luria-Bertani
LC-MS	Liquid-Chromatography coupled to Mass Spectrometry
LLP	Legume lectin like protein
M, or mock	Control treatment
mL	Milliliter(s)
min	Minute(s)
mM, µM	Molarity (molar concentration) [M = mol/L]
NHP	N-hydroxy-Pipecolic acid
NHP-H2	NHP-O-β-glucoside
nm	Nanometers
NO	Nitric oxide
OD	Optical density
ONA	9-oxononanoic acid
PAMP	Pathogen-associated molecular patterns
PCD	Programmed cell death
PCR	Polymerase chain reaction
PetEx	Petiole exudate
Pip	Pipecolic acid
PME	Pectin methylesterase
Ps	*Pseudomonas syringae*
Pst	*Pseudomonas syringae* pv. tomato (DC3000) – virulent
Pst/*AvrRpm1*, or S	*Pseudomonas syringae* pv. tomato (DC3000) – avirulent
PTI	PAMP-triggered immunity
PTP	Plant-to-Plant
qRT-PCR	Quantitative reverse transcription polymerase chain reaction
R	Resistance
RI	Retention Index

RNA	Ribonucleic acid
ROS	Reactive oxygen species
rpm	Revolutions per minute
RPM1	*RESISTANCE TO PSEUDOMONAS SYRINGAE pv. MACULICOLA 1*
RQ	Relative Quantification
RT	Room temperature
SA	Salicylic acid
SAG	SA 0-β-glucoside
SAR	Systemic acquired resistance
sec	second(s)
SGE	Salicyloyl glucose ester
T_m [°C]	Melting temperature
UDP	Uridine diphosphate
UGT	UDP-dependent glycosyltransferase
WT	Wild type
µL	Microliter(s)

Amino acids and nucleotides are expressed according to the IUPAC code (International Union of Pure and Applied Chemistry). All base units and derived units are used following the convention of the SI-system (Système International d'unités).

V List of Figures

Figure 1: Immune responses triggered in plant upon recognition of pathogenic invaders. 2
Figure 2: Model for the combined activation of defense by PTI and ETI. . 4
Figure 3: Model for the cell wall composition-dependent regulation of plant hormonal pathways, gene expression, and associated metabolism. 5
Figure 4: Predicted biosynthesis routes for SA in plants from the precursor chorismate. 8
Figure 5: Regulation in pathways of the JA/ET network after biotic/abiotic stress. 12
Figure 6: Hormonal signaling network shapes plant defense responses. 18
Figure 7: Model for priming of plant defense. 20
Figure 8: Metabolites and pathways involved in the establishment of SAR. 21
Figure 9: Inter-plant communication is promoted by airborne defense signals..... 24
Figure 10: Model for EDS1-dependet regulation of defense. 27
Figure 11: Overview of the leaf architecture in a 4-week-old A. thaliana plant and bacterial infection procedures...... 38
Figure 12: Scheme for bacterial plating (A) and exemplary bacterial growth on a plate at the 2nd day after plating (B). 38
Figure 13: Infection of plants and collection of petiole exudates from infected leaves to determine SAR-inducing capacities...... 39
Figure 14: Plant-to-plant communication set-up using a closed desiccator system. 40
Figure 15: Schematic workflow for the sample preparation for the CoMPP analysis...... 45
Figure 16: Simplified layout to determine the root length of seedlings growing on a treatment plate...... 46
Figure 17: Infection of A. thaliana with Pst/AvrRpm1 induces a local accumulation of BETA-D-XYLOSIDASE 4 (XYL4) transcripts. 48
Figure 18: XYL4 promotes local ETI responses against the (hemi-)biotrophic bacterium Pst/AvrRpm1 in A. thaliana...... 50

Figure 19: Transcript accumulation of defense-associated genes in response to Pst and Pst/AvrRpm1 is comparable in Col-0 and in xyl4 mutant plants. 51
Figure 20: *XYL4* represses an ETI-inducible glucosylation of SA forming SAG. 52
Figure 21: XYL4 promotes Systemic Acquired Resistance (SAR). 54
Figure 22: Early expression of diverse defense-associated genes systemically is related to XYL4. 56
Figure 23: MeJA has no effect on plant defense against *Pst.* 57
Figure 24: XYL4 slightly represses the growth of primary roots in *A. thaliana* seedlings. 59
Figure 25: The generation and transmission of phloem-mobile SAR signals is dependent of XYL4. 62
Figure 26: XYL4 potentially modulates phloem-associated defense signals by regulating the NHP pathway. 64
Figure 27: The generation and perception of airborne SAR signals is dependent of XYL4 65
Figure 28: Exogenous xylose induces EDS1- and LLP1-dependent systemic defense against Pst. 75
Figure 29: Exogenous xylose induces EDS1- and LLP1-dependent systemic defense against Pst. 76
Figure 30: Exogenous xylose and *XYL4* repress the accumulation of NHP-H2 after a challenge with *Pst*. 79
Figure 31: SAR signaling model: locally triggered responses upon a biotic stimulus for ETI/HR. 92
Figure 32: SAR signaling model: systemically mobile signals detectable by XYL4 and LLP1 trigger SAR and potentially induce SA/NHP-dependent signals. 95
Figure 33: **Model for XYL4/*XYL4*-dependent regulation of ETI-associated metabolites.** 112
Figure S34. Infection-associated ion leakage is independent of XYL4. .. 168
Figure S35. Transcript accumulation of JA-related genes and *LLP1* is not affected systemically at later phases. 169
Figure S36: XYL4 has no effect on metabolite accumulation of SA, SAG or AzA after a secondary challenge with Pst 170

Figure S37. XYL4-dependent phloem-mobile SAR signals have no effect on the transcript expression of specific genes in receiver plants. 171
Figure S38. Transgenic xyl4-1 are not inducible for the expression of AvrRpm1 172
Figure S39. Exogenous xylose induces EDS1- and LLP1-dependent defense in distal tissues against Pst. 182
Figure S40. Xylose dose does not affect the growth of *Pst* bacteria in liquid media. 184
Figure S41. Late local and systemic responses after exogenous xylose are not dependent on XYL4, LLP1, or JA signaling. 185

VI List of Tables

Table 1. Bacteria used in this work. 30
Table 2. Kits used in this work. 30
Table 3. Chemicals used in this work. 31
Table 4. Enzymes used in this work. 32
Table 5. Buffers and solutions used in this work. 32
Table 6. Media and their composition as used in this work. 32
Table 7. Antibiotics and their concentrations as used in this work. 33
Table 8. Primers used for qRT-PCR. 33
Table 9. Primers used for genotyping to test for homozygous mutations. 34
Table 10. Devices and instruments used in this work. 34
Table 11. Software and web applications used in this work. 35
Table 12. Pectin accumulation in cell walls is affected by EDS1. 67
Table 13. Accumulation of AGP and pectin in cell walls is modified by EDS1 and XYL4. 69
Table 14*:* SAR- and carbohydrate-related metabolic pathways are regulated in association to EDS1. 71
Table 15. XYL4 and EDS1 modify SAR-inducible metabolic pathways relevant for energy production and lipid synthesis 73
Table S16: Antibodies and carbohydrate binding modules used in CoMPP. 165
Table S17: Details of the one-Way ANOVAs and Tukey tests. 167
Table S18. SAR- and carbohydrate-related metabolic pathways are regulated in association to EDS1. 173

Table S19. XYL4 and EDS1 modify SAR-inducible metabolic pathways relevant for energy production and lipid synthesis 177

1. Introduction

Diverse environmental stimuli challenge plants to continuously adapt to their surroundings. Host-invading pathogens and other stress-associated stimuli, for example, prompt plants to drive up inducible immune responses triggering an intricate network of metabolic signals. By this, defense towards an array of biotic invaders and multiple stress reactions is affected (Spoel and Dong, 2012). There is a broad range of pathogens, with each pest exploiting individual strategies to thrive on infection and proliferate on plants (Sacristán and García-Arenal, 2008). During host-pathogen interaction, the encountering organisms get in close contact, allowing an exchange of chemical compounds and valuable nutrients. A prominent area of direct interaction is the apoplastic space in plants, which constitutes highly dynamic and modifiable extracellular structures like cell walls (Malinovsky et al., 2014). Those walls are mainly composed of interconnected glycan molecules and specialized proteins which can change the functionality of the cell walls. Such regulation is strongly dependent on host-derived signals and manipulative actions triggered by invading pathogens (Jamet and Dunand, 2020). In order to maintain cell wall defensive properties as an active barrier, it is thus of great importance for stressed plants to continuously monitor the extracellular space and adjust its composition (Hamann, 2012). In this way, the pathogenic invaders can be restricted in their propagation during the early phase of interaction with the host, which promotes plant survival (Rui and Dinneny, 2020). Up to date, little is known about how cell wall-related immunity in plants can be successfully induced in order to effectively fend off pathogenic threats, for example in relevant crop plants. In this thesis, I will set out to investigate inducible immune responses by analyzing specific cell wall components (glycans and proteins) and their effect on plant defensive pathways in the model plant *Arabidopsis thaliana* (*A. thaliana*).

1.1 Plant defense

Effective plant defense strategies comprise a two-layered, interactive system of preformed barriers and inducible innate immune responses to maintain health (Thordal-Christensen, 2003; Chisholm et al., 2006; Hématy et al., 2009; Ali et al., 2018). First, when invading microbes try to enter the plant tissues, constitutively present (natural and/or inducible) openings like stomata, pores, or wounding sites need to be overcome (Underwood et al., 2007). Early responses of plant hosts hereby regulate the openness of stomata to restrict pathogenic migration, a reaction that is part of a robust broad spectrum defense response known as non-

host resistance (NHR) (Thordal-Christensen, 2003; Cheng et al., 2012). Whenever pathogens succeed to overcome NHR, they are confronted with the second layer of host defense: plants activate pathogen-associated molecular pattern (PAMP)-triggered immunity (PTI) after the perception of virulent invaders, and ETI upon detection of avirulent attackers (Zhang et al., 2018). The mechanisms of PTI and ETI, which are highly dependent on functional phytohormone networks, are likely exploited by pathogens (Li et al., 2019a).

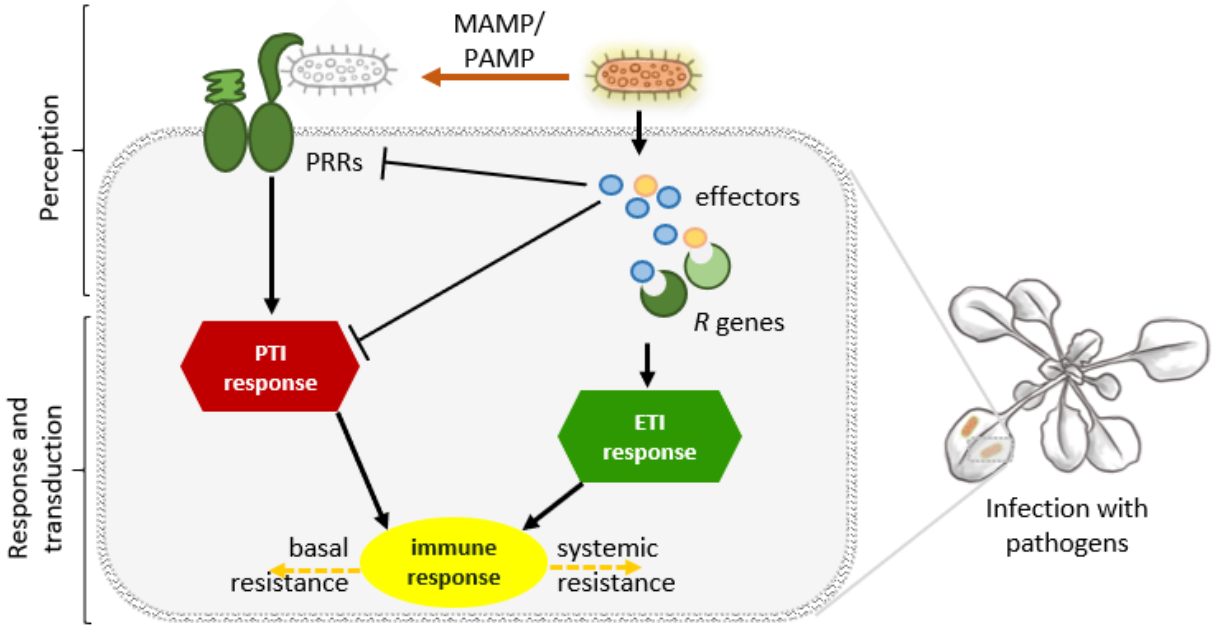

Figure 1: Immune responses triggered in plant upon recognition of pathogenic invaders.
Bacterial pathogen-associated molecular patterns (PAMPs) or microbe-associated patterns (MAMPs; physical outward properties) are detected by plasma membrane bound Pattern Recognition Receptors (PRRs), which culminates in PAMP-triggered immunity (PTI). Bacterial effectors can suppress the PTI response, which results in effector-triggered susceptibility (ETS). Nucleotide-binding, leucine-rich repeat receptors (NLRs) in turn detect pathogenic effectors intracellularly and promote the induction of ETI. Modified from Ali et al. (2018).

Plants recognize pathogenic elicitors (=PAMPs) by Pattern Recognition Receptors (PRRs), which initiates PTI and allows the host to impede propagating invaders (**Figure 1**) (Jones and Dangl, 2006). PAMPs comprise non-race-specific molecules like chitin, bacterial flagellum, lipopolysaccharides (LPS), and further highly conserved pathogen-related surface particles (Zipfel and Felix, 2005; Jones and Dangl, 2006). These elicitors induce signaling cascades in plants involving mitogen-associated protein kinases (MAPKs) (Ishihama and Yoshioka, 2012) and an early induction of transcription factors of the WRKY family (Asai et al., 2002). PTI specifically contributes to the strengthening of plant cell walls, the release of antimicrobial peptides, the limitation of parasitic nutrient acquisition, and the

suppression of the bacterial type III secretion system (Crabill et al., 2010; Voigt, 2014; Bolouri Moghaddam et al., 2016; Yamada et al., 2016a).

However, PTI can be counteracted when pathogens release (race-specific) virulence factors (called effectors) that the plant hosts cannot perceive (Jones and Dangl, 2006). Thus, plants are rendered susceptible (effector-triggered susceptibility, ETS) and pathogen colonization of the host is facilitated. Effectors can specifically interfere with plant immune receptors and host cellular processes including the metabolism of nutrient molecules, phytohormonal pathways, and the production of reactive oxygen species (ROS) (Toruño et al., 2016; Jwa and Hwang, 2017; Han and Kahmann, 2019).

The pathogen-derived and ETS-inducible effectors in turn can be perceived intracellularly (directly or indirectly) in plants which carry appropriate, functional resistance (*R*) genes (**Figure 1**). These *R* genes code for nucleotide-binding, leucine-rich repeat receptors (NLRs) (Cui et al., 2015). Upon successful recognition of effectors, plants are able to initiate ETI downstream signaling providing an effective and long-lasting ("gene-for-gene") resistance to a specific range of pathogens (Jones and Dangl, 2006). At the site of infection, ETI is associated with processes leading to programmed cell death (PCD), which is termed the hypersensitive response (HR) (Jones and Dangl, 2006; Mur et al., 2008). During this process, plants balance directed actions of ROS, nitric oxide (NO), and the formation of hydrogen peroxide (H_2O_2) (Wu et al., 2014).

Interestingly, it was commonly believed for a long time that PTI and ETI represent two independent layers of plant defense due to their differing activation by either PAMPs or effectors, respectively (Thomma et al., 2011). However, PTI and ETI both rely on, for example, the phenolic phytohormone salicylic acid (SA) and fend off (hemi-)biotrophic pathogens in the locally infected (basal) tissues (Bhattacharjee et al., 2011; Doehlemann and Hemetsberger, 2013). Biotrophic pathogens predominantly grow and depend on a living host and thus can be inhibited in their propagation when host plants trigger basal necrosis and SA-associated defense (Glazebrook, 2005). Recent evidence suggests that both PTI and ETI synergistically fortify each other in order to induce the synthesis of ROS and the transcription of SA-related defense genes (**Figure 2**) (Ngou et al., 2021; Yuan et al., 2021). Specifically, PRRs are assumed to fortify ETI-related plant responses associated with HR in order to restrict further pathogen propagation in the host (Ngou et al., 2021). In turn, signaling pathways incorporating the

phytohormone jasmonic acid (JA) are commonly associated with defense to necrotrophic pathogens, herbivory, and wounding (Glazebrook, 2005). Interestingly, pathways signaling via JA and the phytohormone ethylene (ET) are modulated via a synergistic interplay between PTI and ETI (Yuan et al., 2021). ETI specifically enhances the induction of PTI-related defense responses by activating PTI signaling and boosting expression of defense genes and proteins (related to SA, JA and ET) (Ngou et al., 2021). In the models established in Ngou et al. (2021) and in Yuan et al. (2021), PRRs and NLRs cooperatively process activated signaling components that affect effector-inducible reactions and protein turnover in plant defense (**Figure 2**). In sum, a proper ETI defense induction relies on functional PTI recognition and signaling in order to fortify immunity, and PTI in turn consolidates ETI-driven responses.

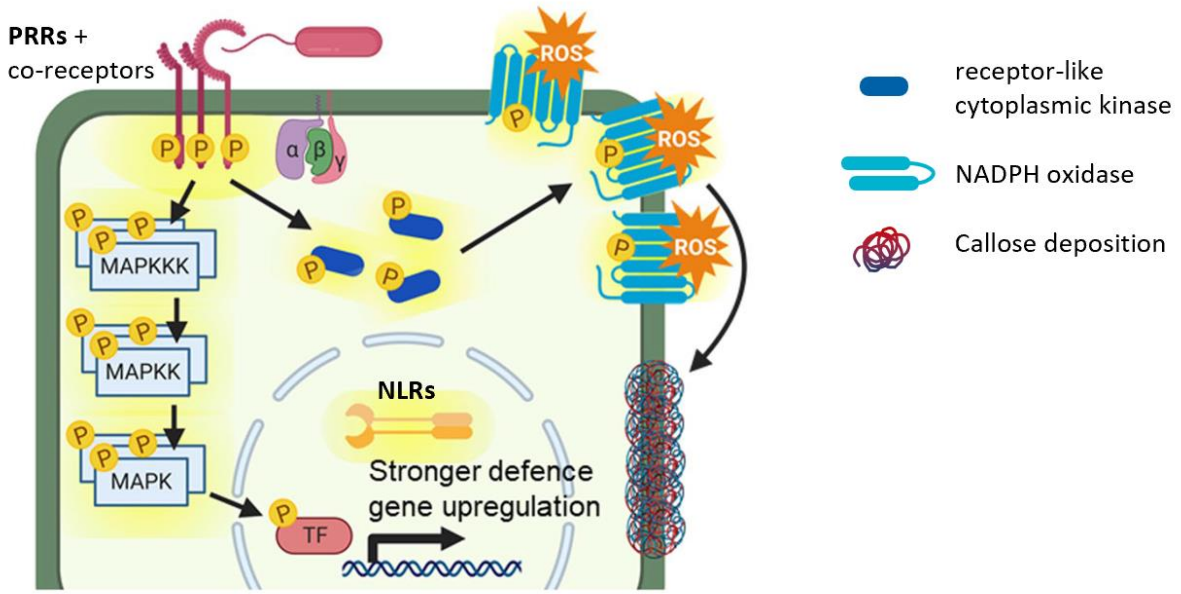

Figure 2: Model for the combined activation of defense by PTI and ETI.
PRRs (necessary for PTI) and NLRs (necessary for ETI) are co-activated to fortify mutual defense responses. This involves downstream signaling cascades that activate mitogen-associated protein kinases (MAPKs), transcription factors (TF), reactive oxygen species ROS, and callose depositions. Adapted from Ngou et al. (2021)

1.2 Cell wall glycans and related molecules shape plant immunity

The extracellular space is a prominent area where host-pathogen interaction takes place (Malinovsky et al., 2014; Smirnova and Kochetov, 2016). Specifically cell walls, which constitute a space where PRRs are localized, play an important role in monitoring and integration of external stimuli that activate downstream signaling (Rui and Dinneny, 2020). Plants perceive PAMPs of pathogens ideally as soon as the attackers start to penetrate or migrate through cell walls (Malinovsky et al., 2014). PRRs moreover sense host-derived damage-associated molecular patterns

(DAMPs), which involve fragments of cell wall glycans and other extracellular molecules like proteins, peptides, amino acids, or nucleotides (Hou et al., 2019). Such DAMPs are primarily released upon breakdown or damage of cells - as induced by pathogenic invaders - or (physical) wounding, which promotes downstream/defense signaling and processes related to cell repair (Hou et al., 2019; Pontiggia et al., 2020). Modifications in the compositional structures of cell walls are anticipated to have a strong effect on immunity, fitness, and developmental adaption in plants via modulations of signaling networks (**Figure 3**) (Rashid, 2016; Vaahtera et al., 2019; Molina et al., 2021).

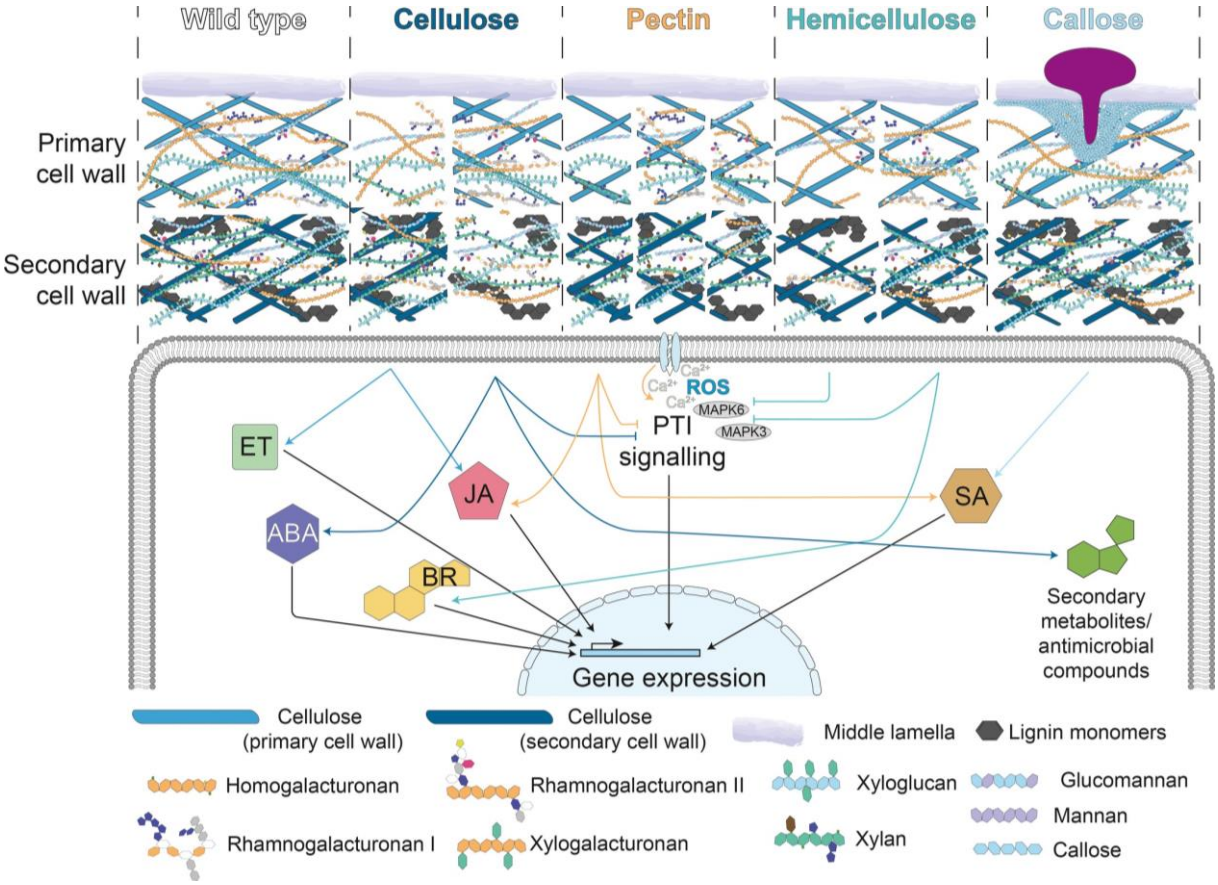

Figure 3: Model for the cell wall composition-dependent regulation of plant hormonal pathways, gene expression, and associated metabolism.
The structural combinations of cellulose, pectin, hemicellulose, lignin, and callose in the primary and secondary cell wall modify signaling cascades. Differences in the presence of these components and moreover the degree of acetylation or methylation (amount of cross-linkage with pectin and hemicellulose) redefine signals. Adapted from Bacete et al. (2018).

The cell wall architecture is plant-regulated in dependence on species, time, and tissue and comprises polysaccharides like cellulose, hemicellulose, pectin, and lignin, as well as proteins (Heredia et al., 1995; Gigli-Bisceglia et al., 2020). Polysaccharides represent ~90% of the dry weight of cell walls, while the rest (~2-12%) is represented by minerals, enzymes, structural phenolic esters, and

glycoproteins (Monro et al., 1976; Houston et al., 2016). In dicotyledonous plants, pectin represent about 20-45% of the total carbohydrate components of plant cell walls (including: rhamnogalacturonan-I and-II (RG-I, RG-II), homogalacturonan (HG)), cellulose ~20-30%, while hemicellulose structures account for ~20-35% (including: xylan, xyloglucan, (gluco)mannans) (Carpita and Gibeaut, 1993; Zablackis et al., 1995; O'Neill and York, 2003). Notably, hydrolyzed glycans associated to HG and cellulose function as DAMPs (De Lorenzo et al., 2018; Pontiggia et al., 2020). Interestingly, plants defective in the cellulose synthase CeSA3 (*cev1*) continuously activate pathways of JA/ET via activation of JA/ET-related defense gene expression (Ellis and Turner, 2001; Ellis et al., 2002). Specifically, pectin- and hemicellulose-associated structures participate in defense induction to pests of different parasitic lifestyles (Bethke et al., 2015; Hou et al., 2019; Molina et al., 2021). Exogenous xyloglucan, for example, effectively induces resistance against a necrotrophic fungal pathogen (*Botrytis cinerea, Bc*) in grapevine and *A. thaliana* (Claverie et al., 2018). Plant defense is dependent on pathways related to SA, and moreover to JA and ET. In addition, other studies describe that an enhanced abundance particularly of xyloglucans, xylose derivatives, galactomannans, and RG-I molecules positively correlates with plant disease resistance (Delgado-Cerezo et al., 2012; Molina et al., 2021). Furthermore, cell wall associated non-enzymatic (glyco)proteins (CWPs) are believed to induce plant defense against diverse pathogens, for example by stiffening of cell walls (solubilization, cross-linking), secretion of arabinogalactan proteins (AGPs), and activation of *PATHOGENESIS-RELATED* (*PR*) gene expression (Rashid, 2016). In sum, cell walls are modifiable targets with versatile functions in plant defense.

It is thus not surprising that parasitic microorganisms manipulate plant cell walls and defense signals for their own benefit – a process plants are trying to effectively resist (Bellincampi et al., 2014). An example: the detection of specific bacterial PAMPs results in a localized deposition of callose to the site of infection (Luna et al., 2011), which provokes (defense) signaling via SA in plants (Bacete et al., 2018). ETS, as one pathogen-inducible immune response, can be promoted after the secretion of the type III effector AvrPto by *Pseudomonas syringae* (*Ps*), suppressing a cell wall-associated callose deposition in *Arabidopsis* plants (Hauck et al., 2003). Secondly, defending plants and invading pathogens actively promote the release of energy-rich monosaccharides from cell walls and carbohydrate storages (sucrose, starch) via mutually suppressive actions to meet the increased

requirement for energy (Fotopoulos et al., 2003; Scharte et al., 2005; Bonfig et al., 2006; Juge, 2006; Bonfig et al., 2010). Taken together, interactions between plants and pathogens redefine and control modifications of cell wall glycans, which affect the breakdown, stiffness, and integrity maintenance of cell walls as described (Bacete and Hamann, 2020). Cell wall compositional modifications further induce signals via a network of phytohormones as depicted in the model (**Figure 3**) of Bacete et al. (2018).

1.3 Phytohormones and crosstalk involved in plant defense

Host-pathogen interactions in a natural environment are indispensably linked to abiotic conditions. Thus, both plant hosts and pathogens cope with an array of factors that simultaneously affect stress responses (Zandalinas et al., 2020). As an effect of combined stresses, plants activate a set of hormonal and metabolic pathways that lead to integrated signal transduction pathways (Peck and Mittler, 2020; Saijo and Loo, 2020). In the end, the timing of defense triggered in plants is crucial for the manifestation of stress tolerance, resistance (e.g. ETI), and survival of plants (Kant et al., 2004; Gómez et al., 2010; Wang et al., 2011b; Mine et al., 2018).

Interconnected mechanisms during plant defense are tightly controlled by signals comprising well-characterized hormones like SA, ET, and JA (Vlot et al., 2021). Related signaling pathways can be modulated by additional hormones like abscisic acid (ABA), auxin, cytokinin (CK), brassinosteroids, gibberellic acid, strigolactone, and peptides (Glazebrook, 2005; Adie et al., 2007b; Spoel et al., 2007; Bari and Jones, 2009; Denancé et al., 2013; Hillmer et al., 2017; Li et al., 2019a). The phytohormonal network simultaneously controls plant stress responses and processes related to growth and development via crosstalk between these pathways (Santner and Estelle, 2009). Within this thesis, I will predominantly focus on the interplay and crosstalk of SA, JA, ET, and ABA.

1.3.1 Salicylic acid

The phenolic compound SA is involved in developmental processes, stomatal movements and furthermore in response to biotic and abiotic stress (Vlot et al., 2009). During defense, SA promotes local and systemic immune responses against a range of predominantly host-specific biotrophic invaders like *Ps* in *A. thaliana* (Li et al., 2019a). SA levels increase during the onset of PTI and/or ETI after plants perceive a stimulus with, for example, an avirulent (hemi-)biotrophic pathogen (Dempsey et al., 1999; DebRoy et al., 2004; Loake and Grant, 2007). As a

consequence, mutant plants deficient in the biosynthesis or perception of SA display enhanced susceptibility to an infection with (hemi-)biotrophic pathogens (Bari and Jones, 2009). SA specifically promotes the establishment of systemic acquired resistance (SAR), which is defined as follows: a localized treatment of plant tissues with, for example, avirulent bacteria initiates systemic signaling that activates SAR against a secondary pathogen infection in distal plant tissues (Alvarez et al., 1998; Shah and Zeier, 2013; Vlot et al., 2021).

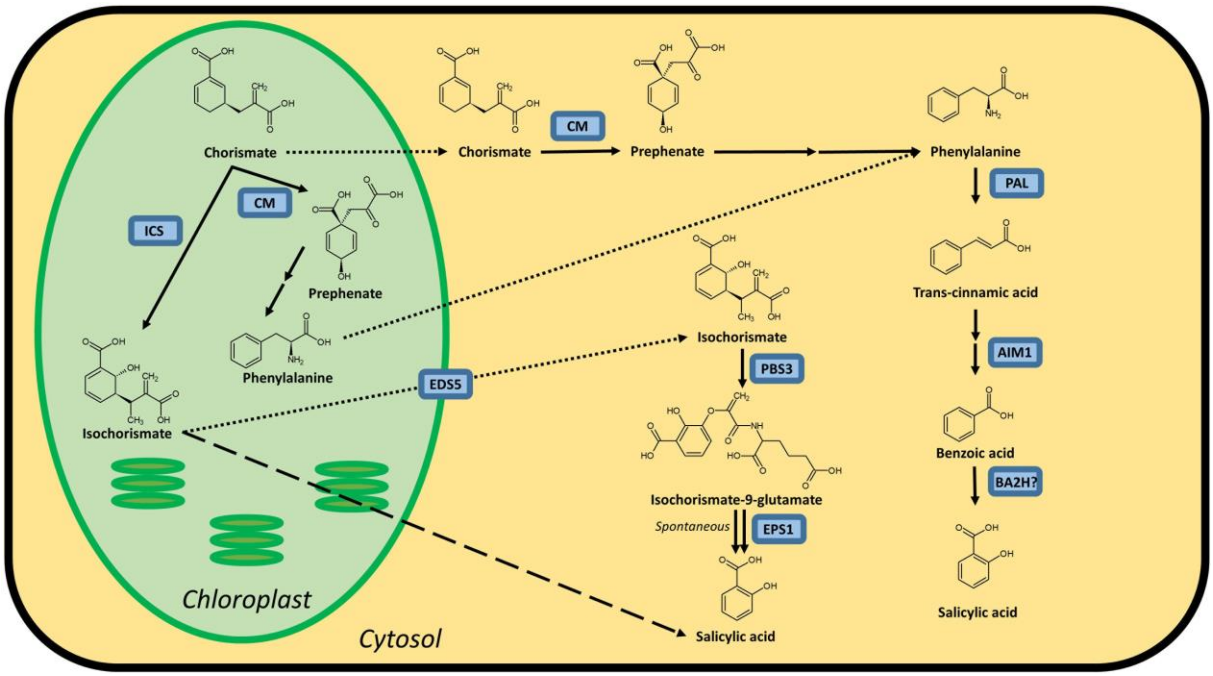

Figure 4: Predicted biosynthesis routes for SA in plants from the precursor chorismate.
Black lines indicate conversion steps, dotted lines depict the intracellular transport from chloroplast to cytosol, the dashed line reflects a route not yet elucidated. Modified from Lefevere et al. (2020).

The biosynthesis of SA (**Figure 4**) is still not fully understood (Lefevere et al., 2020). It is supposedly regulated via two different, chorismate-dependent pathways (Garcion and Métraux, 2006; Chen et al., 2009b). One branch depends on the molecule L-phenylalanine, the enzymatic conversion products *trans*-cinnamic acid (catalyzed by phenylalanine ammonia lyase (PAL)), and benzoic acid, which after hydroxylation ultimately forms SA (Chen et al., 2009b; Li et al., 2019a). The second branch, which is initiated in plastids of *A. thaliana*, depends on the metabolite isochorismate and the pathogen-inducible proteins ISOCHORISMATE SYNTHASE 1 and 2 (ICS1, ICS2), ENHANCED DISEASE SUSCEPTIBILITY 5 (EDS5), and the cytoplasmic avrPphB SUSCEPTIBLE 3 (PBS3) (which is also known as ISOCHORISMATE PYRUVATE LYASE (IPL)) (Verberne et al., 2000; Wildermuth et al., 2001; Rekhter et al., 2019). Notably, cytoplasmic

and nuclear PBS3 interacts with ENHANCED DISEASE SUSCEPTIBILITY 1 (EDS1), thus inhibiting degradation of EDS1 (Chang et al., 2019) and promoting signals in partial dependence of SA (Cui et al., 2017). The expression of, for example, *ICS1* (also known as *SID2*) is inducible by *EDS1* (Lenzoni et al., 2018) after pathogen attack in infected and systemic tissues (Wildermuth et al., 2001). *ICS1* can be modulated by promotor-binding transcription factors like *SYSTEMIC ACQUIRED RESISTANCE-DEFICIENT 1* (*SARD1*), and *CALMODULIN-BINDING PROTEIN 60*-like *g* (*CBPg60*) (Chen et al., 2009a; Zhang et al., 2010c; van Verk et al., 2011). In addition, *ICS1* and *PBS3* are transcriptionally regulated by WRKYs (WRKY28 and WRKY46, respectively) (van Verk et al., 2011), which in sum indicates a complex regulation of SA levels in plants.

The synthesized SA can be further modified on the chemical level via, inter alia, glycosylation, methylation, and amino acid conjugation. SA is reversibly conjugated to either SA *0*-β-glucoside (SAG) or salicyloyl glucose ester (SGE) by specific glucosyltransferases (Dean et al., 2005; Dean and Delaney, 2008). SAG molecules predominate and represent a transportable but inactive form of SA that can be putatively stored long term in vacuoles (Dean et al., 2005). SGE, in turn, is less abundant and an easy hydrolysable form that primarily localizes outside of vacuoles (Thompson et al., 2017; Vaca et al., 2017). Furthermore, SA and its precursor benzoic acid can be reversibly methylated by enzymatic conjugations, producing the volatile molecule methyl salicylate (MeSA) via S-ADENOSYL-L-MET-DEPENDENT METHYLTRANSFERASE 1 (BSMT1) (Shulaev et al., 1997; Song et al., 2009; Tripathi et al., 2010) The expression of *BSMT1* can be transcriptionally modulated by diverse regulators (van Verk et al., 2011; Zheng et al., 2012; Lin et al., 2020), suggesting that versatile plant responses trigger the emission of MeSA.

SA downstream signaling is rather complex and mediated by diverse regulative cascades, including a network incorporating inducible transcription factors (**Figure 6**). The transcription of *PR* genes hereby activates the accumulation of SA via a positive feedback loop (Shirano et al., 2002). The most prominent SA mediator is NONEXPRESSOR OF PR GENES 1 (NPR1) (Fu and Dong, 2013), which is mostly regulated at the post-transcriptional level (Shah, 2003; Wu et al., 2012). *NPR1* modulates basal defense and SAR (Ding et al., 2020). Active NPR1 interacts with TGACG-binding factor (TGA)-proteins, which in turn promote expression of genes like *PATHOGENESIS-RELATED PROTEIN 1* (*PR1*) via binding to its promotor elements (Dong, 2001; Kesarwani et al., 2007; Saleh et al., 2015; Budimir et al., 2021). SA promotes the monomerization of NPR1 from oligomeric complexes and

coordinates the transition of NPR1 from the cytoplasm into the nucleus via modulations of redox homeostasis (Mou et al., 2003; Spoel and Dong, 2012). A subsequent degradation of nucleic NPR1 after ubiquitination functions as key switch for the activation of further SA-dependent signals (Pintard et al., 2004; Spoel et al., 2009).

Interestingly, cytoplasmic NPR1, which is suggested to act as an Cullin 3 Ring E3 ligase adaptor, was shown to include EDS1 as substrate to regulate SA/ETI-associated responses such as the induction of cell death (Zavaliev et al., 2020). NPR3/NPR4, which are paralogues of *NPR1*, interact with EDS1 in order to promote degradational processes and thereby modulate plant defense (Chang et al., 2019). Both NPR3/4 are suggested to work as nuclear SA receptors that regulate SA-induced responses: NPR4 is supposed to either induce the degradation of NPR1 at low SA levels (Fu et al., 2012), or to function as an NPR1-independent transcriptional co-repressor of SA-inducible defense together with NPR3 (Ding et al., 2018). Another possible feature of NPR3 might be the regulation of NPR1-inducible PCD at high SA concentrations (Fu et al., 2012). NPR1 itself, however, was described in other studies to function as a high affinity receptor of SA (Wu et al., 2012; Manohar et al., 2015; Ding et al., 2018), indicating that there are currently different theories about whether or not NPR1 binds SA and thus plays a general role in SA signaling. As plants defective in *NPR1* are still able to induce resistance (to *Ps*) and a simultaneous expression of *PR* genes (Rairdan and Delaney, 2002), this indicates an additional (SA-dependent) defensive regulation independent of *NPR1* (Dong, 2001). Diverse studies showed that SA downstream signals involve cascades independent of *NPR1*, like pathways related to JA and ET and the induction of lipid signals (Penninckx et al., 1996; Clarke et al., 2000; Shah, 2003).

1.3.2 Jasmonic acid

JA and its derivatives play important roles in plant defense to biotic stress (especially against necrotrophic pathogens), wounding responses, and moreover regulate plant growth upon abiotic stress (**Figure 5**) (Okada et al., 2015; Yang et al., 2019). Pathways involving JA act within a network comprising brassinosteroids (BR), gibberellins (GA), ET, SA, and ABA (Yang et al., 2019). Chloroplast-derived JA belongs to the family of oxygenated lipids, is generated from the lipid substrate linolenic acid, of which synthesis is regulated in a positive feedback with JA signals (Wasternack and Hause, 2013). An application of, for example, precursors of JA (like octadecanoid molecules or 12-oxophytodienoic acid (OPDA)) or JA induces

plant responses supposedly by signaling via lipid-based and terpenoid molecules (Farmer and Ryan, 1992; Bosch et al., 2014; Saiman et al., 2015). OPDA is moreover a mobile compound transportable within the plant, for example from shoots to roots (Schulze et al., 2019).

Plant defense is predominantly dependent on interactions of SA signaling within a network of pathways involving JA and ET to activate multifaceted and effective resistance mechanisms (Pieterse and Van Loon, 1999; Koornneef and Pieterse, 2008). Interestingly, mutant plants that are insensitive to ET and JA are susceptible to necrotrophic pathogens (Penninckx et al., 1998; Thomma et al., 1998), and furthermore accumulate lower transcript levels of defense genes like JA/ET-responsive *PLANT DEFENSIN 1.2* (*PDF1.2*) and *PR3,* SA-responsive *PR1b*, and ET-responsive *PR4* (Thomma et al., 1998; Adie et al., 2007a). Furthermore, local defense against *Ps* is regulated by antagonistic actions of SA and JA in *Arabidopsis*, whereas such effect in systemic tissues is not visible (Spoel et al., 2007; Wittek et al., 2015). These findings altogether strongly indicate that crosstalk of ET/JA- and SA-related pathways contributes to local defense against parasitic pathogens (**Figure 6**), as will be discussed later in more detail.

The turnover of JA involves versatile chemical modifications comprising glycosylation, methylation (methyl jasmonate, MeJA), hydroxylation, and decarboxylation, as reviewed elsewhere (Okada et al., 2015). MeJA is a defense-related (volatile) compound that translocates via a sucrose-dependent mechanism in xylem and phloem vessels (Thorpe et al., 2007). JA is further conjugated to amino acids (jasmonoyl-L-isoleucine, JA-Ile) by the catalysator JASMONATE RESISTANT 1 (JAR1) (Suza and Staswick, 2008). The biologically active JA-Ile joins a jasmonate receptor ubiquitin E3 ligase complex - consisting of the Skp1-Cullin-F-(SCF)-box protein and CORONATINE INSENSITIVE 1 (COI1), SCF^{COI1}- that further interacts with JASMONATE ZIM DOMAIN (JAZ) proteins (Staswick and Tiryaki, 2004; Fonseca et al., 2009; Wasternack and Hause, 2013). By this, the binding of stress-inducible JA-Ile to SCF^{COI1} finally results in the degradation of JAZ by the 26S proteasome (Thines et al., 2007).

Activated JA signaling cascades can end in mutually antagonistic pathways of the *ETHYLENE RESPONSE FACTOR* (*ERF*) or the *MYC* branch (**Figure 5**) (Pieterse et al., 2009). Triggers like wounding or insects predominantly activate signaling via the *MYC* branch, transcriptional regulation of the JA signaling marker gene *VEGETATIVE STORAGE PROTEIN 2* (*VSP2)*, and promote the biosynthesis of JA

(Zhang et al., 2015). The induction of a wound-inducible accumulation of JA and *VSP* is dependent on *LIPOXYGENASE 2* (*LOX2*) (Bell et al., 1995).

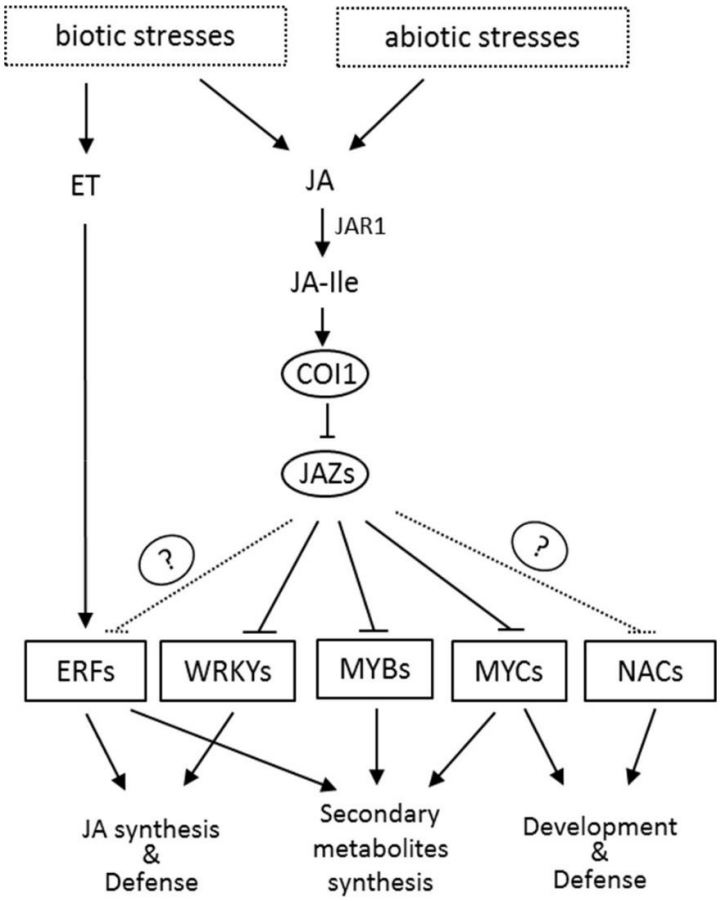

Figure 5: Regulation in pathways of the JA/ET network after biotic/abiotic stress. Question marks indicate a not yet identified adaptor protein regulating the transcription of ERFs or NACs. Modified from Ruan et al. (2019).

Necrotrophic invaders like *Bc*, in turn, stimulate the *APETALA2* (*AP2*)/*ERF* domain-related path which incorporates ET and JA signals and the induction of transcription factors like *ERF1* or *ERF59* (also known as *ORA59*) (Berrocal-Lobo et al., 2002; Lorenzo et al., 2003b; Pré et al., 2008). The *ERF* domain of ERF1 and ORA59 specifically binds to the GCC box motif in elements of defense gene promoters like the fungicidal peptide *PLANT DEFENSIN 1.2* (*PDF1.2*) to further activate transcription (Pré et al., 2008). In this context, JAZ can bind to ETHYLENE INSENSITIVE 3 (EIN3) in order to repress the induction of *ERF1* and *ORA59*, the integrators or JA/ET signals (Zhu et al., 2011). Interestingly, ERFs are additionally targeted by signals downstream of SA or ET (**Figure 6**), as reviewed previously (Yang et al., 2019), indicating that ERFs are key hubs of SA and JA/ET crosstalk. Plants defective in pathways of JA or ET are unable to activate the master regulator *ERF1* and downstream responses (Lorenzo et al., 2003a). Recently, *ERF1* was suggested to modify the generation or transmission of lectin-dependent signals

that function in systemic tissues of locally infected plants (Sales et al., 2021), suggesting that systemically mobile signals are regulated via the interacting pathways of SA and JA/ET.

1.3.3 Ethylene

The volatile compound ET was shown to modulate plant defense responses in multiple ways, interacting with the JA pathway but also with SA signaling (Adie et al., 2007a). JA together with ET synergistically regulates the adaptation to abiotic stress (Kazan, 2015), plant development, and moreover responses in tissues after infestation (with a necrotrophic pathogen) or wounding (Rojo et al., 1999; Glazebrook, 2005; Adie et al., 2007a). Pathogen- and wounding-inducible ET is synthesized from the precursor S-adenosyl methionine (Pierik et al., 2006; Ju and Chang, 2015). The biosynthesis of ET is regulated by diverse enzymes and transcription factors like the JAZ-associated *EIN3* (Adie et al., 2007a; Houben and Van de Poel, 2019), *WRKY33,* and other signals involving calcium (Ca^{2+}) (Wang et al., 2011a; Datta et al., 2015; Jia et al., 2018) and micro RNAs (Huang et al., 2010; Houben and Van de Poel, 2019).

Notably, levels of ET and the antioxidant ascorbic acid (ASA) mutually repress each other in mature leaves (Gergoff et al., 2010; Caviglia et al., 2018), a process potentially regulated by ERFs (Zhang et al., 2012). Changes in the endogenous levels of ET-dependently controlled ASA moreover affect the gene transcription of plant hormonal pathways including that of SA (Caviglia et al., 2018). Interestingly, ASA represses cell division and expansion by stimulating the hydroxylation of proline residues of highly glycosylated hydroxyproline-rich glycoproteins (HRGPs) – a process reversible by the activation of ASA oxidases (Smirnoff and Wheeler, 2000). Further findings describe the oxidative cross-linking of HRGPs as an early pathogen-inducible and ET-related cell wall strengthening response (Toppan et al., 1982; De Cnodder et al., 2005). ROS like H_2O_2 presumably affect the oxidative cross-linking in the cell wall (Lamb and Dixon, 1997), whereby the ASA-associated accumulation of ROS can be repressed by ET via an EIN3-dependent suppression of ABA signaling (Yu et al., 2019). Taken together, this might indicate an ET/ASA(ROS?)/ABA-dependent modulation of cell wall-associated carbohydrates and downstream signaling cascades (**Figure 6**).

Specifically, such regulation might be relevant for basal and systemic defense signaling. Of note is that ET is predominantly relevant in locally infected issues during the establishment of systemic defense responses like SAR (Lawton et al.,

1995; Verberne et al., 2003; Tian et al., 2014). ET-downstream signals are commonly regulated via the JA/*ERF*-branch, with *ERF*s targeting promotor elements of genes with GCC box motifs known as *ETHYLENE RESPONSE ELEMENT* and *DEHYDRATION-RESPONSIVE ELEMENT* (Müller and Munné-Bosch, 2015). Transcription of *ERF*s is moreover a point of hormonal crosstalk (Yamamoto et al., 1999; Devoto et al., 2002; Adie et al., 2007a). Alternatively, JA/ET crosstalk might be dependent on the JAR1-conjugated compound jasmonyl-ACC, as 1-aminocyclopropane-1-carboxylic acid (ACC) is a direct precursor of ethylene (Staswick and Tiryaki, 2004). In sum, potential signaling via ERFs stimulates an ET/SA/JA-dependent crosstalk and thereby affects plant defense.

1.3.4 Abscisic acid

ABA regulates plant responses upon abiotic stress exposure (drought, cold, salinity), developmental processes, stomatal movement, cuticular wax accumulation, and germination (Finkelstein and Gibson, 2002; Li et al., 2019b; Chen et al., 2020). ABA-induced stomatal opening, for example, is modulated by Ca^{2+} signals, protein kinases, and ROS (Jacob et al., 1999; Mustilli et al., 2002; Hunt et al., 2003; Mori et al., 2006; Jammes et al., 2009). Responses involving ABA moreover modify defense upon detection of biotic stressors. Necrotrophic pathogens like *Bc* induce *WRKY33* and by this an elevated synthesis of defense-suppressive ABA (Liu et al., 2015a). Biotrophic fungal pathogens and exogenous ABA were reported to similarly promote a SUGAR TRANSPORTER (STP)-driven accumulation of endogenous ABA and susceptibility in wheat (Huai et al., 2019). In addition, ABA modifies ROS during plant defense (Tan et al., 2019), and affects the redox state, for example by regulating catalase, superoxide dismutase (SOD), peroxidase, ascorbate peroxidase, and ASA (Li et al., 2014).

The synthesis of the isoprenoid ABA derives from the carotenoid pathway and the plastid precursor isopentenyl, which can be produced by either the mevalonic acid (MVA) or the 2-C-methyl-D-erythritol-4-phosphate (MEP) pathway (Eisenreich et al., 2004; Rohmer, 2007). Rate limiting enzymes during the biosynthesis of ABA are enzymes from the 9-cis epoxycarotenoid dioxygenase (NCED) family, like NCED3 (Tan et al., 2003). ABA levels in plants are further controlled by conjugation (glycosylation) and enzymatic hydroxylation. ABA-glucose esters function as a reversible storage form in the cytosol or vacuole (Liu et al., 2015b). The catabolism of ABA leads, for example, to the conversion to phaseic acid, which is retainable in seeds (Weng et al., 2016). During plant stress, translocation of ABA within the plant is directed in dependence of the triggering stimulus (Chen et al., 2020).

ABA is perceived in higher plants by the stress-inducible receptor PYROBACTIN RESISTANCE 1-like (PYL), a repressor of PROTEIN PHOSPHATASE TYPE 2C (PP2C) (Ma et al., 2009; Komatsu et al., 2013). Binding of ABA to PYRABACTIN RESISTANCE (PYR)/REGULATORY COMPONENT OF ABA RECEPTOR (RCAR) suppresses *PP2C,* while it activates a prominent ABA signaling regulator termed SUCROSE NONFERMENTING 1-RELATED PROTEIN KINASE 2 (SnRK2) (Park et al., 2009; Hauser et al., 2011). Increasing ABA levels furthermore lead to the SnRK2-associated induction of transcription and Ca^{2+}-inducible targets involving the activation of components like NAD phosphate (NADPH) oxidases and Ca^{2+} ion channels (Pel et al., 2000; Kwak et al., 2003; Kobayashi et al., 2005; Furihata et al., 2006; Kaplan et al., 2006; Sirichandra et al., 2009). As signaling via ABA and associated glucose pathways moreover comprises regulators that carry an AP2 locus (Finkelstein et al., 1998; Dietz et al., 2010), it can be assumed that such responses might be targeted by JA/ET pathways, as described above. In sum, a network integrating JA/ET, ABA, and additionally SA is suggested to fine-tune plant defense.

1.3.5 Plant hormonal crosstalk

When investigating host-pathogen-associated defense mechanisms in more detail, a strongly modulated crosstalk between SA-, ET-, JA-, and ABA-mediated routes becomes evident that can be antagonistic or synergistic (Li et al., 2019a). Specifically, crosstalk responses are presumably regulated by conserved regulatory mechanisms that control the metabolism of phytohormones, gene transcription, and protein modifications (Spoel and Dong, 2008; Pieterse et al., 2009; Ohri et al., 2015; Yang et al., 2019; Aerts et al., 2021). Ethylene and other plant hormones like auxin, CKs, or JA-mimics are compounds that can be moreover produced and injected into hosts by pathogens, suggesting an active manipulation of plant responses (Weingart et al., 2001; Lorenzo et al., 2003a; Cohn and Martin, 2005; Valls et al., 2006; Kazan and Manners, 2009; Pieterse et al., 2012; Kazan and Lyons, 2014; Chanclud et al., 2016; Ma and Ma, 2016; Han and Kahmann, 2019).

1.3.5.1 SA-JA

Signaling via SA and JA converges in either a simultaneous and synergistic, or an antagonistic fashion in plant defense pathways:

Synergistic actions of SA and JA are detectable during the onset of ETI: during RPS2-dependent ETI, for example, both JA and SA are highly abundant in infected

leaf tissues whereby elevated synthesis of SA precedes that of JA and moreover of JA signaling (Liu et al., 2016b). Here, the early SA-inducible NPR3 and NPR4 appear to act as key regulatory hubs which were suggested to relieve the repressive function of JAZs (like JAZ1) on JA signaling via degradation of these molecules. This mechanism seemingly bypasses modulations of *NPR1* and *COI1*. The authors assume that a signal related to high SA levels in infected tissues during the initial phase of ETI might be necessary to induce a NPR3-driven degradation of NPR1, and to simultaneously activate NPR3/NPR4-triggered signaling and biosynthesis of JA (Fu et al., 2012; Liu et al., 2016b). In support, ETI in a *npr3npr4* double mutant can be rescued after exogenous JA application - this moreover indicates that JA-related signals are relevant for the induction of ETI (Liu et al., 2016b).

On the other hand, many other studies describe SA to predominantly repress the JA(/ET) pathway on the transcriptional level to modulate defense after infection. It is known that especially early defense responses of plants are of highest intensity close to the site of infection, whereas strength declines with increasing distance (Stout et al., 2006; Spoel and Dong, 2008). This allows for defense responses of differing intensity when comparing basal and distal plant parts. In this context, local SA signals strongly suppress JA (or vice versa), while this impact is less detectable systemically. Such effect was previously shown in plants infected with a biotrophic pathogen and challenged with a necrotrophic or herbivore invader (Spoel et al., 2007; Groen et al., 2013; Wittek et al., 2015; Seybold et al., 2020).

Taken together, SA and JA presumably cooperate in a synergistic and antagonistic manner during the onset of ETI defense, dependent on timing, stress intensity, and spatial position.

1.3.5.2 ET-JA-SA

Defending plants regulate hormonal crosstalk in order to prevent spreading invaders. Simultaneously, these plants regulate fitness-related responses after exposure to stress that additionally modulate crosstalk. Such balancing of defense and fitness affects pathways of SA, JA, and the gaseous, non-degradable hormone ET (Vos et al., 2015). Regulations by these three hormones modify defense against a broad spectrum of invaders (Spoel et al., 2007; Li et al., 2019a). Depending on the hormone dose, SA-JA-ET were described to act in either synergistic (low dose, e.g. *PR1* and *PDF1.2* are simultaneously induced) or antagonistic manners (high

dose, e.g. *PR1* is promoted strongly and *PDF1.2* suppressed, or vice versa) (Mur et al., 2006).

Specifically, JA and ET work together to fend off necrotizing pathogens: mutant plants are highly susceptible to an infection with a necrotrophic fungus like *Bc* if they are insensitive to exogenous JA or ET, whereas defense responses to biotrophic pathogens are similar as in wild type plants (Thomma et al., 1998; Thomma et al., 1999). Notably, mutants defective in JA or ET signaling are unable to activate induced systemic resistance (ISR), a response (formerly believed to be SA-independent but) which is *JASMONATE INSENSITIVE 1* (*JAI1* or *MYC2*)- and *NPR1*-dependent and stimulated by beneficial microbes in the rhizosphere (Pieterse et al., 1998; Pozo et al., 2008; Weller et al., 2012; Pieterse et al., 2014; Nie et al., 2017). ISR promotes resistance against a secondary infection with, for example, pathogenic bacteria (Van Loon et al., 1998; Pieterse et al., 1998), and primes plants for a faster induction of JA and ET signals (Pieterse et al., 2000; Choudhary et al., 2007). However, recent studies describe that ISR can be regulated in a host-specific manner involving synergistic actions of JA/ET with SA (Pieterse et al., 2014; Wu et al., 2018a; Yuan et al., 2019; Vlot et al., 2021). It can be assumed that synergistic interactions of the SA and JA/ET pathways form the basis to effectively master a challenge against a broad spectrum of necrotrophic and additionally (hemi-)biotrophic pathogens. Potentially, the regulation of factors like *ORA59* in ISR positively balances signaling by modulating interactions of the SA and JA pathways (Van der Does et al., 2013; Timmermann et al., 2019; Vlot et al., 2021)

Conversely, antagonistic crosstalk is defined as a repression of JA/ET-related signaling by SA, or vice versa, that directly and simultaneously affects defense to biotrophic and necrotrophic pathogens. Presumably, such responses rely on an imbalance of SA versus JA/ET levels. To support this, an infection with the SA-inducing biotrophic pathogen *Ps* suppresses the JA/ET signaling pathway, and furthermore renders plants susceptible to a secondary challenge with a necrotrophic pathogen in the same leaf (Spoel et al., 2007; Wittek et al., 2015). Moreover, plants sensitive to ET accumulate high levels of SA (Thomma et al., 1998). In turn, pathogen-inducible JA biosynthesis or signaling can be counteracted by increasing SA levels in plants (Spoel et al., 2003). Such antagonistic crosstalk can be mediated by *NPR1* and/or transcription factors including *WRKYs*, *EIN3*, or members of the NAC (NAM, ATAF and CUC) transcription factor family like *ANAC019.* In this fashion, for example, expression of biosynthesis

genes like *ICS1* and the accumulation of SA are repressed, while ET and JA signaling pathways are activated (Chen et al., 2009a; Zhang et al., 2010b; Zheng et al., 2012).

1.3.5.3 ET-JA-SA-ABA

ABA exerts crosstalk with JA/ET signaling in order to modulate plant responses after infection with necrotrophic pathogens like *Bc* (Anderson et al., 2004; Adie et al., 2007b; Nguyen et al., 2016; Zhou and Zhang, 2020). Specifically, ABA induces the expression of some JA-related genes during defense except transcripts of *PDF1.2*, which are repressed by ABA. Signaling related to hormonal networking of ABA with JA/ET is dependent on a stress-inducible *ERF* (*ERF4*), of which overexpression renders plants insensitive to ET and ABA, but in turn hypersensitive to salt, for example (Yang et al., 2005). An exogenous application of ABA predominantly represses the JA/ET pathway, whereas endogenous ABA levels promote the same signaling components (Anderson et al., 2004). Defense induced by exogenous ABA during virus-host interaction in rice was shown to repress the JA defensive pathway as well as the accumulation of ROS due to the activation of catalase and SOD (Xie et al., 2018).

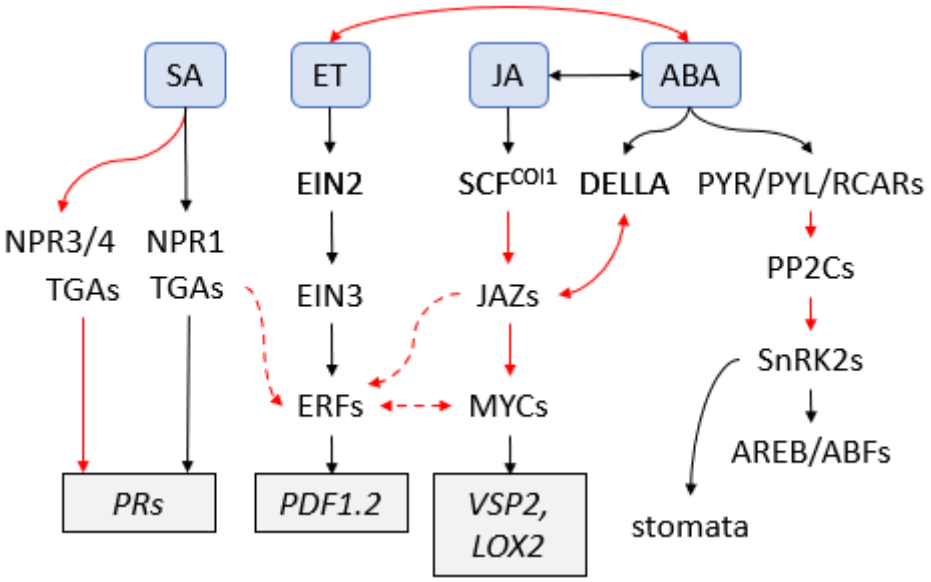

Figure 6: Hormonal signaling network shapes plant defense responses.
Signaling network involving pathways of SA, ET, JA, and ABA in plants affecting downstream signaling and the expression of defense-associated genes. ABRE: ABA-responsive element, ABF: ABRE-binding factors. Black solid line: direct dependent induction, red solid line: dependent repression, red dashed line: predicted repression. Modified after Li et al. (2019a), Zhou et al. (2020), and Nguyen et al. (2016).

An application of SA on the one hand was described to promote a simultaneous accumulation of ABA and H_2O_2 in wheat (Wang et al., 2018b). On the other hand,

signals along the ABA pathway can be suppressed by exogenous SA after plants perceived a stimulus by salt (Yasuda et al., 2008). Notably, an application of SA and additionally ABA results in repression of SA-associated plant responses (Yasuda et al., 2008), indicating a feedback mechanism for ABA to downregulate the SA pathway. Similarly, *Ps* hijacks ABA-inducible responses when injecting COR into plant tissues in order to repress SA and moreover to re-open stomata (De Torres Zabala et al., 2009). ABA additionally regulates the degradation of SA-perceiving NPR1 in *A. thaliana*, which results in suppressed SA signaling (Ding et al., 2016). Similarly, ABA represses *OsNPR1* and SA signaling in rice (Jiang et al., 2010). Exogenous ABA moreover suppresses the accumulation of SA, and presumably the biosynthesis of SA in SAR-induced tomato (Pye et al., 2013; Kusajima et al., 2017). As ABA is additionally a pivotal hormone activated during abiotic stress regulation (as described above), this indicates an important role of ABA in the dual and coordinated regulation of plant responses during abiotic and biotic stress.

As a broad range of gene transcripts in *A. thaliana* plants are modulated during defense, it is further suggested that epigenetic and post-transcriptional regulations shape hormonal networking (Okada et al., 2015; Li et al., 2019a). Histone modifications are assumed to be dispensable for the regulation of SA-JA crosstalk (Koornneef et al., 2008). However, for the JA/ET pathway, HISTONE DEACETYLASE (HAD) 19 and 6 are suggested to modulate plant defense responses via *ERF1* and *EIN3*, respectively (Zhou et al., 2005; Zhu et al., 2011). Recently, another epigenetic regulator belonging to the polycomb repressive complexes termed *LIKE HETEROCHROMATIN PROTEIN 1* (*LHP1*) has been suggested to balance plant developmental responses and stress regulation (Ramirez-Prado et al., 2019). LHP1 is a repressor of the JA/ET-related MYC2 branch that modifies the methylation pattern of the JA- and ABA-inducible NAC-associated genes, *ANAC019* and *ANAC055*. LHP1 regulates the transcription of these two genes and further gene expression, which affects the metabolism of SA involving *ICS1* and *BSMT1*. In the end, resistance against the (hemi-)biotrophic pathogen *Pseudomonas syringae* pv. *tomato* DC3000 (***Pst***) can be modified by LHP1, indicating that LHP1 plays an important role in the regulation of crosstalk between SA, JA/ET, and ABA (Ramirez-Prado et al., 2019).

1.4 Inducible defense responses activate entrainment and priming

Animals, humans and plants share similar immune responses, such as the induction of metabolites, and defense strategies initiated upon exposure to stress (Hunter, 2005; Kim et al., 2020a). Living organisms, which are challenged by stressors, are known to keep memory in order to perform better in a subsequent situation - a feature termed entrainment (Haydon et al., 2013; Netea et al., 2016). For this, plants rely on their innate defense system (Nürnberger et al., 2004).

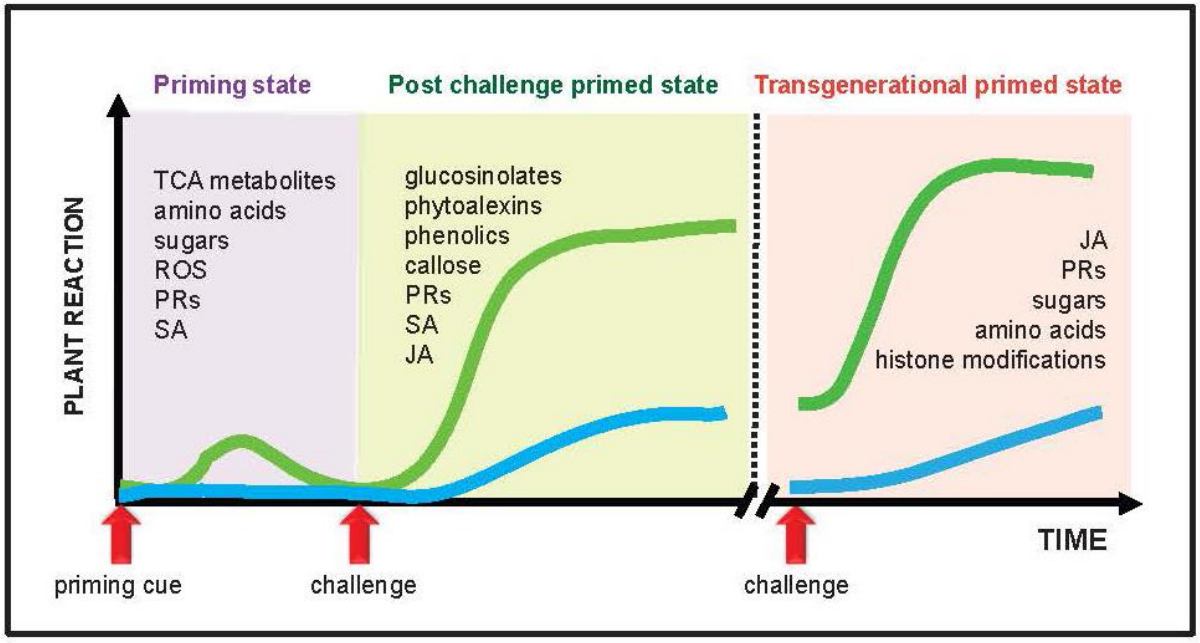

Figure 7: Model for priming of plant defense.
Priming affects the accumulation of metabolites, ROS, defense proteins, plant hormones, and gene transcripts. Green lines indicate the reaction level and speed of primed plants, whereas the blue line indicates that of non-primed plants. Plant reactions get evident especially after a (secondary) challenge with pathogens (left), or after a pathogen challenge in descendants of primed parental plants that transmit a priming memory (transgenerational primed state, right). Adapted from Balmer et al. (2015).

An appropriate stimulus moreover induces priming in plants, an alarmed state of readiness to rapidly fend off subsequent stresses by a faster and/or stronger activation of defense mechanisms (Conrath et al., 2002). The primed status is predominantly based on accumulating levels of metabolites (primary and secondary), enzymes, hormones, and defense-related genes (Balmer et al., 2015). The primed genes display a memory effect with slight expression before and a rapid induction after exposure to subsequent pathogenic stresses (**Figure 7**). This leads to increased stress tolerance and to a stronger induction of, for example, the SA pathway marker gene *PR1* (Jung et al., 2009; Návarová et al., 2012). Notably, priming responses against infections with pathogens can be passed to (at least

two) following generations (Ramírez-Carrasco et al., 2017); this is termed transgenerational priming (**Figure 7**).

1.5 Metabolite signals promote the establishment of systemic acquired resistance

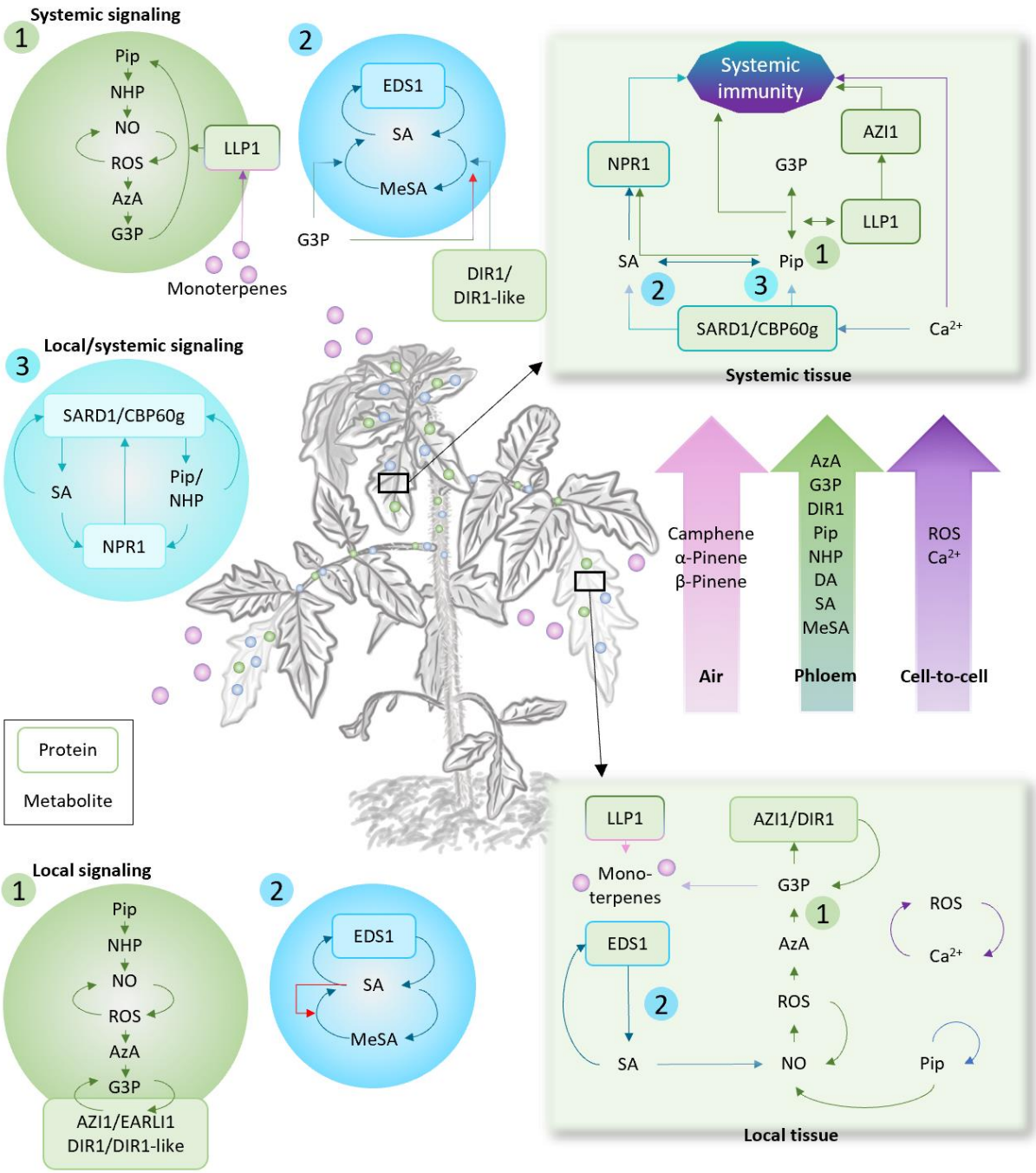

Figure 8: Metabolites and pathways involved in the establishment of SAR.
This signaling model gives an overview of molecular mechanisms relevant for signaling in locally infected (leaves outlined in light grey) and systemic leafy tissues in dicotyledonous plants. The model includes metabolites, hormones, enzymes, and other regulatory components. Adapted from Vlot et al. (2021).

It is of relevance to identify regulators and signaling networks of (early/late) inducible defense responses and priming to elucidate the molecular basis of

interactive pathways in plants. It is known that an effective activation of SAR predominantly depends on two interconnected and synergistically regulated pathways which are associated with SA and pipecolic acid (Pip), respectively (Gao et al., 2015; Kim et al., 2020b; Sun et al., 2020).

Firstly, SA functions during SAR in a positive feedback loop with *EDS1* (**Figure 8**), which is necessary for SAR signal generation and perception (Vlot et al., 2009; Breitenbach et al., 2014; Cui et al., 2017). As EDS1 moreover functions in a regulatory feedback loop together with DELLA proteins to presumably fine-tune SA-associated responses between defense and growth, *EDS1* appears to be a key hub controlling plant responses upon stress (Li et al., 2019c). Inducible signals related to endogenous SA commonly promote the accumulation of *PR* genes (*PR1*, *PR2*, *PR5*) and crosstalk with the JA pathway (affecting *PDF1.2*, *VSP2*) (Pré et al., 2008; Zhang et al., 2015), which is assumed to particularly modify local and systemic plant resistance (Li et al., 2019a). Similarly, exogenous application of SA, SA derivatives, or SA homologues induces defense and the accumulation of PR proteins and *PR* gene expression in diverse plants (White, 1979; Shirano et al., 2002; Vlot et al., 2009). The systemic accumulation of *PR1* transcripts (Malamy et al., 1990; Delaney et al., 1994) as well as elevated SA in local and systemic tissues is essential to mount proper SAR responses (Vlot et al., 2009). Salicylates (SA, methyl salicylate (MeSA)) are described as putative mobile compounds (Park et al., 2007; Lim et al., 2016; Lim et al., 2020). However, long-distance migrating SA molecules are not effectively inducing SAR by themselves (Vernooij et al., 1994; Lim et al., 2020), indicating that (cooperatively) expressed signals are necessary to promote SAR (signaling).

Secondly, the non-protein amino acid Pip and its putatively bioactive conversion product N-hydroxy-pipecolic acid (NHP) promote SAR in dependence of the NHP biosynthesis enzyme FLAVIN-DEPENDENT MONOOXYGENASE 1 (FMO1) (Chen et al., 2018; Hartmann et al., 2018; Wang et al., 2018a). Mutants defective in the synthesis of Pip or NHP (*fmo1*) show an abolished SAR response, whereas mutants compromised in SA (*sid2*) still show moderate SAR responses (Mishina and Zeier, 2006; Bernsdorff et al., 2016; Hartmann et al., 2018). Recently it was shown that exogenously applied NHP promotes SAR in *fmo1*, suggesting that NHP suffices to promote defense (Yildiz et al., 2021). The expression of Pip and NHP is co-regulated with the pathogen-inducible SA synthesis gene *ICS1*, which indicates a synergistic promotion of SAR by Pip-NHP-SA (via *SARD1* and the Ca^{2+}-responsive *CBP60g*) (**Figure 8**) (Wildermuth et al., 2001; Kim et al., 2020b; Sun et al., 2020).

Similarly, exogenously applied Pip or NHP promotes SA signaling and the accumulation of SA (Návarová et al., 2012; Chen et al., 2018; Hartmann et al., 2018). As Pip is assumed to stabilize the predicted SA receptor NPR1 and moreover promotes the expression and priming of *SARD1* and *CBP60g* (Kim et al., 2020b), a synergistic activation of SA and Pip(/NHP) is suggested to regulate SAR (Vlot et al., 2021). Furthermore, Pip and NHP are candidates to function as essential mobile signals in SAR (Návarová et al., 2012; Chen et al., 2018; Hartmann and Zeier, 2018a; Wang et al., 2018c). In addition, the NHP-related conversion metabolite NHP-O-β-glucoside (NHP-H2) was associated to SAR, whose accumulation is suggested as an important negative feedback regulation to avoid NHP overproduction (and negative effects on plant growth) (Bauer et al., 2021; Cai et al., 2021; Holmes et al., 2021; Mohnike et al., 2021). According to the model of Zeier (2021), levels of NHP-H2 more strongly increase in the primary inoculated leaves of SAR-induced plants besides SAG, and to a lesser extent in distal tissues. A local accumulation of NHP-H2 depends on genes of the Pip pathway including *AGD2*-like *DEFENSE RESPONSE PROTEIN 1* (*ALD1) FMO1*, an *URIDINE DIPHOSPHATE (UDP)-DEPENDENT GLYCOSYLTRANSFERASE 76B1* (*UGT76B1*), and moreover on SA-associated routes via *NPR1* and *SID2*, as reviewed (Zeier, 2021). Concluding, it can thus be assumed that NHP-H2 primarily functions in inoculated leaves downstream of Pip and SA. Moreover, other signals generated in defense-stimulated tissues are predicted to translocate towards distal plant organs via either a vascular or airborne route in order to promote SAR:

A former study suggests that the induction of SAR signaling via the phloem is predominantly dependent on biologically active compounds that accumulate in a non-polar fashion (Wittek et al., 2014). Predicted phloem-mobile SAR signals include ROS and Ca^{2+} (Dubiella et al., 2013; Gaupels et al., 2017; Lee et al., 2020; Li et al., 2021b), lipid-derived molecules (glycerol-3-phosphate (G3P), azelaic acid (AzA)) (Chanda et al., 2011; Wittek et al., 2014; Cecchini et al., 2019), extracellular nicotinamide adenine dinucleotides ($eNAD^+$) (Wang et al., 2019), and the diterpene dehydroabietinal (DA) (Chaturvedi et al., 2012). Transportation of these molecules can be promoted by lipid transfer proteins (AZELAIC ACID-INDUCED 1 (AZI1), EARLY ARABIDOPSIS ALUMINUM-INDUCED 1 (EARLI1), DEFECTIVE IN INDUCED RESISTANCE 1 (DIR1), and DIR1-like) (Maldonado et al., 2002; Jung et al., 2009; Cecchini et al., 2015b; Carella et al., 2017), and plasmodesmata-localized proteins (PDLP1,5) (Lim et al., 2016). Interestingly, *PDLP5* was previously shown to additionally affect the movement of bacterial

effectors in *N. benthaminana* (Li et al., 2021c), indicating that this protein influences signaling downstream of effectors.

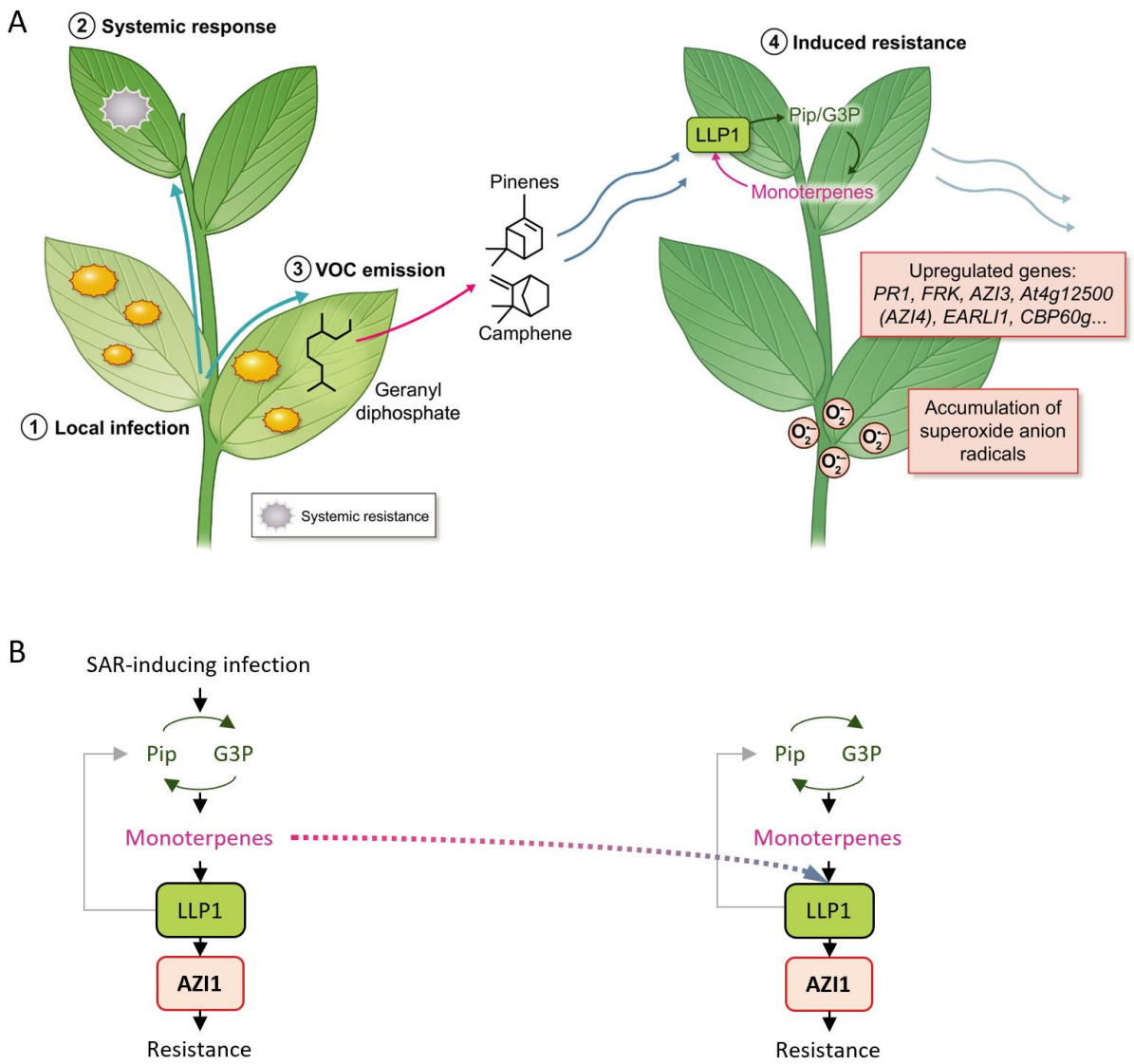

Figure 9: Inter-plant communication is promoted by airborne defense signals. Sender plants (left in A and B) can emit volatile organic compounds (VOC) such as pinenes or camphene from their leaves after a local, SAR-inducing infection. These molecules can be perceived by neighboring plants (right in A and B) in dependence of LLP1 and a signaling fortification loop including Pip/G3P and monoterpenes (A-B). Subsequent downstream signaling cascades promote resistance via AZI1 (B) and activate defense-associated genes and the accumulation of superoxide anion radicals in distal plant parts (A). Adapted from Vlot et al. (2021) and Wenig et al. (2019).

In addition, volatile signals with resistance-inducing capacities are transmittable from SAR-triggered plants to close-by neighbors (inter-plant) or to leaves of the same plant (intra-plant) (Riedlmeier et al., 2017; Wenig et al., 2019; Frank et al., 2021). Such airborne SAR-associated molecules contribute to long-distance signaling and comprise α/β-pinenes and camphene in *A. thaliana* (Riedlmeier et al., 2017; Wenig et al., 2019). Emission of monoterpenes from local tissues is

putatively dependent on Pip (Griebel and Zeier, 2008; Wenig et al., 2019; Vlot et al., 2021). For monoterpenes in particular, a promotive effect on systemic defense rather than on local responses was shown (Riedlmeier et al., 2017). Moreover, an exposure to other terpenoids such as β-caryophyllene, which is emitted from poplar plants, or isoprene (which putatively acts inter-specifically between plants) induces resistance against bacterial infections (Frank et al., 2021).

Interestingly, LEGUME LECTIN LIKE PROTEIN 1 (LLP1) appears to cooperate with AzA, monoterpenes, and G3P via the Pip pathway in order to mount SAR and inter-plant communication (Bartsch et al., 2006; Breitenbach et al., 2014; Wittek et al., 2014; Riedlmeier et al., 2017). *LLP1* was formerly assumed to be regulated via either crosstalk of SA and Pip, or to act in parallel with SA as part of the Pip pathway (Breitenbach et al., 2014; Wenig et al., 2019). As treatments of plants with either AzA or MeSA promote resistance to *Pst* independently of *LLP1*, it seems likely that LLP1 acts in a pathway parallel to SA and AzA (Wenig et al., 2019). Mutant plants defective in *LLP1* or the accumulation of G3P or monoterpenes are likewise un-responsive to a treatment with exogenous Pip and are susceptible to *Pst* (Wang et al., 2018a; Wenig et al., 2019). Consequently, LLP1, G3P and α/β-pinenes are supposed to act downstream of Pip during defense (Wenig et al., 2019). In addition, it was formerly suggested by others that Pip acts upstream of G3P and AZI1 in order to mount SAR (Wang et al., 2018a).

Furthermore, the accumulation of monoterpenes and camphene is suggested to be primarily dependent of *LLP1*, G3P, and Pip, and to a lesser extent on *AZI1* (Wenig et al., 2019), suggesting that monoterpenes function downstream of G3P/Pip and upstream of *LLP1* and (or in parallel to) *AZI1*. Notably, a successful emission of SAR signals is achieved in Pip- or G3P-deficient mutants after the co-application of Pip and G3P (Wenig et al., 2019), which indicates that Pip acts together with (AZI1/DIR1-)G3P in the establishment of systemic resistance. *LLP1* might recognize or amplify such a systemically mobile SAR signal in a mutual pathway with AZI1 and moreover function as receptor of inter-plant signals (**Figure 8**, **9**A-B) (Wenig et al., 2019).

Notably, AZI1 is supposed to act in a feedback loop with G3P and DIR1 in order to establish SAR, whereby *AZI1* and *DIR1* both regulate the accumulation of G3P in local and systemic tissues (Yu et al., 2013). Interestingly, mutants defective in *AZI1* are capable of emitting volatile SAR signals (like monoterpenes), whereas *AZI1* is required to perceive airborne SAR signals (Wenig et al., 2019) and to send

SAR signals via the phloem route (Jung et al., 2009; Yu et al., 2013). The *AZI1* pathway thus seems to represent an important path in plants to convert airborne SAR signals into intra-plant (cell-to-cell and/or long-distance) messages via the phloem. Thus, intra- and inter-plant signaling might be simultaneously affected by *AZI1* (**Figure 9**B). It can moreover be assumed that both pathways, the airborne and the vascular route, synergistically promote inter-specific SAR. Moreover, downstream signaling routes of *LLP1*, *AZI1*, and defense-inducible volatile molecules (like monoterpenes and sesquiterpenes) may be modified by pathways involving SA (*NPR1*) and JA (*JAR1*), respectively (Wenig et al., 2019; Frank et al., 2021).

1.6 *EDS1*-dependent proteins are suggested to modify systemic acquired resistance and are connected to carbohydrate molecules

Signaling via Toll/interleukin-1 receptor (TIR)-type NLRs (TNLs) is assumed to depend on *EDS1*, which promotes two distinct pathways triggering either basal or systemic defense in plants (**Figure 10**) (Aarts et al., 1998). Cell death and local defense is regulated via the branch involving EDS1-SENESCENCE ASSOCIATED GENE 101 (SAG101)-NRG1, while EDS1- PHYTOALEXIN DEFICIENT 4 (PAD4)-ACTIVATED DISEASE RESISTANCE 1 (ADR1) stimulates signaling for systemic resistance (Chini et al., 2004; Wiermer et al., 2005; Roberts et al., 2013; Gantner et al., 2019; Lapin et al., 2019; Song et al., 2020; Pruitt et al., 2021; Sun et al., 2021). NRG1 and ADR1 (coiled-coil-type NLRs) both function as helper-NLRs (Dong et al., 2016), whereby ADR1 carries homologous domains known from protein kinases for serine/threonine (Grant et al., 2003).

Breitenbach et al. (2014) previously identified extracellularly accumulating proteins which are linked to SAR using *Avr RESISTANCE TO PSEUDOMONAS SYRINGAE PV. MACULICOLA 1* (*AvrRpm1*) as a trigger for local ETI responses. In that study, transgenic plants were brought to a state resembling SAR activation by using a pathogen-free, *AvrRpm1* effector-inducible system. SAR-associated proteins were identified by comparing responses in wild type to those in *eds1* mutant plants, which displayed compromised SAR signal generation in response to AvrRpm1. Interestingly, some proteins found in this study, such as the BETA-D-XYLOSIDASE 4 (At5g64570, XYL4) and lectin proteins (including LLP1), putatively relate with regulative pathways involving carbohydrate molecules (Breitenbach et al., 2014).

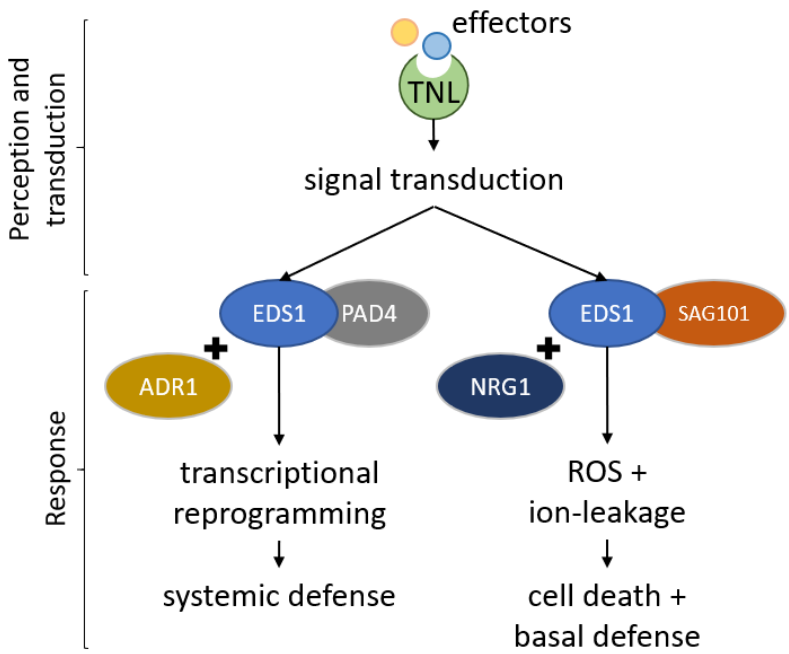

Figure 10: Model for *EDS1*-dependet regulation of defense.
EDS1 promotes basal and systemic responses in effector-triggered plants via two supposedly distinct signaling pathways. Adapted from Song et al. (2020).

Plant lectins carry a conserved carbohydrate binding domain as shown for LLP1, which was previously described to promote SAR (Breitenbach et al., 2014; Wenig et al., 2019; Sales et al., 2021). For the perception of systemic SAR signals, *LLP1* is suggested to potentially sense glycan residues, including soluble sugars or cell wall carbohydrates, or other predicted molecules acting as vascular or airborne mobile signal as discussed before (Wenig et al., 2019; Vlot et al., 2021). As LLP1 is moreover suggested to signal via a route dependent on functional AZI1 (Riedlmeier et al., 2017; Wenig et al., 2019), it can be assumed that subsequent downstream signals are regulated by LLP1-AZI1. Notably, the gene expression of *AZI1* in systemic tissues is positively associated with carbohydrate pathways affecting carbohydrate transporters and the transcription of biosynthesis genes (Wang et al., 2016). It is thus conceivable that sugar signaling (via LLP1-AZI1) might be important for the establishment of an effective SAR response.

XYL4 was identified in the same SAR-associated protein fractions as LLP1 in the proteomic study of Breitenbach et al. (2014) but has so far not been examined for its influence on innate immunity and SAR. *XYL4,* also known as *AtBXL4,* codes for a glycoside hydrolase of which three splice variants are described (Goujon et al., 2003). Interestingly, XYL4 was found to be a cell wall modifying enzyme (Boudart et al., 2005) that can be secreted from plant seedlings (Charmont et al., 2005). This suggests that XYL4 proteins are (partially) mobile within plants or are

potentially released from/to the cell wall space where they presumably get activated (upon stress). According to a phylogenetic analysis comparing different apoplast-derived proteins in *A. thaliana*, XYL4 was found to be homologous to a beta-glucosidase (Iglesias et al., 2006) that was previously described to hydrolyze xyloglucan oligosaccharides (Crombie et al., 1998). Specifically, *Arabidopsis* (*Wassilewskija* ecotype) stem-derived beta-xylosidases, including XYL4 proteins, were classified as xylan-degrading enzymes (Minic et al., 2004). Xyanolytic enzymes like xylosidases were formerly proven to degrade natural substrates including the heteropolysaccharide xylan (Rohman et al., 2019). XYL4 was specifically described to induce the release of D-xylose from hemicellulose structures like xylotetraose, xylobiose, xylan (of oat spelt), arabinoxylan (of rye), and (oligo)arabinoxylan (of wheat), which strongly indicates that XYL4 acts as a beta-D-xylosidase (Minic et al., 2004).

Since XYL4 might alter cell wall glycans by releasing molecules like D-xylose, I hypothesize that a potential XYL4-derived carbohydrate acts as an important signal during SAR. Since LLP1 proteins are predicted to bind carbohydrate-associated molecules and act as systemic SAR signal receptor (Breitenbach et al., 2014; Wenig et al., 2019), I hypothesize that XYL4 action in *A. thaliana* further results in the generation of an LLP1-perceivable substrate. Potentially, such signals comprise derivatives of DAMPs and/or cell wall-associated molecules like xyloglucan residues, as described above.

1.7 Aim of this work

With this study, I aim to characterize *XYL4* for its contribution to plant disease resistance and signaling. I focus on local and systemic responses that shape defense and metabolic pathways in plants that have perceived a bacterial stimulus. In doing so, I intend to characterize XYL4 *in planta* action and to elucidate *XYL4*-dependent signaling during the establishment of SAR.

Cell wall-related immunity is modulated by an intricate, dynamic system regulating cell wall integrity maintenance mechanisms that are likely deployed by plants and pathogens (Gigli-Bisceglia et al., 2020). Particularly, the structure and the composition of cell walls is modified in response to pathogenic stimuli, and assumed to determine plant defense signaling during SAR (Breitenbach et al., 2014). The cell wall-associated protein LLP1 hereby putatively perceives carbohydrate signals in systemic leaves of SAR-triggered plants, which might be generated in dependence to XYL4 or SA.

This study thus initially clarifies if *XYL4* associates with plant defense against (hemi-)biotrophic bacteria in basal tissues, and moreover in SAR. The experiments are performed in wildtype *A. thaliana* and include *xyl4* mutants to additionally assess if defense genes of SA and JA signaling components are (antagonistically) expressed in relation to *XYL4*. In the following, I ascertain if and in which tissues *XYL4* is relevant during SAR signaling that is activated via molecule transmission via the vascular or airborne routes. These analyses provide insights into whether *XYL4* modifies SAR signal generation, propagation, and/or perception in relation to pathways including SA, JA, and Pip.

Finally, this work aims to assess the accumulation of metabolites in (transgenic) *AvrRpm1*-triggered plants in order to identify possible metabolic pathways relevant for SAR. To this end, I use chromatographic approaches and additionally carbohydrate microarrays to reveal differences and patterns in defense-associated molecules including glycan structures. The results presented in this thesis provide promising features of the cell wall and carbohydrates as possible modulators of SAR in *A. thaliana* and call for further studies to uncover their potential in plant protection.

2. Material and methods

2.1 Materials

2.1.1 Plants

A. thaliana ecotype Columbia-0 (Col-0) was used throughout this work. Additionally, I used the mutant lines *eds1-2*, *llp1-1* and *llp3* (SALK_030762), which were previously described (Bartsch et al., 2006; Breitenbach et al., 2014; Wenig et al., 2019; Sales et al., 2021). Moreover, transgenic Col-0 *pDEX:AvrRpm1-HA* and *eds1-2 pDEX:AvrRpm1-HA* were used, as described previously (Mackey et al., 2002; Breitenbach et al., 2014). The mutant lines *xyl4-1* (SALK_071629) and *xyl4-2* (SALK_048903) were obtained from the Nottingham Arabidopsis Stock Centre (Scholl et al., 2000).

2.1.2 Bacteria

Table 1. Bacteria used in this work.

Species	Strain
Pseudomonas syringae pv. *tomato* (*Pst*)	DC3000
	DC3000/*AvrRpm1*
	DC3000-GFP

2.1.3 Kits

Table 2. Kits used in this work.

Kit	Company	Application
QIAprep spin miniprep kit	QIAGEN (Hilden, Germany)	preparation of plasmid DNA
SensiMixSYBR Low-Rox Kit	Bioline Meridian Bioscience Reagents (London, United Kingdom)	qRT-PCR

2.1.4 Chemicals

Chemicals not specifically listed in this table were purchased from either Merck (Darmstadt, Germany), Roth (Karlsruhe, Germany), or Sigma-Aldrich (St. Louis, USA).

Table 3. Chemicals used in this work.

Chemical	Manufacturer
AzA (Azelaic acid)	Sigma-Aldrich (St. Louis, USA)
Camphorsulfonic acid	Sigma-Aldrich (St. Louis, USA)
CTAB (cetyltrimethylammoniumbromid)	Sigma-Aldrich (St. Louis, USA)
DEX (dexamethasone)	Sigma-Aldrich (St. Louis, USA)
Lidocaine	Sigma-Aldrich (St. Louis, USA)
MeJA (methyl jasmonate)	Sigma-Aldrich (St. Louis, USA)
Murashige & Skoog Medium (MS) + vitamins	Duchefa (Haarlem, Netherlands)
p-Nitrophenol	Fluka™, Fisher Scientific (Schwerte, Germany)
Pip (pipecolic acid)	Sigma-Aldrich (St. Louis, USA)
Phytoagar	Duchefa (Haarlem, Netherlands)
Ribitol	Sigma-Aldrich (St. Louis, USA)
SA (salicylic acid)	Roth (Karlsruhe, Germany)
SAG (salicylic acid glucoside)	ChemCruz™ Biochemicals (Huissen, The Netherlands)
NaCl (sodium chloride)	Roth (Karlsruhe, Germany)
^{13}C Sorbitol	Sigma-Aldrich (St. Louis, USA)
Vac-In-Stuff (Silwet L-77)	Lehle Seeds (Texas, USA)
TRI-Reagent®	Sigma-Aldrich (St. Louis, USA)
Tween®-20	Calbiochem (Bioscience) (San Diego, USA)
D-/L-Xylose	ChemCruz™ Biochemicals (Huissen, The Netherlands)
D-Xylose	Acros Organics (New Jersey, USA)
L-Xylose	Acros Organics (New Jersey, USA)

2.1.5 Enzymes

Table 4. Enzymes used in this work.

Enzyme	Manufacturer
Fast Digest restriction enzymes	Thermo Fisher Scientific (Waltham, USA)
MangoTaq™ DNA polymerase	Bioline Reagents (London, United Kingdom)
SensiMix SYBR Low-Rox	Bioline Reagents (London, United Kingdom)
SuperScript II reverse transcriptase	Invitrogen/Thermo Fisher Scientific (Waltham, USA)

2.1.6 Buffers and solutions

Table 5. Buffers and solutions used in this work.

Buffer/solution	Composition	Application
CTAB solution	100 mM Tris, 20 mM EDTA, 1.4 M NaCl, 2% (w/v) CTAB, pH 8.0, autoclave	isolation of genomic DNA
Mock buffer	10 mM $MgCl_2$ / + 0.01% (v:v) Tween-20)	control treatment for infiltration / spray
NTES (gDNA isolation) buffer	250 mM NaCl, 200 mM Tris pH 8, 25 mM EDTA, 0.5% SDS	quick isolation of genomic DNA
RNA-extraction buffer	5 mL glycerol, 3.33 mL 3 M sodium acetate, pH 5.2, 40 mL H2O, adjust pH to 5.0, 38 mL Roti-Aqua-Phenol	RNA isolation
TAE (Tris-acetate-EDTA) buffer	40 mM Tris, 1 mM EDTA, 0.1% (v:v) glacial acetic acid	gel electrophoresis

2.1.7 Media

Table 6. Media and their composition as used in this work.

Medium	Composition	Application
NYGA	5 g proteose peptone 3 g yeast extract 20 mL glycerol 1 L H_2O, adjust pH to 7.0 18 g agar-agar	growth of *Pst* bacteria

MS (Murashige & Skoog)	0.4302% MS salt with vitamins 1% sucrose 0.05% MES buffer, adjust pH to 5.7 1.2% agar-agar	germination of seeds on plates

2.1.8 Antibiotics

Antibiotics were purchased from Roth (Karlsruhe, Germany)

Table 7. Antibiotics and their concentrations as used in this work.

Antibiotic	Final concentration	Use
Ampicillin	100 µg/mL	Petiole exudate buffer
Carbenicillin	250 µg/mL	Sterile media plant
Cefotaxim	100 µg/mL	Sterile media plant
Hygromycin	50 µg/mL	Selection of DEX-transgenic plants
Kanamycin	50 µg/mL	Selection of *Pst* (virulent and avirulent)
Rifampicin	50 µg/mL	Selection of *Pst* (virulent and avirulent)

2.1.9 Primers

Primers were obtained from Metabion (Planegg, Germany)

Table 8. Primers used for qRT-PCR.

Name and description	Sequence 5′ → 3′	T_m [°C]	Reference
UBIQUITIN forward	AGATCCAGGACAAGGAGGTATTC	66	(Sales, 2021)
UBIQUITIN reverse	CGCAGGACCAAGTGAAGAGTAG	67	(Sales, 2021)
XYL4 forward	TGAGACCCGATAAAGCAAGCG	67	
XYL4 reverse	CGAGACCGAGAGAAACGAGAC	67	
PR1 forward	CTACGCAGAACAACTAAGAGGCAAC	68	(Sales, 2021)
PR1 reverse	TTGGCACATCCGAGTCTCACTG	69	(Sales, 2021)
PDF1.2 forward	CCAAGTGGGACATGGTCAG	66	(Sales, 2021)
PDF1.2 reverse	ACTTGTGTGCTGGGAAGACA	67	(Sales, 2021)
VSP2 forward	GTTAGGGACCGGAGCATCAA	60	(Sales, 2021)
VSP2 reverse	AACGGTCACTGAGTATGGGT	63	(Sales, 2021)
LLP1 forward	TGAGTAAACAGCAGTTACGA	60	(Sales, 2021)
LLP1 reverse	TGACGCCATCAGAAGCAGGA	69	(Sales, 2021)
LLP3 forward	TTTGGAGCTGGTCGTTTG	63	(Sales, 2021)
LLP3 reverse	ATTCACTCTACAACAATT	51	(Sales, 2021)
FMO1 forward	ATCCCTTTATCCGCTTCCTCAA	66	(Bauer et al., 2021)

FMO1 reverse	CTCTTCTGCGTGCCGTAGTTTC	68	(Bauer et al., 2021)
AvrRPM1 forward (DEX)	CGAACTCAGCCCCTACAGAC	67	(Breitenbach et al., 2014)
AvrRPM1 reverse (DEX)	GTCGTTCTGCAGCTGAATTG	64	(Breitenbach et al., 2014)

Table 9. Primers used for genotyping to test for homozygous mutations.

Name	Sequence 5' → 3'	Description
LBb1.3	ATTTTGCCGATTTCGGAAC	LB primer for SALK mutants, T-DNA
LB 3 SAIL	TAGCATCTGAATTTCATAACCAAT CTCGATACAC	LB3 primer for SAIL mutants, pCSA110 construct used /7541 bps)
XYL4-1 LP	CCGCTTTCTCCTAAATCGAT	LP primer for XYL4-1, SALK_071629
XYL4-1 RP	TCTCCGACATGAAGAAGA	RP primer for XYL4-1, SALK_071629
XYL4-2 LP	ACTCCATCAAAACAAACGCAC	LP primer for XYL4-2, SALK_048903
XYL4-2 RP	GAATACCGACTCGCTGATCTG	RP primer for XYL4-2, SALK_048903
XYL4-3 LP	AGAGGAAGCAGTTAAGTCGGG	LP primer for BXL4-2, Sail_331_B06 Col-3 background
XYL4-3 RP	GCAAACGTGATTCTCTCCGAG	RP primer for BXL4-2, Sail_331_B06 Col-3 background
EDS1-2 P1	GGCTTGTATTCATCTTCTATC	First primer for EDS1-2, EDS4
EDS1-2 P2	GTGGAAACCAAATTTGACATTAG	Second primer for EDS1-2, EDS6
EDS1-2 P3	ACACAAGGGTGATGCGAGACA	Third primer for EDS1-2, 105/E2
LLP1-1 LP	TTGGGATGCAAAGCAAATTAC	LP primer for LLP1, SALK_036814
LLP1-1 RP	CTTTCTCAGCAACAACGGAAG	RP primer for LLP1, SALK_036814
LLP3 LP	TCCGTGAAGAAAACAAACAA	LP primer for LEC1 SALK_030762
LLP3 RP	GAGACGAAACCCCATTCTCT	RP primer for LEC1 SALK_030762

2.1.10 Devices and instruments

Table 10. Devices and instruments used in this work.

Instrument	Type	Company
Autosampler system	Combi PAL	CTC Analytics AG (Zwingen, Switzerland)
Centrifuges	Heraeus Fresco 21 Heraeus Pico 17 Centrifuge 5415 D Centrifuge 5810 R	Thermo Fisher Scientific (Waltham, USA) Eppendorf (Hamburg, Germany)
Conductivity meter	GLM 020A	Greisinger Electronic (Regenstauf, Germany)
Freeze dryer	ALPHA 2-4 LDplus	Christ (Osterode, Germany)

Gas Chromatography	GC 7890A	Agilent (Santa Clara, USA)
GC-TOF-MS system	Pegasus® HT	Leco (St Joseph, USA)
Gel electrophoresis chamber	PerfectBlue Horizontal Minigelsystems	Peqlab/VWR (Radnor, USA)
Homogenizer	Silamat S6	Ivoclar Vivadent (Ellwangen, Germany)
Metabolite separation	EZ-Guard column	Agilent (Santa Clara, USA)
Microarray instrument	Marathon, Arrayjet	Arrayjet (Roslin, United Kingdom)
PCR cycler	Mastercycler nexus	Eppendorf (Hamburg, Germany)
Photometer	NanoDrop ND-1000	Nanodrop Technologies/ Thermo Fisher Scientific (Waltham, USA)
qRT-PCR cycler	Applied Biosystems 7500 and Applied Biosystems 7500 Fast	Applied Biosystems, Thermo Fisher (Freiburg, Germany)
Rotational vacuum concentrators	RVC 2-25 CDplus SpeedVac™	Christ (Osterode, Germany) Thermo Fisher Scientific (Waltham, USA)
Spectrophotometer	FoodALYT bio	Omnilab (Bremen, Germany)
Microplate reader	Tecan INFINITE M1000 PRO	Tecan (Grödig, Austria)

2.1.11 Software and web applications

Table 11. Software and web applications used in this work.

Software	Version/source	Application
ATTED-II Website	http://atted.jp/	Estimate gene functions due to co-regulation of genes

ChromaTOF & TagFinder Software	ChromaTOF 4.5 TagFinder 4.1	Evaluation of chromatograms and mass spectra
GIMP	Version 2.10.21	Root length measurements
GraphPad Prism	GraphPad Prism 9 for Windows (version 9.1.2)	statistics and graph design
Microsoft Office	Excel, PowerPoint, Word, 2016	data analysis and graph design
Primer Blast	https://www.ncbi.nlm.nih.gov/tools/primer-blast/	qPCR primer design
Real Quantification 7500 Fast System Software	Version 1.5.1	qRT-PCR control and raw data generation
Reference data base metabolome	Golm metabolome database (GMD) (Kopka et al., 2005)	Metabolite profiling and edit

2.2 Methods

2.2.1 Plant material and growth conditions

A. thaliana cultivar Col-0 was used for all experiments. In addition, the T-DNA insertion lines *eds1-2*, *llp1-1*, *llp3*, *xyl4-1*, and *xyl4-2* were examined. Seeds were propagated and tested for homozygosity (O'Malley et al., 2015) using the primers listed in **Table 9**. Plants that were homozygous for the T-DNA insertion were used for all experiments. The T-DNA insertion sites were confirmed in pooled plant samples of at least five individual plants for each T-DNA insertion line. To this end, genomic DNA was isolated from leaves of 5-week-old plants and PCR products were generated using primers as listed in **Table 9**.

Transgenic dexamethasone-inducible (DEX) lines Col-0 *pDEX:AvrRpm1*-HA and *eds1-2 pDEX:AvrRpm1*-HA were previously described in Mackey et al. (2002) and Breitenbach et al. (2014). Constructs for *llp1-1 pDEX:AvrRpm1*-HA, *xyl4-1 pDEX:AvrRpm1*-HA, and *llp3 pDEX:AvrRpm1*-HA were generated by crossing either *llp1-1*, *xyl4-1*, or *llp3* with Col-0 *pDEX:AvrRpm1*-HA. Surface sterilized (70% (v:v) ethanol) seeds of the first (T1) generation were selected for the DEX transgene on MS medium containing 250 µg ml-1 carbenicillin, 100 µg ml-1 cefotaxime, and 50 µg ml-1 hygromycin. DEX transgene-carrying seedlings were subsequently tested for their state of homozygosity by using primers a listed in

Table 9. Homozygous plants of the fourth generation (T4) were used for experiments.

Plants were grown for 4-5 weeks on a mixture of non-fertilized potting soil and silica sand (ratio 5:1) and kept at 22 °C in 10-h days with a light intensity of 100 µmol m^{-2} s^{-1} of photosynthetically active photon flux density, and at 18 °C for 14-h nights. The relative humidity was kept at ~70%.

2.2.2 Pathogens and preparation of bacterial inoculum

Pseudomonas syringae pathovar *tomato* DC3000 (*Pst*) and *Pst*/*AvrRpm1* were used for bacterial inoculation of plants (Breitenbach et al., 2014). Bacteria were grown at 28 °C on NYGA medium (**Table 6**), supplemented with 50 µg mL^{-1} kanamycin and 50 µg mL^{-1} rifampicin. Freshly prepared overnight cultures were used for infection assays and the bacteria were suspended in 10 mM $MgCl_2$ (Wenig et al., 2019). The bacterial density of the suspension was determined by measuring the OD_{600} of the suspension (or a dilution thereof) on a spectrophotometer and by using the formula OD_{600} = 1.0 equals 10^8 colony forming units (cfu) per mL.

2.2.3 Bacterial infections

To investigate bacterial densities in infected leaves, bacterial growth curve assays were performed with *Pst* and *Pst*/*AvrRpm1*. Two fully expanded leaves per plant (e.g. leaves "1" and "2", or "3" and "4", **Figure 11**A) were syringe-infiltrated from the lower (abaxial) side with 10^5 cfu mL^{-1} of bacteria in 10 mM $MgCl_2$ (**Figure 11**B) (Wenig et al., 2019). Alternatively, whole plants were sprayed from the top with 10^8 cfu mL^{-1} of *Pst* or *Pst*/*AvrRpm1* diluted in 10 mM $MgCl_2$ containing 0.01% (v:v) Tween-20. Similarly, corresponding mock solutions were applied by leaf infiltration of 10 mM $MgCl_2$ or by spray application of 10 mM $MgCl_2$ containing 0.01% (v:v) Tween-20 (**Figure 11**C).

Infected leaves were harvested and analyzed for *in planta* bacterial titers, gene expression, or metabolite accumulation at different timepoints as indicated. Additionally, *in planta* bacterial titers were determined as described (Breitenbach et al., 2014). In short, bacteria were extracted from three leaf discs per sample in 500 µL of 10 mM $MgCl_2$, including 0.01% (v:v) Vac-In-Stuff, while shaking (600 rotations per minute (rpm), 26 °C). One hour later, samples were serially diluted and 20 µL per dilution were spotted on NYGA medium, as shown in **Figure *12***A.

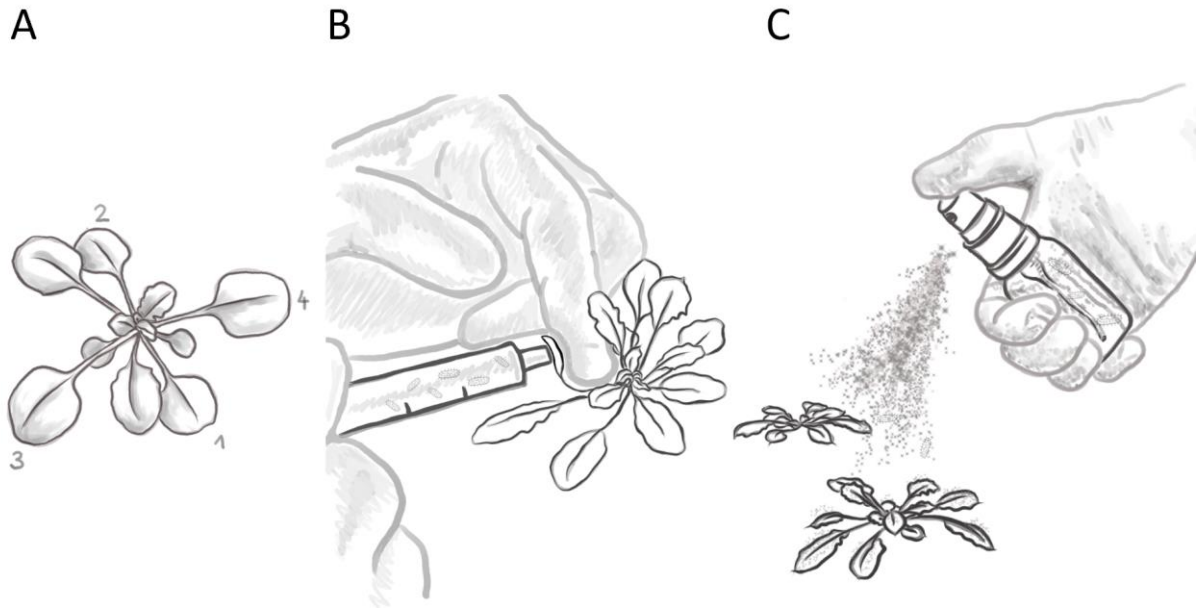

Figure 11: Overview of the leaf architecture in a 4-week-old *A. thaliana* plant and bacterial infection procedures.
Leaves are numbered according to their emergence (**A**). Plants are either inoculated by syringe infiltration (**A**) or spray treatment (**B**). Modified from Wenig et al., 2022.

Bacterial colonies were grown for two days, counted by eye (**Figure *12***B) and subsequently converted to cfu per cm² of leaf tissue. Replicate experiments (one batch) consisted of at least three independent samples per genotype and treatment. Biologically independent datasets were obtained from different experimental rounds, for which seeds were sown independently.

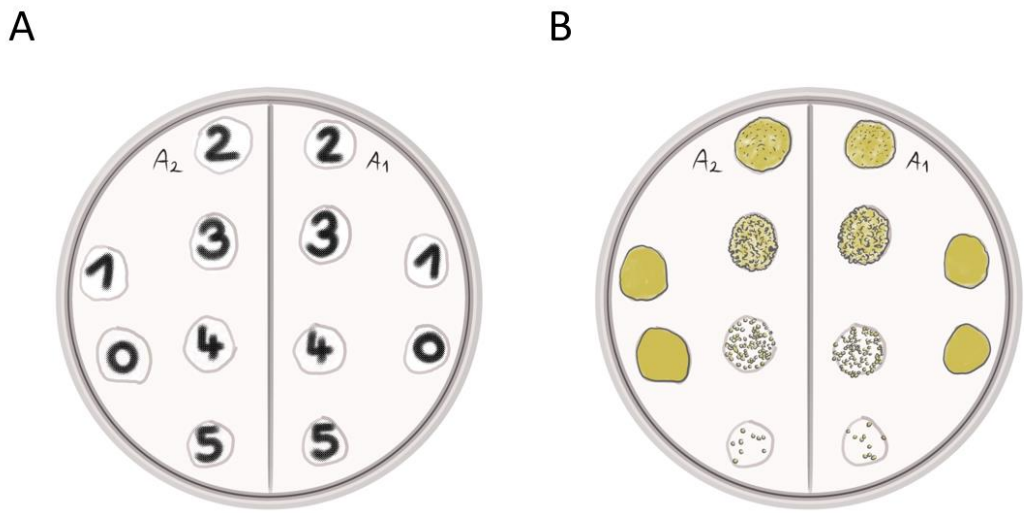

Figure 12: Scheme for bacterial plating (A) and exemplary bacterial growth on a plate at the 2nd day after plating (B).
(**A**) Per sample, 20 µL of each dilution ("0": un-diluted, "1": 1st dilution, "2": 2nd dilution, and so on) was spotted in the place as indicated by numbers on one half of a NYGA plate. (**B**) Bacterial colonies formed were counted at the 2nd day after plating. Modified from Wenig et al., 2022.

To monitor SAR responses in plants, I syringe-inoculated two leaves per plant with 10^6 cfu mL^{-1} of *Pst/AvrRpm1* or the corresponding 10 mM $MgCl_2$ mock solution. Three days later, two distal leaves were challenged with 10^5 cfu mL^{-1} of *Pst* by syringe infiltration. Resulting *in planta Pst* titers were evaluated 4 days later as described above.

In order to evaluate ETI-inducible plant responses at an earlier timepoint, I inoculated two fully expanded leaves with either 10^7 cfu mL^{-1} of *Pst/AvrRpm1*, or a corresponding 10 mM $MgCl_2$ mock solution. 24 hours (h) later, I harvested systemic leaves for the determination of gene expression data by qRT-PCR.

2.2.4 Petiole exudate assays

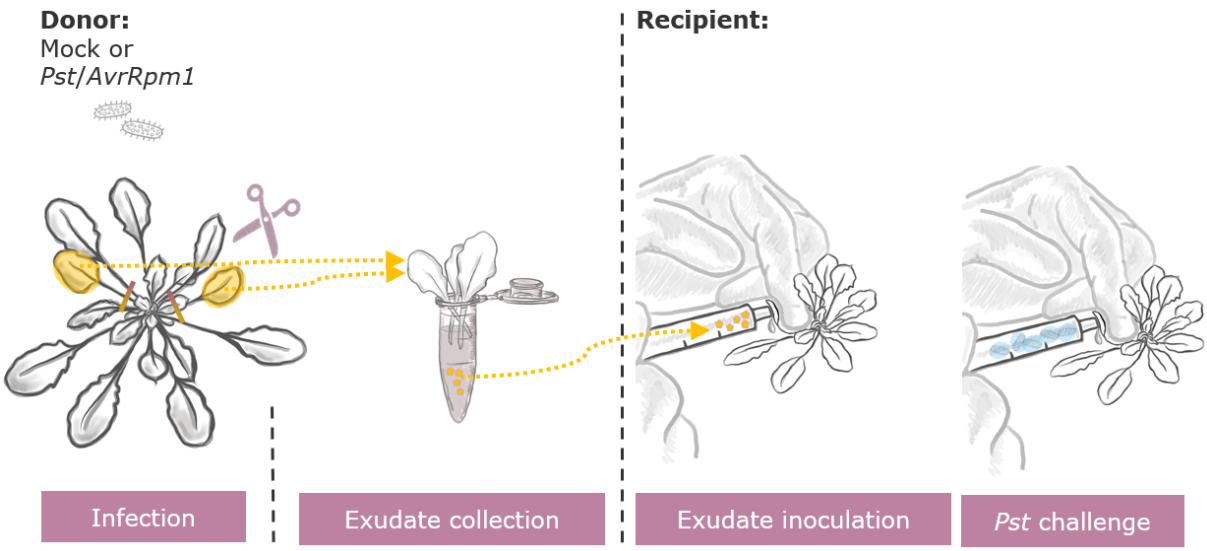

Figure 13: Infection of plants and collection of petiole exudates from infected leaves to determine SAR-inducing capacities.
Yellow marked leaves of donor plants were inoculated by syringe with a bacterial suspension or mock solution. These inoculated leaves were harvested one day later with their petioles cut with scissors at the middle of the rosette (yellow bars indicate the cut site at the lower base of a leaf petiole). Exudates were collected from these harvested leaves in tubes containing water. Prepared exudate solutions were infiltrated into leaves of recipient plants and challenged one day later. Figure contains modifications from Wenig et al., 2022.

Donor plants were inoculated in two fully expanded leaves with either 10^7 cfu mL^{-1} of *Pst/AvrRpm1,* or with a corresponding 10 mM $MgCl_2$ mock solution by syringe infiltration (**Figure 13**). Simultaneously, additional plants were kept untreated. 24 h later, systemic leaves were harvested for gene expression analysis by qRT-PCR. For petiole exudate (PetEx) isolation, the inoculated leaves (or leaves of untreated plants of the same developmental stage) were cut in the middle of the rosette (**Figure 13**). The petioles of six leaves per sample were immersed in 1 mM EDTA for 1 h. Subsequently, the EDTA solution was exchanged for 2 mL of sterilized

water, and PetExs were collected for 48 h in the dark. Afterwards, PetExs were filter-sterilized (Millipore, 0.22 µm), supplemented with $MgCl_2$ to a final concentration of 1 mM, and syringe-infiltrated into fully expanded leaves of naïve recipient plants (**Figure 13**). After 24 h, exudate-treated leaves were either analyzed for gene expression analysis by qRT-PCR or syringe-infiltrated with 10^5 cfu mL^{-1} of *Pst* (**Figure 13**). Resulting *in planta Pst* titers were determined at 4 dpi as described above.

2.2.5 Plant-to-plant (PTP) communication assays

PTP assays were performed as described (Wenig et al., 2019) in 5.5 L glass vacuum desiccators (Rotilabo-Glas-Exsikkatoren, Roth, Germany). 12 sender plants (in 4 pots) were spray-inoculated with either 10^8 cfu mL^{-1} *Pst/AvrRpm1* or with 10 mM $MgCl_2$ containing 0.01% (v:v) Tween-20 as the corresponding mock control. As an additional control, further sender plants were kept untreated. Subsequently, the sender plants were co-incubated with eight naïve receiver plants for 3 days (**Figure 14**A). Thereby, sender and receiver plants were alternately arranged without touching each other. At 24-hour intervals, the lids of the desiccators were lifted to allow air exchange and the release of excess humidity. After co-incubation, fully expanded leaves of the receiver plants were syringe-infiltrated with 10^5 cfu mL^{-1} of *Pst* (**Figure 14**B) and monitored for *in planta Pst* titers at 4 dpi as described above.

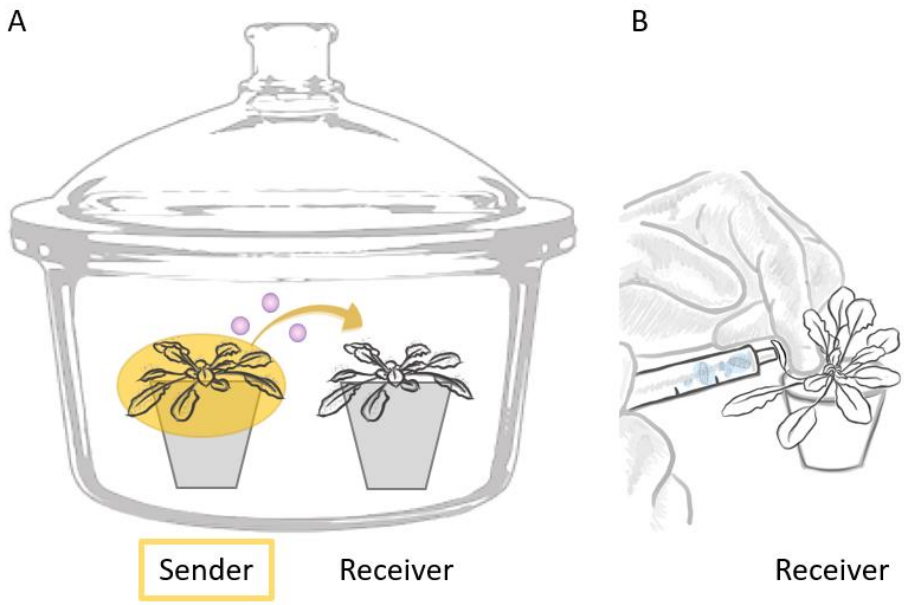

Figure 14: Plant-to-plant communication set-up using a closed desiccator system. (**A**) Spray-inoculated sender plants (encircled in yellow) were co-incubated with receiver plants that are exposed to the emissions (pink bubbles) of senders. (**B**) Two leaves of receiver plants were inoculated with *Pst*. Figure contains modifications from Wenig et al., 2022.

2.2.6 Chemical treatments with xylose

To determine systemic defense responses after a chemical induction with xylose, the first fully expanded leaves per plant were syringe-infiltrated with either a specific xylose (D-/L-Xylose, D-Xylose, or L-Xylose) dose as indicated, or a corresponding 10 mM $MgCl_2$ solution as the mock control. Three days later, from one part of the inoculated plants two systemic leaves per plant were harvested for metabolite extraction by LC-MS (> 20 leaves were pooled per sample). The remaining plants were additionally analyzed for the establishment of systemic resistance. To this end, two distal leaves per plant were challenge-inoculated with 10^5 cfu mL^{-1} of *Pst* by syringe infiltration and evaluated for *in planta* bacterial titers 4 days later as described above.

Moreover, in order to analyze the effect of xylose on bacterial growth rates, I grew 10^7 cfu mL^{-1} of *Pst* and of a GFP-tagged *Pst* strain (*Pst*-GFP) in NYGA liquid medium as quadruplets. This was performed in the wells of 96-well plates, which were supplemented with defined concentrations of D-/L-xylose ranging from 0.1 µM to 1 mM. During a 22 h incubation while shaking (306 rpm), the OD_{600} and/or GFP signal intensity (excitation: 488 ± 10 nm, detection: 508 ± 10 nm) of the bacterial suspensions was monitored every 20 seconds as a measure of bacterial density/growth.

2.2.7 RNA isolation and gene expression analysis by qRT-PCR

RNA was isolated with ice-cooled RNA extraction buffer from **Table 5** following the protocol for an isolation by Tri-Reagent (Sigma-Aldrich). RNA concentration was determined by measuring on the NanoDrop photometer, and cDNA generated on defined RNA amounts by using oligo(dT) (20-mer) and SuperScriptII reverse transcriptase. qRT-PCR was performed on a 7500 Fast real-time qRT-PCR system with the SensiMix SYBR low-ROX kit and with primers from (Breitenbach et al., 2014; Bauer et al., 2021; Sales et al., 2021) and listed in **Table 8**. Transcript accumulation was analyzed with the Real Quantification 7500 Fast System Software and normalized to that of the reference gene *UBIQUITIN*.

2.2.8 Metabolite analysis by Liquid-Chromatography coupled to Mass Spectrometry (LC-MS)

In order to identify metabolites accumulating in plants from either single leaves or whole above-ground plant rosettes, LC-MS analyses were performed with plant extracts in collaboration with Birgit Lange and Anton Schäffner (Helmholtz-Zentrum München (HMGU), Department of Environmental Science, Institute of

Biochemical Plant Pathology). Metabolites from pooled samples comprising a minimum of 12 individual plants (above-ground parts only) were analyzed 2 or 3 days after a treatment (as described above) by either spray or infiltration inoculation, respectively. A minimum of 150 mg fresh weight was extracted as described (Bauer et al., 2021) with some changes. Briefly, the plant tissues were freeze-dried overnight by lyophilization (-50 °C, 0.040 mbar). Next, the tissues were ground with pistil and mortar, and ~20 mg of the dried plant powder were extracted with 1.5 mL of 70% (v:v) ice-cooled methanol containing 333 pg of appropriate internal standards by shaking for 1 h (4 °C, 600 rpm) and centrifugation for 10 min (4 °C, 13,300 rpm). The incurring supernatant was concentrated by two successive steps: firstly, by evaporation for ~2.5 h and secondly, by lyophilization (-50 °C, 0.040 mbar) overnight. The remaining pellet was resuspended in 100 µL of 50% (v:v) acetonitrile and centrifuged for 5 min (14,000 rpm, 4 °C). Finally, 90 µL of this suspension were filtered in microwell plates (0.2 µm, polyvinylidene difluoride), and centrifuged for 10 min (900 rpm, 4 °C) before transfer of the total eluate into LC-MS vials. Simultaneously, metabolite standards were prepared in dilution series (to generate calibration curves) and extracted in the same manner as described above. A volume of 5-10 µL per sample was injected for LC-MS analysis and measured as duplicate. AzA, SA, SAG, and SGE were measured in negative ionization mode, whereas Pip, NHP, and NHP-O-β-glucoside (NHP-H2) were identified in positive ionization mode. Mass spectra were obtained for a range of 50-1300 *m/z*. AzA, SA, SAG, Pip, and NHP were identified using authentic standards. As recommended by Chen et al. (2018), Birgit Lange at HMGU furthermore confirmed NHP levels, which was done by following the protocol of Bauer et al. (2021). Thereby, LC-MS/MS fragmentation patterns of NHP and NHP-H2 were compared to that of synthesized NHP, whose synthesis was formerly described (Hartmann et al., 2018). AzA, SA, and SAG were quantified against an internal standard curve with ten calibration points (100 fg – 500 pg per µL, R = 0.995-0.999) and three internal standards (*p*-nitrophenol, camphorsulfonic acid, lidocaine) at 333 µg L^{-1}. The peak areas of Pip, NHP, NHP-H2, and SGE were quantified against lidocaine (Pip, NHP, NHP-H2) or camphorsulfonic acid (SGE) as internal standard and normalized using the total ion chromatogram during the gradient elution. The retention times and m/z values were: SA 10.0–10.2 min, 137.0250; SAG 8.0–8.5 min, 299.0750; SGE 9.2–9.5 min, 299.0750; AzA 10.4 to 11.4 min, 187.0975; Pip 1.5–1.7 min, 130.0860; NHP 1.4–1.7 min, 146.0817; NHP-H2: 3.3–3.7 min, 308.1346; internal standards:

p-nitrophenol 10.0–10.1 min, 138.0195; camphorsulfonic acid 9.0 min, 231.0695; lidocaine 8.4 min, 235.1805.

2.2.9 Metabolite analysis by Gas Chromatography coupled to Mass Spectrometry *(GC-TOF-MS)*

ETI-associated immune responses were triggered in transgenic plants according to the protocol of Breitenbach et al. (2014) with some minor changes. Briefly, Col-0 *pDEX:AvrRpm1-HA* and *eds1-2 pDEX:AvrRpm1-HA* plants were cultivated for about 5 weeks (3 plants per pot) before spraying the plants with 30 µM dexamethasone containing 0.01% (v:v) Tween-20. After 5 to 6 h of incubation under ambient light and the onset of clear wilting symptoms in plants, the above-ground tissues were harvested by cutting the plants underneath the rosette and freezing in liquid nitrogen. The plant tissues were either analyzed for the induction of *AvrRpm1*-induced transcripts by qRT-PCR or harvested as a pooled sample (> 12 plant rosettes) for further extraction. Next, the plant tissues were ground to a fine powder under liquid nitrogen using mortar and pestle before they were dried by lyophilization for 48 h (-50 °C, 0.040 mbar).

Furthermore, ETI-inducible metabolites were analyzed in wild type and *xyl4* mutant plants. For this purpose, plants were spray-inoculated with either a solution containing 10^8 cfu mL^{-1} of *Pst/AvrRpm1* or with 10 mM $MgCl_2$ each containing 0.01% (v:v) Tween-20 as the corresponding mock control. Two days later, whole above-ground rosettes were harvested, and >12 individual plants were pooled per sample. Subsequently, the plant material was ground to powder and dried as described above.

In the following, samples for ETI-associated and ETI-inducible metabolites were extracted for analysis by GC-TOF-MS. The extracted samples were analyzed by Martin Lehmann and Peter Geigenberger (Ludwig-Maximilians-Universität München (LMU), Department Biology I) in an untargeted approach to detect carbohydrates and other metabolites potentially associated with plant defense. The metabolite analyses were performed using a method that was described previously and slightly modified (Roessner et al., 2001; Lisec et al., 2006; Erban et al., 2007). In brief, 30 mg of the freeze-dried plant powder was extracted in 360 µL of methanol containing 138 µg mL^{-1} of internal standards (ribitol, ^{13}C sorbitol) while shaking for 15 min (950 rpm, 70 °C). After cooling down the sample to room temperature (RT), 200 µL of chloroform and subsequently 400 µL of distilled water was added, followed by vigorous mixing and centrifugation for 15 min (14,000

rpm, 4 °C). An aliquot (50 µL) of the upper, polar phase was transferred into a GC-MS vial (Chromatographie Zubehoer Trott) and dried by evaporation for ~3 h at RT (SpeedVac). The dried samples were further processed by Martin Lehmann (LMU): The pellet was resuspended in 20 µL of methoxyaminhydrochloride (20 mg mL^{-1} in pyridine) and derivatized for 90 min at 37 °C. After the addition of 40 µL of BSTFA (N, O-Bis[trimethylsilyl]-trifluoroacetamide) containing 10 µL retention time standard mixture of linear alkanes (n-decane, n-dodecane, n-pentadecane, n-nonadecane, n-docosane, n-octacosane, n-dotriacontane), the mix was incubated at 37 °C for additional 45 min. One µL of each sample was analyzed using a GC-TOF-MS system. To this end, the metabolites were separated on a 30 m VF-5ms column with a 10 m EZ-Guard column using an GC and an autosampler system. Helium was the carrier gas at a constant flow rate of 1 mL/min. The injection temperature of the split/split-less injector was set to 250 °C. Transfer line and ion source were constant at 250 °C. The initial oven temperature of 70 °C was increased to a final temperature of 320 °C by a rate of 9 °C per minute. The transfer line was set to 250 °C as well as the ion source where the metabolites got ionized and fractionated by an ion pulse of 70 eV. Mass spectra were recorded at 20 scans per second with an m/z 35-800 scanning range. Chromatograms and mass spectra were subsequently evaluated and edited by Martin Lehmann (LMU) using ChromaTOF and TagFinder software (Luedemann et al., 2008).

2.2.10 Comprehensive Microarray Polymer Profiling (CoMPP) for carbohydrates

In order to determine the composition of cell wall polymers in ETI-induced plants, we probed extracted cell wall material with carbohydrate-specific microarrays to generate polymer profiles for single genotypes as indicated. These analyses were performed by Jeanette Hansen and Bodil Jørgensen (University of Copenhagen (UCPH), Section for Plant Glycobiology). For the activation of an ETI response/infection and sampling/harvest/drying of plant material, I followed the same protocol as described for the GC-MS analysis above.

In the following, the dried plant tissues were extracted for alcohol-insoluble residues (AIR, cell wall) for CoMPP as described (Fangel et al., 2021) with some minor changes. AIR was prepared by homogenization in 70% ethanol (EtOH) (v:v) (1.5 mL per 50-100 mg tissue) via vortex and centrifugation for 10 min (max. speed, 4 °C) to discard EtOH. The incurring pellet was dissolved in 3.0 mL of ice-cooled (v:v) methanol:chloroform and subsequently centrifuged for 10 min (max.

speed, 4 °C). In the end, the pellet was washed twice with 100% (v:v) acetone before drying by air overnight.

CoMPP was performed by Jeanette Hansen (UCPH) on extracted AIR (fraction for 1,2-Cyclohexylenedinitrilo- tetraacetic acid (CDTA), sodium hydroxide (NaOH)) with a few modifications (Moller et al., 2007). All samples were printed onto nitrocellulose membranes (pore size 0.45 mm, Whatman) using a microarray instrument. The dried arrays were probed with antibodies and carbohydrate binding modules (CBM) as listed in **Table S16**. All antibodies were supplied by PlantProbes, except BS-400-2 and BS-400-3, which were ordered from BioSupplies (Australia), and INRA-RU1 and INRA-RU2 taken from another study as described (Ralet et al., 2010).

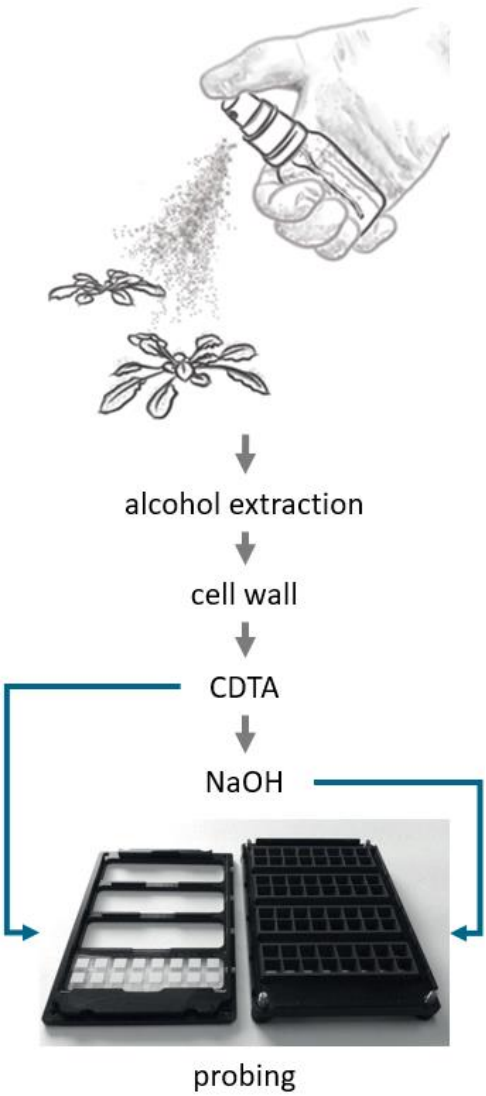

Figure 15: Schematic workflow for the sample preparation for the CoMPP analysis.
Plants were spray-inoculated with either a *Pst* suspension, a mock solution or a dexamethasone solution. Remaining cell wall material of alcohol-extracted plants was dried by before successive fractionation with CDTA and NaOH. The incurring fractions were analyzed on carbohydrate microarrays and probed with suitable antibodies and carbohydrate binding modules. Figure contains modifications from Pedersen et al., 2012, and Wenig et al., 2022.

2.2.11 Determination of electrical conductivity

Following a described protocol (Kasten et al., 2016) with some changes, I determined electrolyte leakage from inoculated and untreated leaves. Ten first true

leaves or six fully expanded leaves were incubated in 30 mL of bi-distilled water. The initial electrical background conductivity (BC) [µS cm^{-2}] was measured with an electrolytic conductivity meter 10 min after leaves were transferred into the water. In the following, the electrical conductivity was consecutively measured after 24 h of rotation (28 rpm, room temperature (RT)) for sample ion leakage (SC), and after transfer to -20 °C overnight and reheating to RT for absolute ion leakage (TC). SC and TC were corrected to BC (SC_c = SC-BC; TC_c = TC-BC) and the relative electrical conductance expressed as a ratio: rel. EC [%] = SC_c /TC_c. This value was used as a measure for a (stress-inducible) regulation of ion leakage for a specific genotype and treatment.

2.2.12 Systemic response regulated by MeJA

To analyze defense responses against *Pst* upon a treatment with MeJA, plants were treated as described previously (Sales et al., 2021). In brief, 5-week-old Col-0 and *xyl4-1* plants were syringe-infiltrated in two leaves with a solution containing either 100 µM MeJA or a control solution (supplemented with 10 mM $MgCl_2$ and 0.025% (v:v) MeOH). Three days later, two systemic leaves were challenged with 10^5 cfu mL^{-1} of *Pst*, and evaluated for bacterial titers 4 days after.

2.2.13 Root growth assays

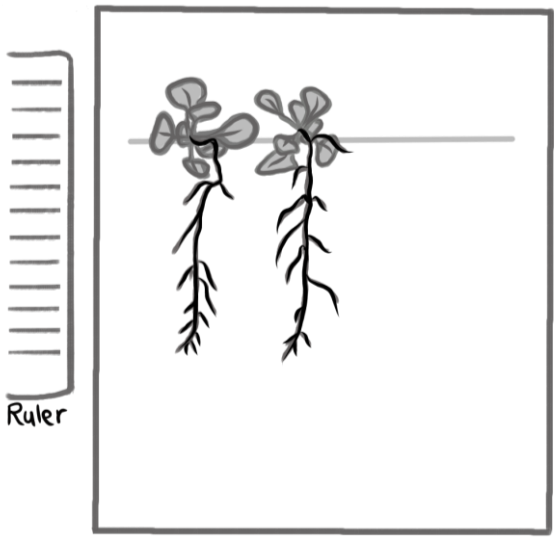

Figure 16: Simplified layout to determine the root length of seedlings growing on a treatment plate.
Seedlings were placed at the same height (indicated with the grey line) on the medium of a treatment plate. Pictures of the plants that had been growing in the plate, were taken with a ruler positioned next to the plate. To this end, I was able to calculate the length of the main roots in a (centi)metric scale.

To measure root growth inhibition, I evaluated root lengths of treated seedling plants. For that case, Jennifer Sales provided help with experiments as described previously (Sales et al., 2021). To this end, seeds of Col-0 and *xyl4-1* plants were sterilized in 75% followed by 100% (v:v) EtOH, dried, and germinated on MS medium containing 0.1% cefotaxim and 0.25% carbenicillin. Six days later, seedlings were transferred to treatment MS plates supplemented with either 100

mM or 300 mM NaCl, or 40 µM MeJA, or with a mock solution. These plates were placed in the growth chamber in a slanted, upright position under long day conditions. The seedlings were photographed 6 and 12 days post transfer from the bottom side of the plates (together with a ruler to size plants, **Figure 16**). I subsequently measured root lengths by using GIMP software. Furthermore, seedlings were harvested after photographing at day 12, pooled per genotype and treatment, and flash frozen in N2 for analysis of RNA.

2.2.14 Statistics

All data presented were evaluated using the statistic software GraphPad Prism. Outliers were excluded according to the result of the Grubb's outlier test with $\alpha=0.05$. Normal distribution was attained after $\log_2$ transformation of the data for qRT-PCR and bacterial titers. Using the Shapiro-Wilk test with $\alpha = 0.01$, the normal distribution of all data sets was verified. Finally, data displaying normal distribution were analyzed by one-way ANOVA analysis with Tukey's multiple testing correction as indicated in the figure legends. Additionally, two-way ANOVA analysis with both Bonferroni correction for multiple testing and False Discovery Rate (FDR) with two-stage linear step-up procedure of Benjamini, Krieger, and Yekutiel was performed for analyzing GC-MS data. Consideration for significant differences was determined for $\alpha = 0.05$.

3. Results

3.1 *XYL4* promotes ETI

XYL4 protein accumulation in the *A. thaliana* apoplast was previously associated with SAR (Breitenbach et al. (2014). Here, I set out to investigate the role of *XYL4* in innate defense responses of plants in more detail.

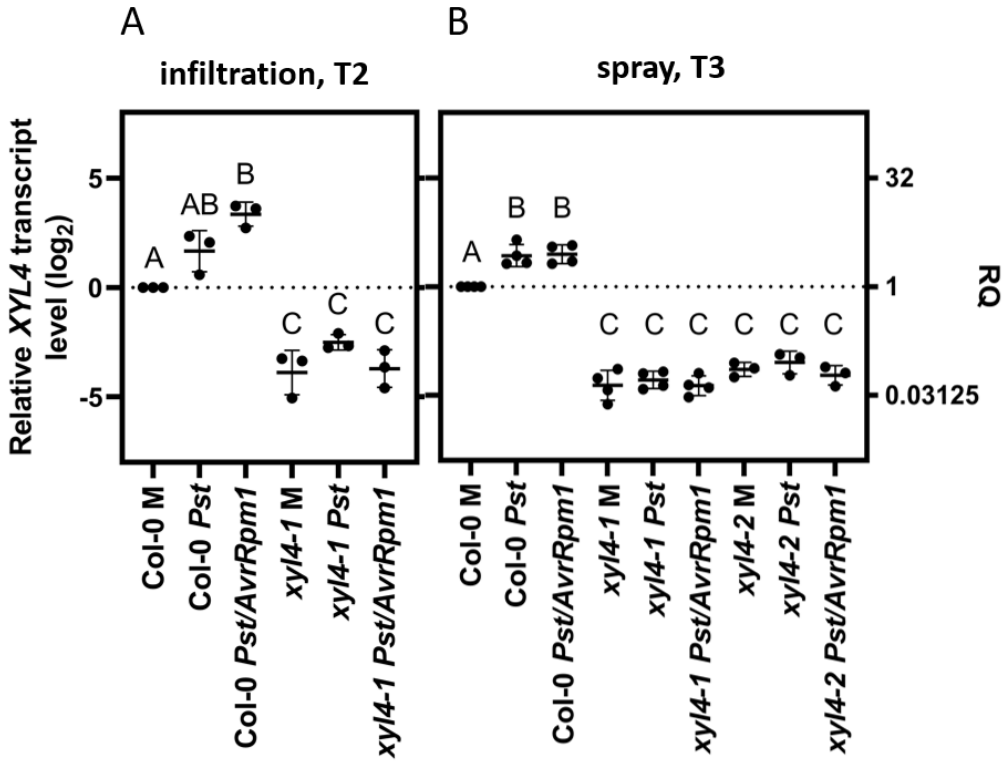

Figure 17: Infection of *A. thaliana* with *Pst/AvrRpm1* induces a local accumulation of *BETA-D-XYLOSIDASE 4* (*XYL4*) transcripts.
Col-0 and *xyl4* plants were inoculated by syringe infiltration with 10^5 cfu/mL of *Pst* or *Pst/AvrRpm1* or by spray treatment with 10^8 cfu/mL of *Pst* or *Pst/AvrRpm1.* The *XYL4* transcript abundance in the inoculated leaves was determined 2 (T2) or 3 days (T3) later by qRT-PCR. Transcript accumulation was normalized to that of *UBIQUITIN* and is shown relative to the normalized transcript levels in the appropriate Col-0 mock (M) controls. Black dots represent biologically independent data points and horizontal lines represent mean values ± SD from three to four biologically independent replicate experiments. The letters above the scatter dot plots indicate statistically significant differences (one-Way ANOVA and Tukey test, P=<0.05, for (*XYL4*: infiltration T2): n=3, F(5, 12)=52.31; for (*XYL4*: spray T3): n=3-4, F(8, 24)=125.8).

First, I monitored the transcript accumulation of *XYL4* in Col-0 wild type plants after inoculation with *Pst* and *Pst/AvrRpm1.* For this reason, I syringe-infiltrated or spray-inoculated plants with either *Pst*, *Pst/AvrRpm1*, or a corresponding mock solution. Transcript abundance was determined at either two or three days post inoculation (dpi) depending on the method of inoculation. Two days after

infiltration, inoculation of the leaves of Col-0 plants with *Pst*/*AvrRpm1*, *XYL4* transcript levels were elevated as compared to mock-treated plants (**Figure 17**A). A treatment with *Pst*, however, caused no significant change in *XYL4* transcript accumulation (**Figure 17**A). The data thus suggest that AvrRpm1 effector-associated responses promote *XYL4* transcript accumulation in wild type plants, whereas infection with virulent *Pst* has no significant effect. By contrast, *XYL4* transcript accumulation was moderately induced in leaves of spray-inoculated Col-0 plants in response to both *Pst* and *Pst/AvrRpm1* (**Figure 17**B). These findings suggest that *Pst*/*AvrRpm1*-infiltrated plants respond with a stronger induction of *XYL4* transcripts than after spray inoculation (**Figure 17**A-B).

In the following, I employed two independent T-DNA insertion lines of *xyl4*, which I refer to as *xyl4-1* and *xyl4-2*, and inoculated these alongside Col-0 plants by spray or infiltration inoculation with either *Pst*, *Pst/AvrRpm1*, or a corresponding mock solution. *XYL4* transcript levels were reduced in both of the *xyl4* lines as compared to Col-0, and did not respond to either of the treatments applied (**Figure 17**A-B).

Subsequently, I investigated whether immune responses towards a bacterial infection with *Pst* or *Pst*/*AvrRpm1* depended on *XYL4*. To this end, I monitored the *in planta* bacterial titers after infiltration inoculation of Col-0 and *xyl4* plants at the day of infection and at 2 and 4 dpi. I detected an increase in bacterial densities over time for both bacterial strains in each of the three plant genotypes (**Figure 18**A-B). The rise in titers of both strains was comparable in wild type and *xyl4* mutant plants, suggesting that after syringe-inoculation, basal immunity against *Pst* and *Pst*/*AvrRpm1* was not regulated in a *XYL4*-dependent manner (**Figure 18**A-B). This was further supported by the fact that differences were not detectable in the infection-associated regulation of known defense-related genes, including *PR1*, *PDF1.2*, *VSP2*, *and LLP1* (**Figure 19**A-D).

However, spray inoculation of Col-0 and the two *xyl4* mutants with *Pst* or *Pst/AvrRpm1* did reveal differences in bacterial growth when I compared titers at 1, 2, and 4 dpi. In contrast to *Pst*, which grew to similar titers in all genotypes (**Figure 18**D), *Pst/AvrRpm1* grew to significantly higher titers at 2 and 4 dpi in both *xyl4* mutants as compared to Col-0 plants (**Figure 18**C).

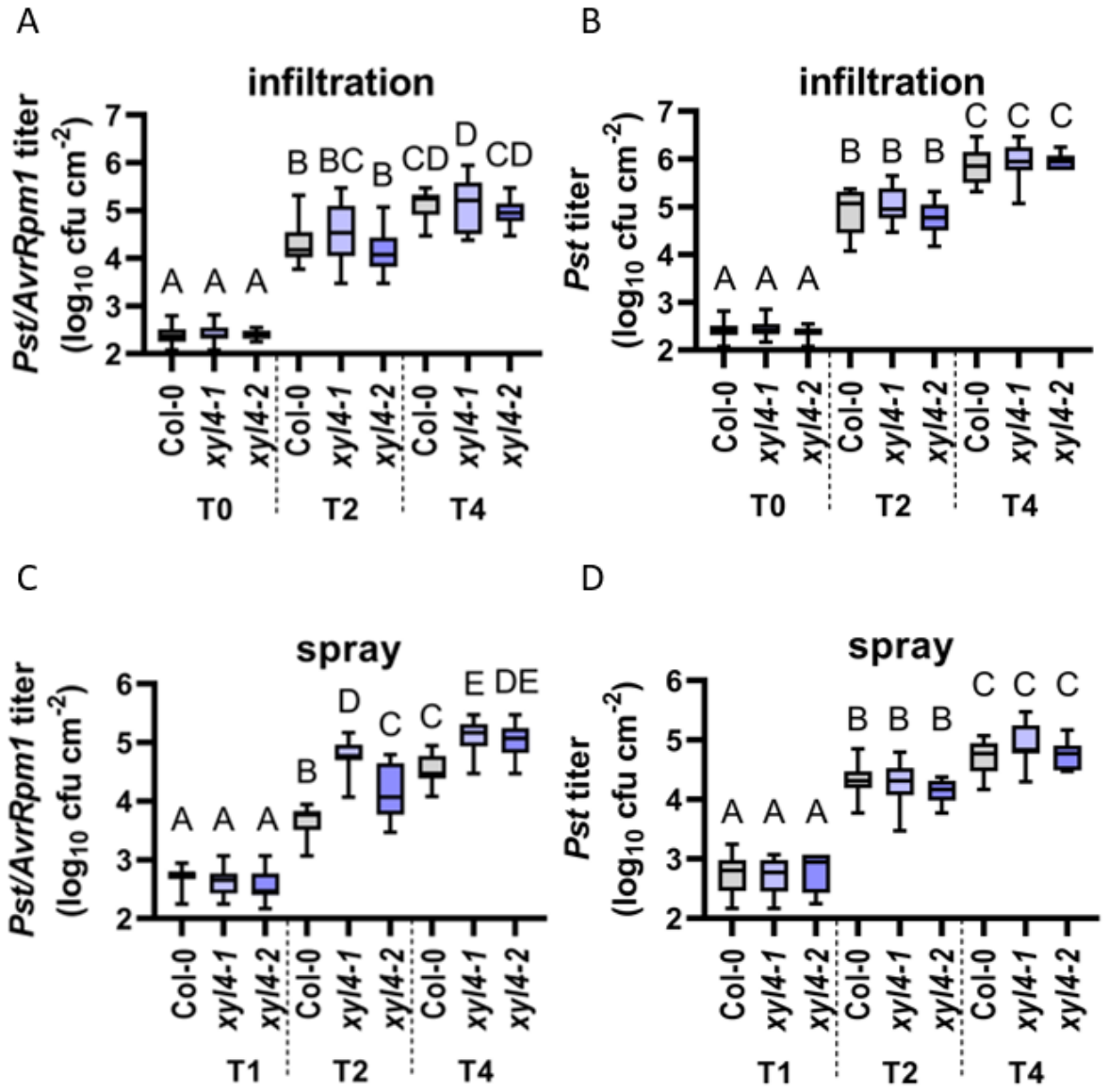

Figure 18: *XYL4* promotes local ETI responses against the (hemi-)biotrophic bacterium *Pst/AvrRpm1* in *A. thaliana*.
Col-0 plants and two independent T-DNA insertion lines of *xyl4* (*xyl4-1* and *xyl4-2*) were inoculated by syringe infiltration with 10^5 cfu/mL of *Pst/AvrRpm1* (**A**) or *Pst* (**B**) or by spray treatment with 10^8 cfu/mL of *Pst/AvrRpm1* (**C**) or *Pst* (**D**). Resulting *in planta* titers of *Pst* and *Pst/AvrRpm1* were determined at the timepoints indicated below the panels at T0: 2 hours post inoculation, T1: one day post inoculation (dpi), T2: 2 dpi, and T4: 4 dpi. Box plots represent average titers from four to seven biologically independent experiments, including at least three replicates each ± min and max values. Different letters above the box plots indicate statistically significant differences for single means (For details of the one-Way ANOVAs and Tukey tests for P=<0.05, see **Table S17**)

Transcript accumulation of *PR1*, *PDF1.2*, *VSP2* and *LLP1* at 3 days post spray inoculation of Col-0 and *xyl4-1* plants treated with *Pst/AvrRpm1* appeared to be regulated in a pathogen-related but *XYL4*-independent manner (**Figure 19**A-D). This leads to the assumption that those defense-related genes might act upstream of *XYL4* or in parallel to it during plant defense.

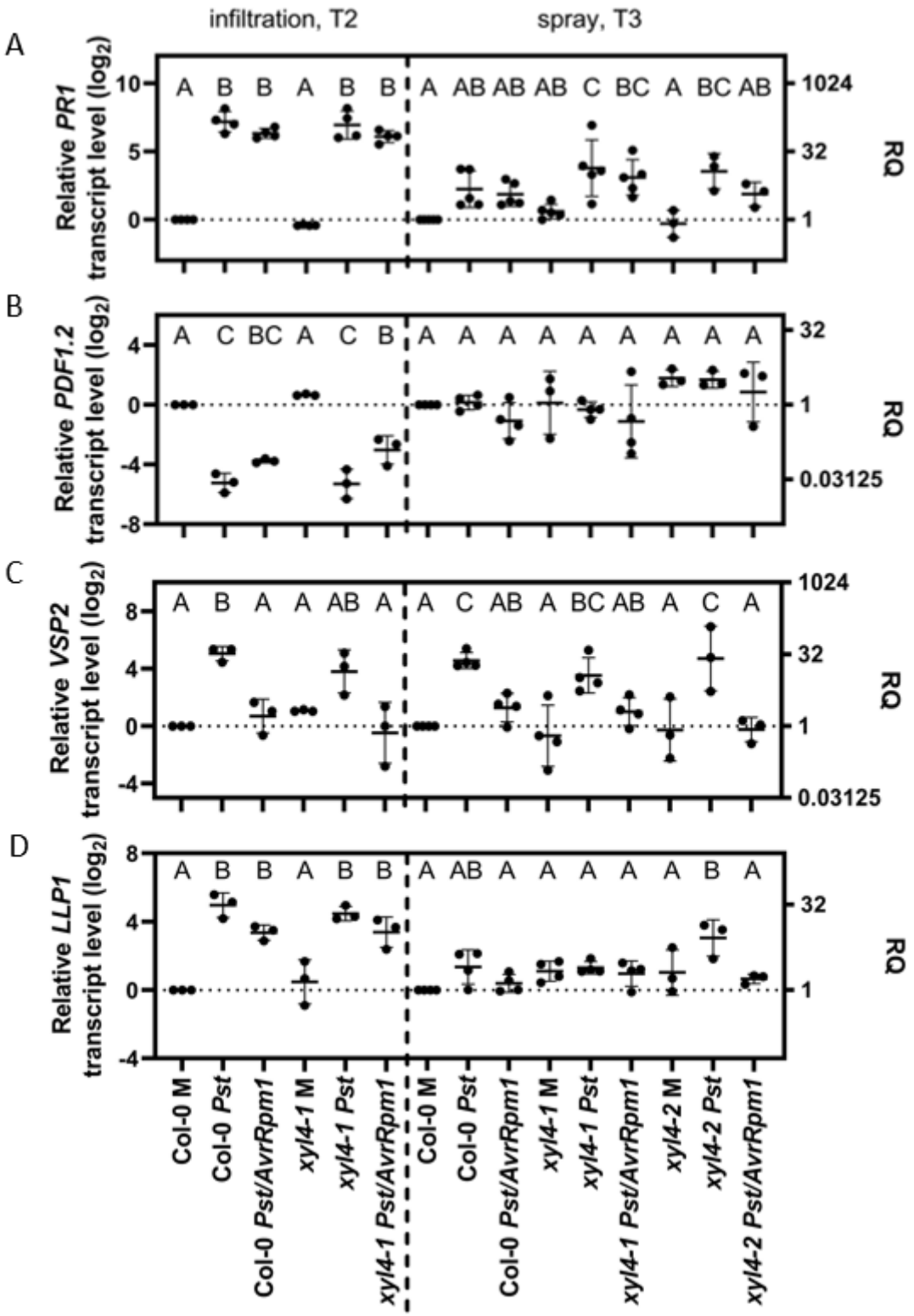

Figure 19: Transcript accumulation of defense-associated genes in response to *Pst* and *Pst/AvrRpm1* is comparable in Col-0 and in *xyl4* mutant plants.
Col-0 and *xyl4-1* plants were inoculated by syringe infiltration with 10^5 cfu/mL of *Pst* or *Pst/AvrRpm1* or by spray treatment with 10^8 cfu/mL of *Pst* or *Pst/AvrRpm1.* Transcript abundance of *PATHOGENESIS-RELATED PROTEIN 1* (*PR1*; **A**), *PLANT DEFENSIN 1.2* (*PDF1.2*; **B**), *VEGETATIVE STORAGE PROTEIN 2* (*VSP2*; **C**), and *LEGUME LECTIN-LIKE PROTEIN 1* (*LLP1*; **D**) in inoculated leaves was determined at 2 (T2) or 3 days (T3) later by qRT-PCR. Transcript accumulation was normalized to that of *UBIQUITIN* and is shown

relative to the normalized transcript levels in the appropriate Col-0 mock (M) controls. Black dots represent biologically independent data points and horizontal lines represent mean values ± SD from three to five biologically independent replicates. The letters above the scatter dot plots indicate statistically significant differences (one-Way ANOVA and Tukey test, P=<0.05, for (*PR1*: infiltration T2): n=4, F(5, 18)=155.3; for (*PR1*: spray T3): n=3-5, F(8, 30)=6.589; for (*PDF1.2*: infiltration T2): n=3, F(5,12)=51.28; for (*PDF1.2*: spray T3): n=3-4, F(8, 23)=2.054; for (*VSP2*: infiltration T2): n=3, F(5, 12)=10.54; for (*VSP2*: spray T3): n3-4, F(8, 24)=8.678; for (*LLP1*: infiltration T2): n=3, F(5, 12)=22.96; for (*LLP1*: spray T3): n=3-4, F(8, 24)=4.504).

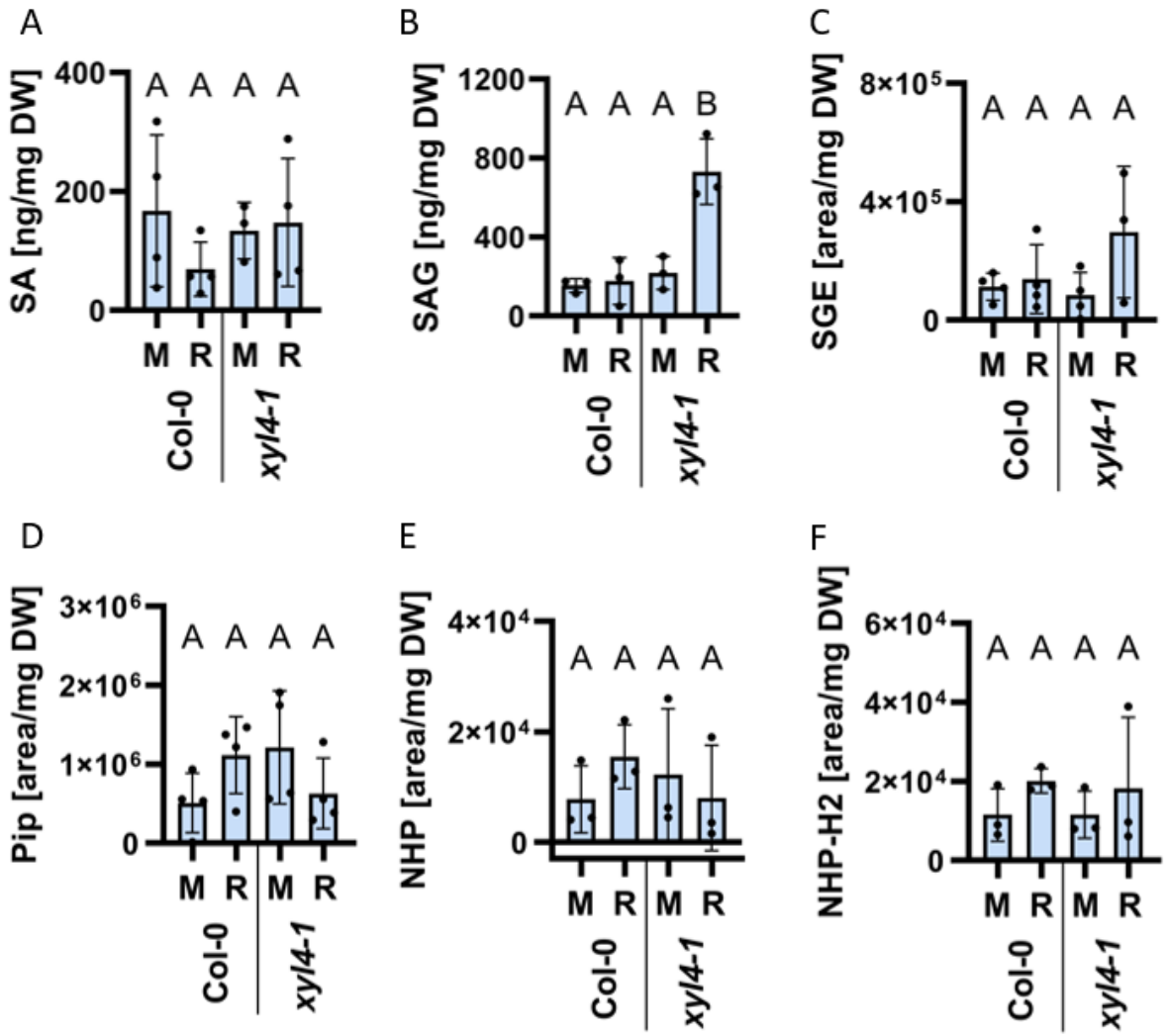

Figure 20: *XYL4* represses an ETI-inducible glucosylation of SA forming SAG.

Col-0 plants and *xyl4-1* mutants were inoculated by spray treatment with 10^8 cfu/mL of *Pst/AvrRpm1* (R) or a mock (M) solution. 48 h later, whole above-ground rosettes were harvested and pooled for a metabolite analysis by LC-MS. The accumulation of SA (A), SAG (B), SGE (C), Pip (D), NHP (E), and NHP-H2 (F) was calibrated to a set of three internal standards and normalized to the individual dry weight. Bars represent average metabolite abundance of 3-4 biologically independent replicates ± SD. Different letters above bars indicate statistically significant differences for means (one-way ANOVA and Tukey test for P=<0.05, for (A): n=3-4, F(3, 14)=15.11; for (B): n=3, F(3, 8)=5.12; for (C): n=3-4, F(3, 15)=13.55; for (D): n=4, F(4, 16)=12.06; for (E): n=3, F(3, 8)=14.01; for (F): n=3, F(3, 8)=15.44).

In addition, *XYL4* obviously has no effect on cellular ion leakage in the inoculated and/or systemic tissues as leaves of *xyl4-1* and *xyl4-2* comparably released ions (detectable by electrical conductivity) as Col-0 after infiltration (**Figure S35**A/B) or spray inoculation (**Figure S35**C/D). This indicates that *XYL4* is not directly regulating cellular ion permeability or related processes like the induction of cell death.

Moreover, we determined the levels of spray inoculation-inducible metabolites SA and Pip (and their derivatives SAG, SGE, NHP, NHP-H2) in Col-0 and *xyl4-1* plants 2 days after inoculation with *Pst*/*AvrRpm1* in collaboration with Birgit Lange (HMGU). SAG accumulated to higher levels in infected *xyl4-1* mutants as compared to wild type plants, while the other metabolites were comparable in both genotypes (**Figure 20**A-F). Taken together, the data suggest that *XYL4* potentially promotes immune responses towards *Pst*/*AvrRpm1* by preventing the conversion of SA to SAG, and thus might stimulate SA-mediated defense and ETI after spray inoculation.

3.2 *XYL4* is essential for SAR

Since local ETI appears to be associated with *XYL4*, I considered if *XYL4* might also modulate responses to a secondary bacterial challenge in distal tissues. In order to test this, I monitored systemic immunity to *Pst* in wild type and *xyl4* mutant plants after a local stimulus. To this end, I inoculated the first two true leaves of Col-0, *xyl4-1*, *xyl4-2* with either a SAR stimulus (here: *Pst*/*AvrRpm1*) or a corresponding mock solution. I further included *eds1-2* and *llp1-1* mutant plants with a known SAR-defective phenotype as control (Breitenbach et al., 2014; Wittek et al., 2014). Three days after the primary stimulus, distal leaves were challenged with virulent *Pst* and monitored for *in planta* bacterial titers 4 days later. The results showed that SAR-induced Col-0 displayed reduced *Pst* titers as compared to mock-treated plants (**Figure 21**A), indicating an activated resistance against the bacterial challenge. In contrast, all mutant genotypes supported similar bacterial densities in both *Pst/AvrRpm1*-stimulated and control-treated plants (**Figure 21**A), indicating that SAR had been abolished in these plants. Consequently, as previously shown for *LLP1* and *EDS1*, the data strongly suggest that *XYL4* is essential for SAR.

I then went on to examine the transcript abundance of stress-associated genes in systemic leaves of Col-0, *xyl4-1*, and *eds1-2* plants 3 days after a local SAR stimulus or a mock treatment. Transcript accumulation of *XYL4*, *PDF1.2*, *VSP2* and

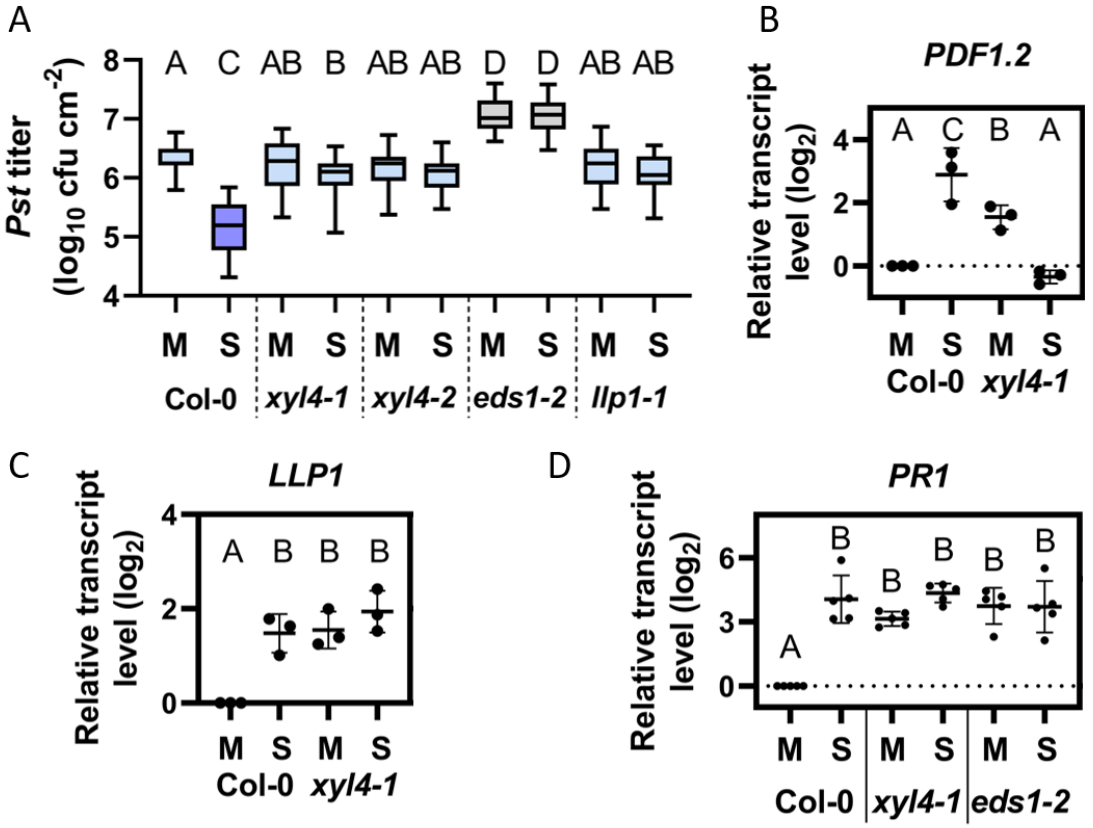

Figure 21: *XYL4* promotes Systemic Acquired Resistance (SAR).
Plants of the genotypes Col-0, *xyl4-1*, *xyl4-2*, *eds1*-2, and *llp1-1* (as indicated below the panels) were syringe-infiltrated in the first two true leaves with either 10^6 (for **A**/**D**) or 10^7 (for **B**/**C**) cfu per mL of *Pst/AvrRpm*1 (S), or a corresponding mock (M) control solution. Distal uninfected leaves were examined for the transcript abundance of *PDF1.2* (B, at 1 dpi), *LLP1* (**C**, at 1 dpi), or *PR1* (**D**, at 3 dpi). Alternatively, plants were challenged at 3 dpi with 10^5 cfu/mL of *Pst* to evaluate SAR. (**A**) *In planta Pst* titers in systemic, challenge-inoculated leaves were measured at 4 dpi. Box plots represent average *Pst* titers from nine biologically independent experiments, including at least 3 replicates each ± min and max values. Letters above the box plots indicate statistically significant differences for means (one-way ANOVA and Tukey test for P=<0.05, F(28, 403)=21.02, Col-0 M n=33, Col-0 S n=37, *xyl4-1* M n=40, *xyl4-1* S n=42, *xyl4-2* M n=21, *xyl4-2* S n=22, *eds1-2* M n=31, *eds1-2* S n=33, *llp1-1* M n=25, *llp1-1* S n=25). (**B**-**D**) Transcript abundance of the genes was measured by qRT-PCR, normalized to that of *UBIQUITIN*, and is shown relative to the normalized transcript levels in the appropriate Col-0 mock (M) controls. Black dots represent three to seven biologically independent data points, and lines indicate the respective mean values ± SD. The letters above the scatter dot plots indicate statistically significant differences (one-Way ANOVA and Tukey test, P=<0.05, for (B): n=3, F(3, 8)=16.74; for (C): n=3, F(3, 8)=29.80; for (D): n=5, F(5, 24)=20.68.

LLP1 was not changed in the systemic tissues of SAR-induced Col-0 or *eds1-2* (**Figure S36**A-D). However, transcript levels of *PR1* were promoted systemically in Col-0 after SAR induction. Here, *xyl4-1* and *eds1-2* displayed elevated *PR1* transcript accumulation after both mock and SAR treatment (**Figure 21**D). This data might indicate that *XYL4* and/or *EDS1* repress the SA signaling component *PR1* or associated pathways. We therefore further determined by LC-MS and

together with Birgit Lange if responses associated with SA, SAG, and AzA – which is supposedly an indirect inducer of SA and *PR1* (Nagy et al., 2017) – might be regulated via *XYL4* after a challenge with *Pst*. Elevated SA in SAR-stimulated plants then could be an indicator for priming in plants (Balmer et al., 2015). However, the levels of SAG and AzA were comparable after a challenge with *Pst* for both plant genotypes and pre-treatments investigated (

Figure S37B-C). Notably, the SAR-stimulated Col-0 and *xyl4-1* plants showed a tendency of only slightly induced SA when compared to mock treated-samples (

Figure S37A), suggesting that these plants showed no strong SA priming at the analyzed timepoint.

To investigate plant responses upon pathogenic infection at earlier timepoints, I further determined the transcript accumulation of defense-related genes in systemic tissues 1 day after a local SAR stimulus or mock treatment. Notably, *XYL4* transcripts were comparable for both treatments in Col-0 (**Figure 22**B), suggesting that *XYL4* gene expression systemically is neither affected at 1 nor at 3 dpi. Notably, transcript levels of *PR1* were moderately elevated after a SAR-stimulus in systemic tissues of Col-0 with a similar intensity to that detected in *xyl4-1* plants after any treatment (**Figure 22**A). Transcripts of the SAR-associated genes *ALD1* (Jong et al., 2004; Song et al., 2004; Cecchini et al., 2015a) and *FMO1* appeared to be regulated in a similar manner as *PR1* (insignificant trends in **Figure 22**A/D-E). Thus, it can be assumed that these three genes are co-expressed systemically. Interestingly, the SAR-related *UGT76B1* (von Saint Paul et al., 2011) was slightly repressed in mock-treated *xyl4-1* plants when compared to Col-0 plants (**Figure *22***F). *XYL4* thus might be involved in the regulation of (wounding) signals related to an inoculation treatment by syringe that represses *PR1*, *ALD1*, *FMO1*, and simultaneously promotes *UGT76B1* (**Figure 22**A/D-F).

In addition, SAR-stimulated *xyl4* mutants expressed lower levels of *LLP3* (**Figure 22**C), which is homologues to *LLP1* and involved in the establishment of SAR (Wenig et al., 2019; Sales et al., 2021). *XYL4* thus might promote early defense responses involving the regulation of *LLP3*. In addition, the expression of *LLP1* was induced in Col-0 after the bacterial infection, and moreover induced in *xyl4-1* after both treatments (**Figure 21**C). These findings suggest that expression of *PR1* and *LLP1* might be similarly regulated in a *Pst/AvrRpm1*-dependent and *XYL4*-modulated manner, whereby the induction of *LLP1* at 1 dpi seems to precede that of *PR1* at 3 dpi (**Figure 21**D). As shown previously, an establishment of SAR

involves an early systemic induction of the JA pathway (Truman et al., 2007). Interestingly, transcript accumulation of the JA marker gene *PDF1.2* was induced systemically during SAR in Col-0 plants one day after the SAR stimulus, whereas such response was absent in *xyl4-1* (**Figure 21**B). This suggests an early systemic induction of JA responses during SAR in dependence of *XYL4* (and potentially *LLP3*).

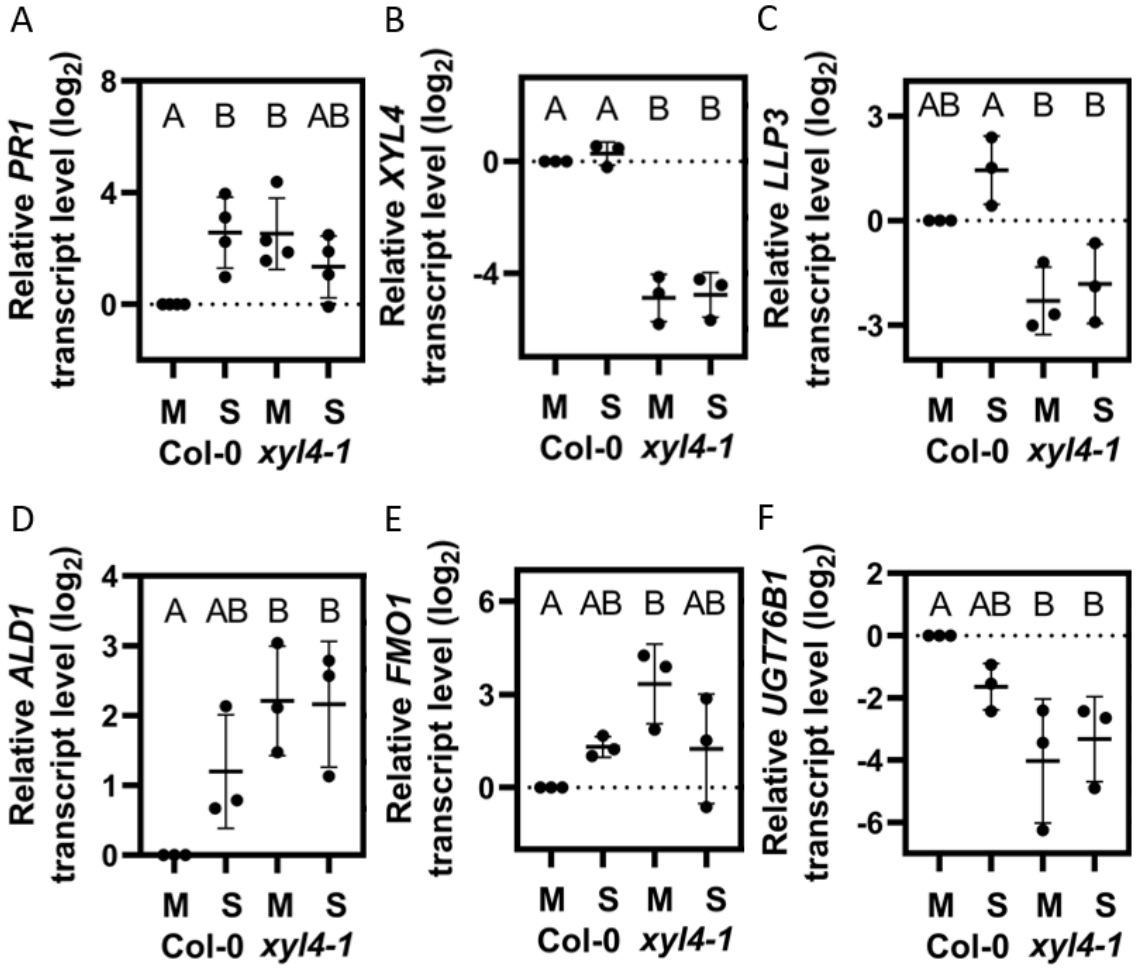

Figure 22: Early expression of diverse defense-associated genes systemically is related to *XYL4*.
(A-F) Col-0 and *xyl4-1* plants were inoculated with either a mock (M) solution or 10^7 cfu/mL of *Pst/AvrRpm1* (S). 24 h later, systemic leaves were harvested to analyze gene transcript levels of *PR1* (**A**), *XYL4* (**B**), *LLP3* (**C**), *ALD1* (**D**), *FMO1* (**E**), and *UGT76B1* (**F**) by RT-qPCR. Transcript accumulation was normalized to that of *UBIQUITIN* and is shown relative to the normalized transcript levels in the appropriate WT mock controls. Black dots and the respective mean values (black line) ± SD represent three to four biologically independent replicates. The letters above the scatter dot plots indicate statistically significant differences (one-Way ANOVA and Tukey test, P=<0.05, for (A): n=4, F(3, 12)=5.285; for (B): n=3, F(3, 8)=1.296; for (C): n=3, F(3, 8)=11.12; for (D): n=3, F(3, 8)=6.196; for (E): n=3, F(3, 8)=4.678; for (F): n=3, F(3, 8)=6.100).

3.3 Systemic defense regulated by *XYL4* is not affected by a treatment with MeJA

Previously it was shown that solutions, which were supplemented with either JA or the volatile MeJA, a JA-derivative, were not as effectively promoting SAR in plants as petiole exudates collected from SAR-stimulated plants (Chaturvedi et al., 2008). This indicates that JA or MeJA alone do not promote systemic defense. Interestingly, an exogenous treatment with a solution containing MeJA induces systemic resistance against *Pst* in *llp1-1* plants, whereas such response was not detectable in wild type plants or another lectin-like mutant that is deficient in *LLP3* (Sales et al., 2021). It is thus suggested that JA might play a distinct role in the establishment of *LLP1*-associated SAR. Interestingly, both *LLP1* and *LLP3* were formerly associated with SAR signaling events, whereby *LLP3* is specifically suggested to act in local tissues affecting SAR signal generation (Wenig et al., 2019; Sales et al., 2021). Notably, mutants defective in *LLP3* are associated with biotic stress regulation involving JA-pathways (Sales et al., 2021), suggesting that local ETI responses promote SAR signaling via triggers of JA. I further ask if such regulation might be additionally modified by *XYL4*.

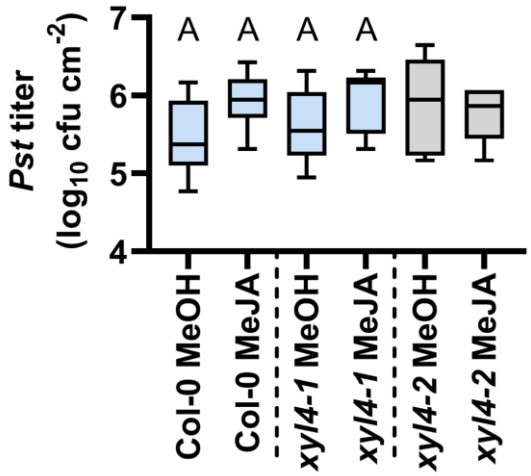

Figure 23: MeJA has no effect on plant defense against *Pst.*

Col-0 and *xyl4* mutants (*xyl4-1*, *xyl4-2*) were infiltrated with a solution containing either 100 µM MeJA or a corresponding mock (MeOH). Subsequently, systemic leaves were challenged with *Pst* at 3 dpi. *In planta Pst* titers in systemic, challenge-inoculated leaves were measured at 4 dpi. Box plots represent average *Pst* titers from two (*xyl4-2*) to four (Col-0, *xyl4-1*) biologically independent experiments, including at least 3 replicates each ± min and max values. Letters above the box plots indicate statistically significant differences for means (one-way ANOVA and Tukey test for $P=<0.05$, $F(5, 57)=2.399$, Col-0 MeOH n=12, Col-0 MeJA n=13, *xyl4-1* MeOH n=14, *xyl4-1* MeJA n=12).

Since my data suggest that early JA responses in systemic tissues are modulated in dependence of *XYL4* (**Figure 21**B), I asked if JA signals moreover involve *XYL4* and *LLP3* or *LLP1* to fortify defense. Consequently, I initially aimed to evaluate

whether plant responses via *XYL4* are similar to those of either *LLP1* or *LLP3* after a trigger by MeJA. In order to investigate this in more detail, Col-0 and two *xyl4* mutant plants (*xyl4-1*, *xyl4-2*) were treated with exogenous MeJA, or a mock solution. In the following, defense of these plants against a systemic challenge with *Pst* was evaluated as described earlier (Sales et al., 2021). Notably, the titers were comparable for both treatments and all genotypes (**Figure 23**), which indicates that MeJA does not affect a *XYL4*-associated systemic defense in *A. thaliana*. These *XYL4*-related and MeJA-inducible responses thus resemble that of *LLP3* (Sales et al., 2021), assuming that *XYL4* might regulate plant defense responses either via the *LLP3* pathway or via one in parallel.

In further experiments, it would be interesting to test if signals other than MeJA can stimulate *XYL4* or *LLP3* to confirm if any JA-related pathway signal additionally acts upstream of *XYL4* and *LLP3* or only downstream via ERF1/*PDF1.2* as shown (**Figure 21**B; Sales et al., 2021).

3.4 *XYL4* moderately affects the root growth of seedlings under abiotic stress and exposure to MeJA

Genes coding for the lectin-like proteins LLP1 and LLP3 were formerly investigated for their influence on SA and JA signaling cascades during biotic defense (Breitenbach et al., 2014) and additionally the regulation of abiotic stress (Sales et al., 2021). It was shown that a treatment with either salt (NaCl) or MeJA inhibits the growth of primary roots in a *LLP1*- and *LLP3*-dependent manner (Sales et al., 2021). Interestingly, salt stress responses are suggested to be regulated by crosstalk of SA and JA signaling cascades in a similar way to the regulation by pathways of the investigated lectins. Specifically, plant responses triggered via *LLP3* and another close homologue, termed *LLP2*, presumably promote ERF1-dependent signals via *PDF1.2* (Sales et al., 2021), a gene potentially modifiable by *XYL4*-associated signals (**Figure 21**B). Therefore, I decided to test whether *XYL4* likewise controls root growth inhibition in seedlings as *LLP3*.

Consequently, root inhibition assays were performed as described previously (Sales et al., 2021), whereby initial focus was on plant responses to high salinity stress. Therefore, seedlings were germinated and cultivated by Jennifer Sales for six days on MS plates before transfer to control or treatment plates supplemented with either 100 µM or 300 µM NaCl. The length of the primary roots was measured at 6 and 12 days post-transfer and normalized to the control plates. The data shows that root growth was inhibited at day 6 and 12 slightly more strongly in salt

dose-treated *xyl4-1* mutants than in Col-0 (**Figure 24**A). This indicates that *XYL4* moderately promotes root growth under salt stress.

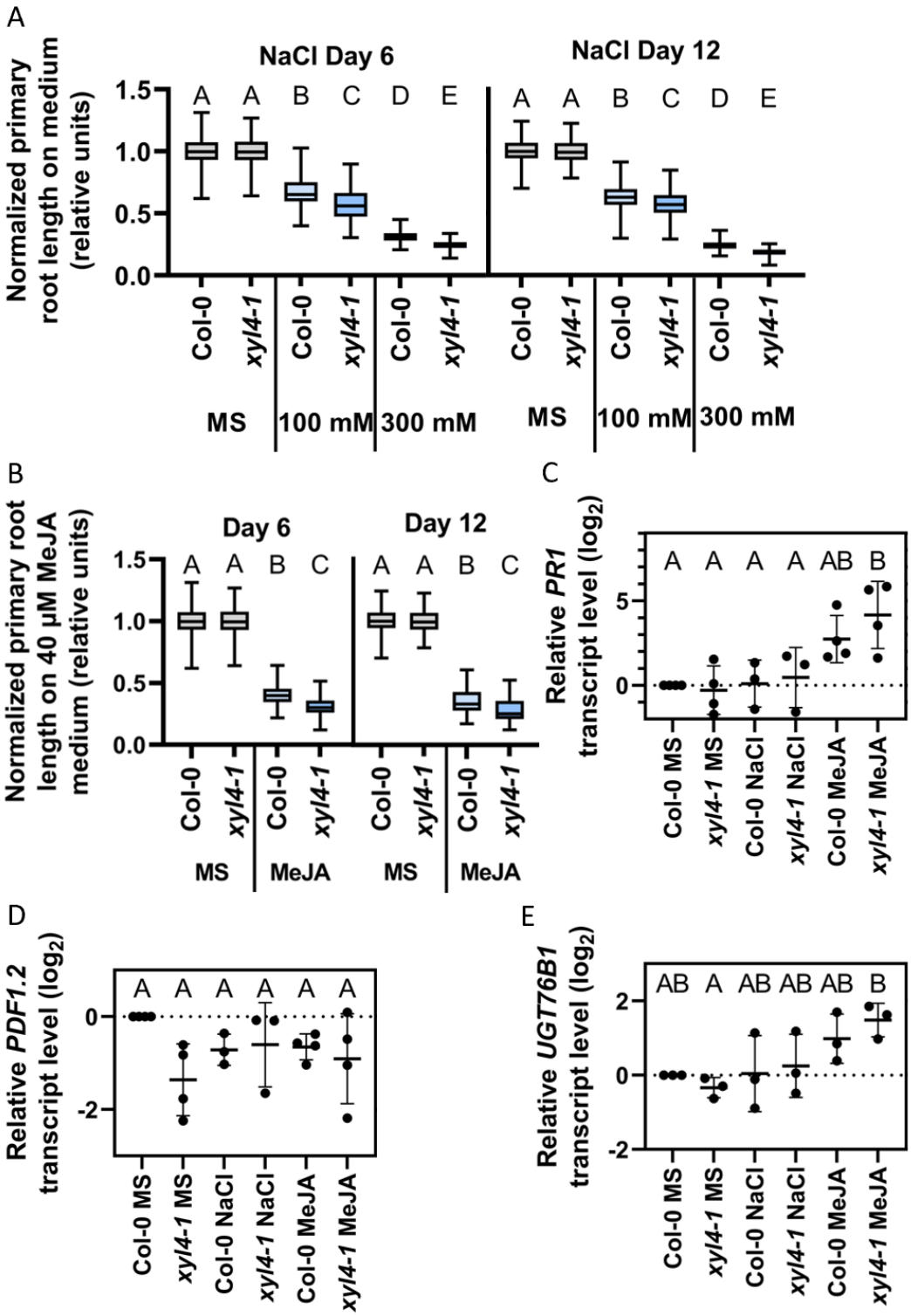

Figure 24: XYL4 slightly represses the growth of primary roots in *A. thaliana* seedlings.

Seedlings of Col-0 and *xyl4-1* plants were germinated on MS plates and transferred after 6 days to either control plates (MS), or to treatment plates supplemented with either 100 mM or 300 mM NaCl (A), or 40 µM MeJA (B). Additionally, whole seedlings (MS; 100 mM NaCl, 40 µM MeJA) at day 12 were analyzed for gene expression for *PR1* (C), *PDF1.2* (D), and *UGT76B1* (E). (**A**-**B**) Primary root length was measured at 6 and 12 days post-transfer

and normalized to that of the same genotype on control plates. Box plots represent average primary root length of four biologically independent experiments ± min and max value. Different letters above box plots indicate statistically significant differences for means (one-way ANOVA and Tukey test for P=<0.05, for (A, day 6): F(5, 677)=1393, Col-0 MS n=115, Col-0 100 mM n=117, Col-0 300 mM n=99, *xyl4-1* MS n=100, *xyl4-1* 100 mM n=126, *xyl4-1* 300 mM n=126; for (A, day 12): F(5, 685)=1970, Col-0 MS n=130, Col-0 100 mM n=129, Col-0 300 mM n=97, *xyl4-1* MS n=100, *xyl4-1* 100 mM n=118, *xyl4-1* 300 mM n=117; for (A, day 6): F(3, 640)=2406, Col-0 MS n=115, Col-0 MeJA n=117, *xyl4-1* MS n=202, *xyl4-1* MeJA n=210; for (A, day 12): F(3, 576)=2475, Col-0 MS n=130, Col-0 MeJA n=129, *xyl4-1* MS n=154, *xyl4-1* MeJA n=167). (**C**-**E**) Gene transcript accumulation was analyzed by qRT-PCR, normalized to that of *UBIQUITIN,* and is shown relative to the normalized transcript levels of the appropriate Col-0 mock (MS) controls. Black dots represent three to four biologically independent data points, and lines indicate the respective mean values ± SD. The letters above the scatter dot plots indicate statistically significant differences (one-Way ANOVA and Tukey test, P=<0.05, for (C): n=3-4, F(5, 16)=6.02; for (D): n=3-4, F(5, 16)=1.859; for (E): n=3, F(5, 12)=0.0379).

In addition, plant performance of seedlings on media supplemented with either 40 µM of MeJA or mock was investigated. Therefore, plants were germinated and cultivated similarly as described above. In a comparable manner as detected in salt-treated plants (**Figure 24**A), the *xyl4-1* plants showed a slightly stronger repression of the growth of primary roots on the MeJA-treatment plates than the control genotype Col-0 (**Figure 24**B). It can be thus assumed that MeJA-triggered responses are partially dependent on *XYL4*.

In order to elucidate plant responses triggered by salt or MeJA on the transcriptional level, I analyzed seedling tissues at day 12. Thereby I determined the transcriptional levels for the SA marker gene *PR1*, the JA signaling component *PDF1.2*, and *UGT76B1*. Regulation of *PDF1.2* at this timepoint was not affected by either treatment or genotype (**Figure 24**D), whereas *PR1* was slightly inducible by MeJA in Col-0 and *xyl4-1* (**Figure 24**C). Potentially an activation of *PR1* resembles a late response of plants to a long-term exposure with MeJA. Notably, such mechanistic regulation of MeJA-inducible *PR1* expression is known from the monocot plant wheat: wheat plants, which repress *PR1* after an exposure to (volatile) MeJA at 1 dpi in root tissues, promote *PR1* in leafy tissues after 24-48 hours and in roots after 72 hours (Lu et al., 2006; Liu et al., 2016a). Similarly, *PR1* is inducible by MeJA in apple after ~48 hours (Zhang et al., 2010a).

Interestingly, the gene *UGT76B1*, which was formerly suggested to promote JA signaling in *Arabidopsis* plants (von Saint Paul et al., 2011), is moderately induced in Col-0 and *xyl4-1* seedlings (**Figure 24**E). Its expressional pattern resembles that of *PR1* (**Figure 24**C/E). This might indicate for a co-regulative (loop-like) path

including MeJA-*UGT76B1/PR1* and the subsequent stimulation of a root growth pathway downstream of it, which is regulated mostly independently of *XYL4*.

3.5 Long-distance SAR signaling via the phloem depends on *XYL4*

Stress signals produced at the site of inoculation can be transmitted towards distal parts within a plant or emitted via airborne molecules to neighboring plants. As *XYL4* is transcriptionally regulated after *Pst/AvrRpm1* in local, infected tissues (**Figure 17**A), but not systemically (**Figure S36**D), I determined if *XYL4* contributes to long-distance signaling in SAR. I initially investigated if *XYL4* modulates the generation of SAR signals and the transmission of molecules via the phloem-mobile route. To this end, I performed petiole exudate experiments with Col-0 and *xyl4-1* plants. For that, I stimulated plants for the generation of phloem sap-associated molecules by syringe-inoculation of either *Pst/AvrRpm1* or a corresponding mock solution. One day later, petiole exudates (PetEx) from the inoculated (donor) leaves were collected, also from (donor) plants that had been kept untreated. To evaluate the SAR-inducing capacities of PetEx, I infiltrated these solutions into naïve Col-0 and *xyl4-1* recipient plants, and one day later challenged the same leaves with *Pst*. *In planta Pst* titers were monitored at 4 dpi. In these experiments the PetEx of bacteria-infected Col-0 donors reduced the propagation of the *Pst* challenge inoculum in Col-0 recipients, thus rendering these plants more resistant against *Pst* compared to recipient plants which had been treated with PetEx of control-treated wild type plants (**Figure 25**A). Notably, PetEx from both mock- and *Pst/AvrRpm1*-treated *xyl4-1* donors reduced the *Pst* titers in Col-0 recipient plants but were neither as effective as PetEx from infected wild type plants (**Figure 25**A). These findings suggest that *XYL4* is necessary for SAR signal generation or transmission from locally infected tissues. Potentially, such a pathway via *XYL4* might co-regulate the generation of SAR signals together with *LLP3* (Sales et al., 2021).

Next, I analyzed the reaction of *xyl4-1* recipient plants to SAR signals in PetEx. To this end, *Pst* titers were analyzed in *xyl4-1* recipient plants that were inoculated with PetEx from infected or mock-treated donors. Notably, the PetEx-treated recipient plants accumulated equal *Pst* densities (**Figure 25**B), indicating that *xyl4-1* is defective in the recognition of SAR-modulating phloem-mobile compounds. Together, these findings suggest that *XYL4* is involved in the perception or propagation of SAR signals in systemic tissues.

Preceding data suggest that PetEx from mock-treated *xyl4-1* donor plants bears resistance-inducing capacities that potentially promote moderate defense (**Figure 25**A). It may be that plants express a (mild?) form of preformed defense by constitutively accumulating defense-modulating compounds in exudates of leafy tissues. I thus set out to test Col-0 and *xyl4-1* recipient plants for their response to PetEx from untreated donors. However, the *Pst* densities detected in the infiltrated Col-0 and *xyl4-1* recipient plants were comparable (**Figure 25**C). The data suggest that *xyl4-1* donors accumulate inoculation-inducible molecules in the defense-promoting PetEx only after an initial infiltration (**Figure 25**A) rather than constantly expressing SAR-promoting compounds. In the greater picture of long-distance signaling in *A. thaliana*, *XYL4* thus appears to control SAR signaling upon inoculation in all relevant tissues involved during defense (from local to systemic).

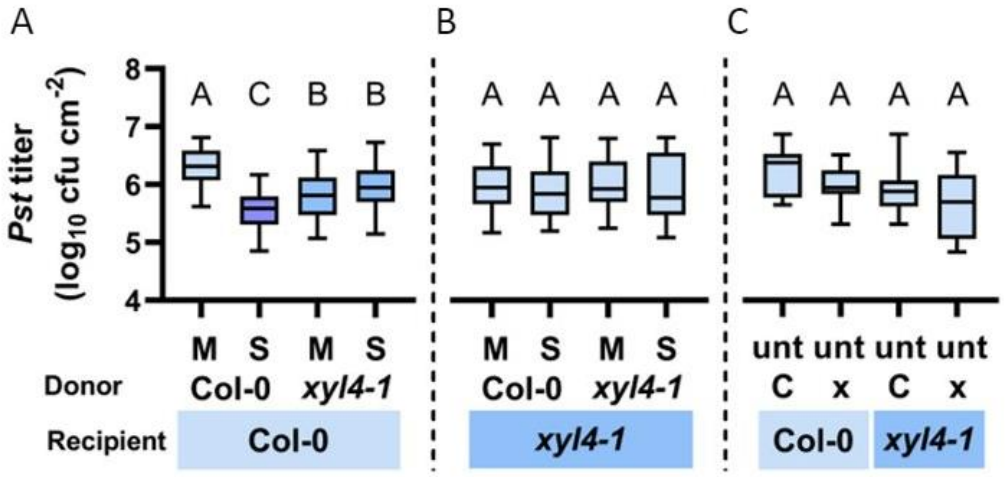

Figure 25: The generation and transmission of phloem-mobile SAR signals is dependent of *XYL4*.
Leaves of Col-0 (C) and *xyl4-1* (x) plants were inoculated with either 10^7 cfu/mL of *Pst/AvrRpm1* (S), a corresponding mock (M) solution, or were kept untreated (unt). One day later, inoculated leaves were cut at the middle of the plant rosette in order to retain their petioles and incubated in water to collect leaf exudates (PetEx). Subsequently, these exudates were syringe-infiltrated into naïve Col-0 and *xyl4-1* recipient plants. Again, one day after, the inoculated recipient leaves were challenged with 10^5 cfu/mL of *Pst*. Bacterial titers in challenge-inoculated receiver plants were monitored at 4 dpi. Box plots represent average single *Pst* titers in Col-0 (**A**/**C**) and *xyl4-1* (**B**/**C**) recipient plants from four to twelve biologically independent experiments ± min and max values. Letters above the box plots indicate statistically significant differences for means (one-way ANOVA and Tukey test for P=<0.05, for (A, Col-0 recipients): F(3, 191)=35.07, Col-0 M n=51, Col-0 S n=48, *xyl4-1* M n=49, *xyl4-1* S n=47; for (B, *xyl4-1* recipients): F(3, 116)=0.4254, Col-0 M n=45, Col-0 S n=44, *xyl4-1* M n=16, *xyl4-1* S n=15; for (C, recipients of PetEx from untreated donors): F(3, 66)=4.705, Col-0 + Col-0 unt n=20, Col-0 + *xyl4-1* unt n=19, *xyl4-1* + Col-0 unt n=16, *xyl4-1* + *xyl4-1* unt n=15).

3.6 *XYL4* putatively regulates *FMO1* during SAR

As the above results suggest that *XYL4* is an important modulator of SAR signals, I aimed to elucidate possible pathways and identify molecules that accumulate in PetEx in association with *XYL4*. I assumed that a *XYL4*-inducible pathway could affect PetEx-triggered gene expression in recipient plants. To elaborate this point, I determined the transcript abundance of the following genes in PetEx-treated leaves of Col-0 and *xyl4-1* recipient plants one day after inoculation: *XYL4*, *PDF1.2*, the lysine catabolism-associated gene *LYSINE-KETOGLUTARATE REDUCTASE* (*LKR*), which triggers an alternative metabolic route of lysine besides the one culminating in Pip biosynthesis (Galili et al., 2001; Návarová et al., 2012), and the SAR-associated genes *ALD1*, *FMO1*, and *UGT76B1.* I found that expression of *XYL4*, *PDF1.2*, *ALD1*, *LKR*, and *UGT76B1* was comparable in response to the different PetEx in Col-0 and *xyl4-1* recipients, respectively (**Figure 26**C, **SFigure S*38***A-D). Interestingly, the gene *FMO1* was induced in Col-0 recipients by PetEx of infected Col-0 in comparison to control-treated plants but suppressed by PetEx of infected *xyl4-1* (**Figure 26**A). This data suggests that *XYL4* modifies phloem-mobile signals that promote a *Pst/AvrRpm1*-related transcript expression of *FMO1* in PetEx-treated wild type receivers.

It was consequently interesting to test if *XYL4* may regulate the accumulation of the *FMO1*-dependent compound NHP, its precursor Pip (Hartmann et al., 2018), and the related conversion metabolite NHP-O-β-glucoside (NHP-H2) (Bauer et al., 2021) during defense. To this end, we set out to determine the levels of those metabolites in the systemic tissues of SAR-induced and additionally *Pst*-challenged plants by LC-MS together with Birgit Lange at HMGU. Col-0 and *xyl4-1* comparably accumulated Pip and NHP (**Figure 26**B/D), while the *FMO1*-dependent abundance of the conversion product NHP-H2 was lower in mock-treated *xyl4-1* plants as in the control Col-0 plants (**Figure 26**E). In sum, the findings as presented in **Figure 26**A/D-E and **Figure S38**D indicate that *XYL4* might promote for a *FMO1*-dependent response that subsequently affects the accumulated portion of NHP-H2 in plants. Such *FMO1*- and NHP-H2-associated modifications may be pivotal for *XYL4*-regulated SAR signaling pathways via the vasculature.

In order to further clarify phloem-related and *XYL4*-dependent signaling mechanisms, it would be further interesting to examine if PetEx of *xyl4-1* donor plants control the accumulation of transcript of defense-associated genes such as *PDF1.2, LLP1*, or *PR1* in inoculated recipients at other timepoints than so far

investigated. As suggested above, those genes might be regulated in dependence of *XYL4* in systemic tissues upon a trigger with *AvrRpm1* (**Figure 21**B-D).

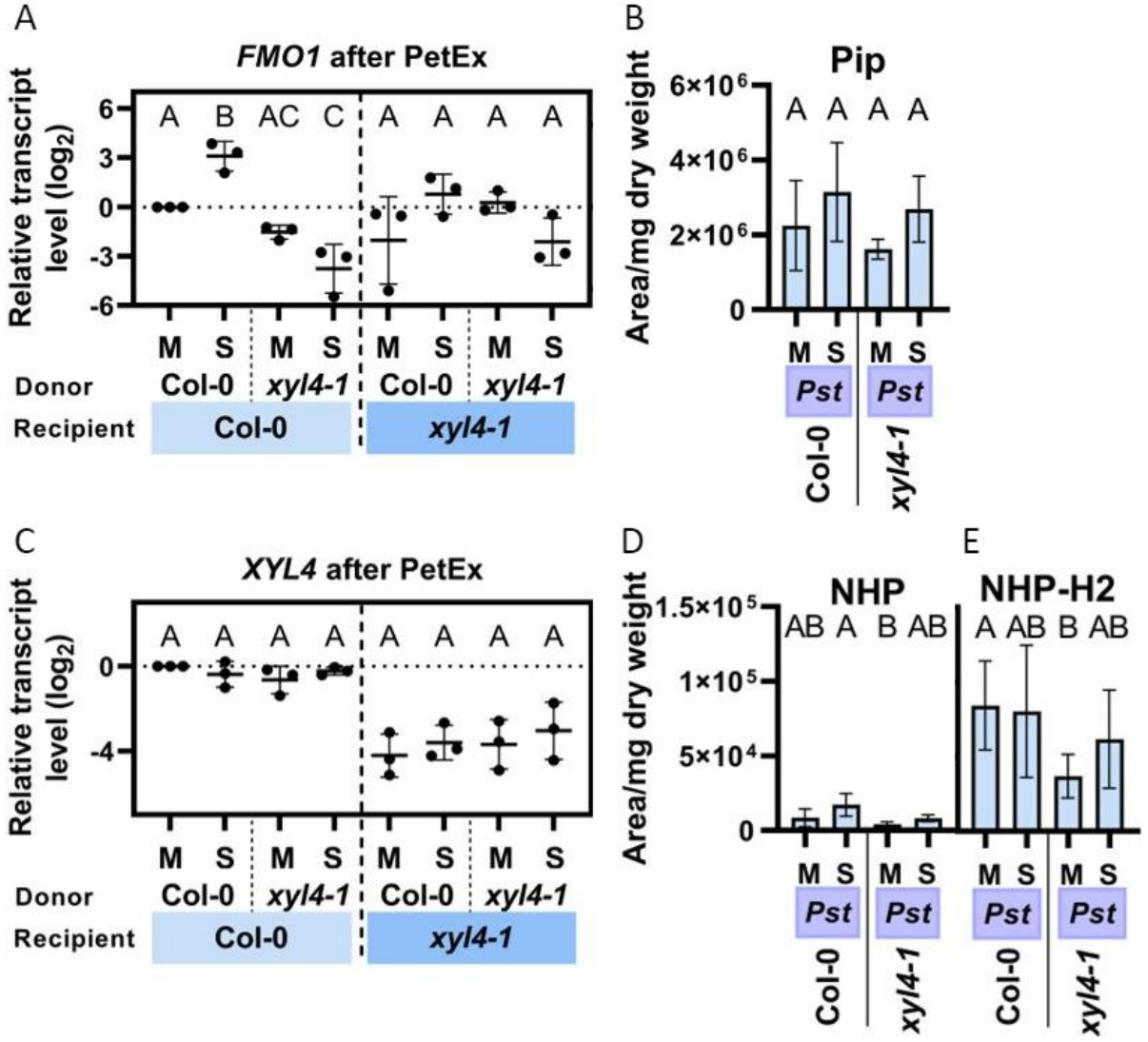

Figure 26: *XYL4* potentially modulates phloem-associated defense signals by regulating the NHP pathway.
Leaves of Col-0 and *xyl4-1* plants were inoculated with either 10^7 cfu/mL of *Pst/AvrRpm1* (S), or a corresponding mock (M) solution. One day later, inoculated leaves were cut at the middle of the plant rosette in order to retain their petioles and incubated in water to collect leaf exudates (PetEx). Subsequently, these exudates were syringe-infiltrated into naïve Col-0 and *xyl4-1* recipient plants. Again, one day after, the inoculated recipient leaves were either collected for determination of gene expression or challenged with 10^5 cfu/mL of *Pst*. (**A**/**C**) Transcript abundance of *FLAVIN-DEPENDENT MONOOXYGENASE 1* (*FMO1*) and *XYL4* was determined by qRT-PCR, normalized to that of *UBIQUITIN*, and is shown relative to the normalized transcript levels of the appropriate Col-0 mock (M) controls. Black dots represent three biologically independent data points, and lines indicate the respective mean values ± SD. The letters above the scatter dot plots indicate statistically significant differences (one-way ANOVA and Tukey test for P=<0.05; for (A): n=3, F(5, 12)=17.77; for (C): n=3, F(5, 12)=2.269). (**B**/**D**/**E**) Col-0 and *xyl4-1* plants were either syringe-inoculated in the first two true leaves with either 10^6 cfu per mL of *Pst/AvrRpm*1 (S), or a corresponding mock (M) control solution. Distal uninfected leaves were challenged at 3 dpi with 10^5 cfu/mL of *Pst*, and analyzed by LC-MS for their metabolite abundance of Pip, NHP, and NHP-H2 one day later to evaluate a priming induction.

Metabolites were calibrated to appropriate internal standards, and normalized to the individual dry weight. Bars represent average metabolite abundance of three to four biologically independent replicates ± SD. Different letters above bars indicate statistically significant differences for means (one-way ANOVA and Tukey test for P=<0.05, for (B, Pip): n=4, F(3, 12)=1.692; for (D, NHP): n=3, F(3, 8)=4.073; for (E, NHP-H2): n=3-4, F(3, 12)=1.826).

3.7 *XYL4* promotes communication via the airborne route

Due to the putatively multifaceted interactions of *XYL4* in signaling via the phloem-mobile route, I speculated that *XYL4* might also interfere with inter-plant communication via volatiles.

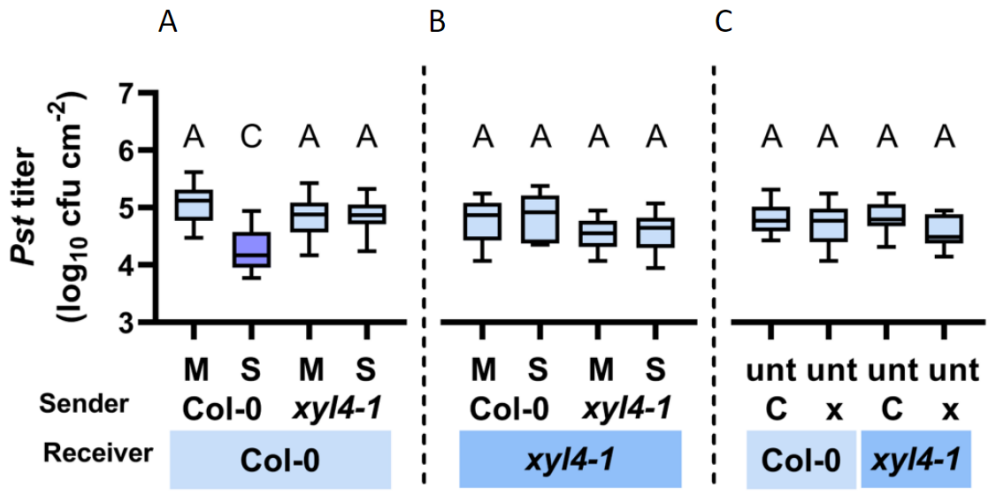

Figure 27: The generation and perception of airborne SAR signals is dependent of *XYL4*
Col-0 (C) and *xyl4-1* (x) sender plants were spray-inoculated with either 10^8 cfu/mL of *Pst/AvrRpm1* (S), with a corresponding mock (M) solution, or kept untreated (unt). Sender plants were co-incubated in closed desiccators with naïve receiver plants. Three days later, leaves of receiver plants were challenged with 10^5 cfu/mL of *Pst*. The resulting *in planta Pst* titers in receiver plants (**A**-**C**) were evaluated at 4 dpi. Box plots represent average *Pst* titers from four to seven biologically independent experiments, including at least 3 replicates each ± min and max values. Letters above the box plots indicate statistically significant differences for means (one-way ANOVA and Tukey test for P=<0.05, for (A, Col-0 receivers): F(3, 118)=37.26, Col-0 M n=30, Col-0 S n=32, *xyl4-1* M n=30, *xyl4-1* S n=30; for (B, *xyl4-1* receivers): F(3, 63)=3.383, Col-0 M n=17, Col-0 S n=17, *xyl4-1* M n=16, *xyl4-1* S n=17; for (C, receivers co-incubated with untreated senders): F(3,62)=2.637, Col-0 + Col-0 unt n=17, Col-0 + *xyl4-1* unt n=16, *xyl4-1* + Col-0 unt n=17, *xyl4-1* + *xyl4-1* unt n=16).

I therefore tested if signaling by airborne signals between ETI-infected sender plants and healthy receivers is dependent on *XYL4*. To address this, I spray-inoculated Col-0 and *xyl4-1* sender plants with either *Pst/AvrRpm1*, or a corresponding mock solution. Subsequently, senders were co-incubated with naïve receiver plants in a closed desiccator to enforce a directed communication. Three days later, the receiver plants were challenged with *Pst* and monitored for bacterial

densities 4 days after. When receivers exhibited lower titers for *Pst* than the corresponding control-treated line, I considered these plants to recognize and respond to airborne molecules from emitting senders. In turn, when receivers did not react with bacterial densities distinct from the control plants, the senders were either not producing or emitting defense-inducing volatiles.

Here, Col-0 receivers, which shared air space with infected wild type senders, responded with reduced *Pst* titers as compared to Col-0 plants co-incubated with mock-treated wild type senders (**Figure 27**A). Nonetheless, when wild type receivers were neighboring *xyl4-1* senders, mostly no differences were detectable in titers of *Pst*. In addition, receivers of either genotype responded similarly to an infection with *Pst* when they had been incubated with untreated senders (**Figure 27**C). Taken together, I suggest that *XYL4* is necessary for the generation of SAR-related volatile signals and hence for defense against *Pst*. Subsequently, I tested *xyl4-1* receiver plants and detected no differences in *Pst* titers after plants were co-incubated with any of the sender plants (**Figure 27**B). Consequently, I propose that *XYL4* acts in the perception of airborne molecules.

3.8 Cell wall composition is affected by ETI in an *EDS1*- and *XYL4*-dependent manner

As formerly described, plant defense against pathogens associates with plant cell wall-mediated immune signals like those inducible by changes in the composition of the walls (Hernandez-Blanco et al., 2007; Reem et al., 2016; Bacete et al., 2018; Vaahtera et al., 2019). XYL4 and other *EDS1*-dependent, ETI-inducible proteins are assumed to modify apoplastic structures such as extracellular carbohydrates like those originating from cell walls (Breitenbach et al., 2014). It was thus of interest to test if SAR-related genes, such as *EDS1* and *XYL4*, contribute to modifications of cell wall carbohydrates. The data so far allows the assumption that *XYL4* activates multiple layers of ETI defense covering intra- and inter-plant communication (**Figure 25**, **Figure *27***). This prompts the question whether actions of XYL4 proteins *in planta* affect associated signaling routes via carbohydrates?

I hypothesize that plant genotypes, including *eds1-2* and *xyl4-1* mutants, display altered compositions in cell wall glycans when compared to the wild type Col-0. To test this, our collaborator Jeanette Hansen at UCPH used Comprehensive Microarray Polymer Profiling (CoMPP) to determine the abundance of specific plant cell wall-related polymeric carbohydrates in these plants. Furthermore, together

with Martin Lehmann at LMU we analyzed the same plant samples for alcohol soluble metabolites by Gas chromatography-mass spectrometry (GC-MS). To this end, lines were selected (Col-0 *pDEX:AvrRpm1-HA* and *eds1-2 pDEX:AvrRpm1-HA*) or newly generated (*xyl4-1 pDEX:AvrRpm1-HA*) that contain a dexamethasone (DEX)-inducible transgene encoding the *P. syringae* effector AvrRpm1. Gene expression analysis of these homozygous lines revealed that *AvrRpm1* transcripts were not induced by DEX treatments in *xyl4-1* plants containing the transgene, although the transgene was induced by DEX in the Col-0 and *eds1-2* transgenic control plants (**Figure S39**). This indicates that the *pDEX:AvrRpm1-HA*-construct was either not successfully integrated into the genome of *xyl4-1* or subjected to RNA-mediated gene silencing in these plants.

Table 12. Pectin accumulation in cell walls is affected by *EDS1*.
Pathogen-free ETI was induced by spray inoculation of transgenic Col-0 and *eds1-2* plants with 30 µM DEX. 6 h later, above-ground tissues were harvested, extracted, and subsequently analyzed for the abundance of carbohydrate polymers by CoMPP. The heat map shows the relative abundance of cell wall glycans epitopes recognized by monoclonal antibodies as listed in **Table S16**. Values of single table cells represent 4 biologically independent replicates and blue color intensity is proportional to the mean spot signal from the microarray. The highest signal in the dataset has been assigned to a value of 100 and all other signals adjusted accordingly. Average abundance values for glycan epitopes labeled with an asterisk (*) are significantly different when comparing *eds1-2* and Col-0 plants (one-way ANOVA and Tukey test for P=<0.05 and n=4: for 2F4 p=0.1602, for JIM5 p=0.0309, for LM19 p=0.0424, for JIM7 p=0.0346, for LM20 p=0.0304, for LM18 p=0.1098, for INRA-RU2 p=0.1031, for INRA-RU1 p=0.0353).

		Pectin														Hemicellulose									Crystalline Cellulose	Proteins											
		Homogalacturonan										Rhamno-galacturonan-I				Xylogalacturonan	Mannan		Xyloglucan			Xylan		Glucan			Arabinogalactan protein									Extensin		
		2F4	JIM5	LM19	JIM7	LM20	LM18	LM7	LM5	LM6	LM13	INRA-RU2	INRA-RU1	LM16	LM8		LM21	LM22	LM15	LM24	LM25	LM11	LM23	BS-400-2	BS-400-3	CBM3a	JIM8	JIM14	JIM15	JIM16	JIM17	JIM4	JIM13	LM2	LM14	Mac207	JIM11	JIM20	LM1
			*	*	*	*							*																										
Col-0	CDTA Fraction	41	70	60	86	86	61	0	15	12	0	36	40	0	0		0	0	0	0	11	0	0	0	0	0	0	0	0	0	0	0	0	0	17	18	0	9	0
		37	55	45	67	66	46	0	15	9	0	34	33	0	0		0	0	0	0	7	0	0	0	0	0	0	0	0	0	0	0	0	0	15	15	0	8	0
		33	54	42	65	64	44	0	18	9	0	30	34	0	0		0	0	0	0	12	0	0	0	0	0	0	0	0	0	0	0	8	6	18	16	0	10	0
		50	62	49	71	72	52	0	10	8	0	31	36	0	0		0	0	0	0	6	0	0	0	0	0	0	0	0	0	0	0	0	0	14	11	0	6	0
eds1-2		53	87	73	98	100	71	0	15	11	0	42	50	0	0		0	0	0	0	9	0	0	0	0	0	0	0	0	0	0	0	5	14	16	0	10	0
		41	68	57	84	83	57	0	15	15	0	45	43	0	0		0	0	0	0	12	0	0	0	0	0	0	0	0	0	0	0	6	15	16	0	9	0
		56	76	62	91	93	65	0	14	11	0	45	45	0	0		0	0	0	0	10	0	0	0	0	0	0	0	0	0	0	0	0	15	15	0	0	0
		52	74	63	88	90	57	0	9	11	0	43	50	0	0		0	0	0	0	8	0	0	0	0	0	0	0	0	0	0	0	0	15	12	0	6	0
Col-0	NaOH Fraction	0	0	0	0	0	0	0	6	0	0	5	7	0	0		35	0	72	6	48	16	0	19	0	27	0	0	0	0	0	0	8	0	13	11	0	15	0
		0	0	0	0	0	0	0	12	0	0	5	9	0	0		40	0	84	8	58	19	0	21	0	32	0	0	0	0	0	0	9	0	13	10	0	14	0
		0	0	0	0	0	0	0	7	0	0	7	7	0	0		32	0	58	0	37	18	0	20	0	22	0	0	0	0	0	0	9	0	13	9	0	15	0
		0	0	0	0	0	0	0	0	0	0	0	0	0	0		32	0	54	6	35	12	0	13	0	22	0	0	0	0	0	0	6	0	12	8	0	12	0
eds1-2		0	0	0	0	0	0	0	8	0	0	0	9	0	0		31	0	59	5	40	0	0	14	0	23	0	0	0	0	0	0	0	0	10	0	0	13	0
		0	0	0	0	0	0	0	6	0	0	8	9	0	0		39	5	72	5	48	15	0	23	0	26	0	0	0	0	0	0	8	0	13	11	0	12	0
		0	0	0	0	0	0	0	7	0	0	7	9	0	0		43	0	77	8	52	18	0	21	0	32	0	0	0	0	0	0	7	0	12	7	0	15	0
		0	0	0	0	0	0	0	0	0	0	0	8	0	0		43	5	77	5	55	8	0	13	0	32	0	0	0	0	0	0	6	0	14	8	0	16	0

I consequently focused on the transgenic Col-0 and *eds1-2* plants, which displayed comparable levels of *AvrRpm1* transcripts (**Figure S39**), and spray-inoculated them with DEX. Five to six hours later, the plants showed clear wilting symptoms, which were indicative of *AvrRpm1*-induced ETI. Therefore, I harvested the above-ground tissues of the plants at this timepoint. The samples of the same genotype and treatment were extracted for either soluble metabolites as used for the analysis by GC-MS (see below, 3.9), or for alcohol insoluble residues (AIR) in order to perform CoMPP. AIR was subsequently subjected by Jeanette Hansen at UCPH to a sequential fractionation with CDTA and NaOH, which respectively released pectin and hemicellulose. After probing the samples with antibodies (for references see **Table S16**), the binding studies of CoMPP revealed greater differences in pectin polysaccharides between the transgenic Col-0 and *eds1-2* plants, and smaller changes for hemicellulose (**Table 12**). In all samples we primarily detected epitopes that belong to homogalaturonan (HG) and rhamnogalacturonan-I (RG-I), as well as those of xyloglucan and mannan (**Table 12**). Notably, the ETI-induced *eds1-2 pDEX:AvrRpm1-HA* plants accumulated significantly higher levels of HG as detected by the antibodies JIM5, JIM7, LM19, and LM20 and of RG-I, whose backbone epitopes were bound to INRA-RU1-1. These results indicate that *EDS1* represses the formation of HG and RG-I pectin polymers in cell walls after the induction of ETI. Consequently, I suggest that *EDS1* might modulate pectin-associated cell wall composition and therefore signal generation and/or transduction during plant defense.

To investigate this point further, I subsequently studied differences in the pectin composition of bacteria-infected plants, more naturally illustrating plant-pathogen interactions. To this end, I spray-inoculated Col-0 plants and additionally *xyl4-1* and *eds1-2* mutants with either *Pst/AvrRpm1*, or a corresponding mock solution. Together with our collaborators at UCPH we determined the cell wall carbohydrate composition of pooled rosettes that were harvested two days later. The heatmap of **Table 13** shows that Col-0 plants were inducible by *Pst/AvrRpm1* for the accumulation of HG-associated carbohydrates detectable by the antibodies JIM5, JIM7, and moreover arabinogalactan proteins (AGPs) as detected by JIM17 when compared to mock-treated plants. To a lesser extent also polymers, as probed with HG-targeting antibodies 2F4, LM18, LM19, LM20, and RG-I-related INRA-RU1/2, were slightly more abundant after infection. Notably, all these epitopes detectable in SAR-induced wild type plants were comparably abundant in inoculated *xyl4-1* mutants and mock-treated Col-0, assuming that SAR-inducible changes are absent

Table 13. Accumulation of AGP and pectin in cell walls is modified by *EDS1* and *XYL4*.

Col-0, *xyl4-1*, and *eds1-2* plants were spray-inoculated with either 10^8 cfu/mL of *Pst/AvrRpm1* (R), or a corresponding mock (M) solution. Two days after, plant rosettes were harvested, extracted, and subsequently analyzed for the abundance of carbohydrate polymers by CoMPP. The heat map shows the most abundant cell wall glycan epitopes recognized by monoclonal antibodies as listed in **Table S16**. Values of single table cells represent 3 biologically independent replicates and blue cell color intensity is proportional to the mean spot antibody signal from the microarray.

| | | | | CDTA Fraction | | | |

in *xyl4-1* plants compared to Col-0. Interestingly, control-treated *eds1-2* plants appeared to accumulate higher (but insignificant) levels of carbohydrate polymers as detected by JIM5, JIM7, JIM17, 2F4, LM18, LM19, LM20, and INRA-RU1/2 when compared to Col-0 and *xyl4-1* mutants. Infected *eds1-2*, however, showed slight reductions in the abundance of the polymers as detected by JIM5, LM19, JIM7, INRA-RU1, LM21, and LM2.

I thus suggest that both *XYL4* and *EDS1* modulate the composition of plant cell walls by affecting pectin, hemicellulose and AGPs (**Table 12**, **Table *13***). Furthermore, *XYL4* and *EDS1* may cooperatively modulate defense responses against an ETI-associated infection and other stress responses (as inducible by spray inoculation). It would thus be interesting to determine exact molecules regulated by either *XYL4* or *EDS1*, and subsequently test if an exogenous application with one of these compounds can affect SAR-like responses in plants.

3.9 *EDS1*- and *XYL4*-associated signals modulate carbohydrate metabolism

Notably, *AvrRpm1*-inducible responses are suggested to trigger pathways involved in the modulation of carbohydrate metabolism (Gao et al., 2020). I thus asked if soluble metabolites and carbohydrate-related molecules aside from cell wall glycans are regulated in an *AvrRpm1*-related and *EDS1*-and/or *XYL4*-dependent manner in *A. thaliana*. For this purpose, we initially analyzed the extracted samples from the same DEX-treated and pooled plant material, of Col-0 *pDEX:AvrRpm1-HA* and *eds1-2 pDEX:AvrRpm1-HA,* as previously used for the first CoMPP study (referring to **Table 12**). Via GC-MS, Martin Lehmann (LMU) determined the abundance of mono- and disaccharides, carbohydrate-derivatives, and amino acids in a semi-targeted approach. An array of 136 shared accumulating metabolites was detectable in the transgenic Col-0 and *eds1-2* plants and was subsequently evaluated for induced or repressed states (given as fold change in **Table 14**). We identified elevated levels of xylulose, spermidine, erythritol, 2,5-dimethoxy-cinnamic acid, and 1,6-anhydro-beta-glucose as well as two unknown metabolites (mass 204 m/z, RI 2534.96, and mass 117 m/z, RI 1539.64), while levels of dihydrosphingosine, Pip, maltose, SA, glucose-6-phosphate (G-6-P), and two unknown molecules (mass 204 m/z, RI 2523.79; mass 259 m/z, RI 2754.92) were reduced in *eds1-2* mutants as compared to wild type (**Table 14**, **Table S18**). These findings suggest that diverse carbohydrate-related compounds and additional molecules are regulated in association with *EDS1*, either due to the *AvrRpm1*-

induced state or as a constitutive response in untreated plants (no untreated samples were included in the analysis).

Table 14*:* SAR- and carbohydrate-related metabolic pathways are regulated in association to EDS1.

Transgenic Col-0 and *eds1-2* plants were spray-inoculated with DEX for the expression of *AvrRpm1*. About 6 h after, rosettes were harvested, pooled for the treatment and genotype, and subsequently extracted in methanol and chloroform to attain soluble metabolites. GC-MS analysis was conducted to determine glycans and further molecules in a semi-targeted manner. The metabolites were and calibrated to two appropriate internal standards and normalized to sample dry weight. Peaks from the chromatograms obtained were evaluated by using available databases and if possible edited for a specific metabolite. Molecules were labeled with "Unknown_mass" when they could not be clearly assigned to a database-saved entry according to their mass and predicted functional groups. For each biologically independent experiment, relative metabolite abundance in comparison to the SAR-induced Col-0 plants was calculated. The table represents mean data expressed as fold-changes merged from four replicates. Numbers in bold indicate for statistically significant differences (two-way ANOVA, and Bonferroni's multiple comparison test or False Discovery Rate (FDR) with two-stage linear step-up procedure of Benjamini, Krieger and Yekutieli; P=<0.05, *p*-values as indicated in the table). Values in green display elevated abundance in metabolites, whereas purple colors indicate lower accumulation.

Metabolite	Fold-change *eds1-2*/Col-0	Bonferroni: adjusted *p*-value	FDR: *p*-value
		Col-0 vs. *eds1-2*	Col-0 vs. *eds1-2*
Xylulose	~3.20	**<0,0001**	**<0,0001**
Unknown_mass204_RI_2534.96	~2.00	**<0,0001**	**<0,0001**
Unknown_mass117_RI_1539.64	~2.00	**<0,0001**	**<0,0001**
Spermidine	~1.75	**<0,0001**	**<0,0001**
Erythritol	~1.65	**0,0002**	**<0,0001**
Unknown_mass237_RI_1522.12	~1.50	**0,0067**	**0,0022**
2,5-Dimethoxy-Cinnamic acid	~1.45	**0,0207**	**0,0069**
1,6-Anhydro-beta-Glucose	~1.45	**0,0273**	**0,0091**
Galactitol	~1.35	0,1324	**0,0441**
Glucose-6-phosphate (G-6-P)	~0.62	**0,0111**	**0,0037**
Unknown_mass204_RI_2523.79	~0.60	**0,0446**	**0,0149**
Unknown_mass259_RI_2754.92	~0.60	**0,0451**	**0,015**
Salicylic acid (SA)	~0.40	**0,0013**	**0,0004**
Maltose	~0.38	**0,0009**	**0,0003**
2-Piperidinecarboxylic acid (Pip)	~0.28	**<0,0001**	**<0,0001**
Dihydrosphingosine	~0.26	**<0,0001**	**<0,0001**

As xylulose, a product metabolizable from xylose as reviewed for other organisms like bacteria, fungi or eukaryotes (Jackson and Nicolson, 2002), accumulated more pronouncedly in the *eds1-2* mutant as compared to Col-0 genetic background (**Table 14**, **Table S18**), I hypothesize that xylose/xylulose-related signals may play an important role in *EDS1*-dependent pathways and ETI.

I further determined if the accumulation of defense-associated metabolites was affected after a bacterial infection in a similar manner as shown for the DEX-induced transgenic plants. To this end, I harvested whole above-ground tissues two days after Col-0, *xyl4-1*, and *eds1-2* plants had been spray-inoculated with *Pst*/*AvrRpm1* or a corresponding mock solution. In total, we detected 138 different metabolites by GC-MS analysis, which was performed by Martin Lehmann. Those compounds were partially comparable with those as listed in **Table S18**. Notably, the accumulation of metabolites as described for the Col-0 and *eds1-2* plants (**Table S18**, **Table S19**) potentially differ due to the harvest timepoint and promoted intensity of *AvrRpm1*-triggered responses: an endogenous activation in the pathogen-free system (with DEX) presumably results in faster (and stronger) plant responses (5-6 h) than an exogenous treatment with a bacterial solution (10^8 cfu/mL of *Pst*/*AvrRpm1*) as analyzed at 2 dpi (at this time, no symptoms of wilting or an indication of strong ETI responses were visible).

Specifically, the compounds asparagine, glutamic acid, fructose, and one additional unknown metabolite (mass 249 m/z, RI 2275.34) accumulated to higher levels in infected as compared to control-treated Col-0 plants (**Table 15**, **Table S19**). Independently of the treatment, the latter unknown compound was comparably elevated in *xyl4-1* and *eds1-2* mutant plants and equated the levels found in infected Col-0 (**Table 15**, **Table S19**). I thus hypothesize that this unknown compound accumulates specifically after infection regardless of whether *XYL4* or *EDS1* is functional. In addition, as levels of this molecule are higher in mock-treated mutant samples than detectable in wild type plants, this might point to a repressive effect of *XYL4* and *EDS1* on the accumulation of this metabolite. Other compounds such as fucose, G3P, serine, and G-6-P accumulated to higher levels after any treatment in *xyl4-1* as compared to Col-0, while this was only the case in *eds1-2* for levels of serine (**Table 15**, **Table S19**). In addition, the abundance of fucose and G3P were higher in *Pst*/*AvrRpm1*-infected *eds1-2* mutant as compared to wild type plants (**Table 15**, **Table S19**). In sum, the data indicate a *XYL4*- and/or *EDS1*-dependent regulation of the above-mentioned metabolites upon inoculation and/or infection.

Table 15. *XYL4* and *EDS1* modify SAR-inducible metabolic pathways relevant for energy production and lipid synthesis

Col-0, *xyl4-1*, and *eds1-2* plants were spray-inoculated with either 10^8 cfu/mL of *Pst/AvrRpm1* (R), or a corresponding mock (M) solution. Two days after, plant rosettes were harvested, pooled for the treatment and genotype, and subsequently extracted in methanol and chloroform to attain soluble metabolites. GC-MS analysis was conducted to determine glycans and further molecules in a semi-targeted manner. 138 metabolites were detected and calibrated to two appropriate internal standards and normalized to sample dry weight. Peaks from the chromatograms obtained were evaluated by using available databases and if possible edited for a specific metabolite. Molecules were labeled with "Unknown_mass" when they could not be clearly assigned to a database-saved entry according to their mass and predicted functional groups. For each biologically independent experiment, a relative metabolite abundance to mock-treated Col-0 plants was calculated. The table represents mean data from three replicates ± SD. Numbers in bold indicate statistically significant differences in comparison to Col-0 M (two-way ANOVA, and Bonferroni's multiple comparison test or False Discovery Rate (FDR) with two-stage linear step-up procedure of Benjamini, Krieger and Yekutieli; P=<0.05, *p*-values as indicated in the table). Values in green display elevated abundance in metabolites, whereas purple colors indicate lower accumulation.

Metabolite	Relative abundance as compared to Col-0 M ± SD				
	Col-0 R	*xyl4-1* M (sorted)	*xyl4-1* R	*eds1-2* M	*eds1-2* R
Unknown_mass249 _RI_2275.34	**2.21 ± 1.04**	**3.18 ± 0.84**	**3.66 ± 0.62**	**2.21 ± 0.23**	**3.11 ± 0.96**
Maleic acid	1.72 ± 1.10	**2.29 ± 0.92**	1.95 ± 0.58	1.54 ± 0.95	**2.17 ± 1.38**
Fucose	1.30 ± 0.29	**2.19 ± 1.89**	**2.22 ± 1.49**	1.18 ± 0.80	**2.42 ± 1.50**
Asparagine	**2.11 ± 1.26**	**2.14 ± 0.57**	**3.16 ± 2.58**	1.31 ± 0.40	**2.36 ± 2.10**
Glycerol-3-phosphate	1.43 ± 0.19	**2.07 ± 0.92**	**2.36 ± 1.24**	1.26 ± 0.82	**2.05 ± 1.37**
Glutamic acid	**2.09 ± 1.06**	**2.05 ± 1.06**	1.92 ± 0.90	1.51 ± 0.20	**2.22 ± 1.24**
Serine	1.43 ± 0.38	**2.00 ± 0.29**	**2.43 ± 0.42**	**1.90 ± 1.18**	**3.60 ± 1.66**
Glucose-6-phosphate	0.98 ± 0.42	**1.99 ± 1.51**	**1.98 ± 1.69**	1.01 ± 0.51	1.72 ± 0.66
Raffinose	0.78 ± 0.23	1.40 ± 0.56	0.79 ± 0.20	**3.19 ± 3.65**	**3.78 ± 4.34**
Unknown_mass103 _RI_2363.76	1.15 ± 0.11	1.40 ± 0.36	1.73 ± 0.64	1.09 ± 0.42	1.52 ± 0.62
Unknown_mass217 _RI_2835.55	1.29 ± 0.32	1.39 ± 0.35	1.72 ± 0.62	**2.31 ± 1.37**	**2.48 ± 1.75**
Glucose	1.32 ± 0.28	1.10 ± 0.24	1.08 ± 0.43	1.46 ± 0.35	**1.85 ± 0.95**
4-hydroxy-Butanoic acid	1.14 ± 0.42	1.10 ± 0.60	**2.37 ± 2.15**	0.97 ± 0.05	1.31 ± 0.27
Putrescine	1.08 ± 0.13	1.09 ± 0.35	**2.03 ± 0.92**	0.78 ± 0.02	**2.54 ± 1.77**
Fructose	**1.27 ± 0.39**	1.08 ± 0.32	1.03 ± 0.37	**1.55 ± 0.64**	**1.58 ± 0.69**
Threonine	0.89 ± 0.27	1.04 ± 0.15	0.98 ± 0.13	**0.68 ± 0.10**	1.00 ± 0.14
Diethylene glycol	1.08 ± 0.35	0.92 ± 0.38	**2.05 ± 1.68**	0.86 ± 0.25	1.04 ± 0.13
Ornithine	0.68 ± 0.32	0.82 ± 0.07	0.80 ± 0.43	0.51 ± 0.23	**2.05 ± 1.32**

In the *eds1-2* mutants, raffinose, fructose, and another unknown metabolite (mass 217 m/z, RI 2835.55) also accumulated to higher levels in both, mock- and

bacteria-treated plants as compared to Col-0 (**Table 15**, **Table S19**). Notably, the compounds glucose and ornithine accumulated only stronger in infected *eds1-2* mutants than in bacteria-inoculated wild type plants, while the expression of threonine was slightly downregulated in mock-treated *eds1-2* plants.

Additionally, putrescine was pronouncedly induced in both infected mutant genotypes, *xyl4-1* and *eds1-2*, when compared to Col-0 plants (**Table 15**, **Table S19**). As the levels of 4-hydroxy-butanoic acid and diethylene glycol were elevated in infected *xyl4-1* plants, it is to determine if these metabolites can be exclusively modified by *XYL4* during defense. Interestingly, derivatives of diethylene glycol were formerly attributed with exhibition of antifungal properties against plant parasitic pathogens (Shukla et al., 2012). In sum, *XYL4* and *EDS1* might affect metabolic pathways via individual and/or mutually stimulated plant responses upon a trigger for ETI.

3.10 *XYL4*-triggered defense responses are putatively linked to a xylose-dependent pathway

As previously described, *EDS1* and *XYL4* have the potential to alter cell wall-associated glycans (**Table 12**, **Table *13***) and metabolic pathways including those involving carbohydrates (**Table S18**, **Table S19**). I consequently intended to further investigate the function of XYL4 and its link to *EDS1* in more detail. The action of XYL4 proteins *in planta* was formerly determined to be that of a functional beta-xylosidase (Minic et al., 2004), whereby XYL4 putatively hydrolyzes carbohydrate molecules comprising multiple xylose units. Hence, I hypothesize that XYL4 potentially promotes the release of xylose-associated molecules, from for example cell walls. Thereby, XYL4 could modulate xylose levels (or that of xylose derivatives) in tissues of (ETI) defense-induced plants. Therefore, I decided to determine how (and if) exogenously applied xylose affects plant immune responses. In order to test this, I inoculated Col-0 and SAR-associated mutant plants including *xyl4-1, eds1-2*, and *llp1-1* with either D-/L-xylose, a corresponding mock solution, or kept plants untreated. At 3 dpi I challenged systemic leaves with *Pst* and examined bacterial titers four days later.

Here, wild type plants, which were pretreated with a dose of 100 nM up to 1 mM of D-/L-xylose, showed reduced bacterial densities when compared to the control plants, regardless of the D-/L-xylose concentration (**Figure 28**A). This indicates an effective, dose-independent induction of plant resistance by xylose, which was comparable for the application of either D- or L-xylose alone (**Figure 29**D).

Interestingly, *xyl4-1* responded with comparable *Pst* titers to Col-0 plants upon a treatment with xylose (**Figure 28**B, **Figure S40**C), suggesting that *xyl4-1* and Col-0 similarly mount a defense response after the xylose application (**Figure 28**A-B). However, *Pst* titers in either *eds1-2* or *llp1-1* were the same after any treatment (**Figure 28**B, **Figure S40**C), which indicates that defense (signaling) related to xylose depends on *EDS1* and *LLP1*. Defense triggered by xylose had no effect on the ion permeability of inoculated and systemic leaves at 3 dpi as determined by measuring the electrical conductivity of the leaves (**Figure S40**A-B). This allows the assumption that xylose-activated signaling does not alter ion leakage events.

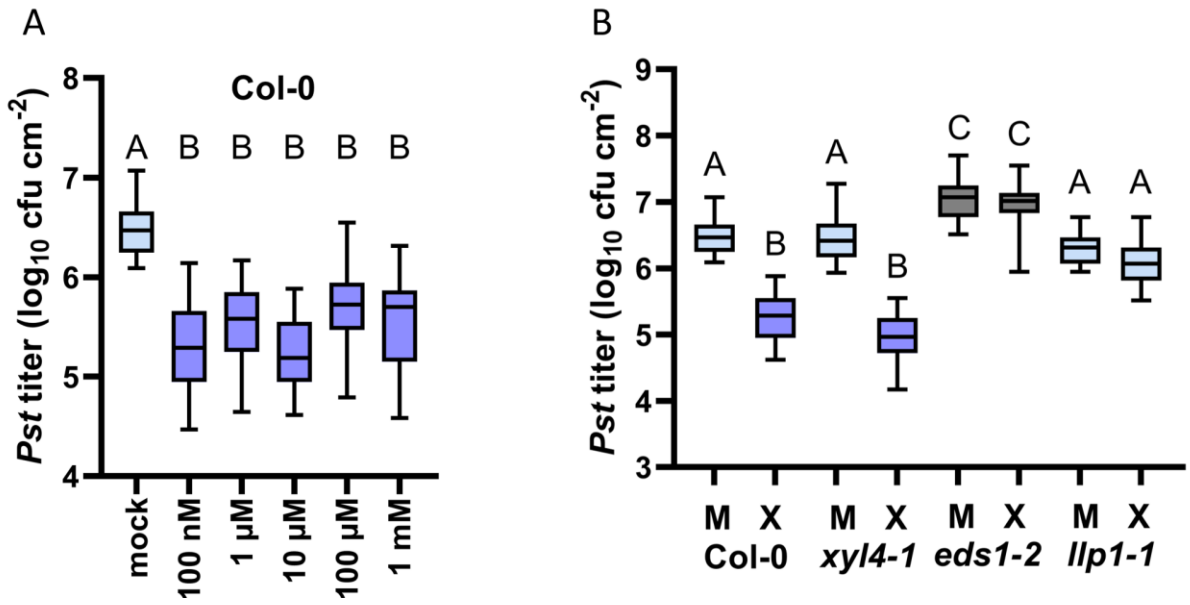

Figure 28: Exogenous xylose induces *EDS1*- and *LLP1*-dependent systemic defense against *Pst*.
Plants of the genotypes Col-0, *xyl4-1*, *eds1-2*, and *llp1-1* were inoculated with a mixture of D- and L-xylose, termed D-/L-xylose (10 µM (X) or another dose as indicated below the panels), or with a corresponding mock (M or mock as indicated below the panels). Three days after, two distal leaves were challenged with 10^5 cfu/mL of *Pst* and monitored for *in planta* bacterial titers 4 days after. *Pst* titers were evaluated in Col-0, *xyl4-1*, *eds1-2,* and *llp1-1* plants as indicated. Box plots represent average *Pst* titers of in total twelve (A) or seven (B) biologically independent experiments ± min and max value. Different letters above box plots indicate statistically significant differences for means (one-way ANOVA and Tukey's test for P=<0.05, for (A, Col-0): F(5, 189)=46.95, mock n=46, 100 nM n=34, 1 µM n=27, 10 µM n=35, 100 µM n=27, 1 mM n=26; for (B): F(7, 284)=43.20, Col-0 M n=46, Col-0 X n=35, xyl4-1 M n=46, xyl4-1 X n=30, eds1-2 M n=41, eds1-2 X n=25, llp1-1 M n=43, llp1-1 X n=26).

In a natural environment, diverse bacteria can perceive and take up D-xylose (Li et al., 2017b) or degrade xylose enzymatically by xylose isomerases, as shown for *Pseudomonas syringae* (*Ps*) strains (Feil et al., 2005). I thus asked myself if the *Pst* bacteria used in the above-described assays could be positively or negatively affected in growth when they get in contact with exogenous xylose. To this end, I

performed an initial test by cultivating *Pst* bacteria on plates with medium fortified with either 100 µM or 1 mM of D-/L-xylose, or a mock solution. By visual evaluation, fewer bacteria were growing on the medium supplemented with 100 µM of xylose when compared to the other two treatment plates (**Figure S41**A-C). This would indicate a suppressive effect of 100 µM of xylose on *Pst* growth.

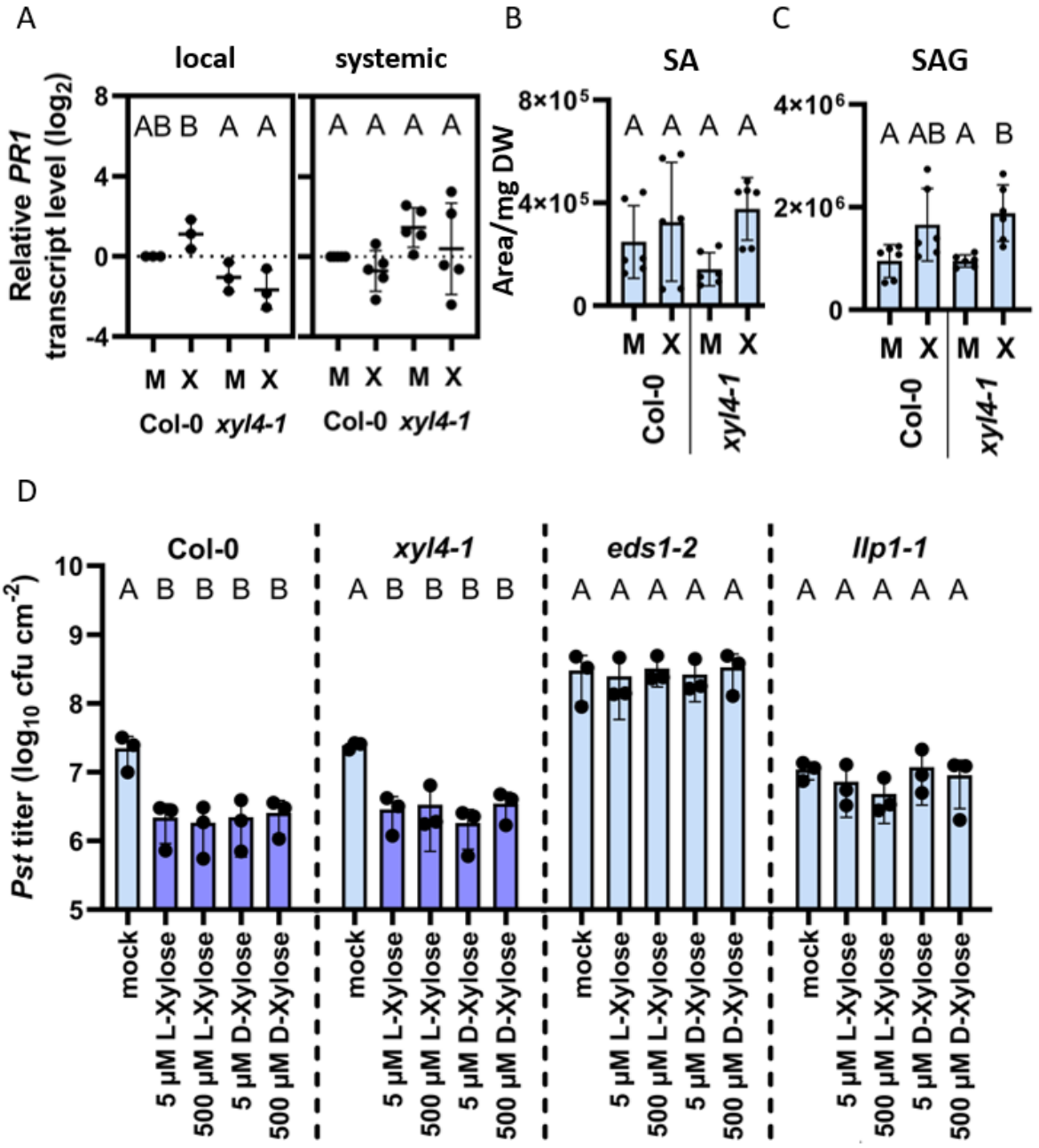

Figure 29: Exogenous xylose induces *EDS1*- and *LLP1*-dependent systemic defense against *Pst*.
Plants of the genotypes Col-0, *xyl4-1*, *eds1-2*, and *llp1-1* were inoculated with D- or L- or D-/L-xylose (10 µM (X) or another dose as indicated below the panels), or with a corresponding mock (M or mock as indicated below the panels). Three days after, gene expression for *PR1* was determined in locally inoculated and systemic leaves. Moreover, two distal leaves were harvested for metabolite analysis of SA (**B**) and SAG (**C**) or challenged with 10^5 cfu/mL of *Pst* and monitored for *in planta* bacterial titers 4 days after.

(**A**) Gene transcript accumulation was analyzed by qRT-PCR, normalized to that of *UBIQUITIN,* and is shown relative to the normalized transcript levels of the appropriate Col-0 mock (M) controls. Black dots represent three to five biologically independent data points, and lines indicate the respective mean values ± SD. The letters above the scatter dot plots indicate statistically significant differences (one-Way ANOVA and Tukey test, P=<0.05, for (local): n=3, F(3, 8)=8.812; for (systemic): n=5, F(5, 22)=2.713). (**B**-**C**) The metabolite accumulation was analyzed by LC-MS, calibrated to three internal standards, and normalized to the individual dry weight. Bars represent average metabolite abundance of six biologically independent replicates ± SD. Different letters above bars indicate statistically significant differences for means (one-way ANOVA and Tukey test for P=<0.05, for (B, SA): n=6, F(6, 18)=5.017; for (C, SAG): n=5-6, F(5, 18)=12.97). (**D**) *Pst* titers were evaluated in Col-0, *xyl4-1*, *eds1-2,* and *llp1-1* plants as indicated. Box plots represent average *Pst* titers of twelve (A-B) or three (F) biologically independent experiments ± min and max value. Different letters above box plots indicate statistically significant differences for means (one-way ANOVA and Tukey test for P=<0.05, for (Col-0): n=3, F(3, 10)=12.66; for (*xyl4-1*): n=3, F(3, 10)= 18.02; for (*eds1-2*): n=3, F(3, 10)=1.06; for (*llp1-1*): n=3, F(3, 10)=0.896).

I consequently conducted further experiments, in which I cultivated two different *Pst* strains in liquid culture in a well-plate format, where the medium was supplemented with either a xylose dose (0.1 µM – 1 mM) or a mock treatment. I subsequently monitored bacterial growth over 22 h. Three replicates with similar results showed that both bacteria comparably increased in density for all the treatments applied (**Figure S41**D/E), indicating that any xylose dose of 0.1 µM - 1 mM did not specifically affect *Pst* growth *in vitro*. I thus suggest that *in planta* growth and responses of *Pst* bacteria were not directly affected by exogenous xylose, and hypothesize that xylose-induced defense (**Figure 28**A-B, **Figure *29***D, **Figure S40**C) exclusively depended on the interaction of the plants with the bacterial counterpart, *Pst*.

3.11 Xylose-inducible defense is putatively linked to pathways involving SA and NHP-H2

In the following I aimed to elucidate possible transcriptional pathways involved in xylose-regulated defense in systemic tissues of Col-0 and *xyl4-1* plants. Therefore, I syringe-inoculated plants with either xylose, a corresponding mock solution, or left them untreated. Three days after, I determined the expression levels of defense-associated genes, including *PR1*, *XYL4*, *PDF1.2*, *VSP2*, and *LLP1* in local and systemic leaves. Interestingly, neither *XYL4,* nor *PDF1.2, VSP2, or LLP1* were specifically regulated in any of these tissues in Col-0 and *xyl4-1* (**Figure S42**A-D). However, *PR1* transcript levels were slightly repressed locally in *xyl4-1* in comparison to Col-0 after a treatment with xylose, whereas they seemed to largely remain unchanged in systemic leaves (**Figure 29**A). These findings suggest a *XYL4*-regulated expression of *PR1* in xylose-inoculated tissues.

I further assumed that xylose might affect relevant SA-associated metabolic pathways in order to modulate systemic defense in *A. thaliana*. For this purpose, we determined levels of systemically accumulating SA and SAG by LC-MS together with Birgit Lange, three days after Col-0 and *xyl4-1* plants had been inoculated with either xylose or a corresponding mock solution. SA levels were comparable for both genotypes and treatments applied (**Figure 29**B), whereas SAG showed a slightly clearer xylose-dependent induction in the *xyl4-1* mutants, which was also detectable, but insignificant in wild type plants (**Figure 29**C). The data indicate a systemic xylose- and SA/SAG-associated plant response, which may be dependent of *XYL4*. Potentially, an *EDS1*-associated pathway involving the xylose-derivative xylulose (e.g. *EDS1*-dependent repression of xylulose/xylose signals) might be necessary to stimulate SA-associated plant responses (**Table S18**) and thereby defense.

I further aimed to identify metabolic plant defensive pathways triggered by xylose against a pathogenic challenge. To this end I applied a secondary treatment with *Pst* in systemic tissues after a local treatment with xylose. Subsequently, Birgit Lange (HMGU) analyzed the accumulation of SA, SAG, AzA, Pip, NHP, and NHP-H2 after 24 h by LC-MS. The abundance of SA and AzA was lower in both genotypes, Col-0 and *xyl4-1* plants, when leaves were induced by xylose and challenged with *Pst* (**Figure 30**A/C). This indicates that metabolic responses prompting xylose-dependent changes in SA and AzA are regulated independent of *XYL4*. Interestingly, the regulation of EDS1 is suggested to modulate levels of SA and AzA during the establishment of SAR (El-Shetehy et al., 2015; Farquharson, 2017), thus xylose responses might control EDS1 action and associated metabolite accumulation at this timepoint investigated. Notably, levels of SAG were comparable for the treatments and genotypes investigated (**Figure 30**B), assuming a *XYL4*- and xylose-independent regulation. Furthermore, Pip and NHP levels were unchanged in Col-0 and *xyl4-1* genotypes after any treatment (**Figure 30**D-E), whereas the levels of NHP-H2 were repressed by xylose in Col-0 and equaled that of inoculated *xyl4-1* plants after any treatment (**Figure 30**F). Potentially, a stress-inducible release of xylose activates plant responses that represses the accumulation of NHP-H2 in order to promote systemic defense against pathogens like *Pst*. Moreover, *XYL4* presumably might interfere with a pathway modulating the accumulation of NHP-H2 (inter alia via a xylose-dependent feedback loop?) in order to control defense against (hemi-)biotrophic pathogens and systemic signaling (**Figure 25**, **Figure *26***).

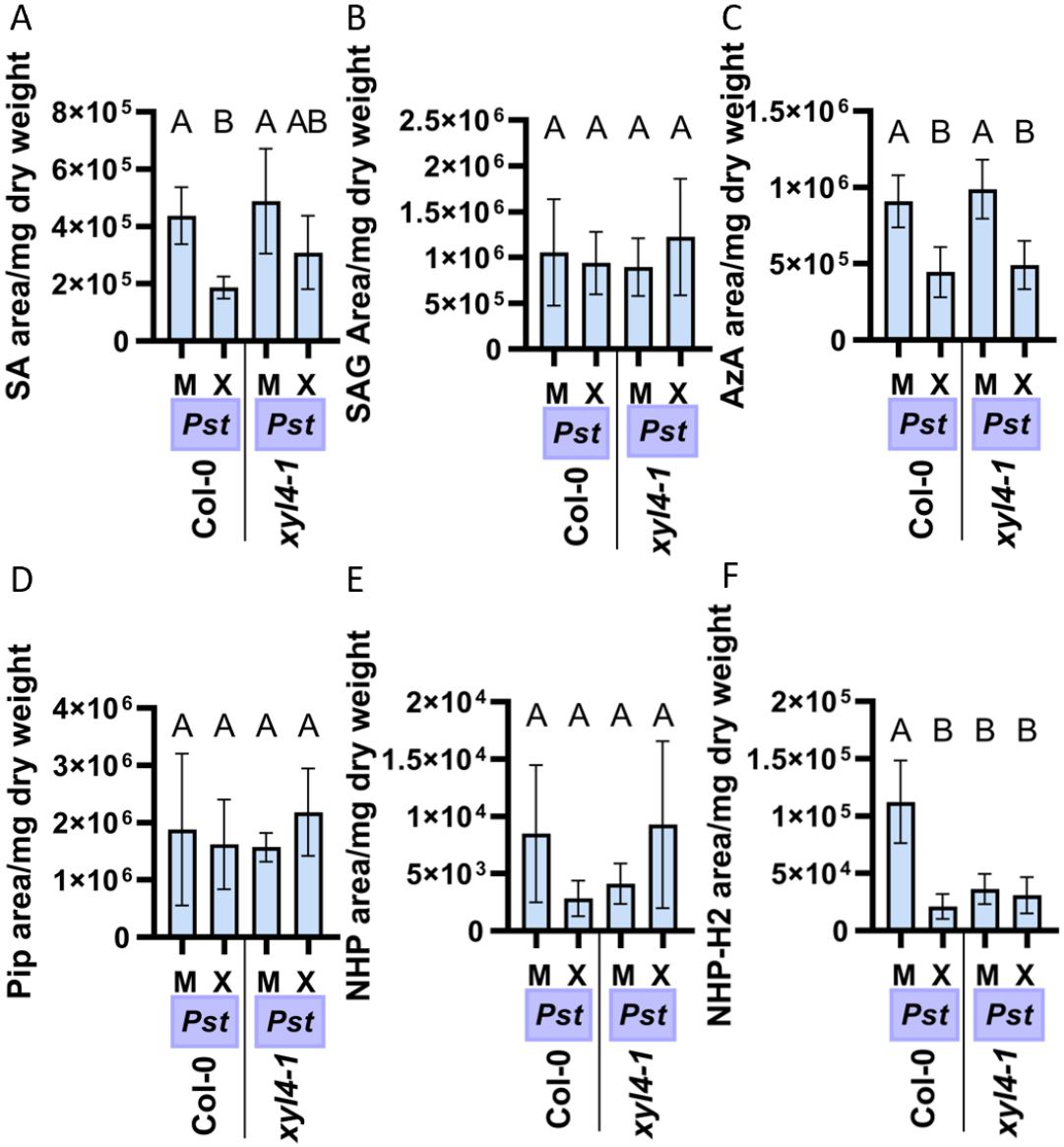

Figure 30: Exogenous xylose and *XYL4* repress the accumulation of NHP-H2 after a challenge with *Pst*.

Plants of the genotypes Col-0 and *xyl4-1* were inoculated with either 10 µM of D-/L-xylose (X), or with a corresponding mock (M). Three days after, two distal leaves were challenged with 10^5 cfu/mL of *Pst* and metabolites like SA (**A**), SAG (**B**), AzA (**C**), Pip (**D**), NHP (**E**) and NHP-H2 (**F**) determined one day after by LC-MS. The metabolite accumulation was calibrated to three internal standards, and normalized to the individual dry weight. Bars represent average metabolite abundance of six biologically independent replicates ± SD. Different letters above bars indicate statistically significant differences for means (one-way ANOVA and Tukey test for P=<0.05, for (A, SA): n=5-6, F(3, 18)=12.53; for (B, SAG): n=5-6, F(3, 18)=0.2313; for (C, AzA): n=5, F(3, 16)=10.53; for (D, Pip): n=5, F(3, 16)=0.4854; for (E, NHP): n=3, F(3, 8)=1.829; for (F, NHP-H2): n=5, F(3, 16)=8.164).

4. Discussion

Since 2014, hunger and numbers of under-nourished people increase worldwide (FAO, 2018). Food security is strongly dependent on key drivers affecting this trend: a direct link can be drawn to varying factors such as climate, landscape, (invasive) pests, and environmental pollution (Carvalho, 2017; FAO, 2018). In future, it will be a great challenge on the global scale to manage land use and crops to meet the need of the steadily growing population, which is predicted to reach 9.7 billion people in 2050 (Molotoks et al., 2021). One central question is to identify opportunities to farm sustainably, for example by reducing the application of chemical agents while improving plant growth, yield, and immunity (Guo et al., 2021; Sible et al., 2021; Yu and Li, 2021). Plants growing outdoors are exposed to diverse biotic and abiotic stimuli that collectively regulate plant yield and stability (Zandalinas et al., 2021). Thus, attention must be paid to investigate stress interactions of plants with their environment in more detail, and establish innovative farming solutions that secure and optimize crop production (Kim et al., 2021; Miladinovic et al., 2021).

In order to evaluate suitable farming methods, it is of fundamental importance to understand the mechanisms of molecular, interacting networks that drive stress and growth responses in plants. Essential interactors are phytohormones that modulate a complex network of synergistic and antagonistic regulations in plants during stress responses (Altmann et al., 2020; Aerts et al., 2021). These plant hormones are pivotal to regulate and balance plant growth, fitness, and yield (Ning et al., 2017; Chandran et al., 2020) and moreover inducible plant defense responses such as ISR and SAR under stress (Vlot et al., 2021). However, signaling pathways and molecular mechanisms promoting (inducible) defense responses and plant growth are still under debate (Park and Ryu, 2021). Recent research suggests that SAR signaling involves the modulation of metabolic pathways (Gao et al., 2021; Zeier, 2021), lipids (Cavaco et al., 2021) and modifications of cell wall components as detectable by specific sensors (Rui and Dinneny, 2020; Lorrai and Ferrari, 2021; Molina et al., 2021). Regulators of such pathways might have a key functional role in the establishment of systemic plant defense and moreover the regulation of crop growth.

In the context of SAR, the role of cell wall components and carbohydrate metabolites for the establishment of an effective defense has yet to be fully elucidated. In this work, I show that the activation of local defense (ETI) and

systemic SAR signaling is promoted by *XYL4*, which putatively codes for a plant growth-related protein that modulates pectin structures. *XYL4*-mediated responses triggered by bacterial stress involve a transcriptional regulation of SA- and JA-related pathways. Moreover, *XYL4* causes alterations in the plant metabolism that presumably modulate glucosylation events, and additionally pathways of the glycolysis and cell wall-bound polyamines.

4.1 *XYL4* potentially modulates ETI via wounding-associated signals

4.1.1 Bacterial treatments (PTI, ETI) trigger local *XYL4* expression

It was previously described that the absence of *EDS1*-dependent signals suffice to eradicate ETI in response to certain groups of pathogenic effectors (Aarts et al., 1998). Moreover, it was shown that inducible defense responses triggered by the pathogenic effector AvrRpm1 induce signaling cascades in *A. thaliana* that culminate in NLR-promoted ETI (Mackey et al., 2002; Jones and Dangl, 2006). In this study, I showed that *XYL4*, of which protein accumulation can be related to *EDS1* (Breitenbach et al., 2014), contributes to local defense (**Figure 18**C) and systemic resistance such as SAR (**Figure 21**A). My findings specifically indicate that an infection by spray or infiltration inoculation with the (hemi-)biotrophic bacterium *Pst/AvrRpm1* induces a local expression of *XYL4* in *A. thaliana* leaves (**Figure 17**A-B). Likewise, *Pst*-inoculated plants were induced for the expression of *XYL4* two or three days after infection (**Figure 17**A-B). However, defense against *Pst* remained unaffected in plants carrying mutations in *XYL4* (**Figure 18**B/D). Furthermore, I suggest that virulent/avirulent status of a pathogen affects the strength of induction of *XYL4* transcription (**Figure *17***A-B) and moreover affects JA-signaling genes *PDF1.2* and *VSP2* (**Figure *19***B-C). Therefore, a pathogen-specific pattern of transcript induction may additionally influence the outcome of *XYL4*-related plant defense responses.

Notably, it may be the case that although *XYL4* transcripts are locally regulated by *Pst* and *Pst/AvrRpm1* (**Figure 17**A-B), *XYL4* functions differently in the *Pst/AvrRpm1*-inducible (NLR-linked) defense pathway that culminates in ETI as compared to *Pst*-induced PTI. Interestingly, another study showed induced *XYL4* transcripts levels already one day after plants had been syringe-infiltrated with a high concentration (10^8 cfu/mL) of *Pst/AvrRpm1* or *Pst*, with *Pst* being more effective to stimulate *XYL4* expression (Kemmerling et al., 2011). This indicates that an early induction of *XYL4* can be stimulated by *Pst*, whereas induction after *Pst/AvrRpm1* at the same timepoint is rather low. Such from my studies differing

pattern for *XYL4* transcription (**Figure 17**A) as described by Kemmerling et al. (2011) will probably be due to the high bacterial titers used for infiltration inoculation, the short exposure time to light during incubation after infection (8 h day/16 h night), and an early sampling 24 h after infection. It would be further interesting to follow the trend of *XYL4* transcript accumulation after prolonged incubation (>24 h) when applying the above-described conditions to *Pst* or *Pst*/*AvrRpm1*-infected plants. It should be moreover clarified which plant- and/or *Pst* virulence-related stimulus – including PAMPs, MAMPs, DAMPs, or a combination thereof due to simultaneous triggers of (mechanical) wounding and pathogen infection promotes *XYL4* expression during defense, besides effectors such as *AvrRpm1* (**Figure 18**C). This information will help to identify triggers and signaling pathways which stimulate *XYL4* expression and thereby triggered stress signaling events. In sum, I hence propose that *XYL4* is a stress-inducible gene whose local expression levels are dependent on pathogen type, amount of inoculum and time of investigation.

4.1.2 *XYL4* is associated with wounding responses rather than with stomatal defense

Stomata, cell walls and the apoplastic space are probable areas of a plant where plant-pathogenic signals can be initially perceived. Upon interaction of a plant with pathogens, downstream responses are launched that can promote transcriptional events and immunity. Interestingly, a *XYL4*-dependent ETI defense was clearly recognizable in spray-inoculated plants but was absent after infiltration inoculation by syringe (**Figure 18**A/C). I consequently hypothesize that the method of plant inoculation might modify *XYL4*-associated pathways, including defense. Possibly, such plant responses are triggered in dependence of the severity of plant cell damage such as mechanical wounding (as incurred, for example, during syringe inoculation); plant responses might thereby associate with stomatal defense (Melotto et al., 2017) or injury-related immunity (Savatin et al., 2014).

Initially, I asked if differences in plant responses after infiltration and spray inoculation were due to *XYL4*-regulated stomatal defense as *Pst*/*AvrRpm1* titers grew to higher levels in spray-inoculated *xyl4* mutants than in wild type plants, whereas bacterial titers in syringe-inoculated plants were comparable (**Figure 18**A/C). Defense responses associated with stomata involve a PAMP-inducible closure of guard cells (e.g. triggered by bacteria) that can restrict the mobility of invading pathogens (Melotto et al., 2006; Schulze-Lefert and Robatzek, 2006). The movements (opening/closure) of stomata and consequently gas exchange and

pathogen entry via these natural pores is suggested to be controlled by either interactions of EDS1/PAD4 (Mateo et al., 2004), xylem-synthesized ABA, climatic factors (involving humidity, water potential, temperature), or carbon dioxide levels (Lim et al., 2015; Li et al., 2019b). Notably, *XYL4* transcript accumulation *in planta* and in suspension cells can be stimulated by treatments with exogenous ABA (Winter et al., 2007; Böhmer and Schroeder, 2011), allowing the assumption that ABA-XYL4 might contribute to stomatal movements. Additionally, the differentiation of meristematic cells into stomata involves the activation of *XYL4* in dependence of epidermis-modifying genes like *SCREAM* and *SPEECHLESS* (Pillitteri et al., 2011). These data suggest that *XYL4* expression is (at least partially) related to the formation and number of functional guard cells. However, if a (ABA-)*XYL4*-asociated pathway affects stomatal regulation during defense, I would expect to find comparable resistance responses in *xyl4* mutant plants after spray inoculation with any bacterial pathogen including both virulent *Pst* and avirulent *Pst*/*AvRpm1*. Because I observed a *XYL4*-dependent defense component after spraying plants with *Pst/AvrRpm1* but detected no differences in *Pst* propagation after inoculation (**Figure 18**C-D) - thus I did not observe consistent plant reactions with multiple pathogens -, the data exclude that *XYL4* participates in stomatal immunity.

Instead, I assume that ETI/basal defense responses upon infection with *Pst* and *Pst*/*AvrRpm1* correlates with *XYL4*-dependent wounding reactions in *A. thaliana*. As transcript levels of *PR1* and *LLP1* were comparably promoted in bacteria-infected leaves of wild type and *xyl4-1* plants at 2 dpi as compared to their control-treated plants (**Figure *19***A), I suppose that *XYL4* does not modulate the local expression of these genes during defense. However, transcript levels of *LLP1* (at 1 dpi) and *PR1* (at 3 dpi) in systemic tissues were elevated in SAR-induced wild type plants and both moreover equaled that of *xyl4-1* mutant plants after any treatment (**Figure *21***C-D). These findings suggest that the systemic expression of *LLP1* and *PR1* may be similarly regulated and in a *XYL4*- and ETI/*Pst*/*AvrRpm1*-dependent manner during defense (**Figure 31**). In addition, *XYL4* transcript accumulation by trend is slightly stronger in *Pst*/*AvrRpm1*-triggered plants after inoculation with pressure and a syringe than after spray inoculation (**Figure 17**A-B), implying that *XYL4* is responsive to mechanical wounding. To that, former studies demonstrated that *XYL4* transcripts considerably increase at 2-12 hours after a wounding stimulus (up to 16-fold when compared to the non-stressed state) (Kilian et al., 2007; Guzha et al., 2022). In sum the data suggests that inoculation-related wounding (infiltration- and spray-inoculation) might interfere

with *XYL4*-associated ETI responses. To understand better which defense signals (early wound-related) may be triggered via *XYL4*, a detailed search for associated signaling pathways should be carried out.

One important *XYL4* signaling route triggered by injury may include JA signals: In my study, SAR-induced wild type plants showed an elevated accumulation of *PDF1.2* systemically at 1 dpi, whereas such promotion was absent in *xyl4-1* mutants (**Figure *21***B). Thus, it is possible that *XYL4* promotes JA-associated responses to wounding, also early after infection of *A. thaliana* with a hemi-biotrophic bacterium such as *Pst/AvrRpm1* used here to induce SAR. Notably, injury responses promote the expression of the genes *PDF1.2* and *JASMONATE-ZIM-DOMAIN PROTEIN 10* (*JAZ10*), and this response is dependent on *XYL4* (Guzha et al., 2022). Moreover, *XYL4* partially regulates the synthesis of JA derivatives (such as jasmonoyl-L-isoleucine, JA-Ile) either after an infection with *Bc* or at about 2 hours after wounding (Guzha et al., 2022). Therefore, I hypothesize that *XYL4* affects early systemic JA signaling during the establishment of SAR. Injury responses could thereby play a role and influence plant defense gene expression as well as metabolite accumulation (Penninckx et al., 1998; Yan et al., 2007; Zhang and Turner, 2008; Jacobo-Velázquez et al., 2015; Howe et al., 2018; Marquis et al., 2020). Years ago, Truman et al. (2007) supposed a pivotal role for jasmonates in the early induction of SAR signaling. These JA signals might compromise SA defense and ETI due to local antagonistic cross talk between the JA and SA signaling sectors in inoculated plants (**Figure *21***A-B). Additionally, because the SAR-deficient phenotype of *xyl4* mutant plants appeared more robust than local defense phenotypes in response to *Pst/AvrRpm1* (**Figure *17***A, **Figure *18***A, **Figure *21***A), I posit that such an additional function of *XYL4* is associated with the establishment of SAR. Together these data suggest that *XYL4* may modulate components of the JA pathway and thereby have a regulative function in an initial phase of SAR.

4.1.3 Crosstalk of JA/ET and SA as modulatory key of *XYL4*-related signaling during defense and plant root growth?

A systemic repression of *PDF1.2* and *LLP1* as an early response (at 1 dpi, **Figure 21**B-C) and a suppressed accumulation of transcripts of the SA-marker *PR1* as a late response (at 3 dpi, **Figure 21**D) potentially points to a cooperatively modulated SA-JA crosstalk during SAR as described earlier (Breitenbach et al., 2014; Sales et al., 2021). Hereby, the regulation of *PDF1.2* expression via pathways of (wounding-inducible) *XYL4* and *LLPs* (LLP1-3) may be essential. Notably, an

infection with necrotrophic *Bc* strongly induces transcription of *PDF1.2* in genetically modified plants that overexpress *XYL4* (Guzha et al., 2022), which indeed suggests that *XYL4* downstream signaling stimulates JA/ET routes and might thus modulate JA-SA crosstalk (**Figure *6***). Interestingly, JAZ10, whose gene is *Pst*-inducible (Demianski et al., 2012) and potentially associates to electric signaling throughout cell membranes (Kumari et al., 2019), was formerly described to bind other proteins like the EDS1/PAD4-controlled transcription factor MYC2 (Moreno et al., 2013; Cui et al., 2018). MYC2, in turn, has diverse regulative functions during a hormonal SA-JA crosstalk by modulating the expression of genes like the SA-related *ICS1* and *BSMT1*, and the JA-related *PDF1.2* (Kazan and Manners, 2013). I therefore assume that pathways following a local SAR stimulus trigger *XYL4* signals that further may affect JAZ10-MYC2 in distal leaves, and by this signal an early induction of *PDF1.2* systemically (**Figure 21**B). Such SA-JA crosstalk may furthermore influence the transmission of vascular and volatile defense-inducing signals (**Figure *25***,**Figure *27***). As an example, the emission of terpenoid volatiles is supposed to be stimulated by regulations of SA-, LLP1-, and JA/*JAR1*-JA-Ile-dependent responses (Wenig et al., 2019; Frank et al., 2021). Possible co-functional roles of *XYL4* with *LLP1* and other *LLP*s during defense (inter- and intra-specific SAR responses) and in conjunction with long-distance signaling and ETI will be discussed later (see section 4.2).

Recent publications suggest that *JAZ10* acts in JA- and NO-controlled root growth inhibition (Barrera-Ortiz et al., 2018; Liu et al., 2021a). Thus, the formation of roots might be partially regulated by concerted modulations of *XYL4*, JA/*JAZ10* and NO. Interestingly, *xyl4* mutants displayed a phenotype with a moderately repressed growth of roots after the exposure to MeJA (or salt) in comparison to wild type plants (**Figure 24**A-B). MeJA-induced *xyl4* seedling and wild type plants responded with similar levels of *PR1* (and a slight but rather negligible induction of *UGT76B1*), while levels of *PDF1.2* were like that of mock-treated plants (**Figure 24**C-E). I therefore assume that *XYL4* at least partially contributes to root growth – potentially via a JA-associated pathway. Additionally, the (marginal) effect of *XYL4* on root development may moreover modulate systemic shoot-root-shoot communication (as part of a signaling loop) which can relate to plant growth and systemic/inducible defense as reviewed (Groen, 2016).

4.2 *XYL4*, *LLP1-3*, and *EDS1* might co-regulate SAR signaling events

4.2.1 Modification of systemic wound responses via *EDS1* and *XYL4*

The data from my studies suggest that systemically expressed *LLP1* (at 1 dpi) and *PR1* (at 3 dpi) transcripts might be regulated via *XYL4*- and/or *EDS1*-dependent wounding signals (see **Figure 21**C-D and compare mock (M) values). However, plant immunity after an additional infection with *Pst* (**Figure 21**A) was not affected, which let assume that slight wound responses upon syringe-inoculation trigger a *XYL4*/*EDS1*-associated but not a defense-inducing expression (level) of *LLP1*/*PR1*. However, these data needs confirmation by also comparing untreated samples against syringe-inoculated plants, as analyzed for tissues of another set of plants (**Figure S42**). Thus, in addition to the injury signals exclusively associated with *XYL4*/*EDS1*, there must be other factors associated with *PstAvrRpm1* that are triggered via *XYL4*/*EDS1* and provide for an effective establishment of SAR (**Figure 21**A). From my own experience, I can confirm that more severe injury to leaves, as occasionally occurs during syringe-infiltration of plants (especially when conducting SAR experiments for the first time), resulted in abolished SAR in all genotypes tested, including wild type plants (data not shown). This was also confirmed in discussions with other laboratory members. These results suggest that severe wounding prevents plants from establishing SAR-like defenses. When performing SAR experiments, plants should be thus infiltrated very carefully to obtain comprehensible results and be able to evaluate plant responses in detail.

In particular, local injury stimuli could influence (*XYL4*) signaling during SAR and/or priming alongside other triggers such as bacteria or chemicals as reviewed (Conrath, 2006). However, hormonal signaling triggered by wounding (or abiotic/biotic stress) may enhance systemic defense responses that depend on PTI/ETI-associated signaling pathways (Peng et al., 2018; Ngou et al., 2021; Yuan et al., 2021). Signals generated upon wounding and modulated by *XYL4* or EDS1 and/or further downstream cascades (see **Figure 21**B-D, **Figure *26***A/E, **Figure 30**F, **Table *13***, **Table S*19***) can potentially be transmitted directly from leaf to leaf or from leaf to root. Proteins that accumulate in the apoplast, like the *EDS1*-dependent and *AvrRpm1*-related XYL4, LLP1 and LLP3 (Breitenbach et al., 2014) could thereby be prominent (co-regulated) modulators for such signaling events upon injury, which then control responses related to SA-JA crosstalk and defense. Interestingly, wound-inducible ROS like singlet oxygen (Prasad et al., 2020) regulate a signaling cascade involving *EDS1*, SA, *PR1*, synthesis of JA precursors (such as oxylipins, OPDA), and induction of cell death responses (Ochsenbein et

al., 2006). Elevated SA levels appear to be relevant to transmit wound responses as a signal downstream of JA signaling pathways in later stages of SAR (Doares et al., 1991; Pena-Cortés et al., 1993), with SA specifically suppressing OPDA and further biosynthesis of oxylipins and JA in local and systemic tissues (Lemos et al., 2016; Gao et al., 2020). It is possible that SA-inducible immunity is thereby regulated by transcriptional reprogramming (including induction of *ICS1* and EDS1 antagonism of the JA-regulator MYC2) via *EDS1*-associated cascades (Cui et al., 2017; Cui et al., 2018; Bhandari et al., 2019). Results from a previous study suggest that *EDS1* transcripts are not regulated 6-24 h after injury, as levels were comparable in untreated and mechanically wounded plant leaves (Falk et al., 1999) – assuming that EDS1 may rather function in later stages of the injury signaling cascade (compare mock-treated plants, **Figure 21**D). It may be worthwhile to investigate whether the expression of *EDS1* in inoculated or systemic tissues is dependent on *XYL4*, which should be also examined for other timepoints than those mentioned in Falk et al. (1999).

In the context of SAR, it would be interesting to investigate whether immunomodulatory PR proteins or peptides could be stimulated by *XYL4* and/or *EDS1* signaling pathways during injury (compare with late *XYL4*/SAR-related induction of *PR1*, **Figure 31**). Previous studies have described promoter-targeted responsiveness of *PR1* and concomitant activation of *PR1*-associated signals like PR peptides after wounding (Warner et al., 1993; Boava et al., 2011; Chen et al., 2014). In tomato, for example, injury (or treatment with MeJA) stimulates the accumulation of PR1b peptides (Chen et al., 2014). PR1b can also induce the expression of stress- and SAR-associated genes when applied exogenously, indicating that PR1b might function as a wounding and MeJA-inducible DAMP that promotes SA-related defense signaling (Chien et al., 2015; Vega-Muñoz et al., 2020). Future analyses could therefore determine if comparable immune-related (SAR-modulating) peptides are triggered via a pathway involving *XYL4* after syringe inoculation or wounding.

4.2.2 *XYL4*-dependent immune signaling involves *FMO1* and DAMPs?

As findings of my studies strongly suggest that *XYL4* controls both SAR signal generation in local, infected tissues and of SAR signal recognition/ propagation in systemic leaves (**Figure 25**, **Figure *27***), I consequently hypothesize that *XYL4* acts upstream in SAR signaling cascades (**Figure 31**, **Figure *32***). This is further corroborated by the fact that *XYL4* signaling in SAR influences both phloem-mediated and airborne systemic signaling (**Figure 21**A, **Figure *25***, **Figure *26***A,

Figure *27*). I therefore wondered what factors are required in a *XYL4*-dependent manner for plants to effectively generate and transmit locally induced signals to distant tissues. I suppose that plants trigger responses after inoculation or infection (for example at the site of inoculation involving cuticle, epidermis, stomata, and cell wall) that could play a central role in the early regulation and/or establishment of SAR.

Results of leaf petiole exudate assays suggest that *Pst*/*AvrRpm1*-associated systemic signaling via the vasculature in petiole exudate-inoculated plants and an effective defense promotion against a secondary infection with *Pst* depends on *XYL4* (**Figure *25***A-B). These data indicate that *Pst*/*AvrRpm1*-*XYL4*-associated immune-modulatory molecules are transmitted via the vasculature to distant leaves, which subsequently trigger systemic defense after passing a *XYL4*-dependent recognition process. *XYL4*-related signaling thereby can be thought to be independent of the accumulation of Pip or its derivatives NHP and NHP-H2 after a secondary challenge with *Pst* (**Figure *26***B,D-E). However, plant responses including an early synthesis of NHP locally, systemically and in phloem sap, as shown for mono- and dicotyledonous species including cucumber (Schnake et al., 2020), might be dependent of a *XYL4*-stimulated expression of (ETI-related) *FMO1* (**Figure *26***A). An ETI-*XYL4*-dependent accumulation of Pip, NHP and NHP-H2 levels might be thus detectable in PetEx-inoculated plants and could be moreover compared to levels in *Pst*/*AvrRpm1*-, PetEx-inoculated, and distal untreated tissues before applying a secondary infection. Notably, *FMO1* might signal the induction of defense in systemic tissues in a manner dependent of *XYL4* and injury-induced responses, (compare responses of recipient plants inoculated with PetEx of those of mock-inoculated wild type plants, **Figure *25***A, **Figure *26***A). Such early *XYL4*-*FMO1*-associated signals could further influence systemic NHP-dependent signals, such as the glycosylation of NHP after secondary infection of the plants with *Pst* (**Figure 26**E). Notably, wild type plants expressed *FMO1* transcripts in slightly higher levels at 1 day after their inoculation with PetEx of SAR-induced wild type donors than after an infection with *Pst*/*AvrRpm1* (compare levels of **Figure 22**E, **Figure *26***A). Such differences may arise because petioles contain an already more developed mixture of molecules and gene transcripts than plants infected ~24 h ago (Note: exudates were taken from infected plants that were incubated with the pathogen for 24 h and leaf petioles immersed in water for an additional 48 h to obtain exudates; a total of thus ~72 h during which exudates could be enriched with immunomodulatory compounds). These findings also indicate, that *FMO1*

might be triggered during both early (**Figure 22**E) and later stages of responses (**Figure *26***A) that modulate SAR signaling (might be triggered via a fortification loop involving *XYL4*).

My studies moreover suggest that *XYL4* may repress an early transcription of *PR1*, *ALD1* and *FMO1* in systemic tissues of mock-treated plants, while he expression of *UGT76B1* seems to be promoted (**Figure 22**A/D-F). A signaling pathway via *XYL4-FMO1* (and maybe therefore also levels of NHP) may thus be (partially) dependent on injury-, SA-, and UTG76B1-(co-)related responses. Wounds (at leafy tissues) as which incurred due to (syringe-) inoculation may trigger responses as known for DAMP signaling. Perception of DAMPs further promotes immune responses in plants in a similar manner as known for PTI (Yamaguchi and Huffaker, 2011), whereby pathways signaling via SA and JA are activated (Wrzaczek et al., 2009; Chen et al., 2014; Ross et al., 2014; Poncini et al., 2017). Interestingly, a Pip-associated activation of SAR is dependent on the MAMP co-receptors BRI1-ASSOCIATED RECEPTOR KINASE1 (BAK1) and BAK1-LIKE1, both of which are suggested to sense DAMPs at the plasma membrane (Krol et al., 2010; Yamada et al., 2016b; Wang et al., 2018c). Consequently, injury/DAMP-driven responses may activate XYL4-dependent and Pip/*FMO1*/NHP-related signals and furthermore modulate SA/JA signaling networks (also systemic SAR-related JA/ET responses as shown **Figure 21**A-B, **Figure *32***) in *A. thaliana* (Hillmer et al., 2017).

As suggested earlier, XYL4 could be involved in the generation or propagation of a signal perceptible by LLP1 that originates from a signaling pathway involving JA, *LLP3*, apoplastic and/or cell wall components (Breitenbach et al., 2014; Wenig et al., 2019; Sales et al., 2021). XYL4 could thus function as an extracellular cell bound PRR that tracks long-distance migrating molecules, including DAMPs near the site of pathogen inoculation or induction of other stress. DAMPs comprise danger or injury signals such as endogenous compounds, for example (stress-inducible) extracellular ATPs or NADPs, fragmented plant self-DNA, nucleotides, fractions of cell wall polymers, proteins, or peptides that can induce cell damage repair or act as inducers of long-distance signaling (Ferrari et al., 2013; Savatin et al., 2014). DAMPs may moreover comprise *XYL4*/*EDS1*-dependent molecules like cell wall structure-associated compounds– and probably molecule(s) as detected in one of the screens that I performed for alcohol-soluble or -insoluble plant materials (**Table 12**, **Table S19**). Notably, DAMPs were previously described to also modulate systemic (SAR) signaling: DAMPs thereby induce transcription of stress-related genes, the accumulation of (PR1) peptides and others stress-related

processes after plants are confronted with microbes, pathogens, or wounding events (Chien et al., 2015; Ádám et al., 2018; Hou et al., 2019; Li et al., 2020b; Vega-Muñoz et al., 2020). During (natural) infection with pathogens, processes related to DAMPs, PAMPs and MAMPs come together to trigger more pronounced plant defense responses than, for example, mechanical wounding alone (which signaled mainly via DAMPs). In sum, I therefore conclude that potential candidate LLP1-perceptible compounds may be closely linked (directly or indirectly) to *XYL4*/*EDS1*-dependent signaling pathways including DAMPs, PAMPs and MAMPs. Interestingly, LLP1 has been shown to support the perception and propagation of systemically mobile signals that originate from interconnected pathways involving SA and/or Pip/G3P (Breitenbach et al., 2014; Wenig et al., 2019; Sales et al., 2021). Notably, ETI-inducible levels of SA, Pip, and G3P were either promoted (SA, Pip) or repressed (G3P) in an *EDS1*- and/or *XYL4*-dependent manner (**Table S18**, **Table S19**). This supports the above-mentioned assumption that pathways via *XYL4* and additionally *EDS1* may contribute to the generation of SAR signals that can be perceived by LLP1 (**Figure 32**) – thus modifying a route (phloem/airborne) of a systemically accumulating substrate.

4.2.3 Local signals via *XYL4* and *LLP3* promote systemic defense

Surprisingly, *xyl4* plants inoculated with PetEx of mock-induced (wounded) wild type plants resulted in less bacterial titers after a challenge infection with *Pst* as compared to wild type recipient plants (**Figure *25***A). It is thus possible that *xyl4* mutants (still) respond to immunomodulatory wound-inducible signals present in PetEx of wild type plants, an effect that was not evident in wild type plants inoculated with the same PetEx solution (**Figure *25***A). *XYL4* might hereby recognize systemically detectable wounding signals involving *XYL4*-dependent regulated transcripts of *PR1*, *LLP3*, *ALD1*, *FMO1*, or *UGT76B1* (**Figure *22***A/C-F). Potentially, XYL4 proteins may detect/respond to (*XYL4*-independent?) signals generated downstream of one of those transcriptional pathways. Additionally, wild type plants and *xyl4* recipient plants both do not respond to any PetEx solution from *xyl4* donors (**Figure *25***B), suggesting that PetEx of *xyl4* donors lack the accumulation of immunity-promoting molecules after any treatment by syringe. However, PetEx of mock-treated, *xyl4* donor plants moderately reduced the propagation of a *Pst* challenge inoculum in wild type recipient plants (**Figure *25***B), suggesting that *XYL4*-dependent and injury-related molecules interfere with systemic defense. Because the same was not observed using PetEx from untreated *xyl4*-donor plants (**Figure 25**C), the dissemination of defense-active signals in *xyl4*

mutant plants might result from responses to wounding, also during a mock, control treatment. In summary, I therefore hypothesize that signals via *XYL4* are involved in the generation/accumulation or transmission of defense-inducing signals in inoculated tissues, involving responses that are partially modulated by injury-related signals.

Recently, a model was elaborated describing that local wounding responses might play a role for SAR signal generation upon infection with pathogens such as bacteria. Sales et al. (2021) proposed that lesions, as formed due to local SA triggers and HR reactions during SAR (Betsuyaku et al., 2018), source JA signaling and initiate long-distance communication within a plant. In support, SAR-inducible signals in tobacco plants prompt a local increase in JA levels (e.g. 6 - 48 hours post infection) that are suggested to precede the fortification of SA signals detectable 72 - 120 hours post infection with a (biotrophic) tobacco mosaic virus (Zhu et al., 2014). Similarly, an exogenous application of JA or the stress signaling molecule MeJA amplifies the production of SA and moreover MeSA (Zhu et al., 2014). As specifically the systemic accumulation of SA is relevant to establish SAR (Vernooij et al., 1994; Vlot et al., 2021), JA thus might play an important role to prepare plants for SA-related defense.

At the site of pathogen infection, JA signaling is presumably associated with the induction of SAR responses in dependence of *LLP3* (Sales et al., 2021). Thereby, a pathway via *LLP3* is assumed to stimulate the generation or transmission of SAR signals from inoculated areas. As the *LLP3* transcript expression can be promoted locally by the exogenous application of MeJA and in a manner independent of *EDS1* (Sales et al., 2021), this indicates that *LLP3* potentially functions downstream of MeJA/JA in a pathway separate from *EDS1*. Notably, a spray treatment with SA in wildtype plants (and *eds1-2* mutants) did not affect transcript accumulation of *LLP3* (Sales, 2021), assuming that *LLP3* predominantly contributes to (local) JA signaling and not to signals via (*EDS1* and) SA in order to establish SAR. If *XYL4* (and JA-Ile) also feeds into a pathway like the so far suggested one for *LLP3* during the exposure to stress, this might indicate that *LLP3* and *XYL4* contribute to an initial defense phase of SAR involving the JA signaling network (**Figure 31**).

It such network, it is possible that *LLP3* might be triggered downstream of *XYL4*. In support, SAR-stimulated *xyl4* mutant plants show lower systemic expression of *LLP3* than wild type plants after an induction with *Pst/AvrRpm1* during the early phase of defense (at 1 dpi, **Figure 22**C), suggesting that *XYL4* might function

upstream of *LLP3*. It would be interesting to further evaluate if a (more pronounced) *XYL4*-dependent induction of *LLP3* can be also detected in pathogen-inoculated tissues. In addition, as the early systemic accumulation of *PDF1.2* transcripts is supposedly regulated in dependence of *XYL4* (at 1 dpi, **Figure 21**B), it needs to be examined if *LLP3* gene expression may be regulated simultaneously with such *XYL4*-associated JA/ET signals during plant-pathogen interaction and SAR. In consequence, I suppose that local signals related to *XYL4*/functional XYL4 might act in the same pathway or in parallel to that of *LLP3*/LLP3 (triggering early XYL4-LLP3 systemic signaling, **Figure 31**) during the onset of SAR signaling events.

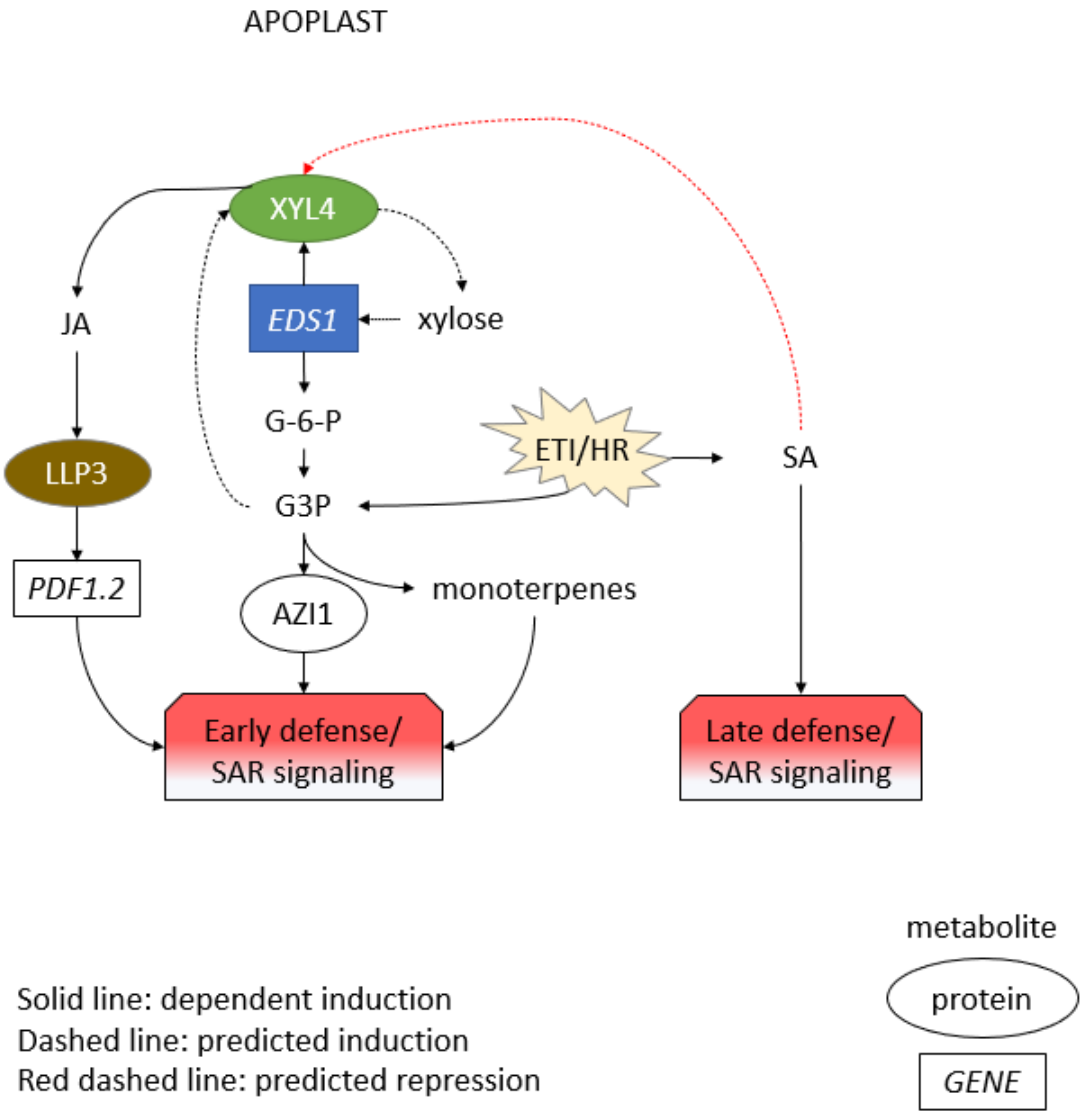

Figure 31: SAR signaling model: locally triggered responses upon a biotic stimulus for ETI/HR.
Pathogen-induced ETI stimulates G3P at the area of infection, which further might trigger early signals over XYL4 and JA. At later phases, SA accumulates in the apoplast and represses pathways including XYL4, while SA-dependent signaling towards distal parts is fortified. Modified after Sales et al. (2021) and Wenig et al. (2019).

Furthermore, *XYL4* potentially affects SAR signal generation or the transmission of vascularly mobile and airborne molecules (**Figure 25**, **Figure *27***) in dependence of pathways including *LLP3* (Wenig et al., 2019; Sales et al., 2021). Their functional proteins XYL4 and LLP3 might hereby (co-)regulate transcription of defense signaling genes and moreover the synthesis of metabolites necessary for intra- and inter-plant communication. It would be thus interesting to determine *in planta* functions of both proteins. I therefore performed modeling analyses to predict protein-ligand binding for XYL4 and LLP3 by using online software tools such as COACH-D (Wu et al., 2018b) and 3DLigandSite with Phyre2 (Wass et al., 2010; Kelley et al., 2015). According to the molecular structure and functional sites, XYL4 proteins are anticipated to have binding sites for diverse glucose derivatives such as ß-D-glucose/ß-D-glucopyranose, glucoside and N-Acetyl-D-Glucosamine (D-GlcNAc). XYL4 might thus function as receptor perceiving changes in levels of D-glucose (a well-known phloem-mobile signaling molecule; Rolland et al., 2006), or specific glucosylated molecules (such as NHP-H2, SAG; Bauer et al., 2021), or biopolymers as formed from the molecule D-GlcNAc (such as fungal chitin, a PAMP; Löffler et al., 2014). Notably, LLP3 proteins are predicted to bind diverse molecules such as manganese, calcium ions, α-D-glucopyranose, α-D-mannopyranose, α-D-galactopyranose and methyl-α-D-galactose (Me-Gal). Interestingly, Me-Gal was found to inhibit protein binding to cell membranes in another lectin of the jacalin-related family, whereby it promoted cell death reactions in human tissues (LUO et al., 2021). It thus might be that LLP3 could have two functional binding sites: one might bind signaling metabolites such as calcium ions and D-glucopyranose upon plant stress (while being anchored to cell membranes), whereas binding of substrates such as Me-Gal may have another function like releasing anchoring of LLP3 from cell membranes. Taken together, further analyses with recombinant XYL4 and LLP3 or proteins extracted from plant tissue would help to evaluate if one of the predicted candidate molecules is a true ligand. Binding and affinity assays could be performed to evaluate protein-substrate relations by means of for instance plant carbohydrate (micro)arrays and microscale thermophoresis.

Surprisingly, an exogenous treatment of plants with the polysaccharide chitin, a potential ligand of XYL4, showed a quick induction (within 30 minutes after exposure) of *LLP3* expression (Zhang et al., 2002; Lyou et al., 2009), assuming that also LLP3 action might be triggered by similar PAMPs as XYL4. Moreover, it was shown that *LLP3* promoter activation is responsive to wounding (presumably regulated independently of JA or ET), exogenous MeJA, and (maybe *XYL4*-JA/ET-

related) ET (Lyou et al., 2009), supporting the fact that (*XYL4*-)*LLP3* signaling functions in modulating local MeJA signals or JA-SA crosstalk (Sales et al., 2021), and additionally injury reactions.

4.2.4 SA-JA crosstalk and systemic defense modified by *XYL4* and *LLP1,3*

It is believed that antagonistic as well as synergistic pathways involving SA and JA modulate ETI (Wittek et al., 2015; Liu et al., 2016b; Hillmer et al., 2017; Kim et al., 2020b). Such hormonal crosstalk of SA and JA is supposedly modified by *EDS1*-dependent transcript regulation, and metabolites involving LLP1-3 (Wenig et al., 2019; Sales et al., 2021) and XYL4 (Breitenbach et al., 2014). However, the contribution of the JA pathway to the consolidation of systemic signaling and SAR is still under debate (Truman et al., 2007; Attaran et al., 2009; Sales et al., 2021). As LLP1-3 proteins are co-expressed with XYL4 upon the induction of ETI and in dependence of *EDS1* (Breitenbach et al., 2014), there might be a co-functional role of these proteins in plant defense and the regulation of hormonal crosstalk. When summarizing the findings of previous studies of Breitenbach et al. (2014), Wenig et al. (2019), and Sales et al. (2021), it can be concluded that LLP1-3 presumably function either via combined or parallel pathways that regulate SA-JA-associated signaling events during local defense and SAR.

As described in the section 4.2.3., *XYL4* presumably promotes SAR signal transmission via the vasculature and is thus required for SAR signal generation/transmission in locally inoculated tissues, as well as in systemic tissues as potential signal receptor or propagator (**Figure 25**). Similarly, volatile signals with defense-inducing effects can also be generated/transmitted from infected senders only when plants carry functional *XYL4*, and are sensed in neighboring wild type plants (**Figure *27***). Mutant *xyl4* sender/receiver plants thus possibly lack the ability to send or perceive immune-promoting signals. These results together suggests that XYL4 is relevant for signal transduction via the vasculature and the airborne route in both, local and systemic tissues of SAR-stimulated plants, as described in the models (**Figure 31**, ***Figure 32***).

Because (SA-responsive) LLP1 is thought to sense/propagate systemic SAR signals (Wenig et al., 2019; Frank et al., 2021; Sales et al., 2021), *LLP1* potentially responds to locally induced signals initiated at the site of pathogen infection (area of HR/lesion formation) involving MeJA/JA and/or *LLP3* (Sales et al., 2021). *LLP1* may be thereby co-regulated with (injury-related responses and) *XYL4*/XYL4 to shape systemic reactions. In support, syringe-infiltrated plants show concomitant

alterations due to *XYL4*-dependent modulation of transcript levels of *PDF1.2* and *LLP1* in distal tissues (**Figure 21**B-C). There, *PDF1.2* transcript were slightly elevated systemically in *xyl4* mutants of mock-treated plants when compared to wild type (**Figure 21**B), suggesting that wounding could lead to slightly higher JA/ET signaling/or express constantly higher levels of *PDF1.2* when plants are defective in *XYL4.* On the contrary, after a bacterial SAR stimulus, levels of *PDF1.2* are comparable for control-treated wild type and SAR-inoculated *xyl4* plants, whereas *Pst/AvrRpm1*-infected wild type plants have significantly higher levels (**Figure 21**B). This suggests systemic promotion of early JA signals via *XYL4* (maybe as induced locally via XYL4/LLP3, **Figure 31**).

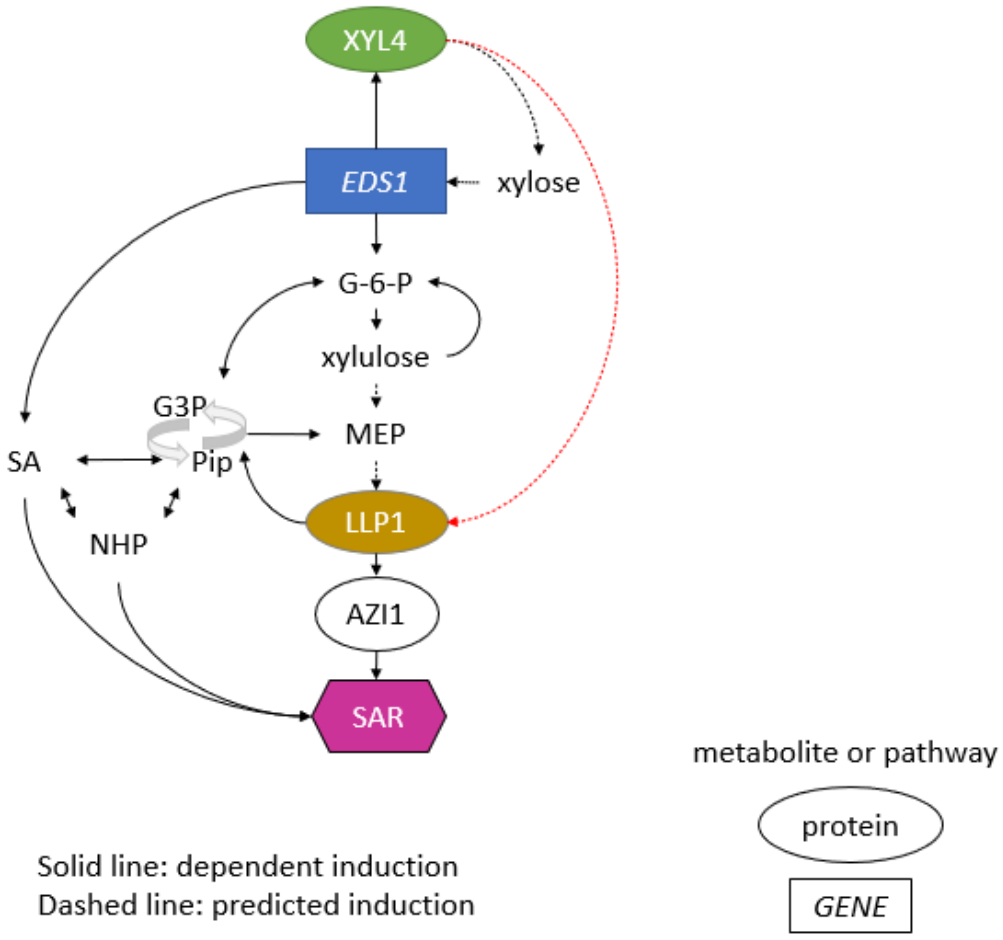

Figure 32: SAR signaling model: systemically mobile signals detectable by *XYL4* and *LLP1* trigger SAR and potentially induce SA/NHP-dependent signals.
Pathways via G-6-P and the loop Pip/G3P fortify systemic signals relevant for the establishment of effective SAR. Modified after Wenig et al. (2019). MEP: 2-C-methyl-D-erythritol 4-phosphate pathway, which includes the synthesis of monoterpenes.

Regarding the second gene, levels of *LLP1* in SAR-stimulated wild type plants and *xyl4* mutants are comparable in each treatment (**Figure 21**C), possibly indicating that *XYL4* can fine tune *LLP1* transcript accumulation at earlier stages after

inoculation (T1) and under wild type conditions (suppression?). However, levels of *LLP1* in *xyl4* mutants may be consistently elevated (**Figure 21**C) - this needs to be tested and compared with levels of untreated samples. When comparing gene expression of plants from another experiment and later timepoints (T3) (including untreated samples), no differences are detectable between mock or untreated wild type and *xyl4* mutants in *LLP1* transcript accumulation (**Figure S42**D). In sum, interrelated signaling pathways of early and late signals need to be triggered during an effective establishment of SAR involving systemic regulations of *XYL4*, *LLP1* and JA/ET signals (**Figure 21**A, ***Figure 32***). Therefore, the precise mechanism(s) by which *XYL4*/XYL4 modulates systemic signaling and defense needs to be investigated. Because XYL4 is necessary in systemic tissues during SAR signaling (**Figure 21**A, **Figure *25***, **Figure *27***), it may function in a mutual pathway or in parallel to that of *LLP1*. Systemically, XYL4 thus potentially locates near entry sites of plant tissues such as stomata, or in close vicinity of cell connecting compartments such as cell wall pore/trans-membrane pumps, along leaf veins or stem tissues in order to quickly detect changes of mobile molecules that are transmittable via air or vasculature. Thereby *XYL4* proteins might be either loosely anchored or predominantly mobile within the tissues in dependence of, for instance, regulation via *EDS1*, upon sensing of immune-signaling molecules such as calcium ions, carbohydrates, hormones, or other putative mobile SAR signaling metabolites as described earlier (**Figure *8***).

4.3 Defense-related metabolism including carbohydrates is regulated by XYL4 and networking pathways

4.3.1 *LLP1, EDS1, XYL4,* and xylose potentially regulate glycosylation events and SAG/NHP-H2-dependent defense

The biosynthesis of SA and the accumulation of NHP are relevant for an effective SAR response, of which both processes can be transcriptionally promoted by *EDS1* upon stress (Hartmann and Zeier, 2019). This indicates a key functional role of *EDS1* and associated pathways in the metabolic regulation of SA and NHP derivatives, SAR signaling, and defense. The balance of SA and NHP and their derivatives SAG and NHP-H2 is suggested to balance growth and defense establishment in stressed plants (Hartmann and Zeier, 2018a; Cai et al., 2021; Mohnike et al., 2021), suggesting that plants actively regulate the conversion of SA/SAG and NHP/NHP-H2 by UGTs, for example, to stimulate SAR.

Specifically, SAG was formerly described to be formed in dependence of specific enzymes (like UGT74F1, UGT74F2, UGT76B1) (Dean and Delaney, 2008; von Saint

Paul et al., 2011) and pH levels (e.g. increased formation of SAG at pH 6-8.5) (Thompson et al., 2017). Potentially *XYL4* signals might modify one or more of the mentioned UGTs and/or cause changes in pH in order to regulate the levels of SA/SAG upon SAR-induction/infection with *Pst*/*AvrRpm1* (**Figure 20**B), or the transcription of UGT76B1 upon wounding (**Figure 22**F). SAG accumulation in *xyl4* mutant plants was about 4-fold compared to levels in wild type plants 2 days after a bacterial infection by spray (**Figure 20**B). This strongly suggests that XYL4 suppresses SAG formation upon infection with SAR-stimulating *Pst*/*AvrRpm1*. This may furthermore indicate that XYL4 has a regulative function on SAG-forming UGTs. It would be further interesting to examine if and how *XYL4* contributes to the regulation of (*NPR1*-independent?) SA/SAG (and JA signaling components) as described earlier (Nandi et al., 2003; Zhang, 2013), while it might promote a wounding-associated expression of *UGT76B1* (von Saint Paul et al., 2011) (**Figure 22**F) and the accumulation of NHP-H2 (**Figure *26***E).

Overexpression of *UGT76B1* commonly results in elevated abundances for SAG and NHP-H2, which is accompanied by the abolishment of SAR (Bauer et al., 2021; Cai et al., 2021). The enzyme UGT76B1 is known to convert NHP (Hartmann and Zeier, 2018b; Bauer et al., 2021; Mohnike et al., 2021; Zeier, 2021), SA, and isoleucic acid into their respective glycosylated derivatives (von Saint Paul et al., 2011), while *UGT76B1* modifies basal defense and SAR (Bauer et al., 2021; Cai et al., 2021; Holmes et al., 2021; Mohnike et al., 2021; Zeier, 2021). Hence, I initially suggested that *XYL4* may modulate SAG/HNP-H2-dependent plant defense by controlling the transcription of *UGT76B1*. The transcription of *UGT76B1* was not affected by *XYL4* at 1 dpi in the systemic tissues of SAR-induced plants (**Figure 22**F), inducating that expression of this *UGT* is not strongly dependent on *XYL4* during defense. However, because expression of *UGT76B1* was significantly more repressed in *xyl4* mutants than in wild type plants by mock solution treatment (**Figure 22**F), a signaling cascade involving *XYL4* could promote transcriptional expression of *UGT76B1* after injury signals. Consequently, it would be interesting to test if *UGT76B1* is responsive to *XYL4*- and (potentially also *LLP3*-related) JA signals in plants (also in other defense-related processed except SAR).

Xylose, which *in planta* is commonly available as free (UDP-)xylose molecules, potentially competes with (UDP-)glucose to be used as activated sugar donor for UGTs, and can consequently inhibit glucosyl transfer reactions (Martin et al., 1999). Since XYL4 action in plants is potentially linked to a function as xylosidase and thus a release of xylose derivatives as described earlier (see section 1.6), I

tested if treatments with exogenous xylose affect the expression of *UGT76B1*. Interestingly, xylose appeared to suppress the conversion of NHP into NHP-H2, which potentially contributes to a fortified systemic defense that associates with NHP in Col-0 and *xyl4-1* (**Figure 28**A-B, **Figure S40**C, **Figure *29***D). These findings support the assumption that xylose can repress UGT function to form glucosylated proteins. As *eds1-2* and *llp1-1* plants did not respond with xylose-inducible resistance against an infection with *Pst* (**Figure S40**C, **Figure *29***D), it would be quite interesting to analyze if an *EDS1*/*LLP1*-dependent effective defense hereby depends on the potential of plants to firstly perceive and respond to xylose-inducible signals, and secondly to promote signals that stimulate the conversion of NHP to NHP-H2. In addition, the control-treated and additionally *Pst*-challenged wild type plants accumulated higher levels of NHP-H2 than *xyl4* mutant plants or those inoculated with xylose (**Figure 30**F), assuming that this plant reaction may partially also be a wound-inducible effect that is dependent on *XYL4*.

Notably, plants defective in *EDS1*, *ALD1*, *FMO1*, *NPR1*, *SID2* or *PAD4* accumulate comparably lower levels of (*UGT76B1*-related) NHP-H2 after a SAR-stimulus (*Ps* pv. *maculicula*) than wild type plants (Bauer et al., 2021). This indicates that Pip-(*ALD1*, *FMO1*) and *EDS1*/SA-related genes (*SID2*, *NPR1*, *PAD4*) are relevant for the accumulation of NHP-H2. In support, a regulation of metabolites such as Pip and SA were detected after an induction for *AvrRpm1*-associated signals in dependence of *XYL4* and *EDS1* (**Table S18**, **Table S*19***). This leads to the assumption that *XYL4* and *EDS1* together may modulate routes to control the accumulation of precursors of NHP-H2 upon (biotic) stress. Interestingly, it was shown that pathogen-infected *eds1* mutant plants are deficient in the accumulation of the senescence-related, xylose-conjugated, and isochorismate-derived 2,3-dihydroxy-benzoic acid (2,3-DHBA) – those plants were lacking 2-hydroxy-3-β-O-d-xylopyranosyloxybenzoic acid (DHB3X) (Bartsch et al., 2010). The availability of xylose, and thus predicted factors able to affect *in planta* xylose concentrations, might be a key to regulate the formation of DHB3X in pathogen-stressed plants. Interestingly, the closely related compound 2,5-DHBA is likewise repressed as 2,3-DHBA in *eds1* mutants, and moreover also in other mutants like *sid2* and *fmo1* (Bartsch et al., 2010). This suggests that these DHBAs are commonly modulated by *EDS1*, SA, and *FMO1*-dependent immune pathways. In sum, as xylose-dependent defense in wild type plants involves the regulation of NHP-H2 (**Figure 30**F) and moreover depends on *LLP1* and *EDS1* (**Figure S40**C, **Figure *29***D), I hypothesize that *XYL4*, *LLP1* and *EDS1* are relevant for the regulation of immune

modulating UGTs in *A. thaliana*. I thus suggest that signaling cascades involving *EDS1*, *LLP1*, xylose, and *XYL4* jointly modulate the local and systemic homeostasis of NHP and SA (**Figure 31**, **Figure *32***). These data prompt the question if *XYL4* may furthermore shape other plant physiological traits besides NHP-H2-dependent defense when interfering UGT glycosylation events with xylose signals.

4.3.2 Xylosidases and AZI1 may regulate an SAR-associated pathway involving lipid-derived molecules and carbohydrates

Besides SA and Pip-derived metabolites, also G3P and AzA-associated routes are presumably relevant for systemic SAR signaling via LLP1 (Wenig et al., 2019). *XYL4*, which is suggested as potential regulative element of phloem-mobile signals during SAR (**Figure 25**A-C), might therefore also affect the transmission or formation of G3P and AzA. Specifically, G3P, Pip, SA and AzA are potential phloem mobile signaling molecules, as described in more detail in the above section 1.5. Thus, any appropriate route during SAR for intra-plant transmission of SA, Pip, G3P, and AzA may be controlled via *XYL4*-associated signals.

The symplastic transport of AzA and G3P is regulated by gating via the interacting proteins PLASMODESMATA LOCALIZING PROTEIN 1 (PDLP1) and 5 (PDLP5) (Lim et al., 2016; Singh et al., 2017). Notably, defense against *Pst* is impaired in *pdlp1* and *pdlp5* mutant plants, or in transgenic genotypes overexpressing *PDLP5* (Lim et al., 2016), which suggest that PDLP1 and PDLP5 contribute to the establishment of effective plant defense. Interestingly, the activation of *Ps*-(pv. *maculicola*)-inducible *PDLP5* (Lee et al., 2011) correlates with a suppressed abundance of AzA and G3P levels in petiole exudates (Lim et al., 2016) and reduced Ca^{2+} signaling (Toyota et al., 2018). This indicates that *PDLP5* functions as negative regulator for the intra-plant transmission of these molecules by regulating traffic via plasmodesmata (Lee et al., 2011). Notably, PDLP1/5 is interacting with lipid transfer protein AZI1 when promoting SAR in dependence of G3P and AzA, whereby the PDLPs presumably stabilize the localization of AZI1 (Lim et al., 2016). Interestingly, BETA-XYLOSIDASE 1 (BXL1), a close homolog of XYL4, can be co-expressed with XYL4 *in planta* (as described in the database ATTED-II: http://atted.jp/) and was shown to interact with PDLP1 (Caillaud et al., 2014). BXL1 and XYL4 seem to have complementing functions during seed mucilage formation (Guzha et al., 2022), assuming that they might also function comparably or in an additive manner in other plant tissues. In sum, a pathway involving BXL1 may potentially affect defense-related pathways of *XYL4* and downstream SAR

signals via AZI1 in parallel to PDLPs. A possible involvement of *BXL1*/BXL1 in SAR and associated signaling routes should consequently be determined.

Notably, *AZI1* regulates sugar signaling, the expression of sugar transporters (Wang et al., 2016), and an SA-related sensing and phloem-associated transmission of hexoses during SAR (Herbers, 1996; Savadi et al., 2018). This strongly indicates that pathways affecting AZI1, including those via BXL1 or PDLPs, could potentially promote sugar signaling. Furthermore, SAR signaling routes involving *AZI1* are suggested to activate defense in association with monoterpenes and LLP1 in *A. thaliana* (Riedlmeier et al., 2017; Wenig et al., 2019). It thus can be hypothesized that defense-stimulated plants activate a pathway via (Pip/G3P-)monoterpenes-LLP1-AZI1 besides sugar signals and XYL4/BXL1 with the purpose of promoting resistance, as shown in the model for systemic SAR signaling (**Figure 32**). Interestingly, a treatment with the *AZI1*-inducer AzA promotes systemic resistance to *Pst* in wildtype and *llp1* mutant plants but not in plants lacking *LLP1-3* (Sales, 2021). These findings suggest that either *LLP2* or *LLP3* or both modulate AzA (and *AZI1*?)-dependent downstream signaling and defense. Notably, *xyl4-1* and Col-0 plants comparably accumulate AzA in dependence to a treatment with either mock, xylose (**Figure 30**C), or an ETI challenge
Figure S37C), suggesting that *XYL4* rather functions downstream or in parallel with a pathway involving the biosynthesis of AzA. In sum, such a AzA/AZI1-related route (including the stimulation of intra-plant sugar signals) might therefore be predominantly dependent on signaling via *LLP2* and/or *LLP3*.

4.3.3 *XYL4* and *EDS1* modify metabolites along the glycolytic pathway

After plants perceive a SAR stimulus, they accumulate G3P besides AzA and SA in locally infected tissues and trigger SAR signaling towards distal parts (Singh et al., 2017). A stimulus for SA production in pathogen-infected plants is regulated in dependence of the SAR-associated digalactosyldiacylglycerol (DGDG), which is synthesized in the inner membranes of chloroplasts (Gao et al., 2014; Lim et al., 2017). Notably, AzA is a nine-carbon fatty acid (FA) derivative that is derived from a ROS-inducible cleavage of a C18 unsaturated FA molecule (Yu et al., 2013; Wang et al., 2014) and its direct SAR-related precursor 9-oxononanoic acid (ONA) (Wittek et al., 2014). As described in Wittek et al. (2014), *EDS1* stimulates SAR via a pathway involving ONA and AzA, which leads to the assumption that *EDS1* is a critical component for the accumulation of AzA upon pathogen infection. Notably, the SAR-inducer G3P can be synthesized (in parallel with a NPR1-inducible pathway) by a stress and NO/ROS-induced lipid peroxidation of AzA, (Chanda et

al., 2011; Wang et al., 2014), indicating that a route via *EDS1* may directly promote levels of both AzA and G3P (along with NO⇔ROS→AzA→G3P). As an exogenous treatment with AzA stimulates the biosynthesis of G3P, this suggests AzA functions upstream of G3P (Yu et al., 2013). It would thus be interesting to determine by which mechanism *EDS1*-dependent signals or EDS1 function modifies the levels of AzA (and G3P, **Table S*19***) in SAR-induced plants.

Notably, G3P *in planta* is suggested to promote the synthesis of fatty acid-derived glycerolipids (Kachroo and Kachroo, 2009), which are important for a DIR1-associated signal transduction (Nandi et al., 2004; Chaturvedi et al., 2008). Since G3P presumably translocates towards distal plant parts in dependence of the transfer proteins DIR1 and AZI1 during SAR (Maldonado et al., 2002; Chanda et al., 2011; Mandal et al., 2011; Yu et al., 2013; Wendehenne et al., 2014), this suggests that G3P levels are regulated via a feedback loop involving DIR1 and AZI1 (Yu et al., 2013). In the first screening performed with transgenic plants sprayed with DEX, no accumulation of G3P or starch was detected. It could be that elevated G3P concentrations are only detectable when plants are infected with a true (bacterial) organism and do not respond with G3P accumulation to an effector-driven stimulus only. In support, G3P utilization-defective plants that were infected with, for example, a true (hemi-)biotrophic fungal pathogen accumulate high levels of G3P (Chanda et al., 2008). Notably, in the second GC-MS screen, elevated G3P levels were detected in *xyl4* mutant plants after each spray treatment (mock- or *Pst*/*AvrRpm1*-treated) and in *eds1-2* only after SAR induction (**Table S19**). Therefore, I hypothesize that *XYL4* and signaling via *EDS1* controls the accumulation of G3P and/or the conversion of AzA to G3P when plants perceive a SAR stimulus. Interestingly, the metabolite G-6-P also accumulated during ETI in a *XYL4*- and *EDS1*-dependent manner with *XYL4* suppressing and *EDS1* promoting G-6-P accumulation (**Table S18**, **Table S19**). By controlling the accumulation of G-6-P putatively other linked pathways branching off the glycolytic pathway may be influenced, including the synthesis of the glycerolipid precursor G3P (Kachroo and Kachroo, 2009; Mandal et al., 2011) and serine (Igamberdiev and Kleczkowski, 2018). Furthermore, besides SA and Pip also levels of maltose – a derivative of starch and a precursor of G-6-P (Weise et al., 2004) – potentially increase upon *AvrRpm1*-associated and *EDS1*-regulated signals that may thus stimulate the breakdown of polysaccharides like starch. Levels of starch or cellulose are *EDS1*-dependently regulated as reduced levels of the starch or cellulose breakdown product 1,6-anhydro-beta-glucose (=Levoglucosan) detected in the GC-MS screen

(**Table S18**). I therefore suggest that *EDS1* might have an important role in the regulation of glycolytic- and thus also energy-associated metabolites (**Figure 33**).

Surprisingly, a comparable pattern of metabolite expression as described for G3P was also detected for another branch-associated metabolite from the glycolytic path: the levels of the SAR-inducible serine (Gao et al., 2020) appear to be suppressed by *XYL4* and *EDS1* upon inoculation (**Table S19**). Notably, serine is a precursor of sphingosines/phospholipids, which likely associate with plant defense signaling responses and PCD (Liang et al., 2003; Sentelle et al., 2012; Young et al., 2013; Wu et al., 2015). As metabolites that are closely associated with the glycolytic pathway, like G-6-P, G3P and serine, more evidently accumulated in *eds1* and *xyl4* mutants upon inoculation or infection (**Table S19**), I suppose that EDS1 and/or XYL4 may suppress the abundance of those compounds to specifically control pathways linked to glycolysis or gluconeogenesis (e.g. pentose phosphate pathway (PPP), secondary metabolites, lipids) during defense (**Figure 33**).

Interestingly, the compounds xylulose and erythritol accumulated *EDS1*-dependently after plants were sprayed with DEX (**Table S*18***). Notably, derivatives of these two compounds xylulose and erythritol (such as 1-deoxy-d-xylulose, erythritol-4-phosphate, 2C-methyl-d-erythritol 4-phosphate) are participating in either the cycle of PPP (Kruger and Von Schaewen, 2003) or MEP, which is needed for isoprenoid biosynthesis (Lichtenthaler, 1999; Hoeffler et al., 2002; Hemmerlin et al., 2006). Notably, one *AvrRpm1*- and folate-associated compound of the PPP (sedoheptulose-1,7-bisphosphate) was formerly suggested to accumulate in an *EDS1*-repressed manner (Wittek, 2013). In addition, the putative nucleotide sugar precursor D-glycero-D-mannoheptose-1,7-bisphosphate also accumulated in association with *AvrRpm1* and *EDS1*; a compound which has a link to the downstream pathway that includes sedoheptulose-1,7-bisphosphate (Wittek, 2013). These data suggest that *EDS1* signals may repress the abundance of xylulose, erythritol, and sedoheptulose-1,7-bisphosphate (and derivatives thereof) during stress to potentially fine-tune PPP- and MEP-related production of terpene/isoprene precursors (Sagner et al., 1998; Jacobsen and Anthonsen, 2015), or an SA precursor and derivative of erythritol-4-phosphate, namely phenylalanine (Barbier et al., 2014). Notably, an enzymatic conversion of erythritol by phosphorylation to erythritol-4-phosphate was shown for proteobacteria (Barbier et al., 2014), however a similar metabolic pathway for erythritol was not yet described in plants. Interestingly, an erythritol derivative in *A. thaliana* termed 2-C-methyl-D-erythritol cyclopyrophosphate is an SA-repressed signaling

metabolite which induces transcription of JA-responsive (in presence of elevated SA levels) and COI1-dependent genes (Lemos et al., 2016). Erythritol-related signals may thus function as a regulatory switch from (high) SA to JA signaling and thereby modulating SA-JA crosstalk and the generation of volatile (immunomodulating) compounds that can further affect plant-to-plant communication (**Figure *27***).

Similarly, the metabolism or catabolism of xylulose in plants was not yet evidenced. As described in an overview for metabolic pathways by Roche (http://biochemical-pathways.com/#/map/1, based on different species including humans), D-xylulose could be directly converted into D-xylose (by xylose isomerase, a pathway not yet associated to plants), while L-xylulose first needs to be converted to xylitol (by L-xylulose reductase, a path already associated to plants) and a final conversion to L-xylose (by aldehyde reductase, a path already associated to plants). It may thus be that xylulose, which accumulated more strongly in *eds1* mutants after a spray with DEX (**Table S*18***), is normally *EDS1*-dependently converted to xylose in wild type plants. This might further indicate that *EDS1*-related signals could interfere with the function of xylulose converting enzymes as listed above. Moreover, UDP-xylulose and UDP-xylose repress the conversion from UDP-glucose to UDP-D-glucuronate (also termed UDP-glucuronic acid, a precursor of UDP-xylose) via a negative feedback loop (Roche pathway, http://biochemical-pathways.com/#/map/1,). Notably, strong repression of glucuronic acid biosynthesis causes swelling of plant cells walls, which is suggested to be related to defects in pectin saccharides (Reboul et al., 2011). Taken together, I suggest that an *EDS1*-xylulose/xylose-dependent regulation of e.g. glucuronic acids and thus pectin may result in alterations of the cell wall composition, which might furthermore cause plant responses that influence xylose-associated systemic defense (**Figure *28***A-B, **Figure *29***D, **Figure *32***), ETI, and SAR (see **Table *12***, **Table *13***, **Table S*18***).

Additionally, since *EDS1* is suggested to stimulate the accumulation of dihydrosphingosine (also known as erythro-D-sphinganine) upon a stimulus with *AvrRpm1* (**Table S18**), *EDS1* may interfere with a path downstream of dihydrosphingoside. Potentially, *eds1-2* mutants might form less complex lipids (and thus have lower levels of sphingosine), which might in turn compromise the induction of HR and PCD (Falk et al., 1999) in relation with SA, *PAD4*, and *FMO1* (Brodersen et al., 2002; König et al., 2021; Rodrigues et al., 2021). Notably, the SA-dependent gene *ACCELERATED-CELL-DEATH 11,* which encodes a mammalian

homologue glycolipid transfer protein, regulates *EDS1*, the accumulation of sphingolipids (Simanshu et al., 2014), and cell wall enzymes involving a pectin esterase and a PME in *A. thaliana* (Brodersen et al., 2002). Sphingolipid-associated PCD was recently shown to be *EDS1*- and SA-dependently regulated (König et al., 2022), supporting a link for co-expression of sphingolipids and EDS1 during stress regulation. Interestingly, mutants lacking specific sphingolipid desaturases were formerly described to resist infections with *Pst* while strongly accumulating sphingolipids and callose in dependence of PDLP5 (Liu et al., 2020b). It thus can be speculated that plants regulate defense and PDLPs by controlling the transcription of *EDS1* and furthermore PCD an the activity of lipase-like EDS1 proteins. Specifically, the regulation of PLDP5 and an associated closure of plasmodesmata is suggested to mediate SA-JA crosstalk and defense by affecting SA-dependent pathways (Lee et al., 2011). Potentially, there is a link between such SA signaling events and the negative modulator of SA-related cell death responses, EDS1-INTERACTING J PROTEIN 1 (EIJ1), which physically interacts with and represses the activity of EDS1 (Liu et al., 2021c). Mutants defective in *EIJ1* activate *EDS1*-dependent cell death comparatively early in leaves after infection with virulent or avirulent *Pst* strains, indicating that EIJ1 is a key regulative component to initiate ETI defense (against biotrophic pathogens).

Taken together, I suggest that *XYL4, EDS1,* xylose/xylulose and (AzA-)G3P promote SAR signaling synergistically (**Figure 32**) and potentially associate with SA pathways to balance/regulate carbohydrate and lipid pathways.

4.4 Cell wall defense and its connection to SAR

4.4.1 Cell wall-associated defense during SAR might be regulated by SA, *EDS1*, and *XYL4*

The SAR-associated hormone SA was formerly shown to promote the synthesis of cell wall polysaccharides and the expression of associated synthase genes (Jia et al., 2021), suggesting that SA-inducible changes in cell wall structures might play a role in SAR establishment. Interestingly, a slight repression of *XYL4* transcripts was formerly associated with signals affecting cell wall modifications and callose deposition in citrus plants that were infected with an SA-degrading biotrophic bacterium (*Candidatus Liberibacter asiaticus*) (Fu et al., 2016), which putatively contains an SA hydroxylase (Li et al., 2017a). Furthermore, exogenous SA results in a slight suppression of *XYL4* in *Arabidopsis* seedlings (Goda et al., 2008), suggesting that *XYL4* may be responsive to SA signals and thus could act

downstream of an *EDS1*-SA pathway. Potentially, *EDS1* and *XYL4* may be pivotal interactors when triggering SA-related signals during the establishment of SAR. It was thus interesting to determine plant resistance against bacterial infections in dependence of *XYL4* and potential associated changes in cell wall patterns.

Cell walls seem to influence defense against bacteria in multiple ways. Inducible changes in the pectin composition of cell walls in common beans (*Phaseolus vulgaris*) were recently suggested to play a role in plant defense against *Ps* pathogens or after the application with the synthetic priming agent 2,6-dichloroisonicotinic acid (INA) (De la Rubia et al., 2021). Thereby, an exogenous application of INA altered the abundance of pectin (methyl-esterificated HGs, RG-I), hemicellulose (xyloglycan, galactan), arabinogalactan, extensin, and cellulose in beans (De la Rubia et al., 2021). Specifically, De la Rubia at al. (2021) suggest that INA stimulates priming resulting in enhanced synthesis of cellulose or callose, and a reinforcement of cell walls. This strengthening effect might be potentiated by strong linkages between single cell wall components (De la Rubia et al., 2021). Notably, the SAR-inducer INA is a functional analogue of the biologically active form of SA (Kauss et al., 1992). In support, INA triggers *PR1* expression similarly as compared to exogenously applied SA (Mou et al., 2003) and, moreover, activates changes in plants that are inheritable to following generations (Martínez-Aguilar et al., 2021). Thus, cell wall-related plant responses, as activated by SA/INA might influence SAR and additionally transgenerational defense.

Cross-linking of cell wall structures may be one modifiable target addressed to fine tune SAR signaling. The process of cross-linking cell walls with, for example, HRGPs, which are highly glycosylated hydroxyproline-rich glycoproteins (Smirnoff and Wheeler, 2000) that function as cross-linking element of cell wall components (Deepak et al., 2010), is thought to depend on the early responses of the plant to infection with a pathogen or induced ET signaling (Toppan et al., 1982; De Cnodder et al., 2005). Interestingly, I suggest that *XYL4* signaling systemically drives an early ETI-associated transcriptional induction of the JA/ET signaling gene *PDF1.2* (**Figure *21***B) and have also detected *EDS1*/*XYL4*-dependent accumulation of the core structural components of HRGPs, designated 4-hydroxy-proline (Owens et al., 2010), in SAR-induced plants (**Table S19**). These findings suggests that early defense responses as triggered via *EDS1* and *XYL4*, such as *XYL4*-JA/ET-associated signaling, might contribute to the modulation of cross-links in systemic tissues and thereby affect immune responses associated to biotic stress tolerance (**Figure 31**). In support of hormone-triggered cell wall remodeling: regulation of gene

expression and the accumulation of HRGPs-related peptides has been described to be inducible by either JA-associated (cell damage/ injury) responses (Taylor et al., 2012), or a treatment with SA (Tiré et al., 1994; Merkouropoulos et al., 1999). Additionally, elevated abundance of HRGP molecules in plants was associated with resistance to *Pst* and *Bc* (Wei and Shirsat, 2006; Reem et al., 2016). I thus suggest that HRGPs may be involved in SA/JA-dependent stress signaling after plants were triggered by (hemi-)biotrophic or necrotrophic pathogens. In summary, I conclude that *XYL4*/*EDS1*-HRGP-related responses are potentially required for an effective establishment of SAR.

Moreover, certainly pectin fragments such as oligogalacturonides (OGs) were proven to have defense-inducing capacities against pathogen attack, specifically in distal, non-inoculated tissues, while basal defense remains unaffected (Gamir et al., 2021). However, others also report PTI-inducing capacities of pectin molecules, thus affecting basal immunity (Lionetti et al., 2010; Raiola et al., 2011). Notably, some pectin polymers such as HGs and RG I were significantly more abundant in *eds1* and Col-0 transgenic plants after DEX spraying (**Table *12***), whereas the composition was comparable in ETI spray-induced plants regardless of plant genotype (*xyl4*, *eds1* and wild type, **Table 13**). This differing pattern in plant response might be an effect of *Pst*/*AvrRmp1*- or SA-dependent signaling, which is altered in the *eds1* mutant background (Venugopal et al., 2009; Cui et al., 2017; Cui et al., 2018). In addition, *xyl4-1* mutants seemed less responsive to induction or suppression of cell wall components upon infection with *Pst*/*AvrRpm1* when compared to wild type plants (**Table 13**). This suggests that *XYL4*-dependent SAR signals might be involved in the transduction of responses relevant to induce alterations or de novo synthesis of cell wall components. A role for a XYL4-related accumulation of pectin during SAR needs to be confirmed with additional experiments.

4.4.2 *EDS1*-dependent cell wall remodeling needed to fine-tune SA-signaling during SAR?

As suggested and discussed earlier, the generation and transmission of SAR signaling events may be regulated by hormonal networks involving systemic JA signaling at early stages (**Figure *21***B) and SA signaling in later phases after infection (**Figure *21***D, **Figure 20**B). Such SAR signaling pathway(s) are thought to be modulated by interconnected pathways of *XYL4*, *EDS1*, and *LLP1-3* and cause modifications at the structure or composition of cell walls (for example depending on *EDS1*, **Table *12***). These alterations on cell wall might trigger SAR signal

generation required for long-distance communication (**Figure *21***A, **Figure *22***C, **Figure *25***, **Figure *26***A, **Figure *27***). I was thus wondering, which modulators (locally and systemically) may affect such cell wall- and/or carbohydrate-related plant responses that could enhance signaling during the establishment of SAR? Potential candidates might be SA and JA signaling-related compounds.

Interestingly, DEX-sprayed *eds1* transgenic plants showed significantly higher values for the abundance of pectin polymers such as de-esterified, partially or heavily (methyl-)esterified HG, and enhanced accumulation of RG-I backbones in comparison to Col-0 plants (**Table *12***). I therefore propose that pathways via *AvrRpm1-EDS1* may regulate pectin accumulation in general, which appears to be independent of esterification status. Future research is therefore needed to determine what mechanisms (including an *EDS1*/xylulose/xylose repressive effect on pectin synthesis, see 4.3.3) plants employ to alter pectin accumulation n an *EDS1*-dependent manner. Notably, *ACCELERATED-CELL-DEATH 11* regulates transcription of *EDS1* and cell wall enzymes involving a pectin esterase and a PME in *A. thaliana* in an SA-dependent manner (Brodersen et al., 2002). In addition, *XYL4* gene appears to be co-expressed with other predicted cell wall modifying enzymes such as xylosidases, pectin acetylesterases, pectin methylesterase (PME), and a xyloglucan endotransglucosylase (http://atted.jp/). This list of commonly expressed enzymes suggests that *EDS1*- and *XYL4*-dependent plant responses may be closely linked to the enzymatic effects of pectin-modulating enzymes such as PMEs (which may be co-expressed by both *XYL4* and *EDS1* pathways). Therefore, for example, PME-related downstream signals may affect the establishment and signaling during SAR as a potential side effect of induced transcription of *XYL4* or *EDS1*.

In my studies, I found that *PR1* transcript levels were significantly increased 3 days after wild type plants perceived a SAR-stimulus compared with control-treated plants (**Figure *21***D). This suggests that enhanced SA signaling at later stages of SAR establishment might downregulate (JA-responsive) PME action (Jia et al., 2021), potentially through SA/JA crosstalk. In support, elevated levels of apoplastically accumulating SA (Lim et al., 2020) and associated downstream signals via *EDS1* (Jirage et al., 1999; Feys et al., 2001; Rietz et al., 2011; Lapin et al., 2020) can repress the JA pathway (Cui et al., 2018). Additionally, exogenously applied SA, pathogenic attack, or wounding (maybe *XYL4*-JA/ET signaled) controls the expression of PME-related genes and the activity of PMEs, with SA suppressing either gene expression or PME activity, as shown in tomato

(Rao et al., 2011; Xu et al., 2015; Fan et al., 2017; Zhu et al., 2020; Jia et al., 2021). As PME action results in the release of compounds including PAL/SA-associated hydroxycinnamic acids (Kim and Carpita, 1992; Carpita, 1996) as well as protons that induce lowering of pH levels (Limberg et al., 2000; Kohli et al., 2015), SA/*EDS1*-PME might be triggering a SA signal-fortification loop. To that, translocation of SA from the cytoplasm to the extracellular space can be promoted by alterations in pH (Rocher et al., 2009; Bonnemain et al., 2013; Lim et al., 2020). Such a PME/pH-SA translocation cascade may furthermore induce the transition of SA into or out of the region of active PMEs. Therefore, I hypothesize that the translocation of SA over short/long distances (and by this intra-plant communication and SAR, **Figure *25***, **Figure *27***, **Figure *21***A) might be (additionally) stimulated in a *XYL4*/*EDS1*-dependent manner via the (SA/EDS-)PME action on cell wall pectin.

Notably, PMEs can be strongly stimulated by JA signals after an infection in *A. thaliana* and potato with, for example, a necrotrophic invader (Raiola et al., 2011; Bethke et al., 2014; Taurino et al., 2014). In addition, JA-inducible PMEs can act independently of SA, ET, and the EDS1 co-regulator PAD4 (Bethke et al., 2014). Therefore, I hypothesized that *XYL4*-dependent stimulation of JA/ET signaling in systemic leaves of SAR-stimulated plants (**Figure *21***B) might promote PME action systemically and, moreover, induce PME-related pectin remodeling in distal leaves. However, pectin polymers of inoculated *xyl4* were comparable in each treatment (mock-treated, SAR-induced, **Table *13***). I thus conclude that PMEs might not have a great effect on pectin methylesterification (as was detectable with the set of epitope antibodies) in dependence of *Pst*/*AvrRpm1*-*XYL4*.

4.4.3 Xylose-associated defense might be modulated by XYL4 and *EDS1*

As XYL4 is a protein that is presumably secreted to the apoplast (Goujon et al., 2003; Breitenbach et al., 2014; Sham et al., 2014; Guzha et al., 2022), its localization close to cell walls and plasma membranes presumably determines where it may function in plants. Interestingly, XYL1 putatively co-localizes with XYL4 in internodes of stems, sepals, developing embryos, and germinating seeds of non-stressed plants (Schmid et al., 2005; Narsai et al., 2011; Klepikova et al., 2016; Hofmann et al., 2019). Notably, stem-derived XYL4 proteins were formerly suggested to participate in developmental processes (Minic et al., 2004). A defect in *XYL4* thus might promote malfunctions of stem- or vasculature-associated processes. Consequently, a *XYL4*-dependent intra-plant transmission or propagation of mobile signals could be inhibited in *xyl4* mutant plants (**Figure 25**).

Interestingly, stem-associated XYL4 spatially co-localizes with three UDP-xylose synthases (USX), which are predominantly expressed in stems, xylem, and interfascicular fibers near vascular tissues (Zhong et al., 2017). I am thus asking if XYL4 proteins may potentially modify the abundance of xylose or the (*EDS1*-associated) xylose-derivative xylulose (**Table S18**) after activation in stems/close to vascular tissues. Such signaling cascade might thereby promote systemically mobile (partially SA/SAG- and *EDS1*-dependent) signals as generated during xylose-inducible defense (**Figure 28**A-B, **Figure 29**C-D). Moreover, stem-derived xylose/xylulose molecules could play a role in the generation or transduction of defense-inducible signals (in an *EDS1*- and *LLP1*-dependent manner?) that trigger vascular or volatile-dependent resistance to *Pst* (**Figure 25**, **Figure 27**). In sum, it would be interesting to determine XYL4 *in planta* function in more detail and elucidate whether (endogenous stem-derived) xylose has the potential to modify systemically mobile defense signals in a manner similar to SAR inducers such as *Pst*/*AvrRpm1* (**Figure 21**A, **Figure 28**A-B).

Guzha et al. (2022) initially described XYL4 functions by comparisons with seed coat-associated XYL1 proteins, which code for bifunctional β-D-xylosidases/ α-arabinofuranosidases (Goujon et al., 2003; Minic et al., 2004) that share 57% identity with XYL4 at the amino acid level (Arsovski et al., 2009). The data suggest that *XYL4* and *XYL1* both modify the composition of seed mucilage, potentially altering monosaccharide levels in dependence of *XYL1* (arabinose) and *XYL4* (xylose) (Guzha et al., 2022). It is suggested that *XYL4* suppresses the accumulation of xylose in mucilage by modifying RG-I components including xylan and arabinan (Williams et al., 2020; Guzha et al., 2022). However, transgenic lines overexpressing *XYL4* (30- to 60-fold higher transcript levels) accumulated equal amounts of xylose and arabinose in rosette leaves when compared to wild type plants (Guzha et al., 2022), suggesting that *XYL4*-inducible plant responses may be regulated in an organ-specific manner and/or in relation to plant development. In support, the leaves of *xyl4* mutant plants in my study also did not accumulate reduced free xylose levels when compared to wild type plants after infection (**Table S*19***). Guzha et al. (2022) investigated a potential function of XYL4 in leaves: in contrast, they detected elevated levels of, for example, arabinose in leaf pectin of non-stressed *xyl4* mutants in comparison to wild type plants, while levels of xylose or other pectin-related monosaccharides were comparable for all *A. thaliana* lines investigated (Guzha et al., 2022). This suggests that XYL4 may specifically alter

pectin structures and the content of cell wall-associated saccharides in leafy tissues.

Notably, LM13-related arabinan epitopes were not detectable in the alcohol-insoluble fraction of leaves taken from stress-induced plants (**Table 12**, **Table 13**). Guzha et al (2022), in contrast detected an elevated accumulation of 1,5-linked arabinosyl residues (as detected with LM13) in seed mucilage. These pectin-related 1,5-linked arabinan molecules thus seem to be formed specifically in seed mucilage, existing in a non-bound (water-extractable) state in seeds (Verhertbruggen et al., 2009b). Other studies suppose XYL4 enzymes to be targeting (water-soluble) arabinan or side chains of RG-I *in planta* (Ridley et al., 2001; Mohnen, 2008; Arsovski et al., 2010; Rossez et al., 2014; Williams et al., 2020). Supplementally, I ultimately suspect that XYL4 acts plant organ-specifically as either xylosidase or arabinosidase, depending on tissues of leaves or seed (pectin, polysaccharides). In future, the function of XYL4 on other cell wall structural components, such as hemicellulose or glycoproteins, needs to be determined.

4.4.4 Fucose-related signals connect different branches of the SAR-signaling network

Interestingly, alcohol-soluble, free fucose levels were repressed in an *XYL4*- and *EDS1*-dependent manner in rosettes of *Pst/AvrRpm1* spray-infected and mock-inoculated plants; in control-treated plants potentially constitutively because fucose levels were elevated independently of *Pst/AvrRpm1* as compared to wild type plants (**Table S19**). Since Guzha et al (2022) detected that non-stressed *xyl4* mutants contain higher fucose levels in leaf pectin than wild type plants, the data suggests that *XYL4* signals control fucose retention in leaf pectin structures. Specifically, pectin components of cell walls and AGPs can be modified by adding fucose side chains by fucosylation events (Puhlmann et al., 1994; Freshour et al., 2003). It can thus be speculated that *XYL4*/*EDS1*-dependent signaling potentially modifies the composition of pectin side chains. As a result, such interlinking of pectin with other components of the wall or the breakdown thereof might greatly affect the flexibility and stiffness of cell walls (Bidhendi and Geitmann, 2016) and thus the ease for pathogens to penetrate tissues. Notably, mutant plants defective in the gene *MURUS 1* (also termed GDP-D-MANNOSE-4,6-DEHYDRATASE 2) have decreased levels of fucose and fucosylated AGPs, and moreover reduced cross-linkages in pectin (Tryfona et al., 2012; Feng et al., 2018). These *MURUS 1*-related alterations in pectin cross-links are suggested to contribute to PTI and ETI, and

additionally stomatal and apoplastic defense (Zhang et al., 2019). Together, this data suggests that modifications of cell wall pectin and fucose levels downstream of XYL4 might also play a role in SAR.

The expression of *MURUS 1* in *A. thaliana* is linked to that of two UDP-glucose 6-dehydrogenases, which promote the xylose-dependent biosynthesis of UDP-glucuronic acid (UDP-GlcA) (Klinghammer and Tenhaken, 2007). Notably, *EDS1* and *XYL4* do not appear to directly affect the accumulation of Glc-A and xylose in alcohol-extractable fractions upon a SAR stimulus (**Table S19**). Potentially, *EDS1*/*LLP1*- or *XYL4*-dependent changes in the xylose monosaccharide content might be detectable in cell-wall associated fractions. Notably, as Glc-A serves as a precursor for UDP-xylose (Li et al., 2015), a co-regulation of Glc-A and xylose levels in plants may be detectable. In support, mutants defective in Glc-A biosynthesis accumulate lower levels of the monosaccharide xylose (and additionally arabinose) and are moreover deficient in xylose-containing pectin side chains and xyloglucan (Reboul et al., 2011). In addition, mutants deficient in, for example, *WALL STRESS RESPONSE 1* (*WSR1*) accumulate elevated levels of xylose (and cellulose) in stems, but levels of glucuronic acid are reduced (Engelsdorf et al., 2019). Interestingly, *WSR1* associates with processes related to cell wall integrity maintenance, the regulation of SA levels and plant resistance to necrotrophic fungal pathogens (Engelsdorf et al., 2019). In sum, I thus propose that *XYL4* and *EDS1*/*LLP1* might have a promotive effect on fucose/Glc-A and thereby on the xylose pathway. Such regulative pathway may suppress fucose levels to modulate cross-linking of pectin and xyloglucan in pathogen-stressed plants.

Interestingly, levels of G3P were likewise accumulating as those of fucose in *eds1* and *xyl4* mutants when compared to wild type after infection with *Pst*/*AvrRpm1*, and additionally in mock-treated *xyl4* plants (**Table S19**). Hence, I hypothesize that pathways downstream of *EDS1* and *XYL4* might modulate the abundance of fucose (originating from pectin components in cell walls or AGPs) and G3P simultaneously during defense. Notably, a local treatment with an exogenously applied fungal, fucose-binding lectin protein induces SAR against *Pst* (Moradi et al., 2021). Thereby, transcripts of genes such as *G3P SYNTHESIS GENE GLY1*, *PR1*, and *RESPIRATORY BURST OXIDASE HOMOLOGS D* and *F* (*RBOHD* and *F*) were induced in lectin-inoculated leaves (Moradi et al., 2021). This suggests that fucose-associated signals may enhance G3P while also boosting ROS signals locally (**Figure 33**).

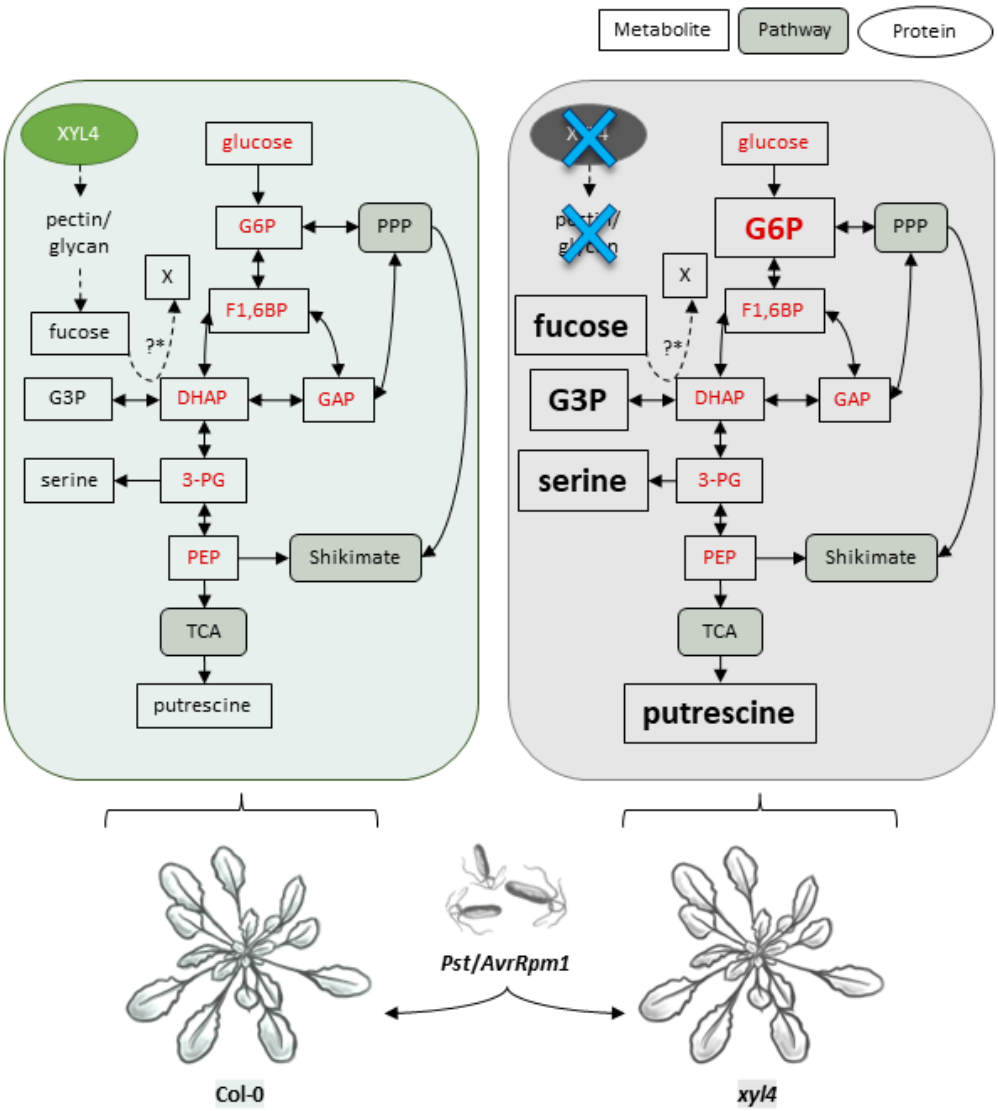

Figure 33: Model for XYL4/*XYL4*-dependent regulation of ETI-associated metabolites.
XYL4 signaling pathways regulate the accumulation of soluble metabolites after an infection with *Pst/AvrRpm1*. This model depicts plant responses detectable 2 days post spray inoculation comparing wild type (Col-0) and *xyl4* mutant plants. Compounds closely related to the pathway of glycolysis/gluconeogenesis are depicted in red. Arrows with dotted lines indicate a supposed induction. Compounds in bold and larger size indicate for higher accumulation after a bacterial infection. "?*" refers to a in plants not yet confirmed pathway converting L-fucose into substrate "X". Such substrate X might be pyruvate or a derivative that consumes dihydroxyacetone phosphate (DHAP) as was shown in *Escherichia coli* bacteria (Hacking and Lin, 1976). G3P: Glycerol-3-phosphate, G6P: Glucose-6-phosphate, F1,6BP: Fructose 1,6-bisphosphate, GAP: Glyceraldehyde 3-phosphate, 3-PG: 3-Phosphoglyceric acid, PPP: Pentose Phosphate Pathway, TCA: Tricarboxylic Acid Cycle. Modified after (Plaxton, 1996; Chanda et al., 2008; Millard et al., 2021).

Defense signaling via RBOHD/F may be furthermore linked to the most abundant polyamine in nature termed putrescine, which was described to be partially dependent on *EDS1*, *NPR1* and SA/*SID2* (Liu et al., 2020a) and to act in local and systemic tissues during defense in *A. thaliana* plants (Liu and Alcázar, 2021). When exogenously applied (500 µM), putrescine triggers SAR and SAR-related gene

expression (Liu and Alcázar, 2021). Putrescine furthermore acts in a positive feedback loop involving apoplastic ROS (hydrogen peroxide) and RBOHD/F (Liu et al., 2019) and regulates stress-responsive MAPK cascades in *A. thaliana* upon infection with bacterial pathogens such as *Pst* (Kim et al., 2013) or treatment with the bacterial PAMP flagellin22 (Liu et al., 2019). As putrescine was exclusively upregulated in *Pst*/*AvrRpm1*-inoculated *eds1* and *xyl4* mutants as compared to wild type plants (**Table S19**), I suggest that XYL4/*XYL4* and EDS1/*EDS1* might have a repressive effect on the accumulation of putrescine as part of a feedback loop after plant infection with avirulent bacteria (maybe this applies also for virulent organisms). Such *EDS1*/*XYL4*-dependent regulation might be a result of an upstream regulation of fucose or by altering levels of SA and JA (**Figure 33**), which both are linked to levels of putrescine: SA is positively and JA negatively associated (Anwar et al., 2015). Interestingly another putrescine-derived polyamine termed spermidine presumably accumulates in an *EDS1*- (and maybe *AvrRpm1*-) dependent manner (**Table S18**), indicating that EDS1/*EDS1* might have an important function in the regulation of levels of diverse polyamines. However, XYL4 alone supposedly has a minor role in an effective basal defense against bacteria (**Figure *18***A-B,D), thus PTI will rather be signaled via EDS1/*EDS1* alone including an *EDS1*-dependent regulation of levels of PCD-related dihydrosphingosines, Pip, SA etc. (**Table S18**).

4.5 Conclusion

The physical barriers formed around plant cells are highly dynamic structures that plants use to continuously adapt to environmental changes induced by abiotic or biotic stressors. Signaling cascades initiated at cell walls or membranes, which embed various receptors for signal perception and transduction, to date are not fully investigated for their contribution to plant defense. Interestingly, the intersecting pathways of *EDS1*- and SA-associated signals involving *LLPs* and *XYL4* can be suggested as important hubs that promote multiple plant stress responses of biotic and moreover abiotic nature. Thereby, a fine tuning of cell wall maintenance mechanisms and glycan metabolites may strongly shape plant defense and inducible responses. Specifically, I hypothesize that *LLP1*, *LLP3*, *EDS1* and *XYL4* synergistically promote SAR signaling via JA, SA, the Pip/G3P-derived pathway and possibly xylose (**Figures 34**, **Figure *32***, **Figure 33**). I propose that SAR signals are associated with cell wall defense and alterations in the carbohydrate metabolism, which are processes that are presumably modified by *XYL4*. In future, an involvement of *EDS1*, *LLPs* and *XYL4* in alterations of structural

components of cell walls should be confirmed. In addition, the contribution of carbohydrates, lectins and cell wall modifying enzymes to plant resistance should be a focus of further studies as they may find applications in plant protection techniques.

5. Outlook

Boosting innate immunity in plants bears great potential to protect plants against a broad spectrum of environmental stresses and diseases. Inducible plant defense responses such as ISR and SAR are very interesting mechanisms to promote plant protection more sustainably without using pesticides or agents harmful to plants or other organisms. As shown within this work, SAR seems to be regulated via interconnected routes including plant glycolytic pathways, which are suggested to modulate plant respiration, energy supply, lipid and carbohydrate metabolism, and the ability to adapt to environmental stresses (Plaxton, 1996; Dumont and Rivoal, 2019; Walker et al., 2021). Enzyme-controlled conversions of glycolytic intermediates relate to multiple defense-inducible reactions and changes in pH (Sakano, 2001). This leads to the assumption that by controlling parts of the glycolysis, a coordination of multiple plant stress responses is possible – including the modulation of systemic defense. It would thus be interesting to test if pathways via *EDS1* or *XYL4* control the activity of glycolysis-related enzymes such as phosphohexose isomerase or the G-6-P forming hexokinase (Plaxton, 1996), with the latter one affecting PCD, defense gene expression (Kim et al., 2006), and sugar signaling (Xiao et al., 2000).

Notably, XYL4 proteins accumulate in the apoplast of *A. thaliana* rosettes after infection with *Pst/AvrRpm1* (Breitenbach et al., 2014) and moreover in xylem tissues of grapevine plants after inoculation with the (hemi-)biotrophic bacterium *Xylella fastidiosa* (Chakraborty et al., 2016). This suggests that a regulation of defense-induced XYL4 might be widespread among different plant species. Additionally, increasing levels of XYL4 in vascular tissues potentially regulate signaling via intra-plant routes of the xylem sap. Since I suggest that *XYL4* contributes to SAR signaling via a vascular/phloem-mobile and airborne route, and moreover seems to modulate wounding-associated responses, it will be necessary to determine if wound-related routes may at least partially contribute to SAR signal generation. To test this, leaf exudates taken from mechanically wounded (e.g. cut with a razor, or pierced with a needle) plant tissues (wildtype and *xyl4* mutant plants) should be evaluated for their defense-inducing capacities in naïve recipient plants that will be challenged with *Pst*. By additionally comparing these results to the efficacy of leaf exudates of untreated, spray-, steam- or dip-inoculated plants in resistance induction, it should be possible to answer if wound signals fortify *XYL4*-dependent defense signaling via the vasculature. For that, plants could be separately infected in single leaves with *Pst/AvrRpm1* by using cotton swab/soft

brushes and ultrasound foggers for example, while covering the rest of the plant. In addition, since repeated wounding events likely lead to a greater accumulation of wound-responsive signals in plants (Zhang and Turner, 2008), it may be also worth investigating the extent to which wound signals affect defense and the establishment of SAR in syringe-inoculated plants via *XYL4* when leaves are inoculated once or several times (a day).

Wounding of plant cells in areas where XYL4 can be expressed such as stems or leaves, may trigger the translocation of JA precursors like OPDA into distal tissues (LaRue, 1941; Schulze et al., 2019; Hoermayer et al., 2020). Notably, JA-pathway dependent signals can be promoted by plasma membrane-localized JA transporters and GLUTAMATE RECEPTOR-LIKE (GLR) channels that allow cell-to-cell and long-distance translocation of molecules upon wounding (Li et al., 2020a; Li et al., 2021a; Uemura et al., 2021), indicating that GLRs may potentially modulate *XYL4*-associated signaling routes. Interestingly, functional GLR3 can be linked to wound-inducible communication within treated cells, signaling towards systemic tissues, and additionally to the production of NO and ROS, calcium ion fluxes and electrical signals during pathogen defense (Manzoor et al., 2013; Vega-Muñoz et al., 2020; Feng et al., 2021). Moreover, GLR3 responds to DAMPs such as degraded pectin of cell walls including OGs, which can stimulate metabolite accumulation in local (e.g. JA-Ile, ET, ABA) and systemic tissues (e.g. OPDA, SA, JA-Ile, ET, ABA), suggesting that GLRs contribute to cell wall-related defense (Ferrari et al., 2013; Davidsson et al., 2017; Gamir et al., 2021). Since I suggest that modifications in the composition of cell wall components such as pectin may influence SAR, it would be interesting to test if GLRs contribute to SAR signaling events.

In the context of wounding, signals initiated at pectin structures of cell walls may trigger a route via airborne molecules such as PME-activated methanol, which is suggested to promote plant-to-plant communication and immunity against a bacterial infection in tobacco plants (Dorokhov et al., 2012; Komarova et al., 2014; Dorokhov et al., 2018). Methanol-inducible genes and other genes coding for serine protease inhibitors - that are known from microbes and animals - are related to bacterial stress and wounding-associated responses in plants (Turra and Lorito, 2011). It will be interesting to test which exogenous volatile signals promote *XYL4*-dependent defense against pathogens such as *Pst*. For this, the ability of sender plants (wild type and *xyl4* mutants), stimulated by different concentrations of known SAR-inducing compounds, such as monoterpenes (pinenes) or

sesquiterpenes (caryophyllene), should be tested for defense induction in receiver plants. In addition to that, to also confirm if the SAR signaling models indeed reflect *in planta* regulated pathways as discussed above under 4., the plant defense-activating metabolites involving SA, SA-derivatives, SA/*PR1* activators (including electrical stimulation as described in Mori et al., 2021), Pip, a combination of Pip and G3P, NHP, AzA, ONA, JA-Ile, xylulose and different OGs should be assessed for their link to *XYL4*.

Other plant hormones that have not yet been investigated in relation to *XYL4* like CK, Auxin and associated pathways may further shape the signaling network of plant growth and defense. CKs, for example, were formerly associated with following aspects: the functionality of phloem, expression of *JAZ10*, leaf injury responses (Schulze et al., 2019), SA and *PR1*-associated defense responses (Choi et al., 2011; Argueso et al., 2012; Naseem and Dandekar, 2012), accumulation of ROS, and moreover the modulation of cell wall loosening enzymes like expansins and pectin modifiers (Brenner et al., 2012). CKs may thus be linked to intra-plant wound signaling, JA-SA crosstalk, cell wall remodeling and by this to responses related to XYL4 or LLPs during SAR. Interestingly, treatments with exogenous CK induces the accumulation of *XYL4* transcripts in plants overexpressing CK-responsive *ARABIDOPSIS RESPONSE REGULATOR 22* (*ARR22*) (Kiba et al., 2004). Because cytoplasmic ARR22 can suppress CK signaling via negative feedback (with no effect on ET, ABA, or auxins), this suggests that ARR22 has a regulatory function for CK-associated responses. Additionally, a promotive effect of *ARR22* on immunity against *Pst* via SA/NPR1-dependent signaling was described (Choi et al., 2010). This suggests that there may be a link between signaling pathways initiated by wounding, triggering CK and a subsequent signaling cascade that might modulate transcription of *ARR22* and *XYL4*, cell wall stiffness, and SA/JA signaling. Such wounding/CK- *XYL4*-associated pathways could affect PTI and/or ETI (*XYL4*-dependent) and trigger plant responses at an early stage of host-pathogen interaction (such as long-distance signaling) as mentioned earlier (Dervinis et al., 2010; Giron et al., 2013). To confirm this, in addition to JA-associated genes, the expression of *ARR22* and CK signaling-related genes should be compared from leavy tissues of SAR-stimulated, PTI-triggered, and wounded plants.

Notably, *A. thaliana* plants regulate *XYL4* upon drought (Clauw et al., 2016), exposure to cold or oxidative stress (Sham et al., 2014) and osmotic stress (Kilian et al., 2007), with an additional infection with *Pst* in drought-recovered plants differently regulating *XYL4* transcript accumulation than in plants undergoing a

drought-stress only (Gupta and Senthil-Kumar, 2017). In sum, *XYL4*/XYL4 may be involved in the regulation of responses to diverse abiotic stimuli besides pathogen defense. Including the results of my formerly described experiments, pathways via *XYL4* should thus be considered when investigating combined stress application (abiotic and biotic) in plants. Hence, a more detailed evaluation of the regulation of *XYL4*/XYL4 *in planta* is needed in a species- and environment-specific context to be able to predict the outcome of plant-pathogen interactions in future.

Following the data, it is consequently necessary to understand how *XYL4* can affect so many signaling pathways and putatively related metabolic routes. At first, XYL4 function *in planta* has to be determined. Secondly, experiments with double/triple mutants defective in SAR-related genes would provide further information of possible co-functional roles within the signaling network involving *XYL4*, *LLPs* and *EDS1*. The overall aim will be to identify pathways solely regulated by XYL4 and those commonly controlled by at least two SAR-associated modulators. For example, basal and systemic immunity could be analyzed in *Pst/AvrRpm1*-induced mutant plants such as *xyl4-llp3* and *xyl4-llp1*. Furthermore, the defense-inducible capacities from leaf exudates of *eds1-2* and *xyl4-llp3*, *xyl4-llp1*, *xyl4-llp1-llp3* should be determined, as well as the ability of such mutant plants to transmit/perceive airborne and immune-modulating compounds. Since *LLP3* presumably functions as modulator of systemic JA signals (Sales, 2021), systemic immune responses of JA-treated *xyl4-llp1* and *xyl4-llp1-llp3* mutants should be compared to that of *llp1-1* and wild type plants. Additionally, since in the context of SAR, I found not yet assignable metabolites in the GC-MS analysis of soluble metabolites, further analyses need to be performed to identify and characterize these *XYL4*- and/or *EDS1*-associated molecules, in order to clarify which metabolic pathways are employed to modulate SAR. Besides knowing predicted functional groups from the unknown molecules (as extractable from our GC-MS data), additional techniques such as infrared absorption spectroscopy or nuclear magnetic resonance would help to reveal the structure/fingerprint of those molecules and model SAR signaling pathways in more detail.

Additionally, the dependency of systemic signaling as triggered by exogenous xylose on *EDS1*, *LLP1* and potentially other *LLPs* should be thoroughly examined (including analyzing *EDS1* and *LLP3* gene transcript accumulation in inoculated and distal leaves). By answering the question which mechanisms via *EDS1*- and *LLP1*-dependent signaling prevent xylose-inducible immunity, it might be possible to elucidate potential signaling routes involving XYL4. For example, an *EDS1*-

triggered localization of XYL4 and LLP3 in the apoplastic space may require xylose signals – also in a time-dependent manner of early or late phase of defense. Potentially, either during translocation of these proteins or during the process of anchoring to the apoplast, phloem loading with SAR-related molecules can occur as described (Singh et al., 2017). It is to investigate if *EDS1* is needed in some capacity (maybe indirectly) for the final localization of XYL4 and also LLP3 to the apoplast (or any other extracellular structure). EDS1/*EDS1* may thereby function as a downstream signaling component, while *EDS1* transcription may not be required upstream of the localization/anchoring induction of XYL4/LLP3 (Breitenbach et al., 2014; Sales et al., 2021).

Furthermore, in the screening of cell wall polymers (CoMPP) of SAR spray-induced plants, further genotypes like *llp1* mutants were included and showed significantly less abundant polymer epitopes detectable by INRA-RU1 and INRA-RU2 as compared to *eds1* mutants and wild type plants (data not shown). Notably, such epitopes are suggested to belong to backbone structures of (unbranched) RG-I, which, in the case of INRA-RU1, do not carry galactosyl side-chains (Ralet et al., 2010). Plants cell walls consist of 5-36% of RG-Is, while within the pectin fraction RG-Is represent 11-85% - depending on plant variety and plant organ (Houben et al., 2011). As RG-Is play an important role in wall biomechanics and moreover affect gelling characteristics of walls (Kaczmarska et al., 2022), I suggest that LLP1/*LLP1* or related downstream signals may either stimulate the synthesis of (branched) RG-I or side branching with e.g. specifically galactosyl residues. Interestingly, by using the online software tool COACH-D (Wu et al., 2018b), predicted protein-ligands for LLP1 include α-D-mannose, α-D-galactose, and β-D-galactose, indicating that LLP1 might respond to (stress-released) molecules like galactose that could originate from RG-I side-branches. Additionally, plant behavior to hydration and dehydration (e.g. reaction to (recurring) drought stress events) and wall firmness/texture might be regulated via *LLP1* and inducible changes in RG-I-related glycan linkages. It would be thus interesting to confirm and examine the exact role of LLP1/*LLP1* in remodeling of cell wall structures.

It should furthermore be considered that *XYL4*-regulated glycosylation events may shape plant physiological traits besides defense. Interestingly, salt-treated mutant plants defective in *N-ACETYLGLUCOSAMINYL-TRANSFERASE I* (also termed *COMPLEX GLYCAN 1*, *CGL1*) – an enzyme involved in protein glycosylation – accumulate about 50% less XYL4 proteins when compared to wild type plants (Liu et al., 2021b). This indicates that there might be a correlation with XYL4 levels *in*

planta and glycosylation events, which, for example, involve the synthesis of complex (osmosis-related) N-glycans in the Golgi apparatus. Notably, *cgl1* mutants showed stunted root growth and altered root hair morphology due to the lack of protein glycosylation (Frank et al., 2008), an effect that might influence root physiological traits such as root length in *xyl4* and *llp3* seedling plants as described above. In addition, plants deficient in either *ARGONAUTE 1* (leaf development) or *SUPERROOT 1/2* (auxin overproduction) displayed elevated *XYL4* transcript levels and more pronounced protein glycosylation than wild type plants (Sorin et al., 2006), suggesting that an indirect *XYL4*-stimulated glycosylation of proteins may simultaneously influence plant growth and defense. Last but not least, *XYL4* transcripts are slightly repressed in mutants deficient in *ARABIDOPSIS BINDING PROTEIN 1*, whose functional protein promotes plant physiological processes such as light-driven cell division and elongation events during the night phase (Paque et al., 2014). Interestingly, fucosylation of xyloglucans thereby influences light-dependent hypocotyl elongation – maybe there is a link between pectin-associated fucose residues and XYL4 required as possible regulatory components to regulate plant growth in absence of light? These findings may point to the fact that pathways via *XYL4* may be involved in the formation of new tissues and/or the differentiation of organs, also during plant defense.

In conclusion, *XYL4* seems to have multifaceted roles in plant development and stress tolerance regulation. Altogether, XYL4 may thus shape inducible defense in diverse plant species and the regulation of its pathway will potentially find application in future plant protection techniques via ISR and SAR as promising alternatives to conventional crop management. Especially in crops of high global gross production and cultivation value such as rice, maize, wheat, or soybean, it needs to be investigated if their innate immunity can be boosted by application of immune-modulating compounds such as oligogalacturonides other cell wall-related molecules, or by exposure to (controlled) abiotic stimuli such as osmotic substances (including sugars or salt), drought, heat etc. As priming for innate immunity involves adaption to stress and improved fitness responses via epigenetic regulations, any mechanisms of the *EDS1*/*LLP*/*XYL4* network could be a target for breeding more tolerant varieties. With further knowledge about SAR, ISR and inter-plant communication, we might be able to grow diverse crops in fields in the future in a more sustainable way.

6. References

Aarts N, Metz M, Holub E, Staskawicz BJ, Daniels MJ, Parker JE (1998) Different requirements for EDS1 and NDR1 by disease resistance genes define at least two R gene-mediated signaling pathways in Arabidopsis. Proc Natl Acad Sci U S A **95**: 10306–10311

Ádám AL, Nagy Z, Kátay G, Mergenthaler E, Viczián O (2018) Signals of systemic immunity in plants: Progress and open questions. Int J Mol Sci **19**: 1–21

Adie B, Chico JM, Rubio-Somoza I, Solano R (2007a) Modulation of plant defenses by ethylene. J Plant Growth Regul **26**: 160–177

Adie BAT, Pérez-Pérez J, Pérez-Pérez MM, Godoy M, Sánchez-Serrano JJ, Schmelz EA, Solano R (2007b) ABA is an essential signal for plant resistance to pathogens affecting JA biosynthesis and the activation of defenses in Arabidopsis. Plant Cell **19**: 1665–81

Aerts N, Pereira Mendes M, Van Wees SCM (2021) Multiple levels of crosstalk in hormone networks regulating plant defense. Plant J **105**: 489–504

Ali S, Mir ZA, Bhat JA, Tyagi A, Chandrashekar N, Yadav P, Rawat S, Sultana M, Grover A (2018) Isolation and characterization of systemic acquired resistance marker gene PR1 and its promoter from Brassica juncea. 3 Biotech **8**: 1–14

Altmann M, Altmann S, Rodriguez PA, Weller B, Elorduy Vergara L, Palme J, Marín-de la Rosa N, Sauer M, Wenig M, Villaécija-Aguilar JA, et al (2020) Extensive signal integration by the phytohormone protein network. Nature **583**: 271–276

Alvarez ME, Pennell RI, Meijer PJ, Ishikawa A, Dixon RA, Lamb C (1998) Reactive oxygen intermediates mediate a systemic signal network in the establishment of plant immunity. Cell **92**: 773–784

Anderson JP, Badruzsaufari E, Schenk PM, Manners JM, Desmond OJ, Ehlert C, Maclean DJ, Ebert PR, Kazan K (2004) Antagonistic interaction between abscisic acid and jasmonate-ethylene signaling pathways modulates defense gene expression and disease resistance in arabidopsis. Plant Cell **16**: 3460–79

Anwar R, Mattoo AK, Handa AK (2015) Polyamine interactions with plant hormones: Crosstalk at several levels. Polyam A Univers Mol Nexus Growth, Surviv Spec Metab. doi: 10.1007/978-4-431-55212-3_22

Argueso CT, Ferreira FJ, Epple P, To JPC, Hutchison CE, Schaller GE, Dangl JL, Kieber JJ (2012) Two-component elements mediate interactions between cytokinin and salicylic acid in plant immunity. PLoS Genet **8**: e1002448

Arsovski AA, Haughn GW, Western TL (2010) Seed coat mucilage cells of Arabidopsis thaliana as a model for plant cell wall research. Plant Signal Behav **5**: 796–801

Arsovski AA, Popma TM, Haughn GW, Carpita NC, McCann MC, Western TL (2009) AtBXL1 encodes a bifunctional β-D-xylosidase/α-L-arabinofuranosidase required for pectic arabinan modification in Arabidopsis mucilage secretory cells. Plant Physiol **150**: 1219–34

Asai T, Tena G, Plotnikova J, Willmann MR, Chiu WL, Gomez-Gomez L, Boller T, Ausubel FM, Sheen J (2002) Map kinase signalling cascade in Arabidopsis innate immunity. Nature **415**: 977–83

Attaran E, Zeier TE, Griebel T, Zeier J (2009) Methyl salicylate production and jasmonate signaling are not essential for systemic acquired resistance in Arabidopsis. Plant Cell **21**: 954–971

Bacete L, Hamann T (2020) The role of mechanoperception in plant cell wall integrity maintenance. Plants **9**: 574–92

Bacete L, Mélida H, Miedes E, Molina A (2018) Plant cell wall-mediated immunity: cell wall changes trigger disease resistance responses. Plant J **93**: 614–636

Balmer A, Pastor V, Gamir J, Flors V, Mauch-Mani B (2015) The "prime-ome": Towards a holistic approach to priming. Trends Plant Sci **20**: 443–452

Barbier T, Collard F, Zúñiga-Ripa A, Moriyón I, Godard T, Becker J, Wittmann C, Van Schaftingen E, Letesson JJ (2014) Erythritol feeds the pentose phosphate pathway via three new isomerases leading to D-erythrose-4-phosphate in Brucella. Proc Natl Acad Sci U S A. doi: 10.1073/pnas.1414622111

Bari R, Jones JDG (2009) Role of plant hormones in plant defence responses. Plant Mol Biol **69**: 473–488

Barrera-Ortiz S, Garnica-Vergara A, Esparza-Reynoso S, García-Cárdenas E, Raya-González J, Francisco Ruiz-Herrera L, López-Bucio J (2018) Jasmonic Acid-Ethylene Crosstalk via ETHYLENE INSENSITIVE 2 Reprograms Arabidopsis Root System Architecture Through Nitric Oxide Accumulation. J Plant Growth Regul **37**: 438–451

Bartsch M, Bednarek P, Vivancos PD, Schneider B, von Roepenack-Lahaye E, Foyer CH, Kombrink E, Scheel D, Parker JE (2010) Accumulation of Isochorismate-derived 2,3-Dihydroxybenzoic 3-O-β-d-Xyloside in Arabidopsis Resistance to Pathogens and Ageing of Leaves. J Biol Chem **285**: 25654–25665

Bartsch M, Gobbato E, Bednarek P, Debey S, Schultze JL, Bautor J, Parker JE (2006) Salicylic Acid – Independent ENHANCED DISEASE SUSCEPTIBILITY1 Signaling

in Arabidopsis Immunity and Cell Death Is Regulated by the Monooxygenase FMO1 and the Nudix Hydrolase NUDT7. Plant Cell **18**: 1038–1051

Bauer S, Mekonnen DW, Hartmann M, Yildiz I, Janowski R, Lange B, Geist B, Scha AR (2021) UGT76B1, a promiscuous hub of small molecule-based immune signaling, glucosylates N-hydroxypipecolic acid, and balances plant immunity. Plant Cell **33**: 714–734

Bell E, Creelman RA, Mullet JE (1995) A chloroplast lipoxygenase is required for wound-induced jasmonic acid accumulation in Arabidopsis. Proc Natl Acad Sci U S A **92**: 8675–79

Bellincampi D, Cervone F, Lionetti V (2014) Plant cell wall dynamics and wall-related susceptibility in plantâ€"pathogen interactions. Front Plant Sci **5**: 1–8

Bernsdorff F, Doering A-C, Gruner K, Schuck S, Bräutigam A, Zeier J (2016) Pipecolic acid orchestrates plant systemic acquired resistance and defense priming via salicylic acid-dependent and independent pathways. Plant Cell **28**: 102–129

Berrocal-Lobo M, Molina A, Solano R (2002) Constitutive expression of Ethylene-Response-Factor1 in arabidopsis confers resistance to several necrotrophic fungi. Plant J **29**: 23–32

Bethke G, Grundman RE, Sreekanta S, Truman W, Katagiri F, Glazebrook J (2014) Arabidopsis PECTIN METHYLESTERASEs contribute to immunity against Pseudomonas syringae. Plant Physiol **164**: 1093–107

Bethke G, Thao A, Xiong G, Li B, Soltis NE, Hatsugai N, Hillmer RA, Katagiri F, Kliebenstein DJ, Pauly M, et al (2015) Pectin Biosynthesis Is Critical for Cell Wall Integrity and Immunity in Arabidopsis thaliana. Plant Cell **28**: 537–556

Betsuyaku S, Katou S, Takebayashi Y, Sakakibara H, Nomura N, Fukuda H (2018) Salicylic Acid and Jasmonic Acid Pathways are Activated in Spatially Different Domains Around the Infection Site During Effector-Triggered Immunity in Arabidopsis thaliana. Plant Cell Physiol **59**: 8–16

Bhandari DD, Lapin D, Kracher B, von Born P, Bautor J, Niefind K, Parker JE (2019) An EDS1 heterodimer signalling surface enforces timely reprogramming of immunity genes in Arabidopsis. Nat Commun **10**: 772–785

Bhattacharjee S, Halane MK, Kim SH, Gassmann W (2011) Pathogen effectors target Arabidopsis EDS1 and alter its interactions with immune regulators. Science (80-) **334**: 1405–08

Bidhendi AJ, Geitmann A (2016) Relating the mechanics of the primary plant cell wall to morphogenesis. J Exp Bot **67**: 449–61

Blake AW, McCartney L, Flint JE, Bolam DN, Boraston AB, Gilbert HJ, Knox JP (2006) Understanding the biological rationale for the diversity of cellulose-directed carbohydrate-binding modules in prokaryotic enzymes. J Biol Chem **281**: 29321–9

Boava LP, Cristofani-Yaly M, Stuart RM, Machado MA (2011) Expression of defense-related genes in response to mechanical wounding and Phytophthora parasitica infection in Poncirus trifoliata and Citrus sunki. Physiol Mol Plant Pathol **76**: 119–125

Böhmer M, Schroeder JI (2011) Quantitative transcriptomic analysis of abscisic acid-induced and reactive oxygen species-dependent expression changes and proteomic profiling in Arabidopsis suspension cells. Plant J **67**: 105–118

Bolouri Moghaddam MR, Vilcinskas A, Rahnamaeian M (2016) Cooperative interaction of antimicrobial peptides with the interrelated immune pathways in plants. Mol Plant Pathol **17**: 464–471

Bonfig KB, Gabler A, Simon UK, Luschin-Ebengreuth N, Hatz M, Berger S, Muhammad N, Zeier J, Sinha AK, Roitsch T (2010) Post-translational derepression of invertase activity in source leaves via down-regulation of invertase inhibitor expression is part of the plant defense response. Mol Plant **3**: 1037–1048

Bonfig KB, Schreiber U, Gabler A, Roitsch T, Berger S (2006) Infection with virulent and avirulent P. syringae strains differentially affects photosynthesis and sink metabolism in Arabidopsis leaves. Planta **225**: 1–12

Bonnemain J-L, Chollet J-F, Rocher F (2013) Transport of Salicylic Acid and Related Compounds. SALICYLIC ACID. pp 43–59

Bosch M, Wright LP, Gershenzon J, Wasternack C, Hause B, Schaller A, Stintzi A (2014) Jasmonic acid and its precursor 12-Oxophytodienoic acid control different aspects of constitutive and induced herbivore defenses in tomato. Plant Physiol **166**: 396–410

Boudart G, Jamet E, Rossignol M, Lafitte C, Borderies G, Jauneau A, Esquerré-Tugayé MT, Pont-Lezica R (2005) Cell wall proteins in apoplastic fluids of Arabidopsis thaliana rosettes: Identification by mass spectrometry and bioinformatics. Proteomics **5**: 212–221

Breitenbach HH, Wenig M, Wittek F, Jorda L, Maldonado-Alconada AM, Sarioglu H, Colby T, Knappe C, Bichlmeier M, Pabst E, et al (2014) Contrasting Roles of the Apoplastic Aspartyl Protease APOPLASTIC, ENHANCED DISEASE SUSCEPTIBILITY1-DEPENDENT1 and LEGUME LECTIN-LIKE PROTEIN1 in Arabidopsis Systemic Acquired Resistance,. Plant Physiol **165**: 791–809

Brenner WG, Ramireddy E, Heyl A, Schmülling T (2012) Gene regulation by cytokinin

in Arabidopsis. Front Plant Sci **3**: 8–30

Brodersen P, Petersen M, Pike HM, Olszak B, Skov S, Ødum N, Jørgensen LB, Brown RE, Mundy J (2002) Knockout of Arabidopsis accelerated-cell-death11 encoding a sphingosine transfer protein causes activation of programmed cell death and defense. Genes Dev **16**: 490–502

Budimir J, Treffon K, Nair A, Thurow C, Gatz C (2021) Redox-active cysteines in TGACG-BINDING FACTOR 1 (TGA1) do not play a role in salicylic acid or pathogen-induced expression of TGA1-regulated target genes in Arabidopsis thaliana. New Phytol **230**: 2420–2432

Cai J, Jozwiak A, Holoidovsky L, Meijler MM, Meir S, Rogachev I, Aharoni A (2021) Glycosylation of N-hydroxy-pipecolic acid equilibrates between systemic acquired resistance response and plant growth. Mol Plant **14**: 440–455

Caillaud MC, Wirthmueller L, Sklenar J, Findlay K, Piquerez SJM, Jones AME, Robatzek S, Jones JDG, Faulkner C (2014) The Plasmodesmal Protein PDLP1 Localises to Haustoria-Associated Membranes during Downy Mildew Infection and Regulates Callose Deposition. PLoS Pathog **10**: e1004496

Carella P, Kempthorne CJ, Wilson DC, Isaacs M, Cameron RK (2017) Exploring the role of DIR1, DIR1-like and other lipid transfer proteins during systemic immunity in Arabidopsis. Physiol Mol Plant Pathol **97**: 49–57

Carpita NC (1996) Structure and biogenesis of the cell walls of grasses. Annu Rev Plant Physiol Plant Mol Biol **47**: 445–476

Carpita NC, Gibeaut DM (1993) Structural models of primary cell walls in flowering plants: Consistency of molecular structure with the physical properties of the walls during growth. Plant J **3**: 1–30

Carvalho FP (2017) Pesticides, environment, and food safety. Food Energy Secur **6**: 48–60

Cavaco AR, Matos AR, Figueiredo A (2021) Speaking the language of lipids: the cross-talk between plants and pathogens in defence and disease. Cell Mol Life Sci **78**: 4399–4415

Caviglia M, Mazorra Morales LM, Concellón A, Gergoff Grozeff GE, Wilson M, Foyer CH, Bartoli CG (2018) Ethylene signaling triggered by low concentrations of ascorbic acid regulates biomass accumulation in Arabidopsis thaliana. Free Radic Biol Med **122**: 130–136

Cecchini NM, Jung HW, Engle NL, Tschaplinski TJ, Greenberg JT (2015a) ALD1 Regulates Basal Immune Components and Early Inducible Defense Responses in

Arabidopsis. Mol Plant-Microbe Interact **28**: 455–466

Cecchini NM, Roychoudhry S, Speed DQJ, Steffes K, Tambe A, Zodrow K, Konstantinoff K, Jung HW, Engle NL, Tschaplinski TJ, et al (2019) Underground azelaic acid–conferred resistance to pseudomonas syringae in arabidopsis. Mol Plant-Microbe Interact **32**: 86–94

Cecchini NM, Steffes K, Schlappi MR, Gifford AN, Greenberg JT (2015b) Arabidopsis AZI1 family proteins mediate signal mobilization for systemic defence priming. Nat Commun **6**: 1–12

Chakraborty S, Nascimento R, Zaini PA, Gouran H, Rao BJ, Goulart LR, Dandekar AM (2016) Sequence/structural analysis of xylem proteome emphasizes pathogenesis-related proteins, chitinases an β-1, 3-glucanases as key players in grapevine defense against Xylella fastidiosa. PeerJ **24**: e2007

Chanclud E, Kisiala A, Emery NRJ, Chalvon V, Ducasse A, Romiti-Michel C, Gravot A, Kroj T, Morel JB (2016) Cytokinin Production by the Rice Blast Fungus Is a Pivotal Requirement for Full Virulence. PLoS Pathog **12**: e1005457

Chanda B, Venugopal SC, Kulshrestha S, Navarre DA, Downie B, Vaillancourt L, Kachroo A, Kachroo P (2008) Glycerol-3-Phosphate Levels Are Associated with Basal Resistance to the Hemibiotrophic Fungus Colletotrichum higginsianum in Arabidopsis. Plant Physiol **147**: 2017–2029

Chanda B, Xia Y, Mandal MK, Yu K, Sekine KT, Gao QM, Selote D, Hu Y, Stromberg A, Navarre D, et al (2011) Glycerol-3-phosphate is a critical mobile inducer of systemic immunity in plants. Nat Genet **43**: 421–429

Chandran V, Shahena S, Rajan M, Mathew L (2020) Controlled Release of Plant Hormones for Modifying Crop Yield. Control. Release Pestic. Sustain. Agric. pp 253–266

Chang M, Zhao J, Chen H, Li G, Chen J, Li M, Palmer IA, Song J, Alfano JR, Liu F, et al (2019) PBS3 Protects EDS1 from Proteasome-Mediated Degradation in Plant Immunity. Mol Plant **12**: 678–688

Charmont S, Jamet E, Pont-Lezica R, Canut H (2005) Proteomic analysis of secreted proteins from Arabidopsis thaliana seedlings: Improved recovery following removal of phenolic compounds. Phytochemistry **66**: 453–461

Chaturvedi R, Krothapalli K, Makandar R, Nandi A, Sparks AA, Roth MR, Welti R, Shah J (2008) Plastid ω3-fatty acid desaturase-dependent accumulation of a systemic acquired resistance inducing activity in petiole exudates of Arabidopsis thaliana is independent of jasmonic acid. Plant J **54**: 106–117

Chaturvedi R, Venables B, Petros RA, Nalam V, Li M, Wang X, Takemoto LJ, Shah J (2012) An abietane diterpenoid is a potent activator of systemic acquired resistance. Plant J **71**: 161–172

Chen H, Xue L, Chintamanani S, Germain H, Lin H, Cui H, Cai R, Zuo J, Tang X, Li X, et al (2009a) ETHYLENE INSENSITIVE3 and ETHYLENE INSENSITIVE3-LIKE1 repress SALICYLIC ACID INDUCTION DEFICIENT2 expression to negatively regulate plant innate immunity in Arabidopsis. Plant Cell **21**: 2527–40

Chen K, Li GJ, Bressan RA, Song CP, Zhu JK, Zhao Y (2020) Abscisic acid dynamics, signaling, and functions in plants. J Integr Plant Biol **62**: 25–54

Chen Y-C, Holmes EC, Rajniak J, Kim J, Tang S, Fischer CR, Mudgett MB, Sattely ES (2018) N-hydroxy-pipecolic acid is a mobile metabolite that induces systemic disease resistance in Arabidopsis. Proc Natl Acad Sci U S A **115**: E4920–E4929

Chen YL, Lee CY, Cheng KT, Chang WH, Huang RN, Nam HG, Chen YR (2014) Quantitative peptidomics study reveals that a wound-induced peptide from PR-1 regulates immune signaling in tomato. Plant Cell **26**: 4135–48

Chen Z, Zheng Z, Huang J, Lai Z, Fan B (2009b) Biosynthesis of salicylic acid in plants. Plant Signal Behav **4**: 493–496

Cheng Y, Zhang H, Yao J, Wang X, Xu J, Han Q, Wei G, Huang L, Kang Z (2012) Characterization of non-host resistance in broad bean to the wheat stripe rust pathogen. BMC Plant Biol **12**: 1–12

Chien PS, Nam HG, Chen YR (2015) A salt-regulated peptide derived from the CAP superfamily protein negatively regulates salt-stress tolerance in Arabidopsis. J Exp Bot **66**: 5301–13

Chini A, Grant JJ, Seki M, Shinozaki K, Loake GJ (2004) Drought tolerance established by enhanced expression of the CC-NBS-LRR gene, ADR1, requires salicylic acid, EDS1 and ABI1. Plant J **38**: 810–822

Chisholm ST, Coaker G, Day B, Staskawicz BJ (2006) Host-microbe interactions: Shaping the evolution of the plant immune response. Cell **124**: 803–814

Choi J, Choi D, Lee S, Ryu CM, Hwang I (2011) Cytokinins and plant immunity: Old foes or new friends? Trends Plant Sci **16**: 388–394

Choi J, Huh SU, Kojima M, Sakakibara H, Paek KH, Hwang I (2010) The cytokinin-activated transcription factor ARR2 promotes plant immunity via TGA3/NPR1-dependent salicylic acid signaling in arabidopsis. Dev Cell **19**: 284–295

Choudhary DK, Prakash A, Johri BN (2007) Induced systemic resistance (ISR) in plants:

Mechanism of action. Indian J Microbiol **47**: 289–297

Clarke JD, Volko SM, Ledford H, Ausubel FM, Dong X (2000) Roles of salicylic acid, jasmonic acid, and ethylene in cpr-Induced resistance in arabidopsis. Plant Cell **12**: 2175–90

Clausen MH, Willats WGT, Knox JP (2003) Synthetic methyl hexagalacturonate hapten inhibitors of anti-homogalacturonan monoclonal antibodies LM7, JIM5 and JIM7. Carbohydr Res **338**: 1797–800

Clauw P, Coppens F, Korte A, Herman D, Slabbinck B, Dhondt S, Van Daele T, De Milde L, Vermeersch M, Maleux K, et al (2016) Leaf growth response to mild drought: Natural variation in arabidopsis sheds light on trait architecture. Plant Cell **28**: 2417–2434

Claverie J, Balacey S, Lemaître-Guillier C, Brulé D, Chiltz A, Granet L, Noirot E, Daire X, Darblade B, Héloir MC, et al (2018) The cell wall-derived xyloglucan is a new DAMP triggering plant immunity in vitis vinifera and arabidopsis thaliana. Front Plant Sci **871**: 1–14

De Cnodder T, Vissenberg K, Van Der Straeten D, Verbelen JP (2005) Regulation of cell length in the Arabidopsis thaliana root by the ethylene precursor 1-aminocyclopropane-1-carboxylic acid: A matter of apoplastic reactions. New Phytol **168**: 541–550

Cohn JR, Martin GB (2005) Pseudomonas syringae pv. tomato type III effectors AvrPto and AvrPtoB promote ethylene-dependent cell death in tomato. Plant J **44**: 139–154

Conrath U (2006) Systemic Acquired Resistance. Plant Signal Behav **1**: 179–184

Conrath U, Pieterse CMJ, Mauch-Mani B (2002) Priming in plant-pathogen interactions. Trends Plant Sci **7**: 210–216

Crabill E, Joe A, Block A, van Rooyen JM, Alfano JR (2010) Plant immunity directly or indirectly restricts the injection of type III effectors by the Pseudomonas syringae type III secretion system. Plant Physiol **154**: 233–244

Crombie HJ, Chengappa S, Hellyer A, Grant Reid JS (1998) A xyloglucan oligosaccharide-active, transglycosylating β-D-glucosidase from the cotyledons of nasturtium (Tropaeolum majus L) seedlings - Purification, properties and characterization of a cDNA clone. Plant J **15**: 27–38

Cui H, Gobbato E, Kracher B, Qiu J, Bautor J, Parker JE (2017) A core function of EDS1 with PAD4 is to protect the salicylic acid defense sector in Arabidopsis immunity. New Phytol **213**: 1802–17

Cui H, Qiu J, Zhou Y, Bhandari DD, Zhao C, Bautor J, Parker JE (2018) Antagonism of Transcription Factor MYC2 by EDS1/PAD4 Complexes Bolsters Salicylic Acid Defense in Arabidopsis Effector-Triggered Immunity. Mol Plant **11**: 1053–1066

Cui H, Tsuda K, Parker JE (2015) Effector-triggered immunity: From pathogen perception to robust defense. Annu Rev Plant Biol **66**: 487–511

Datta R, Kumar D, Sultana A, Hazra S, Bhattacharyya D, Chattopadhyay S (2015) Glutathione regulates 1-aminocyclopropane-1-carboxylate synthase transcription via WRKY33 and 1-aminocyclopropane-1-carboxylate oxidase by modulating messenger RNA stability to induce ethylene synthesis during stress. Plant Physiol **169**: 2963–81

Davidsson P, Broberg M, Kariola T, Sipari N, Pirhonen M, Palva ET (2017) Short oligogalacturonides induce pathogen resistance-associated gene expression in Arabidopsis thaliana. BMC Plant Biol **17**: 19

Dean J V., Delaney SP (2008) Metabolism of salicylic acid in wild-type, ugt74f1 and ugt74f2 glucosyltransferase mutants of Arabidopsis thaliana. Physiol Plant **132**: 417–425

Dean J V., Mohammed LA, Fitzpatrick T (2005) The formation, vacuolar localization, and tonoplast transport of salicylic acid glucose conjugates in tobacco cell suspension cultures. Planta **221**: 287–296

DebRoy S, Thilmony R, Kwack YB, Nomura K, He SY (2004) A family of conserved bacterial effectors inhibits salicylic acid-mediated basal immunity and promotes disease necrosis in plants. Proc Natl Acad Sci U S A **101**: 9927–32

Deepak S, Shailasree S, Kini RK, Muck A, Mithöfer A, Shetty SH (2010) Hydroxyproline-rich Glycoproteins and Plant Defence. J Phytopathol **158**: 585–593

Delaney TP, Uknes S, Vernooij B, Friedrich L, Weymann K, Negrotto D, Gaffney T, Gut-Rella M, Kessmann H, Ward E, et al (1994) A central role of salicylic acid in plant disease resistance. Science (80-) **266**: 1247–50

Delgado-Cerezo M, Sánchez-Rodríguez C, Escudero V, Miedes E, Fernández PV, Jordá L, Hernández-Blanco C, Sánchez-Vallet A, Bednarek P, Schulze-Lefert P, et al (2012) Arabidopsis heterotrimeric G-protein regulates cell wall defense and resistance to necrotrophic fungi. Mol Plant **5**: 98–114

Demianski AJ, Chung KM, Kunkel BN (2012) Analysis of Arabidopsis JAZ gene expression during Pseudomonas syringae pathogenesis. Mol Plant Pathol **13**: 46–57

Dempsey DA, Shah J, Klessig DF (1999) Salicylic acid and disease resistance in plants. CRC Crit Rev Plant Sci **18**: 547–575

Denancé N, Sánchez-Vallet A, Goffner D, Molina A (2013) Disease resistance or growth: The role of plant hormones in balancing immune responses and fitness costs. Front Plant Sci **4**: 1–12

Dervinis C, Frost CJ, Lawrence SD, Novak NG, Davis JM (2010) Cytokinin primes plant responses to wounding and reduces Insect performance. J Plant Growth Regul **29**: 289–296

Devoto A, Nieto-Rostro M, Xie D, Ellis C, Harmston R, Patrick E, Davis J, Sherratt L, Coleman M, Turner JG (2002) COI1 links jasmonate signalling and fertility to the SCF ubiquitin-ligase complex in Arabidopsis. Plant J **32**: 457–466

Dietz KJ, Vogel MO, Viehhauser A (2010) AP2/EREBP transcription factors are part of gene regulatory networks and integrate metabolic, hormonal and environmental signals in stress acclimation and retrograde signalling. Protoplasma **245**: 3–14

Ding Y, Dommel M, Mou Z (2016) Abscisic acid promotes proteasome-mediated degradation of the transcription coactivator NPR1 in Arabidopsis thaliana. Plant J **86**: 20–34

Ding Y, Dommel MR, Wang C, Li Q, Zhao Q, Zhang X, Dai S, Mou Z (2020) Differential Quantitative Requirements for NPR1 Between Basal Immunity and Systemic Acquired Resistance in Arabidopsis thaliana. Front Plant Sci **11**: 1–10

Ding Y, Sun T, Ao K, Peng Y, Zhang Y, Li X, Zhang Y (2018) Opposite Roles of Salicylic Acid Receptors NPR1 and NPR3/NPR4 in Transcriptional Regulation of Plant Immunity. Cell **173**: 1454-1467.e10

Doares SH, Albersheim P, Darvill AG (1991) An improved method for the preparation of standards glycosyl-linkage analysis of complex carbohydrates. **210**: 311–317

Doehlemann G, Hemetsberger C (2013) Apoplastic immunity and its suppression by filamentous plant pathogens. New Phytol **198**: 1001–1016

Van der Does D, Leon-Reyes A, Koornneef A, Van Verk MC, Rodenburg N, Pauwels L, Goossens A, Körbes AP, Memelink J, Ritsema T, et al (2013) Salicylic acid suppresses jasmonic acid signaling downstream of SCFCOI1-JAZ by targeting GCC promoter motifs via transcription factor ORA59. Plant Cell **25**: 744–761

Dong OX, Tong M, Bonardi V, El Kasmi F, Woloshen V, Wünsch LK, Dangl JL, Li X (2016) TNL-mediated immunity in Arabidopsis requires complex regulation of the redundant ADR1 gene family. New Phytol **210**: 960–973

Dong X (2001) Genetic dissection of systemic acquired resistance. Curr Opin Plant Biol **4**: 309–314

Dorokhov YL, Komarova T V., Petrunia I V., Frolova OY, Pozdyshev D V., Gleba YY (2012) Airborne signals from a wounded leaf facilitate viral spreading and induce antibacterial resistance in neighboring plants. PLoS Pathog **8**: e1002640

Dorokhov YL, Sheshukova E V., Komarova T V. (2018) Methanol in plant life. Front Plant Sci **9**: 1–6

Dubiella U, Seybold H, Durian G, Komander E, Lassig R, Witte CP, Schulze WX, Romeis T (2013) Calcium-dependent protein kinase/NADPH oxidase activation circuit is required for rapid defense signal propagation. Proc Natl Acad Sci U S A **110**: 8744–49

Dumont S, Rivoal J (2019) Consequences of oxidative stress on plant glycolytic and respiratory metabolism. Front Plant Sci **10**: 1–16

Eisenreich W, Bacher A, Arigoni D, Rohdich F (2004) Biosynthesis of isoprenoids via the non-mevalonate pathway. Cell Mol Life Sci **61**: 1401–26

El-Shetehy M, Wang C, Shine MB, Yu K, Kachroo A, Kachroo P (2015) Nitric oxide and reactive oxygen species are required for systemic acquired resistance in plants. Plant Signal Behav **10**: e998544

Ellis C, Karafyllidis I, Wasternack C, Turner JG (2002) The Arabidopsis mutant cev1 links cell wall signaling to jasmonate and ethylene responses. Plant Cell **14**: 1557–66

Ellis C, Turner JG (2001) The Arabidopsis mutant cev1 has constitutively active jasmonate and ethylene signal pathways and enhanced resistance to pathogens. Plant Cell **13**: 1025–33

Engelsdorf T, Kjaer L, Gigli-Bisceglia N, Vaahtera L, Bauer S, Miedes E, Wormit A, James L, Chairam I, Molina A, et al (2019) Functional characterization of genes mediating cell wall metabolism and responses to plant cell wall integrity impairment. BMC Plant Biol **19**: 320

Erban A, Schauer N, Fernie AR, Kopka J (2007) Nonsupervised construction and application of mass spectral and retention time index libraries from time-of-flight gas chromatography-mass spectrometry metabolite profiles. Methods Mol Biol **358**: 19–38

Falk A, Feys BJ, Frost LN, Jones JDG, Daniels MJ, Parker JE (1999) EDS1, an essential component of R gene-mediated disease resistance in Arabidopsis has homology to eukaryotic lipases. Proc Natl Acad Sci U S A **96**: 3292–97

Fan H, Dong H, Xu C, Liu J, Hu B, Ye J, Mai G, Li H (2017) Pectin methylesterases contribute the pathogenic differences between races 1 and 4 of Fusarium oxysporum f. sp. cubense. Sci Rep **7**: 13140

Fangel JU, Jones CY, Ulvskov P, Harholt J, Willats WGT (2021) Analytical implications of different methods for preparing plant cell wall material. Carbohydr Polym **261**: 117866

FAO (2018) The State of Food Security and Nutrition in the World 2018. Building climate resilience for food security and nutrition. The State of The World, United Nations 1–202

Farmer EE, Ryan CA (1992) Octadecanoid Precursors of Jasmonic Acid Activate the Synthesis of Wound-Inducible Proteinase Inhibitors. Plant Cell **4**: 129–134

Farquharson KL (2017) Secrets of the forest: Volatiles first discovered in pine trees propagate defense signals within and between plants. Plant Cell **29**: 1181–82

Feil H, Feil WS, Chain P, Larimer F, DiBartolo G, Copeland A, Lykidis A, Trong S, Nolan M, Goltsman E, et al (2005) Comparison of the complete genome sequences of Pseudomonas syringae pv. syringae B728a and pv. tomato DC3000. Proc Natl Acad Sci U S A **102**: 11064–69

Feng S, Pan C, Ding S, Ma Q, Hu C, Wang P, Shi K (2021) The glutamate receptor plays a role in defense against botrytis cinerea through electrical signaling in tomato. Appl Sci **11**: 1–11

Feng W, Kita D, Peaucelle A, Cartwright HN, Doan V, Duan Q, Liu MC, Maman J, Steinhorst L, Schmitz-Thom I, et al (2018) The FERONIA Receptor Kinase Maintains Cell-Wall Integrity during Salt Stress through Ca2+ Signaling. Curr Biol **28**: 666–675

Ferrari S, Savatin D V., Sicilia F, Gramegna G, Cervone F, De Lorenzo G (2013) Oligogalacturonides: Plant damage-associated molecular patterns and regulators of growth and development. Front Plant Sci **4**: 1–9

Feys BJ, Moisan LJ, Newman MA, Parker JE (2001) Direct interaction between the Arabidopsis disease resistance signaling proteins, EDS1 and PAD4. EMBO J **20**: 5400–11

Finkelstein RR, Gibson SI (2002) ABA and sugar interactions regulating development: Cross-talk or voices in a crowd? Curr Opin Plant Biol **5**: 26–32

Finkelstein RR, Li Wang M, Lynch TJ, Rao S, Goodman HM (1998) The arabidopsis abscisic acid response locus ABI4 encodes an APETALA2 domain protein. Plant Cell **10**: 1043–54

Fonseca S, Chini A, Hamberg M, Adie B, Porzel A, Kramell R, Miersch O, Wasternack C, Solano R (2009) (+)-7-iso-Jasmonoyl-L-isoleucine is the endogenous bioactive jasmonate. Nat Chem Biol **5**: 344–350

Fotopoulos V, Gilbert MJ, Pittman JK, Marvier AC, Buchanan AJ, Sauer N, Hall JL, Williams LE (2003) The monosaccharide transporter gene, AtSTP4, and the cell-wall invertase, Atβfruct1, are induced in arabidopsis during infection with the fungal biotroph Erysiphe cichoracearum. Plant Physiol **132**: 821–829

Frank J, Kaulfürst-Soboll H, Rips S, Koiwa H, Von Schaewen A (2008) Comparative analyses of Arabidopsis complex glycan1 mutants and genetic interaction with staurosporin and temperature sensitive3a. Plant Physiol **148**: 1354–67

Frank L, Wenig M, Ghirardo A, Krol A, Vlot AC, Schnitzler J, Rosenkranz M (2021) Isoprene and β-caryophyllene confer plant resistance via different plant internal signaling pathways. Plant Cell Environ **44**: 1151–1164

Freshour G, Bonin CP, Reiter WD, Albersheim P, Darvill AG, Hahn MG (2003) Distribution of fucose-containing xyloglucans in cell walls of the mur1 mutant of Arabidopsis. Plant Physiol **131**: 1602–12

Fu S, Shao J, Zhou C, Hartung JS (2016) Transcriptome analysis of sweet orange trees infected with "Candidatus Liberibacter asiaticus" and two strains of Citrus Tristeza Virus. BMC Genomics **17**: 1–18

Fu ZQ, Dong X (2013) Systemic Acquired Resistance: Turning Local Infection into Global Defense. Annu Rev Plant Biol **64**: 839–863

Fu ZQ, Yan S, Saleh A, Wang W, Ruble J, Oka N, Mohan R, Spoel SH, Tada Y, Zheng N, et al (2012) NPR3 and NPR4 are receptors for the immune signal salicylic acid in plants. Nature **486**: 228–232

Furihata T, Maruyama K, Fujita Y, Umezawa T, Yoshida R, Shinozaki K, Yamaguchi-Shinozaki K (2006) Abscisic acid-dependent multisite phosphorylation regulates the activity of a transcription activator AREB1. Proc Natl Acad Sci U S A **103**: 1988–93

Galili G, Tang G, Zhu X, Gakiere B (2001) Lysine catabolism: A stress and development super-regulated metabolic pathway. Curr Opin Plant Biol **4**: 261–266

Gamir J, Minchev Z, Berrio E, García JM, De Lorenzo G, Pozo MJ (2021) Roots drive oligogalacturonide-induced systemic immunity in tomato. Plant Cell Environ **44**: 275–289

Gantner J, Ordon J, Kretschmer C, Guerois R, Stuttmann J (2019) An EDS1-SAG101 complex is essential for tnl-mediated immunity in nicotiana benthamiana [OPEN]. Plant Cell **31**: 2456–2474

Gao H, Guo M, Song J, Ma Y, Xu Z (2021) Signals in systemic acquired resistance of plants against microbial pathogens. Mol Biol Rep **48**: 3747–3759

Gao H, Zhou Q, Yang L, Zhang K, Ma Y, Xu ZQ (2020) Metabolomics analysis identifies metabolites associated with systemic acquired resistance in Arabidopsis. PeerJ **8**: e10047

Gao Q-M, Zhu S, Kachroo P, Kachroo A (2015) Signal regulators of systemic acquired resistance. Front Plant Sci **6**: 1–12

Gao QM, Yu K, Xia Y, Shine MB, Wang C, Navarre DR, Kachroo A, Kachroo P (2014) Mono- and Digalactosyldiacylglycerol Lipids Function Nonredundantly to Regulate Systemic Acquired Resistance in Plants. Cell Rep **9**: 1681–91

Garcion C, Métraux J (2006) Salicylic acid: biosynthesis, metabolism and signal transduction. Annu. Plant Rev. Vol. 24 Plant Horm. Signal. pp 229–255

Gaupels F, Durner J, Kogel KH (2017) Production, amplification and systemic propagation of redox messengers in plants? The phloem can do it all! New Phytol **214**: 554–560

Gergoff G, Chaves A, Bartoli CG (2010) Ethylene regulates ascorbic acid content during dark-induced leaf senescence. Plant Sci **178**: 207–212

Gigli-Bisceglia N, Engelsdorf T, Hamann T (2020) Plant cell wall integrity maintenance in model plants and crop species - relevant cell wall components and underlying guiding principles. Cell Mol Life Sci **77**: 2049–2077

Giron D, Frago E, Glevarec G, Pieterse CMJ, Dicke M (2013) Cytokinins as key regulators in plant-microbe-insect interactions: Connecting plant growth and defence. Funct Ecol **27**: 599–609

Glazebrook J (2005) Contrasting Mechanisms of Defense Against Biotrophic and Necrotrophic Pathogens. Annu Rev Phytopathol **43**: 205–227

Goda H, Sasaki E, Akiyama K, Maruyama-Nakashita A, Nakabayashi K, Li W, Ogawa M, Yamauchi Y, Preston J, Aoki K, et al (2008) The AtGenExpress hormone and chemical treatment data set: Experimental design, data evaluation, model data analysis and data access. Plant J **55**: 526–542

Gómez S, van Dijk W, Stuefer JF (2010) Timing of induced resistance in a clonal plant network. Plant Biol **12**: 512–517

Goujon T, Minic Z, El Amrani A, Lerouxel O, Aletti E, Lapierre C, Joseleau JP, Jouanin L (2003) AtBXL1, a novel higher plant (Arabidopsis thaliana) putative beta-xylosidase gene, is involved in secondary cell wall metabolism and plant development. Plant J **33**: 677–690

Grant JJ, Chini A, Basu D, Loake GJ (2003) Targeted activation tagging of the

Arabidopsis NBS-LRR gene, ADR1, conveys resistance to virulent pathogens. Mol Plant-Microbe Interact **16**: 669–680

Griebel T, Zeier J (2008) Light regulation and daytime dependency of inducible plant defenses in arabidopsis: Phytochrome signaling controls systemic acquired resistance rather than local defense. Plant Physiol **147**: 790–801

Groen SC (2016) Signalling in systemic plant defence-roots put in hard graft. J Exp Bot. doi: 10.1093/jxb/erw349

Groen SC, Whiteman NK, Bahrami AK, Wilczek AM, Cui J, Russell JA, Cibrian-Jaramillo A, Butler IA, Rana JD, Huang GH, et al (2013) Pathogen-triggered ethylene signaling mediates systemic-induced susceptibility to herbivory in Arabidopsis. Plant Cell **25**: 4755–4766

Guo S, He F, Song B, Wu J (2021) Future direction of agrochemical development for plant disease in China. Food Energy Secur **10**: e293

Gupta A, Senthil-Kumar M (2017) Transcriptome changes in Arabidopsis thaliana infected with Pseudomonas syringae during drought recovery. Sci Rep **7**: 1–14

Guzha A, McGee R, Scholz P, Hartken D, Lüdke D, Bauer K, Wenig M, Zienkiewicz K, Herrfurth C, Feussner I, et al (2022) Cell wall-localized BETA-XYLOSIDASE4 contributes to immunity of Arabidopsis against Botrytis cinerea. Plant Physiol **189**: 1794–1813

Hacking AJ, Lin ECC (1976) Disruption of the fucose pathway as a consequence of genetic adaptation to propanediol as a carbon source in Escherichia coli. J Bacteriol. doi: 10.1128/jb.126.3.1166-1172.1976

Hamann T (2012) Plant cell wall integrity maintenance as an essential component of biotic stress response mechanisms. Front Plant Sci **3**: 1–5

Han X, Kahmann R (2019) Manipulation of phytohormone pathways by effectors of filamentous plant pathogens. Front Plant Sci **10**: 1–13

Hartmann M, Zeier J (2018a) l-lysine metabolism to N-hydroxypipecolic acid: an integral immune-activating pathway in plants. Plant J **96**: 5–21

Hartmann M, Zeier J (2019) N-hydroxypipecolic acid and salicylic acid: a metabolic duo for systemic acquired resistance. Curr Opin Plant Biol **50**: 44–57

Hartmann M, Zeier J (2018b) l-lysine metabolism to N-hydroxypipecolic acid: an integral immune-activating pathway in plants. Plant J **96**: 5–21

Hartmann M, Zeier T, Bernsdorff F, Reichel-Deland V, Kim D, Hohmann M,

Scholten N, Schuck S, Bräutigam A, Hölzel T, et al (2018) Flavin Monooxygenase-Generated N-Hydroxypipecolic Acid Is a Critical Element of Plant Systemic Immunity. Cell **173**: 456-469.e16

Hauck P, Thilmony R, He SY (2003) A Pseudomonas syringae type III effector suppresses cell wall-based extracellular defense in susceptible Arabidopsis plants. Proc Natl Acad Sci U S A **100**: 8577–82

Hauser F, Waadt R, Schroeder JI (2011) Evolution of abscisic acid synthesis and signaling mechanisms. Curr Biol **21**: 346–355

Haydon MJ, Mielczarek O, Robertson FC, Hubbard KE, Webb AAR (2013) Photosynthetic entrainment of the Arabidopsis thaliana circadian clock. Nature **502**: 689–692

Hématy K, Cherk C, Somerville S (2009) Host-pathogen warfare at the plant cell wall. Curr Opin Plant Biol **12**: 406–413

Hemmerlin A, Tritsch D, Hartmann M, Pacaud K, Hoeffler JF, Van Dorsselaer A, Rohmer M, Bach TJ (2006) A cytosolic arabidopsis D-xylulose kinase catalyzes the phosphorylation of 1-deoxy-D-xylulose into a precursor of the plastidial isoprenoid pathway. Plant Physiol. doi: 10.1104/pp.106.086652

Herbers K (1996) Systemic Acquired Resistance Mediated by the Ectopic Expression of Invertase: Possible Hexose Sensing in the Secretory Pathway. Plant Cell Online **8**: 793–803

Heredia A, Jiménez A, Guillén R (1995) Composition of plant cell walls. Z Lebensm Unters Forsch **200**: 24–31

Hernandez-Blanco C, Feng DX, Hu J, Sanchez-Vallet A, Deslandes L, Llorente F, Berrocal-Lobo M, Keller H, Barlet X, Sanchez-Rodriguez C, et al (2007) Impairment of Cellulose Synthases Required for Arabidopsis Secondary Cell Wall Formation Enhances Disease Resistance. Plant Cell Online **19**: 890–903

Hillmer RA, Tsuda K, Rallapalli G, Asai S, Truman W, Papke MD, Sakakibara H, Jones JDG, Myers CL, Katagiri F (2017) The highly buffered Arabidopsis immune signaling network conceals the functions of its components. PLoS Genet **13**: e1006639

Hoeffler J-F, Tritsch D, Grosdemange-Billiard C, Rohmer M (2002) Isoprenoid biosynthesis via the methylerythritol phosphate pathway. Eur J Biochem. doi: 10.1046/j.1432-1033.2002.03150.x

Hoermayer L, Montesinos JC, Marhava P, Benková E, Yoshida S, Friml J (2020) Wounding-induced changes in cellular pressure and localized auxin signalling spatially coordinate restorative divisions in roots. Proc Natl Acad Sci U S A **117**: 15322–31

Hofmann F, Schon MA, Nodine MD (2019) The embryonic transcriptome of Arabidopsis thaliana. Plant Reprod **32**: 77–91

Holmes EC, Chen Y-C, Mudgett MB, Sattely ES (2021) Arabidopsis UGT76B1 glycosylates N-hydroxy-pipecolic acid and inactivates systemic acquired resistance in tomato. Plant Cell **33**: 750–765

Hou S, Liu Z, Shen H, Wu D (2019) Damage-associated molecular pattern-triggered immunity in plants. Front Plant Sci **10**: 1–16

Houben K, Jolie RP, Fraeye I, Van Loey AM, Hendrickx ME (2011) Comparative study of the cell wall composition of broccoli, carrot, and tomato: Structural characterization of the extractable pectins and hemicelluloses. Carbohydr Res. doi: 10.1016/j.carres.2011.04.014

Houben M, Van de Poel B (2019) 1-aminocyclopropane-1-carboxylic acid oxidase (ACO): The enzyme that makes the plant hormone ethylene. Front Plant Sci **10**: 1–15

Houston K, Tucker MR, Chowdhury J, Shirley N, Little A (2016) The Plant Cell Wall: A Complex and Dynamic Structure As Revealed by the Responses of Genes under Stress Conditions. Front Plant Sci **7**: 1–18

Howe GA, Major IT, Koo AJ (2018) Modularity in Jasmonate Signaling for Multistress Resilience. Annu Rev Plant Biol **69**: 387–415

Huai B, Yang Q, Qian Y, Qian W, Kang Z, Liu J (2019) ABA-induced sugar transporter tastp6 promotes wheat susceptibility to stripe rust. Plant Physiol **181**: 1328–43

Huang S, Sawaki T, Takahashi A, Mizuno S, Takezawa K, Matsumura A, Yokotsuka M, Hirasawa Y, Sonoda M, Nakagawa H, et al (2010) Melon EIN3-like transcription factors (CmEIL1 and CmEIL2) are positive regulators of an ethylene- and ripening-induced 1-aminocyclopropane-1-carboxylic acid oxidase gene (CM-ACO1). Plant Sci **178**: 251–257

Hunt L, Mills LN, Pical C, Leckie CP, Aitken FL, Kopka J, Mueller-Roeber B, McAinsh MR, Hetherington AM, Gray JE (2003) Phospholipase C is required for the control of stomatal aperture by ABA. Plant J **34**: 47–55

Hunter P (2005) Common defences. EMBO Rep **6**: 504–507

Igamberdiev AU, Kleczkowski LA (2018) The glycerate and phosphorylated pathways of serine synthesis in plants: The branches of plant glycolysis linking carbon and nitrogen metabolism. Front Plant Sci **9**: 1–12

Iglesias N, Abelenda JA, Rodiño M, Sampedro J, Revilla G, Zarra I (2006) Apoplastic glycosidases active against xyloglucan oligosaccharides of Arabidopsis thaliana. Plant

Cell Physiol **47**: 55–63

Ishihama N, Yoshioka H (2012) Post-translational regulation of WRKY transcription factors in plant immunity. Curr Opin Plant Biol **15**: 431–437

Jackson S, Nicolson S. (2002) Xylose as a nectar sugar: from biochemistry to ecology. Comp Biochem Physiol Part B Biochem Mol Biol **131**: 613–620

Jacob T, Ritchie S, Assmann SM, Gilroy S (1999) Abscisic acid signal transduction in guard cells is mediated by phospholipase D activity. Proc Natl Acad Sci U S A **96**: 12192–97

Jacobo-Velázquez DA, González-Aguëro M, Cisneros-Zevallos L (2015) Cross-talk between signaling pathways: The link between plant secondary metabolite production and wounding stress response. Sci Rep **5**: 1–10

Jacobsen EE, Anthonsen T (2015) 2- C -Methyl- d -erythritol. Produced in plants, forms aerosols in the atmosphere. An alternative pathway in isoprenoid biosynthesis. Biocatal Biotransformation. doi: 10.3109/10242422.2015.1095677

Jamet E, Dunand C (2020) Plant cell wall proteins and development. Int J Mol Sci **21**: 2731

Jammes F, Song C, Shin D, Munemasa S, Takeda K, Gu D, Cho D, Lee S, Giordo R, Sritubtim S, et al (2009) MAP kinases MPK9 and MPK12 are preferentially expressed in guard cells and positively regulate ROS-mediated ABA signaling. Proc Natl Acad Sci U S A **106**: 20520–25

Jia H, Chen S, Liu D, Liesche J, Shi C, Wang J, Ren M, Wang X, Yang J, Shi W, et al (2018) Ethylene-induced hydrogen sulfide negatively regulates ethylene biosynthesis by persulfidation of ACO in tomato under osmotic stress. Front Plant Sci **9**: 1–11

Jia HL, Wang XH, Wei T, Wang M, Liu X, Hua L, Ren XH, Guo JK, Li J (2021) Exogenous salicylic acid regulates cell wall polysaccharides synthesis and pectin methylation to reduce Cd accumulation of tomato. Ecotoxicol Environ Saf **207**: 1–11

Jiang CJ, Shimono M, Sugano S, Kojima M, Yazawa K, Yoshida R, Lnoue H, Hayashi N, Sakakibara H, Takatsuji H (2010) Abscisic acid interacts antagonistically with salicylic acid signaling pathway in rice-magnaporthe grisea interaction. Mol Plant-Microbe Interact **23**: 791–798

Jirage D, Tootle TL, Reuber TL, Frosts LN, Feys BJ, Parker JE, Ausubel FM, Glazebrook J (1999) Arabidopsis thaliana PAD4 encodes a lipase-like gene that is important for salicylic acid signaling. Proc Natl Acad Sci U S A **96**: 13583–88

Jones JDG, Dangl JL (2006) The plant immune system. Nature **444**: 323–329

Jones L, Seymour GB, Knox JP (1997) Localization of pectic galactan in tomato cell walls using a monoclonal antibody specific to (1→4)-β-D-galactan. Plant Physiol **113**: 1405–1412

Jong TS, Lu H, McDowell JM, Greenberg JT (2004) A key role for ALD1 in activation of local and systemic defenses in Arabidopsis. Plant J **40**: 200–212

Ju C, Chang C (2015) Mechanistic insights in ethylene perception and signal transduction. Plant Physiol **169**: 85–95

Juge N (2006) Plant protein inhibitors of cell wall degrading enzymes. Trends Plant Sci **11**: 359–367

Jung HW, Tschaplinski TJ, Wang L, Glazebrook J, Greenberg JT (2009) Priming in Systemic Plant Immunity. Science (80-) **324**: 89–91

Jwa NS, Hwang BK (2017) Convergent evolution of pathogen effectors toward reactive oxygen species signaling networks in plants. Front Plant Sci **8**: 1–12

Kachroo A, Kachroo P (2009) Fatty Acid-derived signals in plant defense. Annu Rev Phytopathol **47**: 153–176

Kaczmarska A, Pieczywek PM, Cybulska J, Zdunek A (2022) Structure and functionality of Rhamnogalacturonan I in the cell wall and in solution: A review. Carbohydr Polym. doi: 10.1016/j.carbpol.2021.118909

Kant MR, Ament K, Sabelis MW, Haring MA, Schuurink RC (2004) Differential timing of spider mite-induced direct and indirect defenses in tomato plants. Plant Physiol **135**: 486–495

Kaplan B, Davydov O, Knight H, Galon Y, Knight MR, Fluhr R, Fromm H (2006) Rapid transcriptome changes induced by cytosolic Ca2+ transients reveal ABRE-related sequences as Ca2+-responsive cis elements in Arabidopsis. Plant Cell **18**: 2733–48

Kasten D, Mithöfer A, Georgii E, Lang H, Durner J, Gaupels F (2016) Nitrite is the driver, phytohormones are modulators while NO and H2O2 act as promoters of NO2-induced cell death. J Exp Bot **67**: 6337–6349

Kauss H, Theisinger-Hinkel E, Mindermann R, Conrath U (1992) Dichloroisonicotinic and salicylic acid, inducers of systemic acquired resistance, enhance fungal elicitor responses in parsley cells. Plant J **2**: 655–660

Kazan K (2015) Diverse roles of jasmonates and ethylene in abiotic stress tolerance. Trends Plant Sci **20**: 219–229

Kazan K, Lyons R (2014) Intervention of phytohormone pathways by pathogen effectors.

Plant Cell **26**: 2285–2309

Kazan K, Manners JM (2009) Linking development to defense: auxin in plant-pathogen interactions. Trends Plant Sci **14**: 373–382

Kazan K, Manners JM (2013) MYC2: The master in action. Mol Plant **6**: 686–703

Kelley LA, Mezulis S, Yates CM, Wass MN, Sternberg MJE (2015) The Phyre2 web portal for protein modeling, prediction and analysis. Nat Protoc **10**: 845–858

Kemmerling B, Halter T, Mazzotta S, Mosher S, Nürnberger T (2011) A genome-wide survey for arabidopsis leucine-rich repeat receptor kinases implicated in plant immunity. Front Plant Sci **2**: 1–6

Kesarwani M, Yoo J, Dong X (2007) Genetic interactions of TGA transcription factors in the regulation of pathogenesis-related genes and disease resistance in Arabidopsis. Plant Physiol **144**: 336–346

Kiba T, Aoki K, Sakakibara H, Mizuno T (2004) Arabidopsis response regulator, ARR22, ectopic expression of which results in phenotypes similar to the wol cytokinin-receptor mutant. Plant Cell Physiol **45**: 1063–77

Kilian J, Whitehead D, Horak J, Wanke D, Weinl S, Batistic O, D'Angelo C, Bornberg-Bauer E, Kudla J, Harter K (2007) The AtGenExpress global stress expression data set: Protocols, evaluation and model data analysis of UV-B light, drought and cold stress responses. Plant J **50**: 347–363

Kim CS, Li JH, Barco B, Park HB, Gatsios A, Damania A, Wang R, Wyche TP, Piizzi G, Clay NK, et al (2020a) Cellular Stress Upregulates Indole Signaling Metabolites in Escherichia coli. Cell Chem Biol **27**: 698–707

Kim J-B, Carpita NC (1992) Changes in Esterification of the Uronic Acid Groups of Cell Wall Polysaccharides during Elongation of Maize Coleoptiles. Plant Physiol **98**: 646–653

Kim JH, Hilleary R, Seroka A, He SY (2021) Crops of the future: building a climate-resilient plant immune system. Curr Opin Plant Biol. doi: 10.1016/j.pbi.2020.101997

Kim M, Lim JH, Ahn CS, Park K, Kim GT, Kim WT, Pai HS (2006) Mitochondria-associated hexokinases play a role in the control of programmed cell death in Nicotiana benthamiana. Plant Cell **18**: 2341–55

Kim SH, Kim SH, Yoo SJ, Min KH, Nam SH, Cho BH, Yang KY (2013) Putrescine regulating by stress-responsive MAPK cascade contributes to bacterial pathogen defense in Arabidopsis. Biochem Biophys Res Commun. doi: 10.1016/j.bbrc.2013.06.080

Kim Y, Gilmour SJ, Chao L, Park S, Thomashow MF (2020b) Arabidopsis CAMTA Transcription Factors Regulate Pipecolic Acid Biosynthesis and Priming of Immunity Genes. Mol Plant **13**: 157–168

Klepikova A V., Kasianov AS, Gerasimov ES, Logacheva MD, Penin AA (2016) A high resolution map of the Arabidopsis thaliana developmental transcriptome based on RNA-seq profiling. Plant J **88**: 1058–70

Klinghammer M, Tenhaken R (2007) Genome-wide analysis of the UDP-glucose dehydrogenase gene family in Arabidopsis, a key enzyme for matrix polysaccharides in cell walls. J Exp Bot **58**: 3609–21

Knox JP, Linstead PJ, Cooper, J. Peart C, Roberts K (1991) Developmentally regulated epitopes of cell surface arabinogalactan proteins and their relation to root tissue pattern formation. Plant J **1**: 317–326

Kobayashi Y, Murata M, Minami H, Yamamoto S, Kagaya Y, Hobo T, Yamamoto A, Hattori T (2005) Abscisic acid-activated SNRK2 protein kinases function in the gene-regulation pathway of ABA signal transduction by phosphorylating ABA response element-binding factors. Plant J **44**: 939–949

Kohli P, Kalia M, Gupta R (2015) Pectin Methylesterases: A Review. J Bioprocess Biotech **5**: 1–7

Komarova T V., Sheshukova E V., Dorokhov YL (2014) Cell wall methanol as a signal in plant immunity. Front Plant Sci **5**: 1–4

Komatsu K, Suzuki N, Kuwamura M, Nishikawa Y, Nakatani M, Ohtawa H, Takezawa D, Seki M, Tanaka M, Taji T, et al (2013) Group A PP2Cs evolved in land plants as key regulators of intrinsic desiccation tolerance. Nat Commun **4**: 1–9

König S, Gömann J, Zienkiewicz A, Zienkiewicz K, Meldau D, Herrfurth C, Feussner I (2021) Sphingolipid-Induced Programmed Cell Death Is a Salicylic Acid and EDS1-Dependent Phenotype in Arabidopsis Running head: Sphingolipid-induced PCD is SA and EDS1-dependent. bioRxiv. doi: 10.1101/2021.04.20.440624

König S, Gömann J, Zienkiewicz A, Zienkiewicz K, Meldau D, Herrfurth C, Feussner I (2022) Sphingolipid-Induced Programmed Cell Death is a Salicylic Acid and EDS1-Dependent Phenotype in Arabidopsis Fatty Acid Hydroxylase (Fah1, Fah2) and Ceramide Synthase (Loh2) Triple Mutants. Plant Cell Physiol. doi: 10.1093/pcp/pcab174

Koornneef A, Pieterse CMJ (2008) Cross Talk in Defense Signaling. Plant Physiol **146**: 839–844

Koornneef A, Rindermann K, Gatz C, Pieterse CMJ (2008) Histone modifications do

not play a major role in salicylate-mediated suppression of jasmonate-induced PDF1.2 gene expression. Commun Integr Biol **1**: 143–145

Kopka J, Schauer N, Krueger S, Birkemeyer C, Usadel B, Bergmüller E, Dörmann P, Weckwerth W, Gibon Y, Stitt M, et al (2005) GMD@CSB.DB: The Golm metabolome database. Bioinformatics. doi: 10.1093/bioinformatics/bti236

Krol E, Mentzel T, Chinchilla D, Boller T, Felix G, Kemmerling B, Postel S, Arents M, Jeworutzki E, Al-Rasheid KAS, et al (2010) Perception of the Arabidopsis danger signal peptide 1 involves the pattern recognition receptor AtPEPR1 and its close homologue AtPEPR2. J Biol Chem **285**: 13471–79

Kruger NJ, Von Schaewen A (2003) The oxidative pentose phosphate pathway: Structure and organisation. Curr Opin Plant Biol. doi: 10.1016/S1369-5266(03)00039-6

Kumari A, Chételat A, Nguyen CT, Farmer EE (2019) Arabidopsis H+-ATPase AHA1 controls slow wave potential duration and wound-response jasmonate pathway activation. Proc Natl Acad Sci U S A **116**: 20226–31

Kusajima M, Okumura Y, Fujita M, Nakashita H (2017) Abscisic acid modulates salicylic acid biosynthesis for systemic acquired resistance in tomato. Biosci Biotechnol Biochem **81**: 1850–53

Kwak JM, Mori IC, Pei ZM, Leonhard N, Angel Torres M, Dangl JL, Bloom RE, Bodde S, Jones JDG, Schroeder JI (2003) NADPH oxidase AtrbohD and AtrbohF genes function in ROS-dependent ABA signaling in arabidopsis. EMBO J **22**: 2623–33

De la Rubia AG, Mélida H, Centeno ML, Encina A, García-Angulo P (2021) Immune priming triggers cell wall remodeling and increased resistance to halo blight disease in common bean. Plants **10**: 1–25

Lamb C, Dixon RA (1997) The oxidative burst in plant disease resistance. Annu Rev Plant Biol **48**: 251–275

Lapin D, Bhandari DD, Parker JE (2020) Origins and Immunity Networking Functions of EDS1 Family Proteins. Annu Rev Phytopathol **58**: 253–276

Lapin D, Kovacova V, Sun X, Dongus JA, Bhandari D, Von Born P, Bautor J, Guarneri N, Rzemieniewski J, Stuttmann J, et al (2019) A coevolved EDS1-SAG101-NRG1 module mediates cell death signaling by TIR-domain immune receptors. Plant Cell **31**: 2430–55

LaRue CD (1941) The Effects of Wounding and Wound Hormones on Root Formation. Proc Natl Acad Sci **27**: 388–392

Laurenzi M, Tipping AJ, Marcus SE, Knox JP, Federico R, Angelini R, McPherson MJ (2001) Analysis of the distribution of copper amine oxidase in cell walls of legume seedlings. Planta **214**: 37–45

Lawton K, Weymann K, Friedrich L, Vernooij B, Uknes S, Ryals J (1995) Systemic acquired resistance in Arabidopsis requires salicylic acid but not ethylene. Mol Plant-Microbe Interact **8**: 863–870

Lee DH, Lal NK, Lin ZJD, Ma S, Liu J, Castro B, Toruño T, Dinesh-Kumar SP, Coaker G (2020) Regulation of reactive oxygen species during plant immunity through phosphorylation and ubiquitination of RBOHD. Nat Commun **11**: 1–16

Lee JY, Wang X, Cui W, Sager R, Modla S, Czymmek K, Zybaliov B, Van Wijk K, Zhang C, Lu H, et al (2011) A plasmodesmata-localized protein mediates crosstalk between cell-to-cell communication and innate immunity in arabidopsis. Plant Cell **23**: 3353–73

Lefevere H, Bauters L, Gheysen G (2020) Salicylic Acid Biosynthesis in Plants. Front Plant Sci **11**: 1–7

Lemos M, Xiao Y, Bjornson M, Wang JZ, Hicks D, Souza A De, Wang CQ, Yang P, Ma S, Dinesh-Kumar S, et al (2016) The plastidial retrograde signal methyl erythritol cyclopyrophosphate is a regulator of salicylic acid and jasmonic acid crosstalk. J Exp Bot **67**: 1557–66

Lenzoni G, Liu J, Knight MR (2018) Predicting plant immunity gene expression by identifying the decoding mechanism of calcium signatures. New Phytol **217**: 1598–1609

Li J, Pang Z, Trivedi P, Zhou X, Ying X, Jia H, Wang N (2017a) "Candidatus liberibacter asiaticus" encodes a functional salicylic acid (SA) hydroxylase that degrades SA to suppress plant defenses. Mol Plant-Microbe Interact **30**: 620–630

Li J, Wang C, Yang G, Sun Z, Guo H, Shao K, Gu Y, Jiang W, Zhang P (2017b) Molecular mechanism of environmental D-xylose perception by a XylFII-LytS complex in bacteria. Proc Natl Acad Sci U S A **114**: 8235–40

Li M, Wang F, Li S, Yu G, Wang L, Li Q, Zhu X, Li Z, Yuan L, Liu P (2020a) Importers Drive Leaf-to-Leaf Jasmonic Acid Transmission in Wound-Induced Systemic Immunity. Mol Plant **13**: 1485–98

Li M, Yu G, Ma J, Liu P (2021a) Interactions of importers in long-distance transmission of wound-induced jasmonate. Plant Signal Behav **16**: 1886490

Li N, Han X, Feng D, Yuan D, Huang LJ (2019a) Signaling crosstalk between salicylic acid and ethylene/Jasmonate in plant defense: Do we understand what they are

whispering? Int J Mol Sci **20**: 671

Li P, Zhao L, Qi F, Htwe NMPS, Li Q, Zhang D, Lin F, Shang-Guan K, Liang Y (2021b) The receptor-like cytoplasmic kinase RIPK regulates broad-spectrum ROS signaling in multiple layers of plant immune system. Mol Plant **14**: 1652–67

Li Q, Wang C, Mou Z (2020b) Perception of damaged self in plants. Plant Physiol **182**: 1545–65

Li S, Li X, Wei Z, Liu F (2019b) ABA-mediated modulation of elevated CO2 on stomatal response to drought. Curr Opin Plant Biol **56**: 174–180

Li SW, Leng Y, Feng L, Zeng XY (2014) Involvement of abscisic acid in regulating antioxidative defense systems and IAA-oxidase activity and improving adventitious rooting in mung bean [Vigna radiata (L.) Wilczek] seedlings under cadmium stress. Environ Sci Pollut Res **21**: 525–537

Li X, Zhang R, Patena W, Gang SS, Blum SR, Ivanova N, Yue R, Robertson JM, Lefebvre PA, Fitz-Gibbon ST, et al (2015) An indexed, mapped mutant library enables reverse genetics studies of biological processes in chlamydomonas reinhardtii. Plant Cell **28**: 367–387

Li Y, Yang Y, Hu Y, Liu H, He M, Yang Z, Kong F, Liu X, Hou X (2019c) DELLA and EDS1 Form a Feedback Regulatory Module to Fine-Tune Plant Growth–Defense Tradeoff in Arabidopsis. Mol Plant **12**: 1485–98

Li Z, Variz H, Chen Y, Liu SL, Aung K (2021c) Plasmodesmata-Dependent Intercellular Movement of Bacterial Effectors. Front Plant Sci **12**: 640277

Liang H, Yao N, Song JT, Luo S, Lu H, Greenberg JT (2003) Ceramides modulate programmed cell death in plants. Genes Dev **17**: 2636–41

Lichtenthaler HK (1999) The 1-deoxy-D-xylulose-5-phosphate pathway of isoprenoid biosynthesis in plants. Annu Rev Plant Biol. doi: 10.1146/annurev.arplant.50.1.47

Lim CW, Baek W, Jung J, Kim JH, Lee SC (2015) Function of ABA in stomatal defense against biotic and drought stresses. Int J Mol Sci **16**: 15251–70

Lim GH, Liu H, Yu K, Liu R, Shine MB, Fernandez J, Burch-Smith T, Mobley JK, McLetchie N, Kachroo A, et al (2020) The plant cuticle regulates apoplastic transport of salicylic acid during systemic acquired resistance. Sci Adv **6**: eaaz0478

Lim GH, Shine MB, De Lorenzo L, Yu K, Cui W, Navarre D, Hunt AG, Lee JY, Kachroo A, Kachroo P (2016) Plasmodesmata Localizing Proteins Regulate Transport and Signaling during Systemic Acquired Immunity in Plants. Cell Host Microbe **19**: 541–549

Lim GH, Singhal R, Kachroo A, Kachroo P (2017) Fatty Acid- and Lipid-Mediated Signaling in Plant Defense. Annu Rev Phytopathol **55**: 505–536

Limberg G, Körner R, Buchholt HC, Christensen TMIE, Roepstorff P, Mikkelsen JD (2000) Analysis of different de-esterification mechanisms for pectin by enzymatic fingerprinting using endopectin lyase and endopolygalacturonase II from A. Niger. Carbohydr Res **327**: 293–307

Lin W, Zhang H, Huang D, Schenke D, Cai D, Wu B, Miao Y (2020) Dual-Localized WHIRLY1 Affects Salicylic Acid Biosynthesis via Coordination of ISOCHORISMATE SYNTHASE1, PHENYLALANINE AMMONIA LYASE1, and *S* -ADENOSYL-L-METHIONINE-DEPENDENT METHYLTRANSFERASE1. Plant Physiol **184**: 1884–1899

Liners F, Van Cutsem P (1992) Distribution of pectic polysaccharides throughout walls of suspension-cultured carrot cells - An immunocytochemical study. Protoplasma **170**: 10–21

Liners F, Letesson J-J, Didembourg C, Van Cutsem P (1989) Monoclonal Antibodies against Pectin: Recognition of a Conformation Induced by Calcium. Plant Physiol **91**: 1491–24

Liners F, Thibault J-F, Van Cutsem P (1992) Influence of the Degree of Polymerization of Oligogalacturonates and of Esterification Pattern of Pectin on Their Recognition by Monoclonal Antibodies. Plant Physiol **99**: 1099–104

Lionetti V, Francocci F, Ferrari S, Volpi C, Bellincampi D, Galletti R, D'Ovidio R, De Lorenzo G, Cervone F (2010) Engineering the cell wall by reducing de-methyl-esterified homogalacturonan improves saccharification of plant tissues for bioconversion. Proc Natl Acad Sci U S A **107**: 616–621

Lisec J, Schauer N, Kopka J, Willmitzer L, Fernie AR (2006) Gas chromatography mass spectrometry-based metabolite profiling in plants. Nat Protoc **1**: 387–396

Liu B, Seong K, Pang S, Song J, Gao H, Wang C, Zhai J, Zhang Y, Gao S, Li X, et al (2021a) Functional specificity, diversity, and redundancy of Arabidopsis JAZ family repressors in jasmonate and COI1-regulated growth, development, and defense. New Phytol **231**: 1525–45

Liu C, Alcázar R (2021) A new insight into the contribution of putrescine to defense in Arabidopsis thaliana. Plant Signal Behav. doi: 10.1080/15592324.2021.1885187

Liu C, Atanasov KE, Arafaty N, Murillo E, Tiburcio AF, Zeier J, Alcázar R (2020a) Putrescine elicits ROS-dependent activation of the salicylic acid pathway in Arabidopsis thaliana. Plant Cell Environ. doi: 10.1111/pce.13874

Liu C, Atanasov KE, Tiburcio AF, Alcázar R (2019) The polyamine putrescine

contributes to H2O2 and RbohD/F-dependent positive feedback loop in arabidopsis pamp-triggered immunity. Front Plant Sci **10**: 1–12

Liu C, Niu G, Li X, Zhang H, Chen H, Hou D, Lan P, Hong Z (2021b) Comparative Label-Free Quantitative Proteomics Analysis Reveals the Essential Roles of N-Glycans in Salt Tolerance by Modulating Protein Abundance in Arabidopsis. Front Plant Sci **12**: 646425

Liu H, Carvalhais LC, Kazan K, Schenk PM (2016a) Development of marker genes for jasmonic acid signaling in shoots and roots of wheat. Plant Signal Behav **11**: e1176654

Liu H, Li Y, Hu Y, Yang Y, Zhang W, He M, Li X, Zhang C, Kong F, Liu X, et al (2021c) EDS1-interacting J protein 1 is an essential negative regulator of plant innate immunity in Arabidopsis. Plant Cell **33**: 153–171

Liu L, Sonbol FM, Huot B, Gu Y, Withers J, Mwimba M, Yao J, He SY, Dong X (2016b) Salicylic acid receptors activate jasmonic acid signalling through a non-canonical pathway to promote effector-triggered immunity. Nat Commun **7**: 13099

Liu NJ, Zhang T, Liu ZH, Chen X, Guo HS, Ju BH, Zhang YY, Li GZ, Zhou QH, Qin YM, et al (2020b) Phytosphinganine Affects Plasmodesmata Permeability via Facilitating PDLP5-Stimulated Callose Accumulation in Arabidopsis. Mol Plant **13**: 128–143

Liu S, Kracher B, Ziegler J, Birkenbihl RP, Somssich IE (2015a) Negative regulation of ABA Signaling By WRKY33 is critical for Arabidopsis immunity towards Botrytis cinerea 2100. Elife. doi: 10.7554/eLife.07295

Liu Z, Yan JP, Li DK, Luo Q, Yan Q, Liu Z Bin, Ye LM, Wang JM, Li XF, Yang Y (2015b) UDP-glucosyltransferase71C5, a major glucosyltransferase, mediates abscisic acid homeostasis in Arabidopsis. Plant Physiol **167**: 1659–70

Loake G, Grant M (2007) Salicylic acid in plant defence-the players and protagonists. Curr Opin Plant Biol **10**: 466–472

Löffler G, Pedrides PE, Müller M, Heinrich PC, Graeve L (2014) Pathobiochemie des Kohlehydratstoffwechsels. Biochem. und Pathobiochemie. pp 222–225

Van Loon LC, Bakker PAHM, Pieterse CMJ (1998) Systemic resistance induced by rhizosphere bacteria. Annu Rev Phytopathol **36**: 453–483

De Lorenzo G, Ferrari S, Cervone F, Okun E (2018) Extracellular DAMPs in Plants and Mammals: Immunity, Tissue Damage and Repair. Trends Immunol **39**: 937–950

Lorenzo O, Piqueras R, Sánchez-serrano JJ, Solano R (2003a) Integrates Signals from

Ethylene and Jasmonate Pathways in Plant Defense. Plant Cell **15**: 165–178

Lorenzo O, Piqueras R, Sánchez-Serrano JJ, Solano R (2003b) ETHYLENE RESPONSE FACTOR1 integrates signals from ethylene and jasmonate pathways in plant defense. Plant Cell **15**: 165–178

Lorrai R, Ferrari S (2021) Host cell wall damage during pathogen infection: Mechanisms of perception and role in plant-pathogen interactions. Plants **10**: 399

Lu ZX, Gaudet D, Puchalski B, Despins T, Frick M, Laroche A (2006) Inducers of resistance reduce common bunt infection in wheat seedlings while differentially regulating defence-gene expression. Physiol Mol Plant Pathol **67**: 138–148

Luedemann A, Strassburg K, Erban A, Kopka J (2008) TagFinder for the quantitative analysis of gas chromatography - Mass spectrometry (GC-MS)-based metabolite profiling experiments. Bioinformatics **24**: 732–737

Luna E, Pastor V, Robert J, Flors V, Mauch-Mani B, Ton J (2011) Callose deposition: A multifaceted plant defense response. Mol Plant-Microbe Interact **24**: 183–193

LUO Y, ZENG LJ, LIU XQ, LI L, ZENG QY (2021) cDNA cloning of a novel lectin that induce cell apoptosis from Artocarpus hypargyreus. Chin J Nat Med **19**: 81–89

Lyou SH, Park HJ, Jung C, Sohn HB, Lee G, Kim CH, Kim M, Choi Y Do, Cheong JJ (2009) The Arabidopsis AtLEC gene encoding a lectin-like protein is up-regulated by multiple stimuli including developmental signal, wounding, jasmonate, ethylene, and chitin elicitor. Mol Cells **27**: 75–81

Ma KW, Ma W (2016) Phytohormone pathways as targets of pathogens to facilitate infection. Plant Mol Biol **91**: 713–725

Ma Y, Szostkiewicz I, Korte A, Moes D, Yang Y, Christmann A, Grill E (2009) Regulators of PP2C phosphatase activity function as abscisic acid sensors. Science (80-) **324**: 1064–68

Mackey D, Holt BF, Wiig A, Dangl JL (2002) RIN4 interacts with *Pseudomonas syringae* type III effector molecules and is required for RPM1-mediated resistance in *Arabidopsis*. Cell **108**: 743–754

Malamy J, Carr JP, Klessig DF, Raskin I (1990) Salicylic acid: A likely endogenous signal in the resistance response of tobacco to viral infection. Science (80-) **250**: 1002–04

Maldonado AM, Doerner P, Dixonk RA, Lamb CJ, Cameron RK (2002) A putative lipid transfer protein involved in systemic resistance signalling in Arabidopsis. Nature **419**: 399–403

Malinovsky FG, Fangel JU, Willats WGT (2014) The role of the cell wall in plant immunity. Front Plant Sci **5**: 1–12

Manabe Y, Nafisi M, Verhertbruggen Y, Orfila C, Gille S, Rautengarten C, Cherk C, Marcus SE, Somerville S, Pauly M, et al (2011) Loss-of-function mutation of REDUCED WALL ACETYLATION2 in Arabidopsis leads to reduced cell wall acetylation and increased resistance to Botrytis cinerea. Plant Physiol **155**: 1068–78

Mandal MK, Chanda B, Xia Y, Yu K, Sekine KT, Gao QM, Selote D, Kachroo A, Kachroo P (2011) Glycerol-3-phosphate and systemic immunity. Plant Signal Behav **6**: 1871–74

Manohar M, Tian M, Moreau M, Park SW, Choi HW, Fei Z, Friso G, Asif M, Manosalva P, Von Dahl CC, et al (2015) Identification of multiple salicylic acid-binding proteins using two high throughput screens. Front Plant Sci **5**: 1–14

Manzoor H, Kelloniemi J, Chiltz A, Wendehenne D, Pugin A, Poinssot B, Garcia-Brugger A (2013) Involvement of the glutamate receptor AtGLR3.3 in plant defense signaling and resistance to Hyaloperonospora arabidopsidis. Plant J **76**: 466–480

Marcus SE, Blake AW, Benians TAS, Lee KJD, Poyser C, Donaldson L, Leroux O, Rogowski A, Petersen HL, Boraston A, et al (2010) Restricted access of proteins to mannan polysaccharides in intact plant cell walls. Plant J **64**: 191–203

Marcus SE, Verhertbruggen Y, Hervé C, Ordaz-Ortiz JJ, Farkas V, Pedersen HL, Willats WG, Knox JP (2008) Pectic homogalacturonan masks abundant sets of xyloglucan epitopes in plant cell walls. BMC Plant Biol **8**: 1–12

Marquis V, Smirnova E, Poirier L, Zumsteg J, Schweizer F, Reymond P, Heitz T (2020) Stress- and pathway-specific impacts of impaired jasmonoyl-isoleucine (JA-Ile) catabolism on defense signalling and biotic stress resistance. Plant Cell Environ **43**: 1158–70

Martin RC, Mok MC, Mok DWS (1999) A gene encoding the cytokinin enzyme zeatin O-xylosyltransferase of Phaseolus vulgaris. Plant Physiol **120**: 553–558

Martínez-Aguilar K, Hernández-Chávez JL, Alvarez-Venegas R (2021) Priming of seeds with INA and its transgenerational effect in common bean (Phaseolus vulgaris L.) plants. Plant Sci **305**: 110834

Mateo A, Mühlenbock P, Rustérucci C, Chang CCC, Miszalski Z, Karpinska B, Parker JE, Mullineaux PM, Karpinski S (2004) LESION SIMULATING DISEASE 1 is required for acclimation to conditions that promote excess excitation energy. Plant Physiol **136**: 2818–30

McCabe PF, Valentine TA, Forsberg LS, Pennell RI (1997) Soluble signals from cells

identified at the cell wall establish a developmental pathway in carrot. Plant Cell **9**: 2225–41

McCartney L, Marcus SE, Knox JP (2005) Monoclonal antibodies to plant cell wall xylans and arabinoxylans. J Histochem Cytochem **53**: 543–546

Meikle PJ, Bonig I, Hoogenraad NJ, Clarke AE, Stone BA (1991) The location of (1→3)-β-glucans in the walls of pollen tubes of Nicotiana alata using a (1→3)-β-glucan-specific monoclonal antibody. Planta **185**: 1–8

Meikle PJ, Hoogenraad NJ, Bonig I, Clarke AE, Stone BA (1994) A (1→3,1→4)-β-glucan-specific monoclonal antibody and its use in the quantitation and immunocytochemical location of (1→3,1→4)-β-glucans. Plant J **5**: 1–9

Melotto M, Underwood W, Koczan J, Nomura K, He SY (2006) Plant Stomata Function in Innate Immunity against Bacterial Invasion. Cell **126**: 969–980

Melotto M, Zhang L, Oblessuc PR, He SY (2017) Stomatal defense a decade later. Plant Physiol. doi: 10.1104/pp.16.01853

Merkouropoulos G, Barnett DC, Shirsat AH (1999) The Arabidopsis extensin gene is developmentally regulated, is induced by wounding, methyl jasmonate, abscisic and salicylic acid, and codes for a protein with unusual motifs. Planta **208**: 212–219

Miladinovic D, Antunes D, Yildirim K, Bakhsh A, Cvejić S, Kondić-Špika A, Marjanovic Jeromela A, Opsahl-Sorteberg HG, Zambounis A, Hilioti Z (2021) Targeted plant improvement through genome editing: from laboratory to field. Plant Cell Rep **40**: 935–951

Millard P, Pérochon J, Letisse F (2021) Functional analysis of deoxyhexose sugar utilization in Escherichia coli reveals fermentative metabolism under aerobic conditions. Appl Environ Microbiol. doi: 10.1128/aem.00719-21

Mine A, Seyfferth C, Kracher B, Berens ML, Becker D, Tsuda K (2018) The defense phytohormone signaling network enables rapid, high-amplitude transcriptional reprogramming during effector-triggered immunity. Plant Cell **30**: 1199–1219

Minic Z, Rihouey C, Do CT, Lerouge P, Jouanin L (2004) Purification and characterization of enzymes exhibiting beta-D-xylosidase activities in stem tissues of Arabidopsis. Plant Physiol **135**: 867–878

Mishina TE, Zeier J (2006) The *Arabidopsis* Flavin-Dependent Monooxygenase FMO1 Is an Essential Component of Biologically Induced Systemic Acquired Resistance. Plant Physiol **141**: 1666–1675

Mohnen D (2008) Pectin structure and biosynthesis. Curr Opin Plant Biol **11**: 266–277

Mohnike L, Rekhter D, Huang W, Feussner K, Tian H, Herrfurth C, Zhang Y, Feussner I (2021) The glycosyltransferase UGT76B1 modulates N-hydroxy-pipecolic acid homeostasis and plant immunity. Plant Cell **33**: 735–749

Molina A, Miedes E, Bacete L, Rodríguez T, Mélida H, Denancé N, Sánchez-Vallet A, Rivière MP, López G, Freydier A, et al (2021) Arabidopsis cell wall composition determines disease resistance specificity and fitness. Proc Natl Acad Sci U S A **118**: e2010243118

Moller I, Marcus SE, Haeger A, Verhertbruggen Y, Verhoef R, Schols H, Ulvskov P, Mikkelsen JD, Knox JP, Willats W (2008) High-throughput screening of monoclonal antibodies against plant cell wall glycans by hierarchical clustering of their carbohydrate microarray binding profiles. Glycoconj J **25**: 37–48

Moller I, Sørensen I, Bernal AJ, Blaukopf C, Lee K, Øbro J, Pettolino F, Roberts A, Mikkelsen JD, Knox JP, et al (2007) High-throughput mapping of cell-wall polymers within and between plants using novel microarrays. Plant J **50**: 1118–28

Molotoks A, Smith P, Dawson TP (2021) Impacts of land use, population, and climate change on global food security. Food Energy Secur **10**: 1–20

Monro JA, Penny D, Bailey RW (1976) The organization and growth of primary cell walls of lupin hypocotyl. Phytochemistry **15**: 532–541

Moradi A, El-Shetehy M, Gamir J, Austerlitz T, Dahlin P, Wieczorek K, Künzler M, Mauch F (2021) Expression of a Fungal Lectin in Arabidopsis Enhances Plant Growth and Resistance Toward Microbial Pathogens and a Plant-Parasitic Nematode. Front Plant Sci. doi: 10.3389/fpls.2021.657451

Moreno JE, Shyu C, Campos ML, Patel LC, Chung HS, Yao J, He SY, Howe GA (2013) Negative feedback control of jasmonate signaling by an alternative splice variant of JAZ10. Plant Physiol **162**: 1006–17

Mori D, Moriyama A, Kanamaru H, Aoki Y, Masumura Y, Suzuki S (2021) Electrical stimulation enhances plant defense response in grapevine through salicylic acid-dependent defense pathway. Plants **10**: 1316

Mori IC, Murata Y, Yang Y, Munemasa S, Wang YF, Andreoli S, Tiriac H, Alonso JM, Harper JF, Ecker JR, et al (2006) CDPKs CPK6 and CPK3 function in ABA regulation of guard cell S-type anion- and Ca2+- permeable channels and stomatal closure. PLoS Biol **4**: e327

Mou Z, Fan W, Dong X (2003) Inducers of plant systemic acquired resistance Regulate NPR1 function through redox changes. Cell **113**: 935–944

Müller M, Munné-Bosch S (2015) Ethylene response factors: A key regulatory hub in

hormone and stress signaling. Plant Physiol **169**: 32–41

Mur LAJ, Kenton P, Atzorn R, Miersch O, Wasternack C (2006) The outcomes of concentration-specific interactions between salicylate and jasmonate signaling include synergy, antagonism, and oxidative stress leading to cell death. Plant Physiol **140**: 249–262

Mur LAJ, Kenton P, Lloyd AJ, Ougham H, Prats E (2008) The hypersensitive response; The centenary is upon us but how much do we know? J Exp Bot **59**: 501–520

Mustilli AC, Merlot S, Vavasseur A, Fenzi F, Giraudat J (2002) Arabidopsis OST1 protein kinase mediates the regulation of stomatal aperture by abscisic acid and acts upstream of reactive oxygen species production. Plant Cell **14**: 3089–99

Nagy Z, Kátay G, Gullner G, Király L, Ádám AL (2017) Azelaic acid accumulates in phloem exudates of TMV-infected tobacco leaves, but its application does not induce local or systemic resistance against selected viral and bacterial pathogens. Acta Physiol Plant **39**: 1–9

Nandi A, Kachroo P, Fukushige H, Hildebrand DF, Klessig DF, Shah J (2003) Ethylene and jasmonic acid signaling affect the NPR1-independent expression of defense genes without impacting resistance to Pseudomonas syringae and Peronospora parasitica in the Arabidopsis ssi1 mutant. Mol Plant-Microbe Interact **16**: 588–599

Nandi A, Welti R, Shah J (2004) The Arabidopsis thaliana Dihydroxyacetone Phosphate Reductase Gene Suppressor of Fatty Acid Desaturase Deficiency1 Is Required for Glycerolipid Metabolism and for the Activation of Systemic Acquired Resistance. Plant Cell **16**: 465–477

Narsai R, Law SR, Carrie C, Xu L, Whelan J (2011) In-depth temporal transcriptome profiling reveals a crucial developmental switch with roles for RNA processing and organelle metabolism that are essential for germination in Arabidopsis. Plant Physiol **157**: 1342–62

Naseem M, Dandekar T (2012) The Role of Auxin-Cytokinin Antagonism in Plant-Pathogen Interactions. PLoS Pathog **8**: e1003026

Návarová H, Bernsdorff F, Doring A-C, Zeier J (2012) Pipecolic Acid, an Endogenous Mediator of Defense Amplification and Priming, Is a Critical Regulator of Inducible Plant Immunity. Plant Cell **24**: 5123–5141

Netea MG, Joosten LAB, Latz E, Mills KHG, Stunnenberg HG, O'Neill LAJ, Xavier RJ (2016) Trained immunity: a program of innate immune memory in health and disease. Scince **352**: 1–23

Ngou BPM, Ahn HK, Ding P, Jones JDG (2021) Mutual potentiation of plant immunity by cell-surface and intracellular receptors. Nature **592**: 110–115

Nguyen D, Rieu I, Mariani C, van Dam NM (2016) How plants handle multiple stresses: hormonal interactions underlying responses to abiotic stress and insect herbivory. Plant Mol Biol **91**: 727–740

Nie P, Li X, Wang S, Guo J, Zhao H, Niu D (2017) Induced systemic resistance against botrytis cinerea by Bacillus cereus AR156 through a JA/ET- and NPR1-dependent signaling pathway and activates PAMP-triggered immunity in Arabidopsis. Front Plant Sci **8**: 1–12

Ning Y, Liu W, Wang GL (2017) Balancing Immunity and Yield in Crop Plants. Trends Plant Sci **22**: 1069–79

Nürnberger T, Brunner F, Kemmerling B, Piater L (2004) Innate immunity in plants and animals: Striking similarities and obvious differences. Immunol Rev **198**: 249–266

O'Malley RC, Barragan CC, Ecker JR (2015) A user's guide to the arabidopsis T-DNA insertion mutant collections. Plant Funct. Genomics Methods Protoc. Second Ed. pp 323–342

O'Neill MA, York WS (2003) The Plant Cell Wall. Annu Plant Rev Plant Rev. doi: 10.1093/aob/mch185

Ochsenbein C, Przybyla D, Danon A, Landgraf F, Göbel C, Imboden A, Feussner I, Apel K (2006) The role of EDS1 (enhanced disease susceptibility) during singlet oxygen-mediated stress responses of Arabidopsis. Plant J **47**: 445–456

Ohri P, Bhardwaj R, Bali S, Kaur R, Jasrotia S, Khajuria A, Parihar R (2015) The Common Molecular Players in Plant Hormone Crosstalk and Signaling. Curr Protein Pept Sci **16**: 369–388

Okada K, Abe H, Arimura G-I (2015) Jasmonates Induce Both Defense Responses and Communication in Monocotyledonous and Dicotyledonous Plants. Plant Cell Physiol **56**: 16–27

Owens NW, Stetefeld J, LattovaÌ E, Schweizer F (2010) Contiguous O-galactosylation of 4(R)-hydroxy-l-proline residues forms very stable polyproline II helices. J Am Chem Soc **132**: 5036–42

Paque S, Mouille G, Grandont L, Alabadí D, Gaertner C, Goyallon A, Muller P, Primard-Brisset C, Sormani R, Blázquez MA, et al (2014) AUXIN BINDING PROTEIN1 links cellwall remodeling, auxin signaling, and cell expansion in Arabidopsis. Plant Cell **26**: 280–295

Park SW, Kaimoyo E, Kumar D, Mosher S, Klessig DF (2007) Methyl salicylate is a critical mobile signal for plant systemic acquired resistance. Science (80-) **318**: 113–116

Park SY, Fung P, Nishimura N, Jensen DR, Fujii H, Zhao Y, Lumba S, Santiago J, Rodrigues A, Chow TFF, et al (2009) Abscisic acid inhibits type 2C protein phosphatases via the PYR/PYL family of START proteins. Science (80-) **324**: 1068–71

Park YS, Ryu CM (2021) Understanding plant social networking system: Avoiding deleterious microbiota but calling beneficials. Int J Mol Sci. doi: 10.3390/ijms22073319

Pattathil S, Avci U, Baldwin D, Swennes AG, McGill JA, Popper Z, Bootten T, Albert A, Davis RH, Chennareddy C, et al (2010) A comprehensive toolkit of plant cell wall glycan-directed monoclonal antibodies. Plant Physiol **153**: 514–525

Peck S, Mittler R (2020) Plant signaling in biotic and abiotic stress. J Exp Bot **71**: 1649–51

Pedersen HL, Fangel JU, McCleary B, Ruzanski C, Rydahl MG, Ralet MC, Farkas V, Von Schantz L, Marcus SE, Andersen MCF, et al (2012) Versatile high resolution oligosaccharide microarrays for plant glycobiology and cell wall research. J Biol Chem **287**: 39429–39438

Pel ZM, Murata Y, Benning G, Thomine S, Klüsener B, Allen GJ, Grill E, Schroeder JI (2000) Calcium channels activated by hydrogen peroxide mediate abscisic acid signalling in guard cells. Nature **406**: 731–734

Pena-Cortés H, Albrecht T, Prat S, Weiler EW, Willmitzer L (1993) Aspirin prevents wound-induced gene expression in tomato leaves by blocking jasmonic acid biosynthesis. Planta **191**: 123–128

Peng Y, Van Wersch R, Zhang Y (2018) Convergent and divergent signaling in PAMP-triggered immunity and effector-triggered immunity. Mol Plant-Microbe Interact **31**: 403–409

Penninckx IAMA, Eggermont K, Terras FRG, Thomma BPHJ, De Samblanx GW, Buchala A, Métraux JP, Manners JM, Broekaert WF (1996) Pathogen-Induced Systemic Activation of a Plant Defensin Gene in Arabidopsis Follows a Salicylic Acid-Independent Pathway. Plant Cell **8**: 2309–23

Penninckx IAMA, Thomma BPHJ, Buchala A, Métraux JP, Broekaert WF (1998) Concomitant activation of jasmonate and ethylene response pathways is required for induction of a plant defensin gene in Arabidopsis. Plant Cell **10**: 2103–13

Pierik R, Tholen D, Poorter H, Visser EJW, Voesenek LACJ (2006) The Janus face of ethylene: growth inhibition and stimulation. Trends Plant Sci **11**: 176–183

Pieterse CMJ, Van Der Does D, Zamioudis C, Leon-Reyes A, Van Wees SCM (2012) Hormonal modulation of plant immunity. Annu Rev Cell Dev Biol **28**: 489–521

Pieterse CMJ, Leon-Reyes A, Van Der Ent S, Van Wees SCM (2009) Networking by small-molecule hormones in plant immunity. Nat Chem Biol **5**: 308–316

Pieterse CMJ, Van Loon LC (1999) Salicylic acid-independent plant defence pathways. Trends Plant Sci **4**: 52–58

Pieterse CMJ, Van Pelt JA, Ton J, Parchmann S, Mueller MJ, Buchala AJ, Métraux JP, Van Loon LC (2000) Rhizobacteria-mediated induced systemic resistance (ISR) in Arabidopsis requires sensitivity to jasmonate and ethylene but is not accompanied by an increase in their production. Physiol Mol Plant Pathol **57**: 123–134

Pieterse CMJ, Van Wees SCM, Van Pelt JA, Knoester M, Laan R, Gerrits H, Weisbeek PJ, Van Loon LC (1998) A novel signaling pathway controlling induced systemic resistance in arabidopsis. Plant Cell **10**: 1571–80

Pieterse CMJ, Zamioudis C, Berendsen RL, Weller DM, Van Wees SCM, Bakker PAHM (2014) Induced systemic resistance by beneficial microbes. Annu Rev Phytopathol **52**: 347–375

Pillitteri LJ, Peterson KM, Horst RJ, Torii KU (2011) Molecular profiling of stomatal meristemoids reveals new component of asymmetric cell division and commonalities among stem cell populations in Arabidopsis. Plant Cell **23**: 3260–75

Pintard L, Willems A, Peter M (2004) Cullin-based ubiquitin ligases: Cul3-BTB complexes join the family. EMBO J **23**: 1681–87

Plaxton WC (1996) The organization and regulation of plant glycolysis. Annu Rev Plant Physiol Plant Mol Biol **47**: 185–214

Poncini L, Wyrsch I, Tendon VD, Vorley T, Boller T, Geldner N, Métraux JP, Lehmann S (2017) In roots of Arabidopsis thaliana, the damage-associated molecular pattern AtPep1 is a stronger elicitor of immune signalling than flg22 or the chitin heptamer. PLoS One **12**: e0185808

Pontiggia D, Benedetti M, Costantini S, De Lorenzo G, Cervone F (2020) Dampening the DAMPs: How Plants Maintain the Homeostasis of Cell Wall Molecular Patterns and Avoid Hyper-Immunity. Front Plant Sci **11**: 613259

Pozo MJ, Van Der Ent S, Van Loon LC, Pieterse CMJ (2008) Transcription factor MYC2 is involved in priming for enhanced defense during rhizobacteria-induced systemic

resistance in Arabidopsis thaliana. New Phytol **180**: 511–523

Prasad A, Sedlářová M, Balukova A, Rác M, Pospíšil P (2020) Reactive Oxygen Species as a Response to Wounding: In Vivo Imaging in Arabidopsis thaliana. Front Plant Sci **10**: 1660

Pré M, Atallah M, Champion A, De Vos M, Pieterse CMJ, Memelink J (2008) The AP2/ERF domain transcription factor ORA59 integrates jasmonic acid and ethylene signals in plant defense. Plant Physiol **147**: 1347–57

Pruitt RN, Locci F, Wanke F, Zhang L, Saile SC, Joe A, Karelina D, Hua C, Fröhlich K, Wan WL, et al (2021) The EDS1–PAD4–ADR1 node mediates Arabidopsis pattern-triggered immunity. Nature **598**: 495–499

Puhlmann J, Bucheli E, Swain MJ, Dunning N, Abersheim P, Darvill AG, Hahn MG (1994) Generation of monoclonal antibodies against plant cell-wall polysaccharides. I.Characterization of a monoclonal antibody to a terminal alpha-(1==2)-linked fucosyl-containing epitope. Plant Physiol **104**: 699–710

Pye MF, Hakuno F, MacDonald JD, Bostock RM (2013) Induced resistance in tomato by SAR activators during predisposing salinity stress. Front Plant Sci **4**: 1–9

Raiola A, Lionetti V, Elmaghraby I, Immerzeel P, Mellerowicz EJ, Salvi G, Cervone F, Bellincampi D (2011) Pectin methylesterase is induced in Arabidopsis upon infection and is necessary for a successful colonization by necrotrophic pathogens. Mol Plant-Microbe Interact **24**: 432–440

Rairdan GJ, Delaney TP (2002) Role of salicylic acid and NIM1/NPR1 in race-specific resistance in arabidopsis. Genetics **161**: 803–811

Ralet MC, Tranquet O, Poulain D, Moïse A, Guillon F (2010) Monoclonal antibodies to rhamnogalacturonan I backbone. Planta **231**: 1373–83

Ramírez-Carrasco G, Martínez-Aguilar K, Alvarez-Venegas R (2017) Transgenerational defense priming for crop protection against plant pathogens: A hypothesis. Front Plant Sci **8**: 1–8

Ramirez-Prado JS, Latrasse D, Rodriguez-Granados NY, Huang Y, Manza-Mianza D, Brik-Chaouche R, Jaouannet M, Citerne S, Bendahmane A, Hirt H, et al (2019) The Polycomb protein LHP1 regulates Arabidopsis thaliana stress responses through the repression of the MYC2-dependent branch of immunity. Plant J **100**: 1118–31

Rao TVR, Gol NB, Shah KK (2011) Effect of postharvest treatments and storage temperatures on the quality and shelf life of sweet pepper (Capsicum annum L.). Sci Hortic (Amsterdam) **132**: 18–26

Rashid A (2016) Defense responses of plant cell wall non-catalytic proteins against pathogens. Physiol Mol Plant Pathol **94**: 38–46

Reboul R, Geserick C, Pabst M, Frey B, Wittmann D, Lütz-Meindl U, Léonard R, Tenhaken R (2011) Down-regulation of UDP-glucuronic acid biosynthesis leads to swollen plant cell walls and severe developmental defects associated with changes in pectic polysaccharides. J Biol Chem **286**: 39982–92

Reem NT, Pogorelko G, Lionetti V, Chambers L, Held MA, Bellincampi D, Zabotina OA (2016) Decreased polysaccharide feruloylation compromises plant cell wall integrity and increases susceptibility to necrotrophic fungal pathogens. Front Plant Sci **7**: 1–7

Rekhter D, Lüdke D, Ding Y, Feussner K, Zienkiewicz K, Lipka V, Wiermer M, Zhang Y, Feussner I (2019) Isochorismate-derived biosynthesis of the plant stress hormone salicylic acid. Science (80-) **365**: 498–502

Ridley BL, O'Neill MA, Mohnen D (2001) Pectins: Structure, biosynthesis, and oligogalacturonide-related signaling. Phytochemistry **57**: 929–967

Riedlmeier M, Ghirardo A, Wenig M, Knappe C, Koch K, Georgii E, Dey S, Parker JE, Schnitzler J-P, Vlot C (2017) Monoterpenes support systemic acquired resistance within and between plants. Plant Cell **29**: 1440–1459

Rietz S, Stamm A, Malonek S, Wagner S, Becker D, Medina-Escobar N, Corina Vlot A, Feys BJ, Niefind K, Parker JE (2011) Different roles of Enhanced Disease Susceptibility1 (EDS1) bound to and dissociated from Phytoalexin Deficient4 (PAD4) in Arabidopsis immunity. New Phytol **191**: 107–119

Roberts M, Tang S, Stallmann A, Dangl JL, Bonardi V (2013) Genetic Requirements for Signaling from an Autoactive Plant NB-LRR Intracellular Innate Immune Receptor. PLoS Genet **9**: e1003465

Rocher F, Chollet JF, Legros S, Jousse C, Lemoine R, Faucher M, Bush DR, Bonnemain JL (2009) Salicylic acid transport in Ricinus communis involves a pH-dependent carrier system in addition to diffusion. Plant Physiol **150**: 2081–91

Rodrigues JM, Coutinho FS, dos Santos DS, Vital CE, Ramos JRLS, Reis PB, Oliveira MGA, Mehta A, Fontes EPB, Ramos HJO (2021) BiP-overexpressing soybean plants display accelerated hypersensitivity response (HR) affecting the SA-dependent sphingolipid and flavonoid pathways. Phytochemistry **185**: 112704

Roessner U, Luedemann A, Brust D, Fiehn O, Linke T, Willmitzer L, Fernie AR (2001) Metabolic profiling allows comprehensive phenotyping of genetically or environmentally modified plant systems. Plant Cell **13**: 11–29

Rohman A, Dijkstra BW, Puspaningsih NNT (2019) β-xylosidases: Structural diversity, catalytic mechanism, and inhibition by monosaccharides. Int J Mol Sci **20**: 5524

Rohmer M (2007) Diversity in isoprene unit biosynthesis: The methylerythritol phosphate pathway in bacteria and plastids. Pure Appl Chem **79**: 739–751

Rojo E, León J, Sánchez-Serrano JJ (1999) Cross-talk between wound signalling pathways determines local versus systemic gene expression in Arabidopsis thaliana. Plant J **20**: 135–142

Rolland F, Baena-Gonzalez E, Sheen J (2006) SUGAR SENSING AND SIGNALING IN PLANTS: Conserved and Novel Mechanisms. Annu Rev Plant Biol **57**: 675–709

Ross A, Yamada K, Hiruma K, Yamashita-Yamada M, Lu X, Takano Y, Tsuda K, Saijo Y (2014) The Arabidopsis PEPR pathway couples local and systemic plant immunity. EMBO J **33**: 62–75

Rossez Y, Holmes A, Lodberg-Pedersen H, Birse L, Marshall J, Willats WGT, Toth IK, Holden NJ (2014) Escherichia coli common pilus (ECP) targets arabinosyl residues in plant cell walls to mediate adhesion to fresh produce plants. J Biol Chem **289**: 34349–34365

Rui Y, Dinneny JR (2020) A wall with integrity: surveillance and maintenance of the plant cell wall under stress. New Phytol **225**: 1428–1439

Ruprecht C, Bartetzko MP, Senf D, Dallabernardina P, Boos I, Andersen MCF, Kotake T, Knox JP, Hahn MG, Clausen MH, et al (2017) A synthetic glycan microarray enables epitope mapping of plant cell wall glycan-directed antibodies. Plant Physiol **175**: pp.00737.2017

Sacristán S, García-Arenal F (2008) The evolution of virulence and pathogenicity in plant pathogen populations. Mol Plant Pathol **9**: 369–384

Sagner S, Eisenreich W, Fellermeier M, Latzel C, Bacher A, Zenk MH (1998) Biosynthesis of 2-C-methyl-D-erythritol in plants by rearrangement of the terpenoid precursor, 1-deoxy-D-xylulose 5-phosphate. Tetrahedron Lett. doi: 10.1016/S0040-4039(98)00296-2

Saijo Y, Loo EP iian (2020) Plant immunity in signal integration between biotic and abiotic stress responses. New Phytol **225**: 87–104

Saiman MZ, Mustafa NR, Choi YH, Verpoorte R, Schulte AE (2015) Metabolic alterations and distribution of five-carbon precursors in jasmonic acid-elicited Catharanthus roseus cell suspension cultures. Plant Cell Tissue Organ Cult **122**: 351–362

von Saint Paul V, Zhang W, Kanawati B, Geist B, Faus-Keßler T, Schmitt-Kopplin P, Schäffner AR (2011) The arabidopsis glucosyltransferase UGT76B1 conjugates isoleucic acid and modulates plant defense and senescence. Plant Cell **23**: 4124–4145

Sakano K (2001) Metabolic regulation of pH in plant cells: Role of cytoplasmic pH in defense reaction and secondary metabolism. Int Rev Cytol **206**: 1–44

Saleh A, Withers J, Mohan R, Marqués J, Gu Y, Yan S, Zavaliev R, Nomoto M, Tada Y, Dong X (2015) Posttranslational modifications of the master transcriptional regulator NPR1 enable dynamic but tight control of plant immune responses. Cell Host Microbe **18**: 169–182

Sales J, Pabst E, Wenig M, Breitenbach HH, Perez G, Knappe C, Hammerl R, Liu J, Rozhon W, Poppenberger B, et al (2021) Local jasmonic acid cues drive systemic acquired resistance signal generation. bioRxiv

Sales JH (2021) Phytohormone crosstalk via legume lectin like-proteins regulates systemic acquired resistance and abiotic stress tolerance. TUM School of Life Sciences

Santner A, Estelle M (2009) Recent advances and emerging trends in plant hormone signalling. Nature **459**: 1071–78

Savadi S, Prasad P, Bhardwaj SC, Kashyap PL, Gangwar OP, Khan H, Kumar S (2018) Temporal Transcriptional Changes in SAR and Sugar Transport-Related Genes During Wheat and Leaf Rust Pathogen Interactions. J Plant Growth Regul **37**: 826–839

Savatin D V., Gramegna G, Modesti V, Cervone F (2014) Wounding in the plant tissue: The defense of a dangerous passage. Front Plant Sci. doi: 10.3389/fpls.2014.00470

Scharte J, Schön H, Weis E (2005) Photosynthesis and carbohydrate metabolism in tobacco leaves during an incompatible interaction with Phytophthora nicotianae. Plant, Cell Environ **28**: 1421–35

Schmid M, Davison TS, Henz SR, Pape UJ, Demar M, Vingron M, Schölkopf B, Weigel D, Lohmann JU (2005) A gene expression map of Arabidopsis thaliana development. Nat Genet **37**: 501–506

Schnake A, Hartmann M, Schreiber S, Malik J, Brahmann L, Yildiz I, Von Dahlen J, Rose LE, Schaffrath U, Zeier J (2020) Inducible biosynthesis and immune function of the systemic acquired resistance inducer N-hydroxypipecolic acid in monocotyledonous and dicotyledonous plants. J Exp Bot. doi: 10.1093/JXB/ERAA317

Scholl RL, May ST, Ware DH (2000) Seed and molecular resources for Arabidopsis. Plant Physiol **124**: 1477–80

Schulze-Lefert P, Robatzek S (2006) Plant Pathogens Trick Guard Cells into Opening the Gates. Cell **126**: 831–834

Schulze A, Zimmer M, Mielke S, Stellmach H, Melnyk C, Hause B, Gasperini D (2019) Shoot-to-root translocation of the jasmonate precursor 12-oxo-phytodienoic acid (OPDA) coordinates plant growth responses following tissue damage. bioRxiv. doi: 10.1101/517193

Sentelle RD, Senkal CE, Jiang W, Ponnusamy S, Gencer S, Panneer Selvam S, Ramshesh VK, Peterson YK, Lemasters JJ, Szulc ZM, et al (2012) Ceramide targets autophagosomes to mitochondria and induces lethal mitophagy. Nat Chem Biol **8**: 831–838

Seybold H, Demetrowitsch TJ, Hassani MA, Szymczak S, Reim E, Haueisen J, Lübbers L, Rühlemann M, Franke A, Schwarz K, et al (2020) A fungal pathogen induces systemic susceptibility and systemic shifts in wheat metabolome and microbiome composition. Nat Commun **11**: 1910

Shah J (2003) The salicylic acid loop in plant defense. Curr Opin Plant Biol **6**: 365–371

Shah J, Zeier J (2013) Long-distance communication and signal amplification in systemic acquired resistance. Front Plant Sci **4**: 1–16

Sham A, Al-Azzawi A, Al-Ameri S, Al-Mahmoud B, Awwad F, Al-Rawashdeh A, Iratni R, AbuQamar S (2014) Transcriptome analysis reveals genes commonly induced by Botrytis cinerea infection, cold, drought and oxidative stresses in Arabidopsis. PLoS One **9**: e113718

Shirano Y, Kachroo P, Shah J, Klessig DF (2002) A gain-of-function mutation in an Arabidopsis Toll Interleukin-1 Receptor-Nucleotide Binding Site-Leucine-Rich Repeat type R gene triggers defense responses and results in enhanced disease resistance. Plant Cell **14**: 3149–3162

Shukla P, Walia S, Ahluwalia V, Parmar BS, Nair MG (2012) Activity of alkanediol alkanoates against pathogenic plant fungi Rhizoctonia solani and Sclerotium rolfsii. Nat Prod Commun **7**: 1219–1222

Shulaev V, Silverman P, Raskin I (1997) Airborne signalling by methyl salicylate in plant pathogen resistance. Nature **385**: 718–721

Sible CN, Seebauer JR, Below FE (2021) Plant biostimulants: A categorical review, their implications for row crop production, and relation to soil health indicators. Agronomy **11**: 1297

Simanshu DK, Zhai X, Munch D, Hofius D, Markham JE, Bielawski J, Bielawska A, Malinina L, Molotkovsky JG, Mundy JW, et al (2014) Arabidopsis accelerated cell

death 11, ACD11, Is a ceramide-1-phosphate transfer protein and intermediary regulator of phytoceramide levels. Cell Rep. doi: 10.1016/j.celrep.2013.12.023

Singh A, Lim GH, Kachroo P (2017) Transport of chemical signals in systemic acquired resistance. J Integr Plant Biol **59**: 336–344

Sirichandra C, Gu D, Hu HC, Davanture M, Lee S, Djaoui M, Valot B, Zivy M, Leung J, Merlot S, et al (2009) Phosphorylation of the Arabidopsis AtrbohF NADPH oxidase by OST1 protein kinase. FEBS Lett **583**: 2982–2986

Smallwood M, Beven A, Donovan N, Neill SJ, Peart J, Roberts K, Knox JP (1994) Localization of cell wall proteins in relation to the developmental anatomy of the carrot root apex. Plant J **5**: 237–246

Smirnoff N, Wheeler GL (2000) Ascorbic acid in plants: Biosynthesis and function. CRC Crit Rev Plant Sci **35**: 291–314

Smirnova OG, Kochetov A V. (2016) Plant cell wall and mechanisms of resistance to pathogens. Russ J Genet Appl Res **6**: 622–631

Song JT, Koo YJ, Park JB, Seo YJ, Cho YJ, Seo HS, Choi Y Do (2009) The expression patterns of AtBSMT1 and AtSAGT1 encoding a salicylic acid (SA) methyltransferase and a SA glucosyltransferase, respectively, in Arabidopsis plants with altered defense responses. Mol Cells **28**: 105–109

Song JT, Lu H, Greenberg JT (2004) Divergent Roles in Arabidopsis thaliana Development and Defense of Two Homologous Genes, Aberrant Growth and Death2 And AGD2-Like Defense Response Protein 1, Encoding Novel Aminotransferases. Plant Cell **16**: 353–366

Song W, Forderer A, Yu D, Chai J (2020) Structural biology of plant defence. New Phytol **229**: 692–711

Sorin C, Negroni L, Balliau T, Corti H, Jacquemot MP, Davanture M, Sandberg G, Zivy M, Bellini C (2006) Proteomic analysis of different mutant genotypes of Arabidopsis led to the identification of 11 proteins correlating with adventitious root development. Plant Physiol **140**: 349–364

Spoel SH, Dong X (2012) How do plants achieve immunity? Defence without specialized immune cells. Nat Rev Immunol **12**: 89–100

Spoel SH, Dong X (2008) Making Sense of Hormone Crosstalk during Plant Immune Responses. Cell Host Microbe **3**: 348–351

Spoel SH, Johnson JS, Dong X (2007) Regulation of tradeoffs between plant defenses against pathogens with different lifestyles. Proc Natl Acad Sci U S A **104**: 18842–47

Spoel SH, Koornneef A, Claessens SMC, Korzelius JP, Van Pelt JA, Mueller MJ, Buchala AJ, Métraux JP, Brown R, Kazan K, et al (2003) NPR1 modulates cross-talk between salicylate- and jasmonate-dependent defense pathways through a novel function in the cytosol. Plant Cell **15**: 760–770

Spoel SH, Mou Z, Tada Y, Spivey NW, Genschik P, Dong X (2009) Proteasome-Mediated Turnover of the Transcription Coactivator NPR1 Plays Dual Roles in Regulating Plant Immunity. Cell **137**: 860–872

Stacey NJ, Roberts K, Knox JP (1990) Patterns of expression of the JIM4 arabinogalactan-protein epitope in cell cultures and during somatic embryogenesis in Daucus carota L. Planta **180**: 285–292

Staswick PE, Tiryaki I (2004) The oxylipin signal jasmonic acid is activated by an enzyme that conjugate it to isoleucine in Arabidopsis W inside box sign. Plant Cell **16**: 2117–27

Stout MJ, Thaler JS, Thomma BPHJ (2006) Plant-mediated interactions between pathogenic microorganisms and herbivorous arthropods. Annu Rev Entomol **51**: 663–689

Sun T, Huang J, Xu Y, Verma V, Jing B, Sun Y, Orduna AR, Tian H, Huang X, Xia S, et al (2020) Redundant CAMTA transcription factors negatively regulate the biosynthesis of salicylic acid and N-hydroxypipecolic acid by modulating the expression of SARD1 and CBP60g. Mol Plant **13**: 144–156

Sun X, Lapin D, Feehan JM, Stolze SC, Kramer K, Dongus JA, Rzemieniewski J, Blanvillain-Baufumé S, Harzen A, Bautor J, et al (2021) Pathogen effector recognition-dependent association of NRG1 with EDS1 and SAG101 in TNL receptor immunity. Nat Commun **12**: 3335

Suza WP, Staswick PE (2008) The role of JAR1 in Jasmonoyl-l-isoleucine production during Arabidopsis wound response. Planta **227**: 1221–32

Tan BC, Joseph LM, Deng WT, Liu L, Li QB, Cline K, McCarty DR (2003) Molecular characterization of the Arabidopsis 9-cis epoxycarotenoid dioxygenase gene family. Plant J **35**: 44–56

Tan L, Liu Q, Song Y, Zhou G, Luan L, Weng Q, He C (2019) Differential function of endogenous and exogenous abscisic acid during bacterial pattern-induced production of reactive oxygen species in arabidopsis. Int J Mol Sci **20**: 2544

Taurino M, Abelenda JA, Río-Alvarez I, Navarro C, Vicedo B, Farmaki T, Jiménez P, García-Agustín P, Lõpez-Solanilla E, Prat S, et al (2014) Jasmonate-dependent modifications of the pectin matrix during potato development function as a defense

mechanism targeted by Dickeya dadantii virulence factors. Plant J **77**: 418–429

Taylor CM, Karunaratne C V., Xie N (2012) Glycosides of hydroxyproline: Some recent, unusual discoveries. Glycobiology **22**: 757–767

Thines B, Katsir L, Melotto M, Niu Y, Mandaokar A, Liu G, Nomura K, He SY, Howe GA, Browse J (2007) JAZ repressor proteins are targets of the SCF(COI1) complex during jasmonate signalling. Nature **448**: 661–665

Thomma BPHJ, Eggermont K, Penninckx IAMA, Mauch-Mani B, Vogelsang R, Cammue BPA, Broekaert WF (1998) Separate jasmonate-dependent and salicylate-dependent defense-response pathways in arabidopsis are essential for resistance to distinct microbial pathogens. Proc Natl Acad Sci U S A **95**: 15107–11

Thomma BPHJ, Eggermont K, Tierens KFMJ, Broekaert WF (1999) Requirement of functional ethylene-insensitive 2 gene for efficient resistance of Arabidopsis to infection by Botrytis cinerea. Plant Physiol **121**: 1093–102

Thomma BPHJ, Nürnberger T, Joosten MHAJ (2011) Of PAMPs and effectors: The blurred PTI-ETI dichotomy. Plant Cell **23**: 4–15

Thompson AMG, Iancu C V., Neet KE, Dean J V., Choe JY (2017) Differences in salicylic acid glucose conjugations by UGT74F1 and UGT74F2 from Arabidopsis thaliana. Sci Rep **4**: 46629

Thordal-Christensen H (2003) Fresh insights into processes of nonhost resistance. Curr Opin Plant Biol **6**: 351–357

Thorpe MR, Ferrieri AP, Herth MM, Ferrieri RA (2007) 11C-imaging: Methyl jasmonate moves in both phloem and xylem, promotes transport of jasmonate, and of photoassimilate even after proton transport is decoupled. Planta **226**: 541–551

Tian D, Peiffer M, De Moraes CM, Felton GW (2014) Roles of ethylene and jasmonic acid in systemic induced defense in tomato (Solanum lycopersicum) against helicoverpa zea. Planta **239**: 577–589

Timmermann T, Poupin MJ, Vega A, Urrutia C, Ruz GA, González B (2019) Gene networks underlying the early regulation of Paraburkholderia phytofirmans PsJN induced systemic resistance in Arabidopsis. PLoS One **14**: 1–24

Tiré C, De Rycke R, De Loose M, Inzé D, Van Montagu M, Engler G (1994) Extensin gene expression is induced by mechanical stimuli leading to local cell wall strengthening in Nicotiana plumbaginifolia. Planta **195**: 175–181

Toppan A, Roby D, Esquerré-Tugayé M-T (1982) Cell Surfaces in Plant-Microorganism Interactions. Plant Physiol **70**: 82–86

Torode TA, Marcus SE, Jam M, Tonon T, Blackburn RS, Hervé C, Knox JP (2015) Monoclonal antibodies directed to fucoidan preparations from brown algae. PLoS One **10**: e0118366

De Torres Zabala M, Bennett MH, Truman WH, Grant MR (2009) Antagonism between salicylic and abscisic acid reflects early host-pathogen conflict and moulds plant defence responses. Plant J **59**: 375–386

Toruño TY, Stergiopoulos I, Coaker G (2016) Plant-Pathogen Effectors: Cellular Probes Interfering with Plant Defenses in Spatial and Temporal Manners. Annu Rev Phytopathol **54**: 419–441

Toyota M, Spencer D, Sawai-Toyota S, Jiaqi W, Zhang T, Koo AJ, Howe GA, Gilroy S (2018) Glutamate triggers long-distance, calcium-based plant defense signaling. Science (80-) **361**: 1112–1115

Tripathi D, Jiang YL, Kumar D (2010) SABP2, a methyl salicylate esterase is required for the systemic acquired resistance induced by acibenzolar-S-methyl in plants. FEBS Lett **584**: 3458–63

Truman W, Bennett MH, Kubigsteltig I, Turnbull C, Grant M (2007) *Arabidopsis* systemic immunity uses conserved defense signaling pathways and is mediated by jasmonates. Proc Natl Acad Sci **104**: 1075–1080

Tryfona T, Liang HC, Kotake T, Tsumuraya Y, Stephens E, Dupree P (2012) Structural characterization of Arabidopsis leaf arabinogalactan polysaccharides. Plant Physiol **160**: 653–666

Turra D, Lorito M (2011) Potato Type I and II Proteinase Inhibitors: Modulating Plant Physiology and Host Resistance. Curr Protein Pept Sci. doi: 10.2174/138920311796391151

Uemura T, Wang J, Aratani Y, Gilroy S, Toyota M (2021) Wide-field, real-time imaging of local and systemic wound signals in Arabidopsis. J Vis Exp **2021**: e62114

Underwood W, Melotto M, He SY (2007) Role of plant stomata in bacterial invasion. Cell Microbiol **9**: 1621–29

Vaahtera L, Schulz J, Hamann T (2019) Cell wall integrity maintenance during plant development and interaction with the environment. Nat Plants **5**: 924–932

Vaca E, Behrens C, Theccanat T, Choe JY, Dean J V. (2017) Mechanistic differences in the uptake of salicylic acid glucose conjugates by vacuolar membrane-enriched vesicles isolated from Arabidopsis thaliana. Physiol Plant **161**: 332–338

Valls M, Genin S, Boucher C (2006) Integrated regulation of the type III secretion

system and other virulence determinants in Ralstonia solanacearum. PLoS Pathog **2**: 798–807

VandenBosch KA, Bradley DJ, Knox JP, Perotto S, Butcher GW, Brewin NJ (1989) Common components of the infection thread matrix and the intercellular space identified by immunocytochemical analysis of pea nodules and uninfected roots. EMBO J **8**: 335–341

Vega-Muñoz I, Duran-Flores D, Fernández-Fernández ÁD, Heyman J, Ritter A, Stael S (2020) Breaking Bad News: Dynamic Molecular Mechanisms of Wound Response in Plants. Front Plant Sci **11**: 610445

Venugopal SC, Jeong RD, Mandal MK, Zhu S, Chandra-Shekara AC, Xia Y, Hersh M, Stromberg AJ, Navarre DR, Kachroo A, et al (2009) Enhanced disease susceptibility 1 and salicylic acid act redundantly to regulate resistance gene-mediated signaling. PLoS Genet **5**: e1000545

Verberne MC, Hoekstra J, Bol JF, Linthorst HJM (2003) Signaling of systemic acquired resistance in tobacco depends on ethylene perception. Plant J **35**: 27–32

Verberne MC, Verpoorte R, Bol JF, Mercado-Blanco J, Linthorst HJM (2000) Overproduction of salicylic acid in plants by bacterial transgenes enhances pathogen resistance. Nat Biotechnol **18**: 779–783

Verhertbruggen Y, Marcus SE, Haeger A, Ordaz-Ortiz JJ, Knox JP (2009a) An extended set of monoclonal antibodies to pectic homogalacturonan. Carbohydr Res **344**: 1858–1862

Verhertbruggen Y, Marcus SE, Haeger A, Verhoef R, Schols HA, McCleary B V., McKee L, Gilbert HJ, Knox JP (2009b) Developmental complexity of arabinan polysaccharides and their processing in plant cell walls. Plant J **59**: 413–425

van Verk MC, Bol JF, Linthorst HJM (2011) WRKY Transcription Factors Involved in Activation of SA Biosynthesis Genes. BMC Plant Biol **11**: 1–12

Vernooij B, Friedrich L, Morse A, Reist R, Kolditz-Jawhar R, Ward E, Uknes S, Kessmann H, Ryals J (1994) Salicylic acid is not the translocated signal responsible for inducing systemic acquired resistance but is required in signal transduction. Plant Cell **6**: 959–965

Vlot AC, Dempsey DA, Klessig DF (2009) Salicylic Acid, a Multifaceted Hormone to Combat Disease. Annu Rev Phytopathol **47**: 177–206

Vlot AC, Sales JH, Lenk M, Bauer K, Brambilla A, Sommer A, Chen Y, Wenig M, Nayem S (2021) Systemic propagation of immunity in plants. New Phytol **229**: 1234–50

Voigt CA (2014) Callose-mediated resistance to pathogenic intruders in plant defense-related papillae. Front Plant Sci **5**: 1–6

Vos IA, Moritz L, Pieterse CMJ, Van Wees SCM (2015) Impact of hormonal crosstalk on plant resistance and fitness under multi-attacker conditions. Front Plant Sci **6**: 1–13

Walker RP, Chen ZH, Famiani F (2021) Gluconeogenesis in Plants: A Key Interface between Organic Acid/Amino Acid/Lipid and Sugar Metabolism. Molecules **26**: 5129

Wang C, El-Shetehy M, Shine MB, Yu K, Navarre D, Wendehenne D, Kachroo A, Kachroo P (2014) Free Radicals Mediate Systemic Acquired Resistance. Cell Rep **7**: 348–355

Wang C, Huang X, Li Q, Zhang Y, Li JL, Mou Z (2019) Extracellular pyridine nucleotides trigger plant systemic immunity through a lectin receptor kinase/BAK1 complex. Nat Commun **10**: 4810

Wang C, Liu R, Lim GH, de Lorenzo L, Yu K, Zhang K, Hunt AG, Kachroo A, Kachroo P (2018a) Pipecolic acid confers systemic immunity by regulating free radicals. Sci Adv **4**: eaar4509

Wang H, Mei W, Qin Y, Zhu Y (2011a) 1-Aminocyclopropane-1-carboxylic acid synthase 2 is phosphorylated by calcium-dependent protein kinase 1 during cotton fiber elongation. Acta Biochim Biophys Sin (Shanghai) **43**: 654–661

Wang W, Barnaby JY, Tada Y, Li H, Tör M, Caldelari D, Lee DU, Fu XD, Dong X (2011b) Timing of plant immune responses by a central circadian regulator. Nature **470**: 110–114

Wang W, Wang X, Huang M, Cai J, Zhou Q, Dai T, Cao W, Jiang D (2018b) Hydrogen peroxide and abscisic acid mediate salicylic acid-induced freezing tolerance in wheat. Front Plant Sci **9**: 1–13

Wang X-Y, Li D-Z, Li Q, Ma Y-Q, Yao J-W, Huang X, Xu Z-Q (2016) Metabolomic analysis reveals the relationship between AZI1 and sugar signaling in systemic acquired resistance of Arabidopsis. Plant Physiol Biochem **107**: 273–287

Wang Y, Schuck S, Wu J, Yang P, Döring AC, Zeier J, Tsuda K (2018c) A MPK3/6-WRKY33-ALD1-Pipecolic Acid Regulatory Loop Contributes to Systemic Acquired Resistance. Plant Cell **30**: 2480–2494

Warner SAJ, Scott R, Draper J (1993) Isolation of an asparagus intracellular PR gene (AoPR1) wound-responsive promoter by the inverse polymerase chain reaction and its characterization in transgenic tobacco. Plant J **3**: 191–201

Wass MN, Kelley LA, Sternberg MJE (2010) 3DLigandSite: Predicting ligand-binding sites using similar structures. Nucleic Acids Res **38(Web Ser**: W469-73

Wasternack C, Hause B (2013) Jasmonates: Biosynthesis, perception, signal transduction and action in plant stress response, growth and development. An update to the 2007 review in Annals of Botany. Ann Bot **111**: 1021–58

Wei G, Shirsat AH (2006) Extensin over-expression in Arabidopsis limits pathogen invasiveness. Mol Plant Pathol **7**: 579–592

Weingart H, Ullrich H, Geider K, Völksch B (2001) The role of ethylene production in virulence of Pseudomonas syringae pvs. glycinea and phaseolicola. Phytopathology **91**: 511–518

Weise SE, Weber APM, Sharkey TD (2004) Maltose is the major form of carbon exported from the chloroplast at night. Planta **218**: 474–482

Weller DM, Mavrodi D V., Van Pelt JA, Pieterse CMJ, Van Loon LC, Bakker PAHM (2012) Induced systemic resistance in Arabidopsis thaliana against Pseudomonas syringae pv. tomato by 2,4-diacetylphloroglucinol-producing Pseudomonas fluorescens. Phytopathology **102**: 403–412

Wendehenne D, Gao Q, Kachroo A, Kachroo P (2014) Free radical-mediated systemic immunity in plants. Curr Opin Plant Biol **20**: 127–134

Weng JK, Ye M, Li B, Noel JP (2016) Co-evolution of Hormone Metabolism and Signaling Networks Expands Plant Adaptive Plasticity. Cell **166**: 881–893

Wenig M, Ghirardo A, Sales JH, Pabst ES, Breitenbach HH, Antritter F, Weber B, Lange B, Lenk M, Cameron RK, et al (2019) Systemic acquired resistance networks amplify airborne defense cues. Nat Commun **10**: 3813

White RF (1979) Acetylsalicylic acid (aspirin) induces resistance to tobacco mosaic virus in tobacco. Virology **99**: 410–412

Wiermer M, Feys BJ, Parker JE (2005) Plant immunity: The EDS1 regulatory node. Curr Opin Plant Biol **8**: 383–389

Wildermuth MC, Dewdney J, Wu G, Ausubel FM (2001) Isochorismate synthase is required to synthesize salicylic acid for plant defence. Nature **414**: 562–565

Willats WG t., Marcus SE, Knox JP (1998) Generation of a monoclonal antibody specific to (1 → 5)-α-L-arabinan. Carbohydr Res **308**: 149–152

Willats WGT, Limberg G, Buchholt HC, Van Alebeek GJ, Benen J, Christensen TMIE, Visser J, Voragen A, Mikkelsen JD, Knox JP (2000) Analysis of pectic epitopes

recognised by hybridoma and phage display monoclonal antibodies using defined oligosaccharides, polysaccharides, and enzymatic degradation. Carbohydr Res **327**: 309–320

Willats WGT, McCartney L, Steele-King CG, Marcus SE, Mort A, Huisman M, Van Alebeek GJ, Schols HA, Voragen AGJ, Le Goff A, et al (2004) A xylogalacturonan epitope is specifically associated with plant cell detachment. Planta **218**: 673–681

Willats WGT, Orfila C, Limberg G, Buchholt HC, van Alebeek G-JWM, Voragen AG., Marcus SE, Christensen TMIE, Mikkelsen JD, Murray BS, et al (2001) Modulation of the Degree and Pattern of Methyl-esterification of Pectic Homogalacturonan in Plant Cell Walls. J Biol Chem. doi: 10.1074/jbc.m011242200

Williams MAK, Cornuault V, Irani AH, Symonds VV, Malmström J, An Y, Sims IM, Carnachan SM, Sallé C, North HM (2020) Polysaccharide Structures in the Outer Mucilage of Arabidopsis Seeds Visualized by AFM. Biomacromolecules **21**: 1450–1459

Winter D, Vinegar B, Nahal H, Ammar R, Wilson G V., Provart NJ (2007) An "electronic fluorescent pictograph" Browser for exploring and analyzing large-scale biological data sets. PLoS One **2**: e718

Wittek F (2013) Identification of systemic acquired resistance-inducing molecules in plants by a new metabolomic approach. TUM

Wittek F, Hoffmann T, Kanawati B, Bichlmeier M, Knappe C, Wenig M, Schmitt-Kopplin P, Parker JE, Schwab W, Vlot AC (2014) Arabidopsis ENHANCED DISEASE SUSCEPTIBILITY1 promotes systemic acquired resistance via azelaic acid and its precursor 9-oxo nonanoic acid. J Exp Bot. doi: 10.1093/jxb/eru331

Wittek F, Kanawati B, Wenig M, Hoffmann T, Franz-Oberdorf K, Schwab W, Schmitt-Kopplin P, Vlot AC (2015) Folic acid induces salicylic acid-dependent immunity in Arabidopsis and enhances susceptibility to Alternaria brassicicola. Mol Plant Pathol **16**: 616–622

Wrzaczek M, Brosché M, Kollist H, Kangasjärvi J (2009) Arabidopsis GRI is involved in the regulation of cell death induced by extracellular ROS. Proc Natl Acad Sci U S A **106**: 5412–5417

Wu JX, Li J, Liu Z, Yin J, Chang ZY, Rong C, Wu JL, Bi FC, Yao N (2015) The Arabidopsis ceramidase AtACER functions in disease resistance and salt tolerance. Plant J **81**: 767–780

Wu L, Chen H, Curtis C, Fu ZQ (2014) Go in for the kill: How plants deploy effector-triggered immunity to combat pathogens. Virulence **5**: 710–721

Wu L, Huang Z, Li X, Ma L, Gu Q, Wu H, Liu J, Borriss R, Wu Z, Gao X (2018a)

Stomatal closure and SA-, JA/ET-signaling pathways are essential for Bacillus amyloliquefaciens FZB42 to restrict leaf disease caused by Phytophthora nicotianae in Nicotiana benthamiana. Front Microbiol **9**: 847

Wu Q, Peng Z, Zhang Y, Yang J (2018b) COACH-D: Improved protein-ligand binding sites prediction with refined ligand-binding poses through molecular docking. Nucleic Acids Res **46**: 438–442

Wu Y, Zhang D, Chu JY, Boyle P, Wang Y, Brindle ID, De Luca V, Després C (2012) The Arabidopsis NPR1 Protein Is a Receptor for the Plant Defense Hormone Salicylic Acid. Cell Rep **1**: 639–947

Xiao W, Sheen J, Jang JC (2000) The role of hexokinase in plant sugar signal transduction and growth and development. Plant Mol Biol **44**: 451–461

Xie K, Li L, Zhang H, Wang R, Tan X, He Y, Hong G, Li J, Ming F, Yao X, et al (2018) Abscisic acid negatively modulates plant defence against rice black-streaked dwarf virus infection by suppressing the jasmonate pathway and regulating reactive oxygen species levels in rice. Plant Cell Environ **41**: 2504–2514

Xu G, Liu D, Wu Y, Gao PP, Xiao Y, Cao L, Liu P (2015) Effects of exogenous salicylic acid on cell wall polysaccharides and aluminum tolerance of Trichosanthes kirilowii under aluminum toxicity. Pakistan J Bot **47**: 1649–1655

Yamada K, Saijo Y, Nakagami H, Takano Y (2016a) Regulation of sugar transporter activity for antibacterial defense in Arabidopsis. Science (80-) **354**: 1427–30

Yamada K, Yamashita-Yamada M, Hirase T, Fujiwara T, Tsuda K, Hiruma K, Saijo Y (2016b) Danger peptide receptor signaling in plants ensures basal immunity upon pathogen-induced depletion of BAK 1. EMBO J **35**: 46–61

Yamaguchi Y, Huffaker A (2011) Endogenous peptide elicitors in higher plants. Curr Opin Plant Biol **14**: 351–357

Yamamoto S, Suzuki K, Shinshi H (1999) Elicitor-responsive, ethylene-independent activation of GCC box-mediated transcription that is regulated by both protein phosphorylation and dephosphorylation in cultured tobacco cells. Plant J **20**: 571–579

Yan Y, Stolz S, Chételat A, Reymond P, Pagni M, Dubugnon L, Farmer EE (2007) A downstream mediator in the growth repression limb of the jasmonate pathway. Plant Cell **19**: 2470–2483

Yang J, Duan G, Li C, Liu L, Han G, Zhang Y, Wang C (2019) The Crosstalks Between Jasmonic Acid and Other Plant Hormone Signaling Highlight the Involvement of Jasmonic Acid as a Core Component in Plant Response to Biotic and Abiotic Stresses. Front Plant Sci **10**: 1–12

Yang Z, Tian L, Latoszek-Green M, Brown D, Wu K (2005) Arabidopsis ERF4 is a transcriptional repressor capable of modulating ethylene and abscisic acid responses. Plant Mol Biol **58**: 585–596

Yasuda M, Ishikawa A, Jikumaru Y, Seki M, Umezawa T, Asami T, Maruyama-Nakashita A, Kudo T, Shinozaki K, Yoshida S, et al (2008) Antagonistic interaction between systemic acquired resistance and the abscisic acid-mediated abiotic stress response in Arabidopsis. Plant Cell **20**: 1678–1692

Yates EA, Valdor JF, Haslam SM, Morris HR, Dell A, Mackie W, Knox JP (1996) Characterization of carbohydrate structural features recognized by anti-arabinogalactan-protein monoclonal antibodies. Glycobiology **6**: 131–139

Yildiz I, Mantz M, Hartmann M, Zeier T, Kessel J, Thurow C, Gatz C, Petzsch P, Köhrer K, Zeier J (2021) The mobile SAR signal N-hydroxypipecolic acid induces NPR1-dependent transcriptional reprogramming and immune priming. Plant Physiol **186**: 1679–1705

Young MM, Kester M, Wang HG (2013) Sphingolipids: Regulators of crosstalk between apoptosis and autophagy. J Lipid Res **54**: 5–19

Yu H, Li J (2021) Short-and long-term challenges in crop breeding. Natl Sci Rev **8**: nwab00

Yu K, Soares JM, Mandal MK, Wang C, Chanda B, Gifford AN, Fowler JS, Navarre D, Kachroo A, Kachroo P (2013) A Feedback Regulatory Loop between G3P and Lipid Transfer Proteins DIR1 and AZI1 Mediates Azelaic-Acid-Induced Systemic Immunity. CellReports **3**: 1266–1278

Yu Y, Wang J, Li S, Kakan X, Zhou Y, Miao Y, Wang F, Qin H, Huang R (2019) Ascorbic acid integrates the antagonistic modulation of ethylene and abscisic acid in the accumulation of reactive oxygen species. Plant Physiol **179**: 1861–1875

Yuan M, Huang Y, Huang Y, Ge W, Jia Z, Song S, Zhang L (2019) Involvement of jasmonic acid, ethylene and salicylic acid signaling pathways behind the systemic resistance induced by Trichoderma longibrachiatum H9 in cucumber. BMC Genomics **20**: 144

Yuan M, Jiang Z, Bi G, Nomura K, Liu M, Wang Y, Cai B, Zhou JM, He SY, Xin XF (2021) Pattern-recognition receptors are required for NLR-mediated plant immunity. Nature **592**: 105–109

Zablackis E, Huang J, Muller B, Darvill AG, Albersheim P (1995) Characterization of the Cell-Wall Polysaccharides of Arabidopsis thaliana Leaves. Plant Physiol **107**: 1129–1138

Zandalinas SI, Fritschi FB, Mittler R (2020) Signal transduction networks during stress

combination. J Exp Bot **71**: 1734–41

Zandalinas SI, Fritschi FB, Mittler R (2021) Global Warming, Climate Change, and Environmental Pollution: Recipe for a Multifactorial Stress Combination Disaster. Trends Plant Sci **26**: 588–599

Zavaliev R, Mohan R, Chen T, Dong X (2020) Formation of NPR1 Condensates Promotes Cell Survival during the Plant Immune Response. Cell **182**: 1093–1108

Zeier J (2021) Metabolic regulation of systemic acquired resistance. Curr Opin Plant Biol **62**: 102050

Zhang B, Ramonell K, Somerville S, Stacey G (2002) Characterization of early, chitin-induced gene expression in Arabidopsis. Mol Plant-Microbe Interact **15**: 963–970

Zhang F, Yao J, Ke J, Zhang L, Lam VQ, Xin XF, Zhou XE, Chen J, Brunzelle J, Griffin PR, et al (2015) Structural basis of JAZ repression of MYC transcription factors in jasmonate signalling. Nature **525**: 269–273

Zhang J, Du X, Wang Q, Chen X, Lv D, Xu K, Qu S, Zhang Z (2010a) Expression of pathogenesis related genes in response to salicylic acid, methyl jasmonate and 1-aminocyclopropane-1-carboxylic acid in Malus hupehensis (Pamp.) Rehd. BMC Res Notes **3**: 1–6

Zhang L, Paasch BC, Chen J, Day B, He SY (2019) An important role of l-fucose biosynthesis and protein fucosylation genes in Arabidopsis immunity. New Phytol **222**: 981–994

Zhang W (2013) Impact of glycosyltransferase UGT76B1 in Arabidopsis thaliana and its substrate isoleucic acid on plant defense. Ludwig-Maximilians-University Munich, Fuzhou, Jiangxi, P.R. China

Zhang W, Zhao F, Jiang L, Chen C, Wu L, Liu Z (2018) Different Pathogen Defense Strategies in Arabidopsis: More than Pathogen Recognition. Cells **7**: 252

Zhang X, Chen S, Mou Z (2010b) Nuclear localization of NPR1 is required for regulation of salicylate tolerance, isochorismate synthase 1 expression and salicylate accumulation in Arabidopsis. J Plant Physiol **167**: 144–148

Zhang Y, Turner JG (2008) Wound-induced endogenous jasmonates stunt plant growth by inhibiting mitosis. PLoS One **3**: e3699

Zhang Y, Xu S, Ding P, Wang D, Cheng YT, He J, Gao M, Xu F, Li Y, Zhu Z, et al (2010c) Control of salicylic acid synthesis and systemic acquired resistance by two members of a plant-specific family of transcription factors. Proc Natl Acad Sci U S A **107**: 18220–25

Zhang Z, Wang J, Zhang R, Huang R (2012) The ethylene response factor AtERF98 enhances tolerance to salt through the transcriptional activation of ascorbic acid synthesis in Arabidopsis. Plant J **71**: 273–287

Zheng XY, Spivey NW, Zeng W, Liu PP, Fu ZQ, Klessig DF, He SY, Dong X (2012) Coronatine promotes pseudomonas syringae virulence in plants by activating a signaling cascade that inhibits salicylic acid accumulation. Cell Host Microbe **11**: 587–596

Zhong R, Teng Q, Haghighat M, Yuan Y, Furey ST, Dasher RL, Ye ZH (2017) Cytosol-localized UDP-xylose synthases provide the major source of UDP-xylose for the biosynthesis of Xylan and xyloglucan. Plant Cell Physiol **58**: 156–174

Zhou C, Zhang L, Duan J, Miki B, Wu K (2005) Histone Deacetylase19 is involved in jasmonic acid and ethylene signaling of pathogen response in Arabidopsis. Plant Cell **17**: 1196–1204

Zhou JM, Zhang Y (2020) Plant Immunity: Danger Perception and Signaling. Cell **181**: 978–989

Zhu CQ, Hu WJ, Cao XC, Zhu LF, Bai ZG, Huang J, Liang QD, Jin QY, Zhang JH (2020) Role of salicylic acid in alleviating the inhibition of root elongation by suppressing ethylene emission in rice under Al toxicity conditions. Plant Growth Regul **90**: 475–487

Zhu F, Xi DH, Yuan S, Xu F, Zhang DW, Lin HH (2014) Salicylic acid and jasmonic acid are essential for systemic resistance against tobacco mosaic virus in nicotiana benthamiana. Mol Plant-Microbe Interact **27**: 567–577

Zhu Z, An F, Feng Y, Li P, Xue L, A M, Jiang Z, Kim JM, To TK, Li W, et al (2011) Derepression of ethylene-stabilized transcription factors (EIN3/EIL1) mediates jasmonate and ethylene signaling synergy in Arabidopsis. Proc Natl Acad Sci U S A **108**: 12539–44

Zipfel C, Felix G (2005) Plants and animals: A different taste for microbes? Curr Opin Plant Biol **8**: 353–360

7. Supplemental data

Table S16: Antibodies and carbohydrate binding modules used in CoMPP.

Antibody /CBM	Specificity	Reference
JIM5	Partially methyl-esterified homogalacturonan	(VandenBosch et al., 1989; Willats et al., 2000; Clausen et al., 2003)
JIM7	Heavily methyl-esterified homogalacturonan	(VandenBosch et al., 1989; Willats et al., 2000; Clausen et al., 2003)
LM18	De-esterified homogalacturonan	(Verhertbruggen et al., 2009a)
LM19	De-esterified homogalacturonan	(Verhertbruggen et al., 2009a)
LM20	Methyl-esterified homogalacturonan	(Verhertbruggen et al., 2009a)
LM7	Partially methyl-esterified homogalacturonan	(Laurenzi et al., 2001; Willats et al., 2001)
INRA-RU2	Backbone of rhamnogalacturonan I	(Ralet et al., 2010)
INRA-RU1	Backbone of rhamnogalacturonan I	(Ralet et al., 2010)
LM5	(1–4)-ß-D-galactan	(Jones et al., 1997)
LM6	(1,5)-α-L-arabinan	(Willats et al., 1998)
LM13	Linear arabinan	(Moller et al., 2008)
LM16	Galactan	(Verhertbruggen et al., 2009a)
LM8	Xylogalacturonan	(Willats et al., 2004)

LM22	(1,4)-β-D-Mannan/galactomannan	(Marcus et al., 2010)
LM21	(1,4)-β-D-Mannan/galactomannan	(Marcus et al., 2010)
LM15	Xyloglucan	(Marcus et al., 2008; Ruprecht et al., 2017)
LM24	Xyloglucan	(Pedersen et al., 2012)
LM25	Xyloglucan	(Pedersen et al., 2012)
LM11	Unsubstituted xylans	(McCartney et al., 2005)
LM23	Xylogalacturonan, xylan, fucoidan preps	(Manabe et al., 2011; Pedersen et al., 2012; Torode et al., 2015)
BS-400-2	(1→3)-β-glucans	(Meikle et al., 1991)
BS-400-3	(1-3;1-4)-beta-D-glucan	(Meikle et al., 1994)
JIM8	Arabinogalactan protein	(McCabe et al., 1997)
JIM13	Arabinogalactan protein	(Knox et al., 1991; Yates et al., 1996)
JIM14	Arabinogalactan protein	(Knox et al., 1991; Yates et al., 1996)
JIM15	Arabinogalactan protein	(Knox et al., 1991; Yates et al., 1996)
JIM16	Arabinogalactan protein	(Knox et al., 1991; Yates et al., 1996; Ruprecht et al., 2017)
JIM17	Arabinogalactan protein	(Pattathil et al., 2010)
JIM4	Arabinogalactan protein glycan	(Stacey et al., 1990; Knox et al., 1991; Yates et al., 1996)
JIM20	Extensin	(Smallwood et al., 1994)

LM2	Arabinogalactan protein	(Yates et al., 1996)
LM14	Arabinogalactan protein	(Moller et al., 2008; Pedersen et al., 2012)
Mac207	Arabinogalactan protein	(Yates et al., 1996)
CBM3a	Crystalline cellulose	(Blake et al., 2006)
2F4	Homogalacturonan	(Liners et al., 1989; Liners et al., 1992; Liners and Van Cutsem, 1992)
LM1	Extensin	(Smallwood et al., 1994)
JIM11	Extensin	(Smallwood et al., 1994)

Table S17: Details of the one-Way ANOVAs and Tukey tests.

For P=<0.05 of Fig. 18. T0: two hours after inoculation at the day of infection, T1: one dpi, T2: 2 dpi, and T4: 4 dpi.

Details for statistics
For (**A**): F(8, 136)=144.3, Col-0 T0 n=15**,** Col-0 T2 n=17**,** Col-0 T4 n=22**,** *xyl4-1* T0 n=15**,** *xyl4-1* T2 n=18**,** *xyl4-1* T4 n=22**,** *xyl4-2* T0 n=12**,** *xyl4-2* T2 n=12**,** *xyl4-2* T4 n=12; for (**B**): F(8, 137)=361.6, Col-0 T0 n=15**,** Col-0 T2 n=18**,** Col-0 T4 n=22**,** *xyl4-1* T0 n=15**,** *xyl4-1* T2 n=18**,** *xyl4-1* T4 n=22**,** *xyl4-2* T0 n=12**,** *xyl4-2* T2 n=12**,** *xyl4-2* T4 n=12; for (**C**): F(8, 132)=285.3, Col-0 T1 n=21**,** Col-0 T2 n=27**,** Col-0 T4 n=32**,** *xyl4-1* T1 n=20**,** *xyl4-1* T2 n=27**,** *xyl4-1* T4 n=32**,** *xyl4-2* T1 n=9**,** *xyl4-2* T2 n=12**,** *xyl4-2* T4 n=12; for (**D**): F(8, 164)=169.7, Col-0 T1 n=18**,** Col-0 T2 n=24**,** Col-0 T4 n=28**,** *xyl4-1* T1 n=18**,** *xyl4-1* T2 n=24**,** *xyl4-1* T4 n=28, *xyl4-2* T1 n=9, *xyl4-2* T2 n=12, *xyl4-2* T4 n=12)

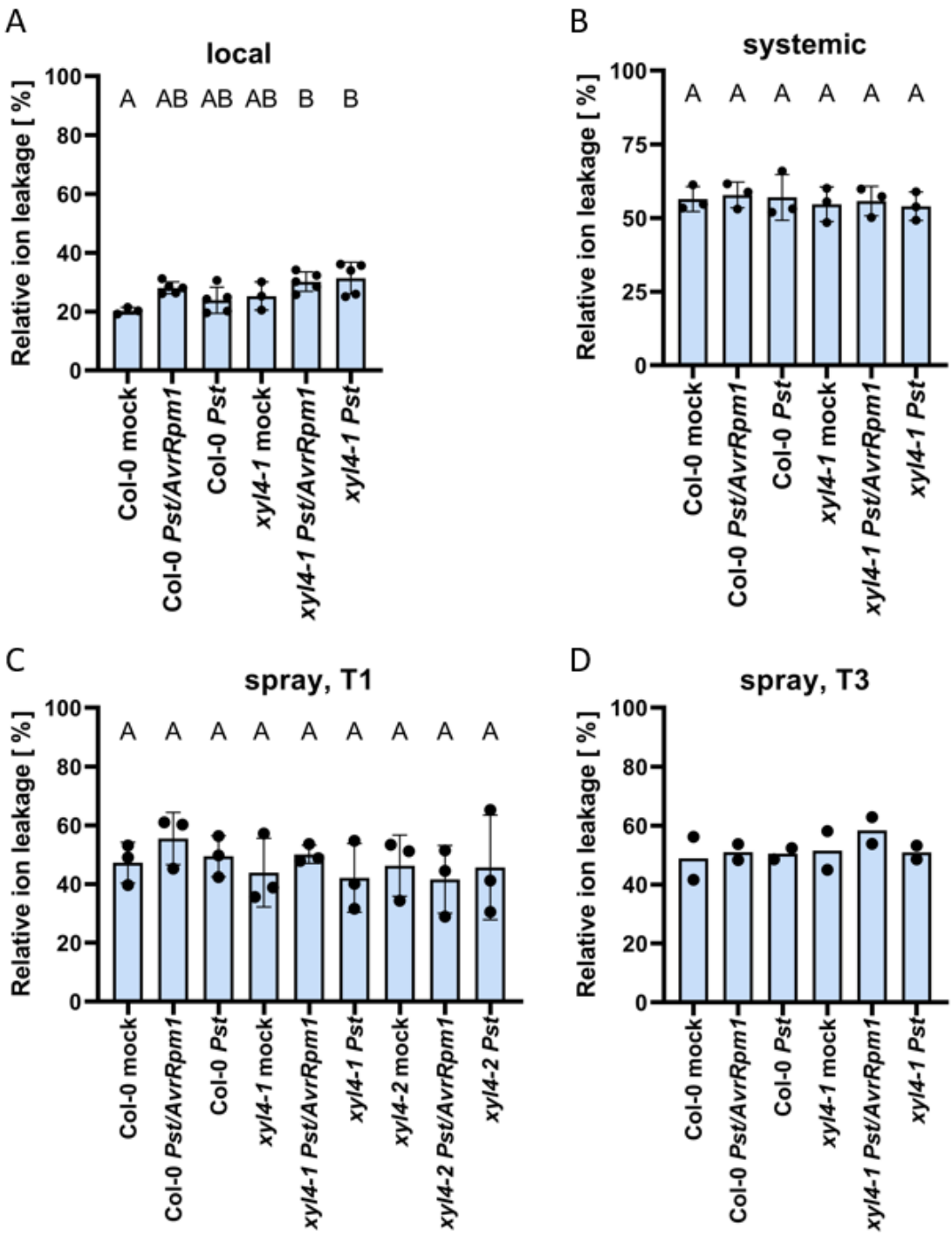

Figure S35. Infection-associated ion leakage is independent of XYL4.

Plants (Col-0, *xyl4-1*) were infiltrated with either a control solution (mock) or 10^5 cfu/mL of *Pst* or *Pst*/*AvrRpm1*. Alternatively, Col-0, *xyl4-1* and additionally *xyl4-2* plants were spray-inoculated with either 10^8 cfu/mL of *Pst* or *Pst*/*AvrRpm1*, or a mock solution. One (or three) day(s) later, infected (A), systemic (B), or spray-inoculated (C/D) leaves were harvested and subsequently incubated in water to determine the electrical conductivity as a measure for ion leakage. Bars represent the average electrical conductivity of two to five independent experiments relative to background conductivity (black dots represent individual data points) ± SD. Different letters above the bars indicate statistically significant differences (one-way ANOVA and Tukey test for P=<0.05, for (A): F(5, 20)=4.517, Col-0 mock n=3, Col-0 Pst n=5, Col-0 Pst/AvrRpm1 n=5, xyl4-1 mock n=3, xyl4-1 Pst n=5, xyl4-1 Pst/AvrRpm1 n=5; for (B): n=3, F(5, 12)=0.2054; for (C): n=3, F(8, 18)=0.5074).

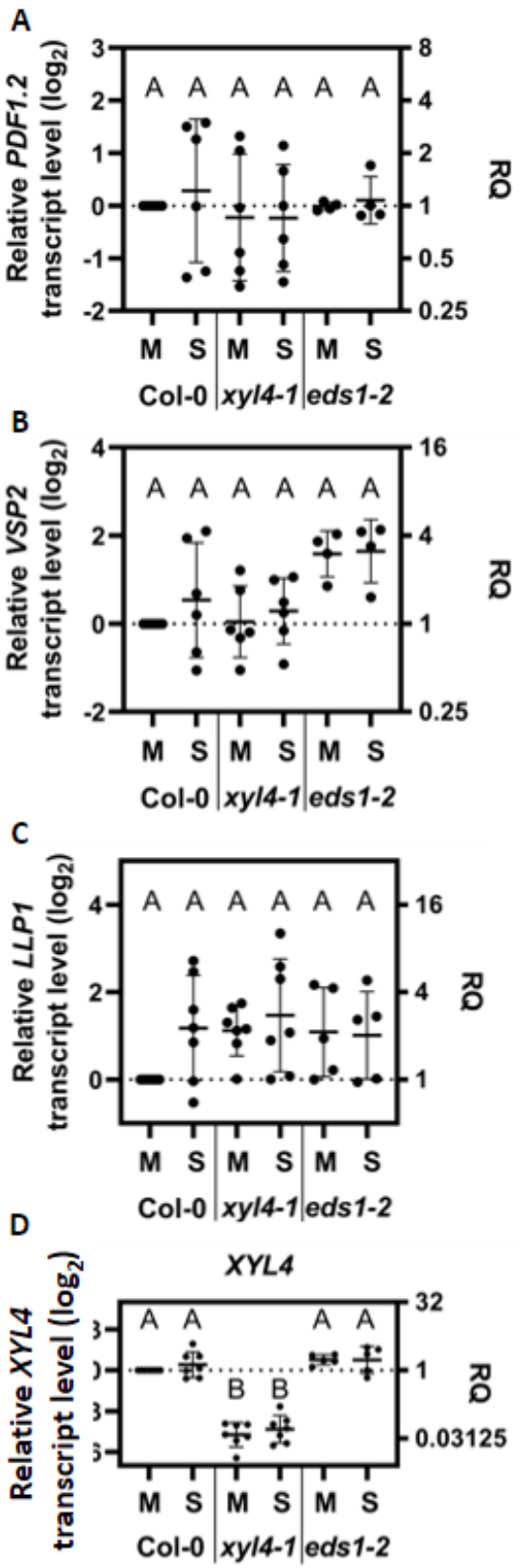

Figure S36. Transcript accumulation of JA-related genes and *LLP1* is not affected systemically at later phases.

(A-C) Col-0, *xyl4-1*, and *eds1-2* plants were inoculated with either a mock (M) solution or 10^6 cfu/mL of *Pst/AvrRpm1* (S). Three days later, systemic leaves were harvested to analyze gene transcript levels of *PDF1.2*, *VSP2, LLP1* and *XYL4* by RT-qPCR. Transcript accumulation was normalized to that of *UBIQUITIN* and is shown relative to the normalized transcript levels in the appropriate WT mock controls. Black dots and the respective mean values (black line) ± SD represent four to seven biologically independent replicates. The letters above the scatter dot plots indicate statistically significant differences (one-Way ANOVA and Tukey test, P=<0.05, for (A): n=4-6, F(5, 26)=0.2675; for (B): n=4-6, F(5, 26)=3.95; for (C): n=5-7, F(5, 32)=1.966; for (D): n=7, F(5, 32)=68.60).

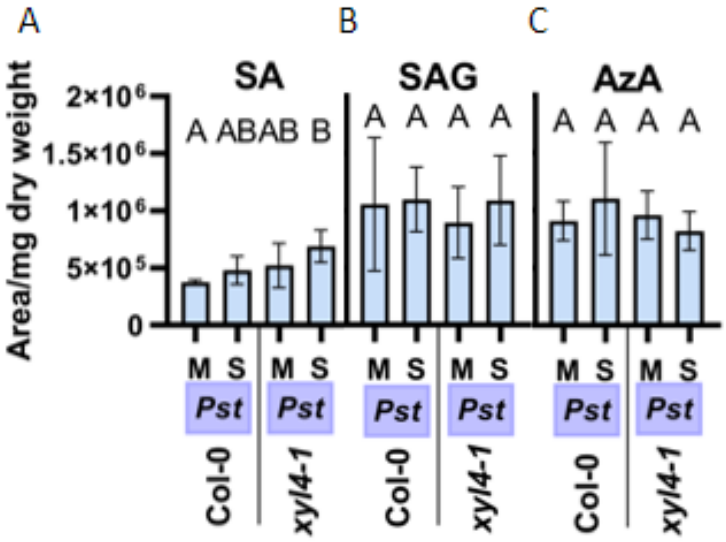

Figure S37: *XYL4* has no effect on metabolite accumulation of SA, SAG or AzA after a secondary challenge with *Pst*

Plants of the genotypes Col-0 and *xyl4-1* were syringe-infiltrated in the first two true leaves with 10^7 cfu per mL of *Pst/AvrRpm*1 (S), or a corresponding mock (M) control solution. The plants were challenged at 3 dpi with 10^5 cfu/mL of *Pst*. One day later, the inoculated leaves were pooled for each treatment and genotype and determined for the metabolites SA (A), SAG (B), and AzA (C). The metabolites were analyzed by LC-MS, calibrated to appropriate internal standards, and normalized to the individual dry weight. Bars represent average metabolite abundance of four to five biologically independent replicates ± SD. Different letters above bars indicate statistically significant differences for means (one-way ANOVA and Tukey test for P=<0.05, for (A): n=4, F(3, 12)=3.896; for (B): n=5, F(3, 18)=0.3146; for (C): n=4, F(3, 14)=0.572).

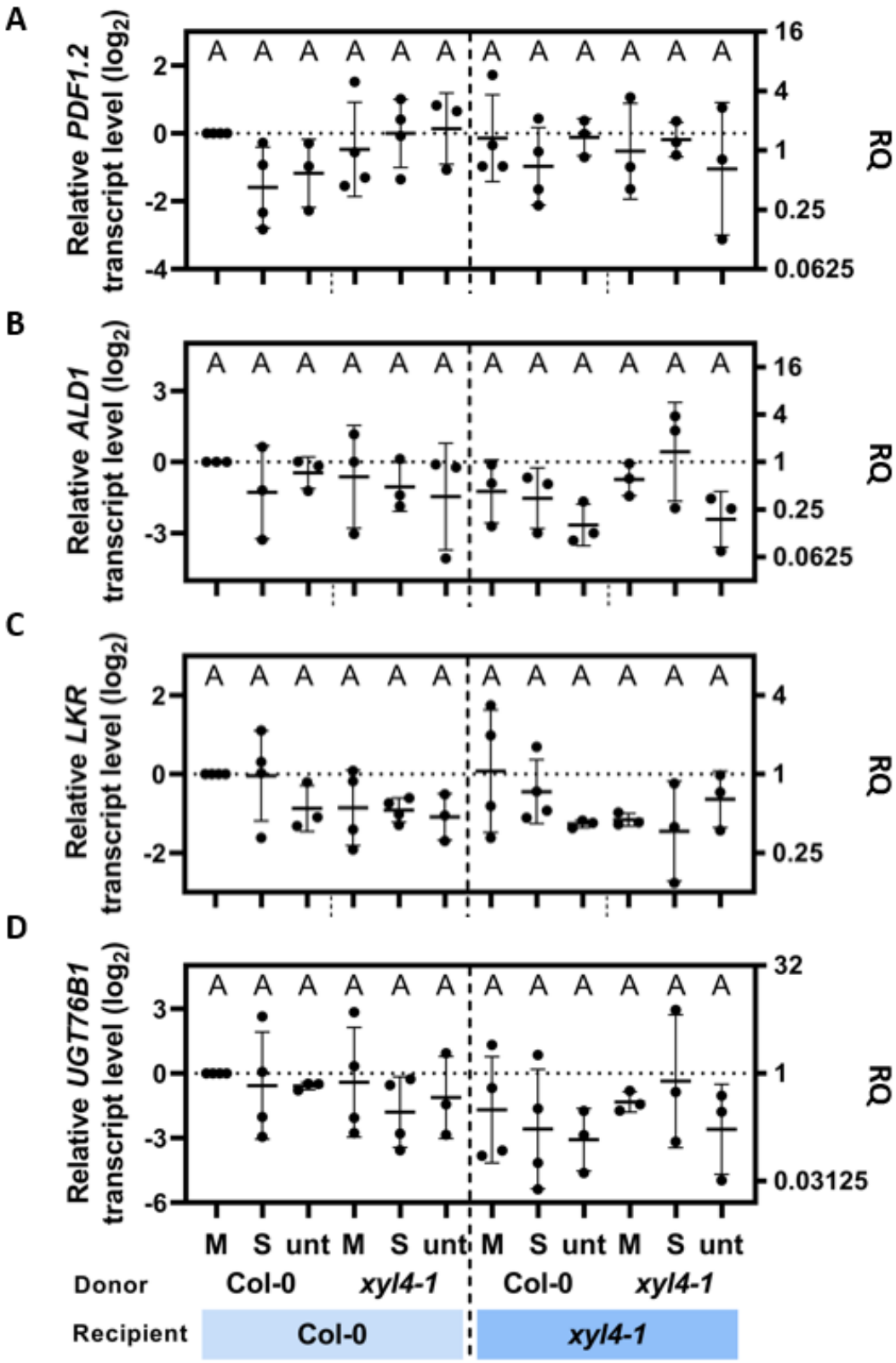

Figure S38. *XYL4*-dependent phloem-mobile SAR signals have no effect on the transcript expression of specific genes in receiver plants.
(A-D) WT (Col-0) and *xyl4-1* plants were inoculated with either a mock (M) solution or 10^7 cfu/mL of *Pst/AvrRpm1* (S) or kept untreated (unt). 24 hours later, distal leaves were cut at the middle of the plant rosette with the petiole and incubated in water in the dark for to

days to collect leaf exudates. Subsequently, these exudates from donor plants were fortified with 10mM $MgCl_2$ and syringe-infiltrated into naïve recipient plants. On day later, the inoculated leaves were collected to analyze gene transcript levels by RT-qPCR. Transcript accumulation was normalized to that of *UBIQUITIN* and is shown relative to the normalized transcript levels in the appropriate WT mock controls. Black dots and the respective mean values ± SD represent three to four biologically independent replicates. The letters above the scatter dot plots indicate statistically significant differences (one-Way ANOVA and Tukey test, P=<0.05, for (A, Col-0 receiver):: n=3-4, F(5, 16)=1.728; for (A, *xyl4-1* receiver): n=3-4, F(5, 14)=0.3952; for (B, Col-0 receiver): n=3, F(5, 12)=0.3615; for (B, *xyl4-1* receiver): n=3, F(5, 12)=0.117; for (C, Col-0 receiver): n=3-4, F(5, 16)=1.636; for (C, *xyl4-1* receiver): n=3-4, F(5, 14)=1.216; for (D, Col-0 receiver): n=3-4, F(5, 16)=0.5325; for (D, *xyl4-1* receiver): n=3-4, F(5, 14)=0.595).

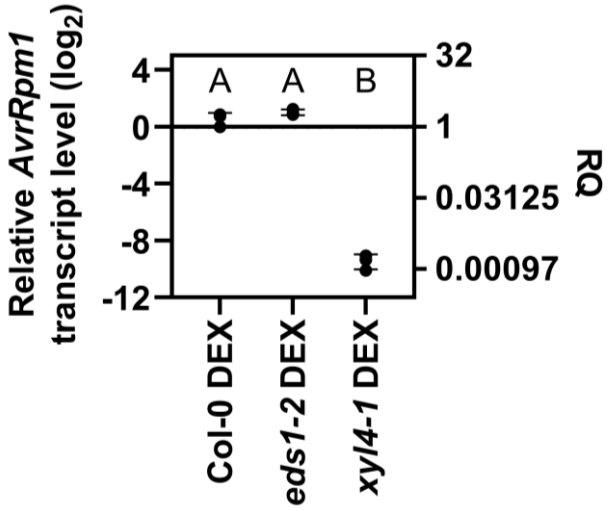

Figure S39. Transgenic *xyl4-1* are not inducible for the expression of *AvrRpm1*
Transgenic Col-0, *eds1-2*, and *xyl4-1* plants were spray-inoculated with DEX and harvested for the gene expression analysis 6 h later. Transcript abundance of *AvrRpm1* was determined by qRT-PCR, normalized to that of *UBIQUITIN*, and is shown relative to the normalized transcript levels of an appropriate Col-0 control. Black dots represent three biologically independent data points, and lines indicate the respective mean values ± SD. The letters above the scatter dot plots indicate statistically significant differences (n=3, F(2, 6)=593.2).

Table S18. SAR- and carbohydrate-related metabolic pathways are regulated in association to *EDS1*.

Transgenic Col-0 and *eds1-2* plants were spray-inoculated with DEX for the expression of *AvrRpm1*. About 6 h after, rosettes were harvested, pooled for the treatment and genotype, and subsequently extracted in methanol and chloroform to attain soluble metabolites. GC-MS analysis was conducted to determine glycans and further molecules in a semi-targeted manner. 136 metabolites were detected and calibrated to two appropriate internal standards and normalized to sample dry weight. Peaks from the chromatograms obtained were evaluated by using available databases and if possible edited for a specific metabolite. Molecules were labeled with "Unknown_mass" when they could not be clearly assigned to a database-saved entry according to their mass and predicted functional groups. For each biologically independent experiment I calculated the average abundance normalized to sample dry weight and relative to SAR-induced Col-0 plants from four biologically independent replicates ± SD. Values in bold are significant different from SAR-induced Col-0 (two-way ANOVA, and Bonferroni's multiple comparison test or False Discovery Rate (FDR) with two-stage linear step-up procedure of Benjamini, Krieger and Yekutieli; P=<0.05, *p*-values as indicated in the table).

Metabolite	Relative abundance ± SD		Bonferroni: adjusted *p*-value	FDR: *p*-value
	Col-0	***eds1-2* (sorted)**	**Col-0 vs. *eds1-2***	**Col-0 vs. *eds1-2***
Xylulose	1.00	3.23 ± 1.05	**<0.0001**	**<0.0001**
Unknown_mass204_RI_2534.96	1.00	2.05 ± 0.82	**<0.0001**	**<0.0001**
Unknown_mass117_RI_1539.64	1.00	1.99 ± 0.37	**<0.0001**	**<0.0001**
Spermidine	1.00	1.74 ± 0.75	**<0.0001**	**<0.0001**
Erythritol	1.00	1.67 ± 0.14	**0.0002**	**<0.0001**
Unknown_mass237_RI_1522.12	1.00	1.52 ± 0.99	**0.0067**	**0.0022**
2,5-Dimethoxy-Cinnamic acid	1.00	1.46 ± 0.54	**0.0207**	**0.0069**
1,6-Anhydro-beta-Glucose	1.00	1.44 ± 0.31	**0.0273**	**0.0091**
Aspartic acid	1.00	1.35 ± 0.16	0.1815	0.0605
Galactitol	1.00	1.34 ± 0.54	0.1324	**0.0441**
Unknown_mass249_RI_2269.03	1.00	1.31 ± 0.43	0.2059	0.0686
Glycinamide	1.00	1.30 ± 0.48	0.2277	0.0759
Lysine	1.00	1.30 ± 0.44	0.2285	0.0762
Glycerol	1.00	1.29 ± 0.54	0.2536	0.0845
2-Amino-Butanoic acid	1.00	1.29 ± 0.38	0.274	0.0913
Ethanolamine	1.00	1.28 ± 0.58	0.3154	0.1051
Phosphoenolpyruvic acid (PEP)	1.00	1.26 ± 0.07	0.3796	0.1265
Diethylenglycol	1.00	1.25 ± 0.51	0.4216	0.1405
4-Hydroxy-Butanoic acid	1.00	1.25 ± 0.32	0.4426	0.1475
Citric acid	1.00	1.24 ± 0.68	0.4754	0.1585
Threonic acid	1.00	1.24 ± 0.20	0.5006	0.1669
Xylose	1.00	1.22 ± 0.27	0.5628	0.1876
Glycolic acid	1.00	1.22 ± 0.15	0.5693	0.1898
Threose	1.00	1.22 ± 0.14	0.576	0.192
Erythrose	1.00	1.22 ± 0.26	0.5848	0.1949
Unknown_mass234_RI_1466.08	1.00	1.22 ± 0.32	0.6111	0.2037

Galactaric acid	1.00	1.19 ± 0.44	0.7588	0.2529
Unknown_mass204_RI_2293.26	1.00	1.18 ± 0.20	0.8746	0.2915
Maleic acid	1.00	1.18 ± 0.09	0.8943	0.2981
Galactonic acid	1.00	1.18 ± 0.24	0.8959	0.2986
Unknown_mass73_RI_1454.79	1.00	1.18 ± 0.13	0.9094	0.3031
Ribose	1.00	1.17 ± 0.35	0.9416	0.3139
Unknown_mass204_RI_3085.34	1.00	1.16 ± 0.19	>0.9999	0.3393
Unknown_mass103_RI_1464.64	1.00	1.16 ± 0.13	>0.9999	0.3616
Unknown_mass217_RI_1743.32	1.00	1.15 ± 0.23	>0.9999	0.3732
Proline	1.00	1.15 ± 0.52	>0.9999	0.3775
myo-Inositol	1.00	1.14 ± 0.12	>0.9999	0.3937
Unknown_mass204_RI_2491.98	1.00	1.14 ± 0.07	>0.9999	0.4096
Arginine	1.00	1.14 ± 0.51	>0.9999	0.4232
Unknown_mass217_RI_1760.67	1.00	1.14 ± 0.08	>0.9999	0.4279
Alanine	1.00	1.13 ± 0.36	>0.9999	0.4328
Benzoic acid	1.00	1.12 ± 0.45	>0.9999	0.4698
Unknown_mass156_RI_1221.66	1.00	1.12 ± 0.22	>0.9999	0.4771
Xylitol	1.00	1.12 ± 0.09	>0.9999	0.5116
Nicotinic acid	1.00	1.12 ± 0.12	>0.9999	0.4786
Unknown_mass204_RI_3155.42	1.00	1.11 ± 0.18	>0.9999	0.5318
Arabinose	1.00	1.11 ± 0.16	>0.9999	0.5343
Fumaric acid	1.00	1.10 ± 0.43	>0.9999	0.5426
Ribonic acid	1.00	1.10 ± 0.24	>0.9999	0.5501
Glycine	1.00	1.10 ± 0.05	>0.9999	0.5814
Urea	1.00	1.10 ± 0.19	>0.9999	0.5532
Benzene-1,2,4-triol	1.00	1.10 ± 0.03	>0.9999	0.6023
Ornithine	1.00	1.09 ± 0.50	>0.9999	0.5778
Unknown_mass217_RI_1555.05	1.00	1.07 ± 0.17	>0.9999	0.6872
Glycylglycylglycine	1.00	1.06 ± 0.31	>0.9999	0.7339
Unknown_mass117_RI_1796.22	1.00	1.05 ± 0.13	>0.9999	0.759
Unknown_mass117_RI_1572.75	1.00	1.05 ± 0.15	>0.9999	0.7628
2,4-Dihydroxy-Butanoic acid	1.00	1.05 ± 0.14	>0.9999	0.7768
Psicose	1.00	1.04 ± 0.18	>0.9999	0.7948
Shikimic acid	1.00	1.04 ± 0.08	>0.9999	0.7972
Threitol	1.00	1.04 ± 0.23	>0.9999	0.8094
6-Hydroxy-nicotinic acid	1.00	1.04 ± 0.10	>0.9999	0.8164
Leucine	1.00	1.04 ± 0.23	>0.9999	0.8348
Valine	1.00	1.03 ± 0.22	>0.9999	0.8681
Fucose	1.00	1.03 ± 0.09	>0.9999	0.877
Unknown_mass84_RI_1824.17	1.00	1.02 ± 0.23	>0.9999	0.8907
Malic acid	1.00	1.02 ± 0.51	>0.9999	0.8961
Isoleucine	1.00	1.02 ± 0.21	>0.9999	0.901
Unknown_mass204_RI_2762.02	1.00	1.02 ± 0.21	>0.9999	0.9013
Erythronic acid	1.00	1.02 ± 0.18	>0.9999	0.9185
Glyceric acid	1.00	1.01 ± 0.16	>0.9999	0.9341
Phenylalanine	1.00	1.01 ± 0.14	>0.9999	0.936
5-Methylthio-Adenosine	1.00	1.01 ± 0.23	>0.9999	0.9518
Unknown_mass204_RI_2400.4	1.00	1.01 ± 0.12	>0.9999	0.9669

Galactose	1.00	1.01 ± 0.16	>0.9999	0.9695
Gluconic acid	1.00	1.00 ± 0.53	>0.9999	0.9826
Unknown_mass73_RI_1577.68	1.00	0.99 ± 0.28	>0.9999	0.9734
Unknown_mass204_RI_2333.62	1.00	0.99 ± 0.03	>0.9999	0.9609
Threonic acid-1,4-lactone	1.00	0.99 ± 0.14	>0.9999	0.9574
4-Amino-Butanoic acid	1.00	0.98 ± 0.61	>0.9999	0.9283
Adenine	1.00	0.98 ± 0.29	>0.9999	0.9032
Glutamic acid	1.00	0.98 ± 0.26	>0.9999	0.9001
Serine	1.00	0.98 ± 0.17	>0.9999	0.8971
Raffinose	1.00	0.98 ± 0.70	>0.9999	0.8962
Unknown_mass73_RI_1590.44	1.00	0.98 ± 0.27	>0.9999	0.8852
Unknown_mass73_RI_2212.85	1.00	0.97 ± 0.22	>0.9999	0.8544
Octadecanoic acid	1.00	0.96 ± 0.42	>0.9999	0.831
Pyruvic acid (Pyruvate)	1.00	0.96 ± 0.22	>0.9999	0.8309
Unknown_mass204_RI_2407.6	1.00	0.96 ± 0.20	>0.9999	0.8295
Unknown_mass204_RI_2138.52	1.00	0.96 ± 0.19	>0.9999	0.8232
Tyrosine	1.00	0.95 ± 0.09	>0.9999	0.7896
O-Acetyl-Serine	1.00	0.95 ± 0.13	>0.9999	0.782
Hydroquinone	1.00	0.94 ± 0.16	>0.9999	0.7466
Unknown_mass204_RI_2163.04	1.00	0.94 ± 0.09	>0.9999	0.7245
Unknown_mass217_RI_1833.63	1.00	0.94 ± 0.23	>0.9999	0.7238
Uracil	1.00	0.93 ± 0.19	>0.9999	0.737
Unknown_mass202_RI_2845.92	1.00	0.93 ± 0.38	>0.9999	0.6842
2-Hydroxy-Glutaric acid	1.00	0.93 ± 0.15	>0.9999	0.6634
Unknown_mass204_RI_2157.94	1.00	0.92 ± 0.07	>0.9999	0.6544
Glucuronic acid	1.00	0.92 ± 0.21	>0.9999	0.6389
Butyro-1,4-lactam	1.00	0.92 ± 0.35	>0.9999	0.619
4-Acetamido-Butanoic acid	1.00	0.91 ± 0.24	>0.9999	0.6134
Methionine	1.00	0.91 ± 0.13	>0.9999	0.5936
alpha,alpha'-Trehalose	1.00	0.91 ± 0.21	>0.9999	0.5921
Nicotinamide	1.00	0.91 ± 0.07	>0.9999	0.5896
Unknown_mass98_RI_1660.12	1.00	0.91 ± 0.25	>0.9999	0.6393
Pyroglutamic acid	1.00	0.89 ± 0.19	>0.9999	0.5189
beta-Alanine	1.00	0.88 ± 0.08	>0.9999	0.5146
2-Deoxy-Galactose	1.00	0.88 ± 0.25	>0.9999	0.4734
trans-4-Hydroxy-Proline	1.00	0.87 ± 0.03	>0.9999	0.5209
Allose (?)	1.00	0.87 ± 0.11	>0.9999	0.4375
Glucose	1.00	0.87 ± 0.16	>0.9999	0.4354
2-Deoxy-Ribose	1.00	0.86 ± 0.23	>0.9999	0.4161
Threonine	1.00	0.86 ± 0.03	>0.9999	0.4636
Putrescine	1.00	0.84 ± 0.12	>0.9999	0.4288
Succinic acid	1.00	0.83 ± 0.13	0.9465	0.3155
Glycerophosphoglycerol	1.00	0.82 ± 0.09	0.9119	0.304
Glutamine	1.00	0.82 ± 0.38	0.8422	0.2807
Mannose	1.00	0.80 ± 0.19	0.7314	0.2438
Fructose	1.00	0.78 ± 0.21	0.5665	0.1888
Sinapic acid	1.00	0.77 ± 0.15	0.5541	0.1847
3-Cyano-Alanine	1.00	0.77 ± 0.27	0.5153	0.1718

Asparagine	1.00	0.76 ± 0.33	0.4798	0.1599
2-oxo-Glutaric acid	1.00	0.76 ± 0.23	0.4705	0.1568
Phosphoric acid	1.00	0.72 ± 0.25	0.305	0.1017
Sucrose	1.00	0.70 ± 0.23	0.2503	0.0834
Tryptophan	1.00	0.68 ± 0.38	0.1887	0.0629
Glucose-6-phosphate (G-6-P)	1.00	0.62 ± 0.40	**0.0111**	**0.0037**
Ribulose	1.00	0.62 ± 0.15	0.1544	0.0515
3-oxalo-Malic acid	1.00	0.60 ± 0.08	0.0924	0.0716
Unknown_mass204_RI_2523.79	1.00	0.60 ± 0.11	**0.0446**	**0.0149**
Unknown_mass259_RI_2754.92	1.00	0.59 ± 0.13	**0.0451**	**0.015**
Salicylic acid (SA)	1.00	0.40 ± 0.08	**0.0013**	**0.0004**
Maltose	1.00	0.38 ± 0.20	**0.0009**	**0.0003**
2-Piperidinecarboxylic acid (Pip)	1.00	0.28 ± 0.12	**<0.0001**	**<0.0001**
Dihydrosphingosine	1.00	0.26 ± 0.02	**<0.0001**	**<0.0001**

Table S19. XYL4 and EDS1 modify SAR-inducible metabolic pathways relevant for energy production and lipid synthesis.
Col-0, *xyl4-1*, and *eds1-2* plants were spray-inoculated with either 10^8 cfu/mL of *Pst/AvrRpm1* (R), or a corresponding mock (M) solution. Two days after, plant rosettes were harvested, pooled for the treatment and genotype, and subsequently extracted in methanol and chloroform to attain soluble metabolites. GC-MS analysis was conducted to determine glycans and further molecules in a semi-targeted manner. 137 metabolites were detected and calibrated to two appropriate internal standards and normalized to sample dry weight. Peaks from the chromatograms obtained were evaluated by using available databases and if possible edited for a specific metabolite. Molecules were labeled with "Unknown_mass" when they could not be clearly assigned to a database-saved entry according to their mass and predicted functional groups. For each biologically independent experiment, a relative metabolite abundance as compared to mock-treated Col-0 plants was calculated. Data represents the average abundance normalized to sample dry weight and relative to mock-treated Col-0 wild type plants from three biologically independent replicates ± SD. Values in bold are significantly different from mock-treated Col-0 plants (two-way ANOVA, and Bonferroni's multiple comparison test or False Discovery Rate (FDR) with two-stage linear step-up procedure of Benjamini, Krieger and Yekutieli; P=<0.05, *p*-values as indicated in the table).

Number	**Metabolite**	Relative abundance ± SD					
		Col-0 M	**Col-0 R**	***xyl4-1* M (sorted)**	***xyl4-1* R**	***eds1-2* M**	***eds1-2* R**
1	**Unknown_mass249_RI_2275.34**	1.00	**2.21 ± 1.04**	**3.18 ± 0.84**	**3.66 ± 0.62**	**2.21 ± 0.23**	**3.11 ± 0.96**
2	**Maleic acid**	1.00	1.72 ± 1.10	**2.29 ± 0.92**	1.95 ± 0.58	1.54 ± 0.95	**2.17 ± 1.38**
3	**Fucose**	1.00	1.30 ± 0.29	**2.19 ± 1.89**	**2.22 ± 1.49**	1.18 ± 0.80	**2.42 ± 1.50**
4	**Asparagine**	1.00	**2.11 ± 1.26**	**2.14 ± 0.57**	**3.16 ± 2.58**	1.31 ± 0.40	**2.36 ± 2.10**
5	**Glycerol-3-phosphate**	1.00	1.43 ± 0.19	**2.07 ± 0.92**	**2.36 ± 1.24**	1.26 ± 0.82	**2.05 ± 1.37**
6	**Glutamic acid**	1.00	**2.09 ± 1.06**	**2.05 ± 1.06**	1.92 ± 0.90	1.51 ± 0.20	**2.22 ± 1.24**
7	**Serine**	1.00	1.43 ± 0.38	**2.00 ± 0.29**	**2.43 ± 0.42**	**1.90 ± 1.18**	**3.60 ± 1.66**
8	**Glucose-6-phosphate**	1.00	0.98 ± 0.42	**1.99 ± 1.51**	**1.98 ± 1.69**	1.01 ± 0.51	1.72 ± 0.66
9	**Malic acid**	1.00	1.38 ± 0.10	1.96 ± 1.84	1.09 ± 0.31	1.58 ± 0.77	1.33 ± 0.35
10	**Fumaric acid**	1.00	1.46 ± 0.48	1.86 ± 1.39	1.33 ± 0.60	1.12 ± 0.36	1.09 ± 0.19
11	**Glycerophosphoglycerol**	1.00	1.15 ± 0.16	1.74 ± 0.80	1.79 ± 0.92	1.39 ± 0.74	2.05 ± 1.09
12	**2-oxo-Glutaric acid**	1.00	1.18 ± 0.45	1.67 ± 0.81	1.47 ± 0.79	1.09 ± 0.38	1.33 ± 0.26
13	**Erythronic acid**	1.00	1.29 ± 0.11	1.67 ± 1.17	1.64 ± 0.83	1.15 ± 0.39	1.26 ± 0.22
14	**Glycine**	1.00	1.18 ± 0.38	1.67 ± 0.57	1.73 ± 0.91	0.73 ± 0.22	1.07 ± 0.38
15	**Phosphoric acid**	1.00	1.21 ± 0.40	1.58 ± 0.78	1.58 ± 0.51	1.17 ± 0.70	1.43 ± 0.91
16	**Unknown_mass245_RI_1560.09**	1.00	1.15 ± 0.20	1.56 ± 0.44	1.65 ± 0.53	1.11 ± 0.71	1.77 ± 1.00

17	**Glyceric acid**	1.00	1.08 ± 0.39	1.54 ± 0.25	1.43 ± 0.15	1.18 ± 0.38	1.21 ± 0.32
18	**Unknown_mass133_RI_2263.58**	1.00	1.28 ± 0.25	1.53 ± 0.65	1.74 ± 0.80	1.26 ± 0.60	1.46 ± 0.54
19	**Sinapic acid**	1.00	1.25 ± 0.45	1.53 ± 0.85	1.70 ± 0.67	0.87 ± 0.30	1.42 ± 0.64
20	**Palatinose**	1.00	1.19 ± 0.32	1.51 ± 0.83	2.02 ± 0.83	1.58 ± 0.61	1.83 ± 0.78
21	**beta-Alanine**	1.00	1.06 ± 0.10	1.50 ± 0.48	1.24 ± 0.41	0.78 ± 0.07	1.18 ± 0.30
22	**Galactinol**	1.00	0.97 ± 0.18	1.48 ± 0.38	1.39 ± 0.25	1.13 ± 0.28	1.36 ± 0.31
23	**Uracil**	1.00	1.33 ± 0.32	1.48 ± 0.47	1.54 ± 0.41	1.17 ± 0.66	1.38 ± 0.35
24	**Salicylic acid-glucopyranoside**	1.00	1.34 ± 0.38	1.45 ± 0.51	1.85 ± 0.67	1.01 ± 0.38	1.31 ± 0.61
25	**Unknown_mass191_RI_2913.87**	1.00	1.13 ± 0.28	1.44 ± 0.26	1.73 ± 0.62	1.00 ± 0.51	1.51 ± 0.40
26	**Mannose**	1.00	1.12 ± 0.18	1.42 ± 0.46	1.02 ± 0.48	1.03 ± 0.20	1.23 ± 0.35
27	**Proline**	1.00	0.91 ± 0.31	1.41 ± 0.53	1.10 ± 0.40	0.75 ± 0.22	1.08 ± 0.30
28	**Raffinose**	1.00	0.78 ± 0.23	1.40 ± 0.56	0.79 ± 0.20	**3.19 ± 3.65**	**3.78 ± 4.34**
29	**Unknown_mass103_RI_2363.76**	1.00	1.15 ± 0.11	1.40 ± 0.36	1.73 ± 0.64	1.09 ± 0.42	1.52 ± 0.62
30	**Unknown_mass217_RI_2835.55**	1.00	1.29 ± 0.32	1.39 ± 0.35	1.72 ± 0.62	**2.31 ± 1.37**	**2.48 ± 1.75**
31	**2-deoxy-Galactose**	1.00	0.99 ± 0.30	1.39 ± 0.67	1.49 ± 0.19	1.02 ± 0.15	1.59 ± 0.31
32	**Rhamnose**	1.00	1.07 ± 0.35	1.35 ± 0.23	1.56 ± 0.25	0.92 ± 0.33	1.61 ± 0.47
33	**Mannitol**	1.00	1.17 ± 0.15	1.34 ± 0.28	1.15 ± 0.47	1.03 ± 0.18	1.61 ± 0.60
34	**Shikimic acid**	1.00	1.00 ± 0.17	1.34 ± 0.41	1.21 ± 0.15	0.78 ± 0.18	0.98 ± 0.10
35	**Uric acid**	1.00	1.05 ± 0.32	1.32 ± 0.36	1.19 ± 0.50	0.99 ± 0.26	1.09 ± 0.37
36	**Unknown_mass117_RI_2167.52**	1.00	1.14 ± 0.35	1.32 ± 0.31	1.33 ± 0.24	1.10 ± 0.15	1.24 ± 0.08
37	**2-Piperidinecarboxylic acid**	1.00	0.89 ± 0.11	1.32 ± 0.17	1.24 ± 0.32	1.04 ± 0.41	0.91 ± 0.17
38	**Unknown_mass89_RI_1951.54**	1.00	1.23 ± 0.44	1.30 ± 0.62	0.93 ± 0.49	1.01 ± 0.12	1.20 ± 0.50
39	**Maltose**	1.00	1.21 ± 0.35	1.30 ± 0.34	1.38 ± 0.51	1.17 ± 0.37	1.20 ± 0.37
40	**Unknown_mass204_RI_2340.64**	1.00	1.11 ± 0.26	1.27 ± 0.22	1.38 ± 0.41	1.07 ± 0.25	1.22 ± 0.30
41	**Erythrose**	1.00	1.00 ± 0.11	1.27 ± 0.64	1.11 ± 0.21	0.80 ± 0.15	0.83 ± 0.11
42	**Spermidine**	1.00	1.12 ± 0.19	1.27 ± 0.35	1.71 ± 0.72	0.93 ± 0.25	1.58 ± 0.84
43	**Benzoic acid**	1.00	1.01 ± 0.38	1.26 ± 0.55	1.34 ± 0.62	1.34 ± 0.19	1.51 ± 1.05
44	**Leucine**	1.00	1.16 ± 0.15	1.25 ± 0.14	1.47 ± 0.48	1.05 ± 0.13	1.43 ± 0.22
45	**Sucrose**	1.00	1.15 ± 0.59	1.25 ± 0.25	0.93 ± 0.10	0.92 ± 0.11	1.06 ± 0.26
46	**Unknown_mass177_RI_1131.54**	1.00	0.97 ± 0.13	1.25 ± 0.26	1.33 ± 0.36	0.96 ± 0.06	1.04 ± 0.10
47	**Citric acid**	1.00	1.36 ± 0.05	1.25 ± 0.69	1.04 ± 0.14	1.29 ± 0.55	1.31 ± 0.19

48	**O-acetyl-Serine**	1.00	0.81 ± 0.38	1.25 ± 0.73	1.06 ± 0.48	0.60 ± 0.11	0.90 ± 0.35
49	**Pyroglutamic acid**	1.00	1.02 ± 0.10	1.24 ± 0.42	1.25 ± 0.49	0.74 ± 0.11	1.14 ± 0.20
50	**3-oxalo-Malic acid**	1.00	1.08 ± 0.25	1.23 ± 0.30	1.58 ± 0.63	0.93 ± 0.22	1.38 ± 0.53
51	**Succinic acid**	1.00	1.26 ± 0.22	1.22 ± 0.37	1.19 ± 0.18	0.89 ± 0.07	1.07 ± 0.21
52	**Methionine**	1.00	0.82 ± 0.21	1.21 ± 0.38	1.13 ± 0.15	0.67 ± 0.15	1.06 ± 0.15
53	**alpha,alpha'-Trehalose**	1.00	0.96 ± 0.03	1.21 ± 0.20	1.29 ± 0.25	1.01 ± 0.21	1.29 ± 0.21
54	**Unknown_mass191_RI_2399.64**	1.00	1.06 ± 0.32	1.19 ± 0.24	1.25 ± 0.34	0.96 ± 0.25	1.03 ± 0.25
55	**Unknown_mass117_RI_1574.04**	1.00	1.11 ± 0.22	1.19 ± 0.28	1.37 ± 0.47	0.96 ± 0.20	1.05 ± 0.20
56	**2-methyl-Malic acid**	1.00	0.98 ± 0.09	1.19 ± 0.22	1.58 ± 0.78	0.99 ± 0.36	1.04 ± 0.05
57	**6-hydroxy-Nicotinic acid**	1.00	1.15 ± 0.19	1.18 ± 0.22	1.15 ± 0.19	1.03 ± 0.06	1.38 ± 0.33
58	**Unknown_mass204_RI_2496.1**	1.00	1.04 ± 0.15	1.18 ± 0.24	1.30 ± 0.26	0.96 ± 0.18	1.15 ± 0.11
59	**Glutamine**	1.00	0.80 ± 0.44	1.18 ± 0.60	1.27 ± 0.53	0.51 ± 0.27	1.31 ± 0.30
60	**Unknown_mass205_RI_2123.68**	1.00	1.18 ± 0.31	1.18 ± 0.23	1.10 ± 0.11	1.10 ± 0.13	1.63 ± 0.65
61	**Xylose**	1.00	0.89 ± 0.04	1.17 ± 0.34	1.20 ± 0.11	0.84 ± 0.24	1.26 ± 0.31
62	**Unknown_mass204_RI_2537.62**	1.00	0.92 ± 0.22	1.16 ± 0.19	1.12 ± 0.14	0.86 ± 0.11	0.88 ± 0.03
63	**Unknown_mass117_RI_1796.92**	1.00	1.12 ± 0.18	1.16 ± 0.39	1.31 ± 0.36	0.98 ± 0.23	1.11 ± 0.16
64	**Nicotinic acid**	1.00	0.96 ± 0.36	1.15 ± 0.30	1.13 ± 0.06	0.72 ± 0.33	0.98 ± 0.38
65	**Galactonic acid**	1.00	1.10 ± 0.16	1.14 ± 0.18	1.33 ± 0.36	0.85 ± 0.14	1.23 ± 0.32
66	**Pyruvic acid**	1.00	1.09 ± 0.15	1.14 ± 0.24	1.24 ± 0.03	0.95 ± 0.24	1.29 ± 0.28
67	**Unknown_mass117_RI_1367.42**	1.00	0.99 ± 0.16	1.14 ± 0.31	1.16 ± 0.22	0.77 ± 0.13	0.89 ± 0.09
68	**Phenylalanine**	1.00	0.93 ± 0.15	1.13 ± 0.28	1.26 ± 0.49	0.79 ± 0.22	1.07 ± 0.17
69	**Butyro-1,4-lactam**	1.00	1.12 ± 0.34	1.13 ± 0.27	0.90 ± 0.12	0.78 ± 0.08	0.96 ± 0.17
70	**N-acetyl-Mannosamine**	1.00	1.07 ± 0.22	1.13 ± 0.11	1.18 ± 0.19	1.01 ± 0.09	1.19 ± 0.14
71	**Tyrosine**	1.00	1.15 ± 0.44	1.13 ± 0.19	1.53 ± 0.82	1.08 ± 0.60	1.57 ± 0.65
72	**Unknown_mass373_RI_2103.6**	1.00	1.47 ± 1.08	1.13 ± 0.55	1.58 ± 1.12	0.67 ± 0.66	1.25 ± 0.15
73	**Ethanolamine**	1.00	0.89 ± 0.33	1.13 ± 0.57	0.99 ± 0.51	1.15 ± 0.53	1.60 ± 0.95
74	**Unknown_mass133_RI_2352.3**	1.00	1.05 ± 0.20	1.11 ± 0.13	1.18 ± 0.20	0.97 ± 0.10	1.12 ± 0.27
75	**Threose**	1.00	0.98 ± 0.04	1.11 ± 0.21	0.89 ± 0.38	0.81 ± 0.12	0.93 ± 0.08
76	**Isoleucine**	1.00	1.07 ± 0.21	1.11 ± 0.10	1.29 ± 0.47	0.87 ± 0.15	1.19 ± 0.16
77	**Hydroquinone**	1.00	1.15 ± 0.24	1.11 ± 0.06	1.05 ± 0.30	0.88 ± 0.30	1.07 ± 0.13
78	**Unknown_mass117_RI_1542.02**	1.00	0.81 ± 0.07	1.10 ± 0.24	0.99 ± 0.26	0.85 ± 0.21	1.00 ± 0.06

79	**Unknown_mass204_RI_2286.26**	1.00	1.05 ± 0.21	1.10 ± 0.25	1.22 ± 0.18	1.01 ± 0.13	1.14 ± 0.10
80	**Valine**	1.00	0.97 ± 0.27	1.10 ± 0.17	1.20 ± 0.40	0.85 ± 0.11	1.26 ± 0.27
81	**2,5-dimethoxy-Cinnamic acid**	1.00	0.92 ± 0.21	1.10 ± 0.14	1.14 ± 0.31	1.26 ± 0.47	1.09 ± 0.37
82	**Glucose**	1.00	1.32 ± 0.28	1.10 ± 0.24	1.08 ± 0.43	1.46 ± 0.35	**1.85 ± 0.95**
83	**4-hydroxy-Butanoic acid**	1.00	1.14 ± 0.42	1.10 ± 0.60	**2.37 ± 2.15**	0.97 ± 0.05	1.31 ± 0.27
84	**Putrescine**	1.00	1.08 ± 0.13	1.09 ± 0.35	**2.03 ± 0.92**	0.78 ± 0.02	**2.54 ± 1.77**
85	**Xylulose**	1.00	0.89 ± 0.23	1.09 ± 0.16	1.02 ± 0.24	0.86 ± 0.15	0.97 ± 0.15
86	**Threonic acid**	1.00	0.91 ± 0.14	1.09 ± 0.09	1.28 ± 0.47	0.78 ± 0.16	1.25 ± 0.46
87	**Unknown_mass117_RI_1732.76**	1.00	1.11 ± 0.24	1.09 ± 0.09	1.32 ± 0.40	0.94 ± 0.13	1.15 ± 0.19
88	**Unknown_mass218_RI_1762.04**	1.00	1.00 ± 0.22	1.09 ± 0.15	1.34 ± 0.11	0.87 ± 0.18	1.28 ± 0.01
89	**Erythritol**	1.00	0.94 ± 0.24	1.09 ± 0.25	1.07 ± 0.19	0.78 ± 0.02	0.77 ± 0.14
90	**Unknown_mass204_RI_2483.53**	1.00	1.11 ± 0.29	1.09 ± 0.18	1.31 ± 0.28	0.88 ± 0.16	0.97 ± 0.21
91	**Arabinose**	1.00	1.03 ± 0.14	1.08 ± 0.14	1.20 ± 0.20	0.86 ± 0.06	1.05 ± 0.09
92	**Psicose**	1.00	0.94 ± 0.14	1.08 ± 0.10	1.03 ± 0.13	0.85 ± 0.04	0.96 ± 0.11
93	**Unknown_mass157_RI_2407.09**	1.00	1.00 ± 0.24	1.08 ± 0.21	1.17 ± 0.29	0.93 ± 0.18	0.99 ± 0.21
94	**Gluconic acid**	1.00	1.25 ± 0.54	1.08 ± 0.04	1.63 ± 0.77	1.09 ± 0.64	1.54 ± 0.73
95	**Fructose**	1.00	**1.27 ± 0.39**	1.08 ± 0.32	1.03 ± 0.37	**1.55 ± 0.64**	**1.58 ± 0.69**
96	**Unknown_mass103_RI_2355.38**	1.00	1.04 ± 0.21	1.07 ± 0.04	1.18 ± 0.17	0.96 ± 0.11	1.13 ± 0.16
97	**Glycerol**	1.00	1.07 ± 0.52	1.07 ± 0.53	1.37 ± 0.62	1.01 ± 0.37	1.41 ± 0.76
98	**Unknown_mass234_RI_1466.24**	1.00	0.95 ± 0.14	1.07 ± 0.07	1.07 ± 0.06	0.82 ± 0.17	1.11 ± 0.20
99	**2-amino-Butyric acid**	1.00	0.98 ± 0.12	1.06 ± 0.10	1.09 ± 0.33	0.91 ± 0.05	1.05 ± 0.16
100	**Allose**	1.00	1.14 ± 0.20	1.06 ± 0.14	1.27 ± 0.19	1.06 ± 0.01	1.27 ± 0.12
101	**3-cyano-Alanine**	1.00	1.01 ± 0.74	1.06 ± 0.58	1.06 ± 0.35	0.50 ± 0.10	1.19 ± 0.55
102	**Unknown_mass204_RI_2526.77**	1.00	1.05 ± 0.22	1.06 ± 0.08	1.15 ± 0.70	0.84 ± 0.10	0.94 ± 0.12
103	**Glycinamide**	1.00	0.92 ± 0.11	1.06 ± 0.39	1.40 ± 0.70	0.92 ± 0.31	0.89 ± 0.09
104	**Arginine**	1.00	0.67 ± 0.32	1.05 ± 0.59	1.06 ± 0.68	0.48 ± 0.32	1.33 ± 0.58
105	**Nonanoic acid**	1.00	0.96 ± 0.31	1.05 ± 0.01	1.10 ± 0.13	0.81 ± 0.11	0.93 ± 0.17
106	**Threonine**	1.00	0.89 ± 0.27	1.04 ± 0.15	0.98 ± 0.13	**0.68 ± 0.10**	1.00 ± 0.14
107	**Unknown_mass249_RI_2163.22**	1.00	1.05 ± 0.35	1.04 ± 0.21	1.10 ± 0.33	1.02 ± 0.14	1.10 ± 0.22
108	**Unknown_mass217_RI_1834.98**	1.00	0.96 ± 0.19	1.04 ± 0.20	1.40 ± 0.83	1.06 ± 0.17	1.09 ± 0.28
109	**Unknown_mass262_RI_1464.64**	1.00	0.93 ± 0.14	1.04 ± 0.38	1.44 ± 0.71	0.91 ± 0.34	0.85 ± 0.14

110	**Dihydrosphingosine**	1.00	0.98 ± 0.25	1.04 ± 0.14	1.06 ± 0.35	0.88 ± 0.10	1.07 ± 0.14
111	**Unknown_mass116_RI_1377.22**	1.00	0.92 ± 0.18	1.03 ± 0.11	1.03 ± 0.12	0.73 ± 0.06	1.06 ± 0.20
112	**Unknown_mass217_RI_1557.51**	1.00	1.28 ± 0.40	1.03 ± 0.21	1.07 ± 0.15	1.08 ± 0.47	1.21 ± 0.66
113	**4-acetamido-Butanoic acid**	1.00	0.81 ± 0.19	1.02 ± 0.66	1.19 ± 0.80	0.54 ± 0.12	0.95 ± 0.43
114	**Galactose**	1.00	0.99 ± 0.05	1.01 ± 0.05	1.01 ± 0.24	1.17 ± 0.20	1.29 ± 0.31
115	**myo-Inositol**	1.00	1.05 ± 0.13	1.00 ± 0.20	1.00 ± 0.26	1.01 ± 0.16	1.07 ± 0.07
116	**Unknown_mass117_RI_1908.82**	1.00	1.01 ± 0.15	1.00 ± 0.23	0.89 ± 0.42	0.87 ± 0.20	1.05 ± 0.21
117	**Alanine**	1.00	0.99 ± 0.34	0.99 ± 0.33	0.96 ± 0.27	0.65 ± 0.07	1.09 ± 0.47
118	**Glycolic acid**	1.00	0.94 ± 0.29	0.99 ± 0.25	1.10 ± 0.46	0.94 ± 0.62	1.16 ± 0.63
119	**Ribose**	1.00	1.02 ± 0.18	0.98 ± 0.14	1.02 ± 0.31	1.02 ± 0.33	1.06 ± 0.12
120	**Ribonic acid-1,4-lactone**	1.00	0.98 ± 0.26	0.98 ± 0.08	1.06 ± 0.22	0.82 ± 0.10	0.88 ± 0.08
121	**Diethylene glycol**	1.00	1.08 ± 0.35	0.92 ± 0.38	**2.05 ± 1.68**	0.86 ± 0.25	1.04 ± 0.13
122	**Aconitic acid**	1.00	1.00 ± 0.14	0.92 ± 0.14	0.95 ± 0.04	0.80 ± 0.09	1.04 ± 0.03
123	**1,8-diamino-Octane**	1.00	0.74 ± 0.34	0.88 ± 0.26	1.04 ± 0.22	0.72 ± 0.09	0.82 ± 0.10
124	**Urea**	1.00	0.91 ± 0.32	0.87 ± 0.53	1.83 ± 1.59	0.76 ± 0.06	0.94 ± 0.15
125	**Arabinonic acid**	1.00	0.89 ± 0.11	0.85 ± 0.04	0.86 ± 0.20	0.79 ± 0.17	0.97 ± 0.20
126	**Aspartic acid**	1.00	0.89 ± 0.17	0.84 ± 0.07	0.66 ± 0.29	0.75 ± 0.15	0.92 ± 0.21
127	**3-oxo-Glutaric acid**	1.00	0.97 ± 0.16	0.82 ± 0.20	0.74 ± 0.26	0.72 ± 0.17	0.91 ± 0.17
128	**Ornithine**	1.00	0.68 ± 0.32	0.82 ± 0.07	0.80 ± 0.43	0.51 ± 0.23	**2.05 ± 1.32**
129	**3-deoxy-Glucose**	1.00	0.94 ± 0.20	0.76 ± 0.13	0.72 ± 0.26	0.66 ± 0.26	0.80 ± 0.24
130	**Glyceraldehyde-3-phosphate**	1.00	0.85 ± 0.19	0.75 ± 0.03	0.62 ± 0.39	0.76 ± 0.29	0.82 ± 0.29
131	**Benzene-1,2,4-triol**	1.00	1.00 ± 0.70	0.75 ± 0.47	0.82 ± 0.53	0.86 ± 0.03	0.97 ± 0.57
132	**Glucuronic acid**	1.00	1.16 ± 0.35	0.73 ± 0.60	0.45 ± 0.14	1.82 ± 0.80	0.50 ± 0.25
133	**Unknown_mass204_RI_2299.77**	1.00	0.82 ± 0.35	0.71 ± 0.29	0.88 ± 0.24	0.75 ± 0.19	0.86 ± 0.36
134	**Unknown_mass129_RI_2138.23**	1.00	0.68 ± 0.58	0.71 ± 0.31	0.69 ± 0.29	0.78 ± 0.25	0.58 ± 0.24
135	**Threonic acid-1,4-lactone**	1.00	0.77 ± 0.01	0.68 ± 0.30	0.66 ± 0.10	0.52 ± 0.42	0.59 ± 0.21
136	**4-amino-Butanoic acid**	1.00	0.98 ± 0.08	0.62 ± 0.57	0.97 ± 0.11	0.93 ± 0.35	1.73 ± 1.86
137	**4-hydroxy-Proline**	1.00	1.29 ± 0.48	0.38 ± 0.08	1.38 ± 0.63	0.62 ± 0.21	0.76 ± 0.15

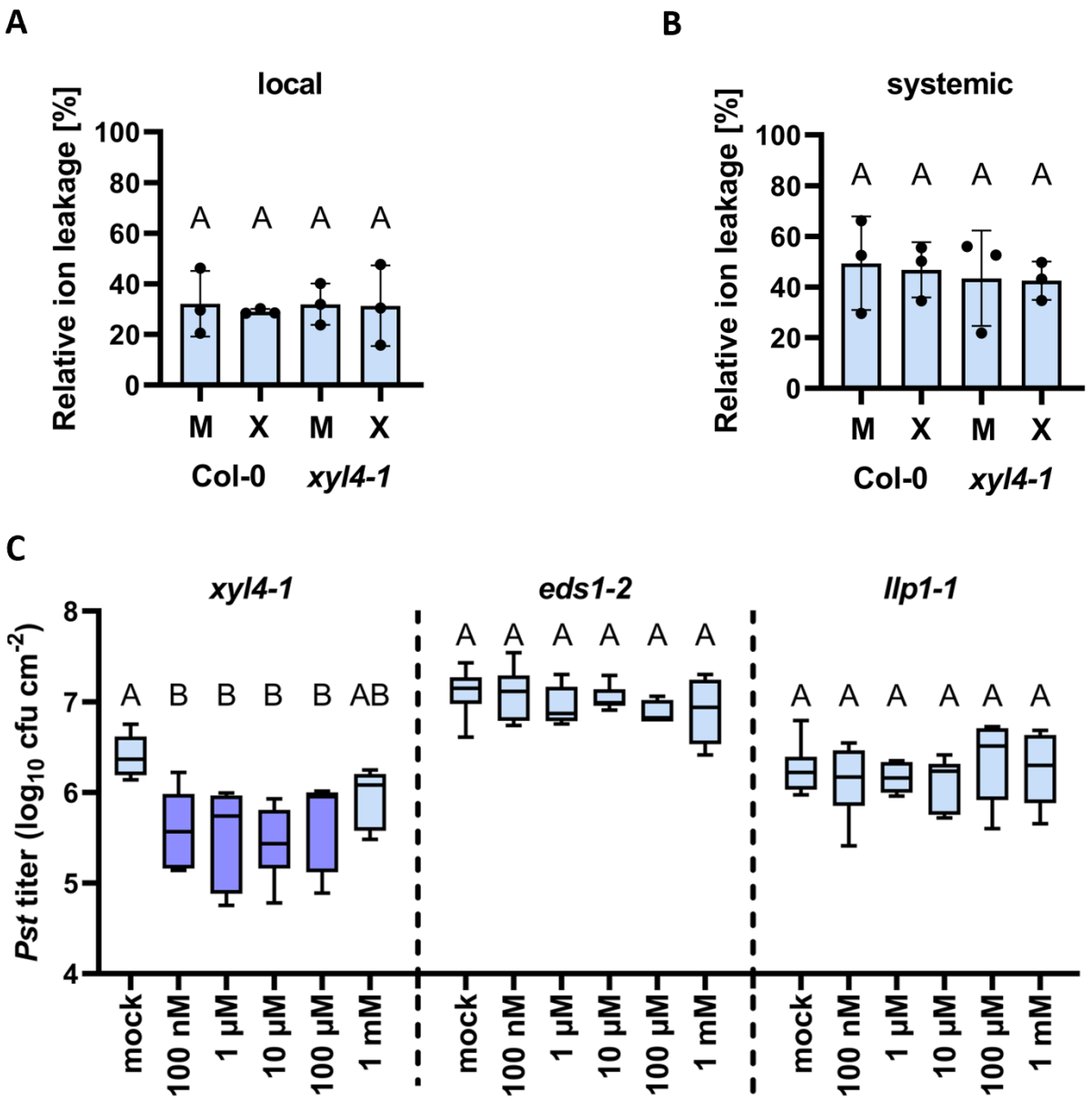

Figure S40. Exogenous xylose induces *EDS1*- and *LLP1*-dependent defense in distal tissues against *Pst*.

Plants of the genotypes Col-0, *xyl4-1*, *eds1-2*, and *llp1-1* were inoculated with either D-/L-xylose (10 µM (X) or another dose as indicated below the panels), or a corresponding mock (M) solution. Three days after, electrical conductivity was measured for the inoculated and distal leaves in order to obtain a measure for ion leakage. Additionally, systemic leaves were challenged with 10^5 cfu/mL of *Pst* to monitor xylose dose-dependent systemic defense in the mutant lines. (A-B) Electrical conductivity was monitored at 3 dpi in inoculated (A) and distal leaves (B). Bars represent the average electrical conductivity of three independent experiments relative to the background conductivity (black dots represent individual data points) ± SD. Different letters above the box plots indicate statistically significant differences (one-way ANOVA and Tukey test for P=<0.05, for (A): F(3, 8)=0.0499; for (B): n=3, F(3, 8)=0.137). (C) *In planta Pst* titers in distal leaves were monitored at 4 dpi. Box plots represent average *Pst* titers of twelve biologically independent replicates ± min and max value. Different letters above box plots indicate statistically significant differences for means (one-way ANOVA and Tukey test for P=<0.05, for *xyl4-1*: F(5, 30)=4.909, mock n=7, 100 nM n=7, 1 µM n=5, 10 µM n=7, 100 µM n=5, 1 mM

n=5; for *eds1-2*: F(5, 32)=0.9567, mock n=9, 100 nM n=8, 1 µM n=5, 10 µM n=6, 100 µM n=5, 1 mM n=5; for *llp1-1*: F(5, 32)=0.3751, mock n=9, 100 nM n=8, 1 µM n=5, 10 µM n=6, 100 µM n=5, 1 mM n=5).

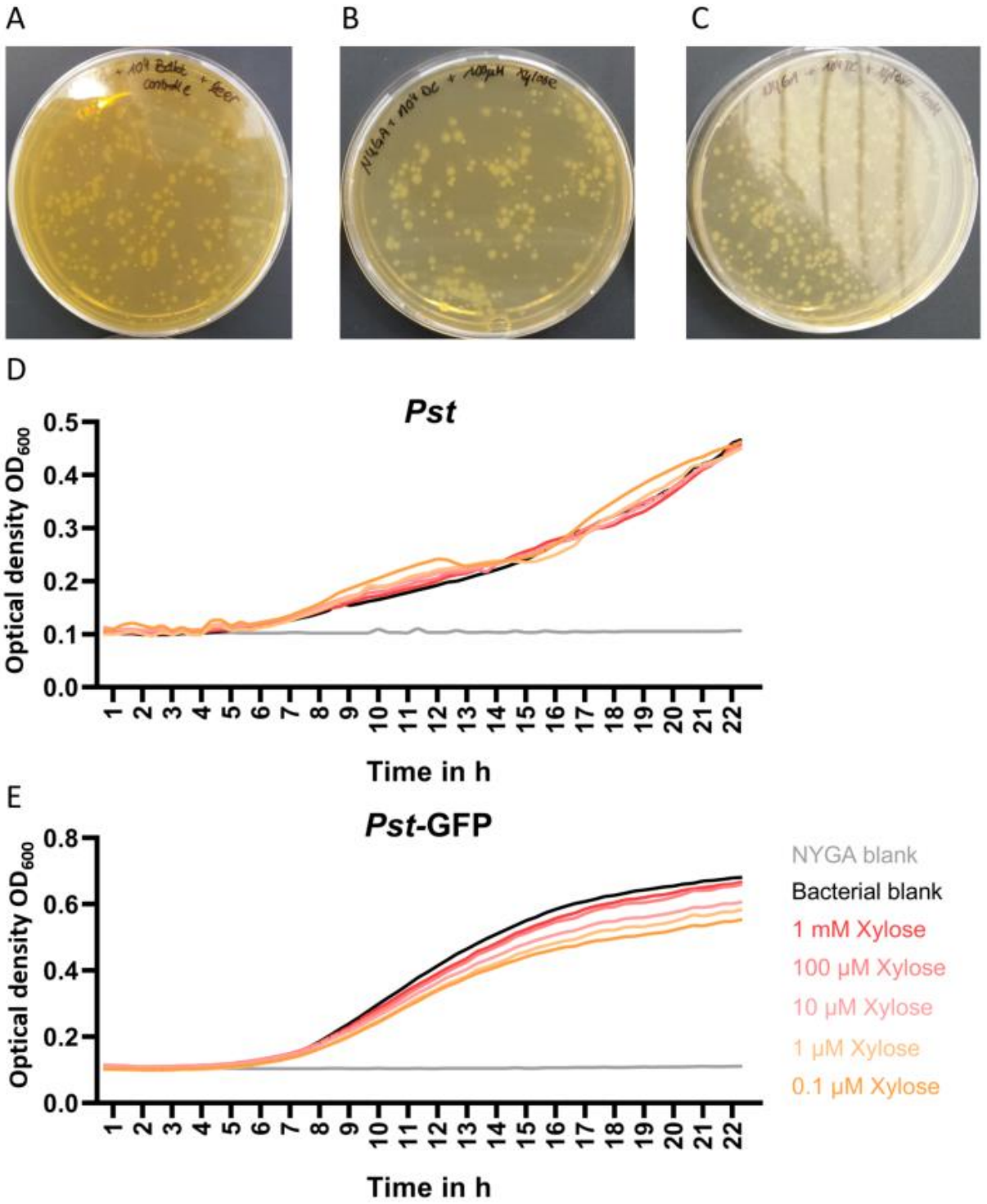

Figure S41. Xylose dose does not affect the growth of *Pst* bacteria in liquid media. (**A**-**C**) NYGA media were supplemented with either D-/-L-xylose (100 µM, 1 mM), or a corresponding mock solution. To determine bacterial growth on plates, 10^4 cfu/mL of *Pst* was streaked out an monitored by eye for the formation of cfu two days later. (**D**/**E**) An initial inoculum with 10^7 cfu/mL *Pst* (D) or fluorescently tagged *Pst*-GFP (E) bacteria were grown for 22 h in liquid NYGA medium supplemented with either a specific D-/L-xylose dose (as indicated) or mock (NYGA blank). The optical density at 600 nm (OD_{600}) of the bacterial suspensions was monitored every 20 seconds as a measure of bacterial density/growth, whereby NYGA blank was added as control. The OD_{600} mean values (n=4) were plotted.

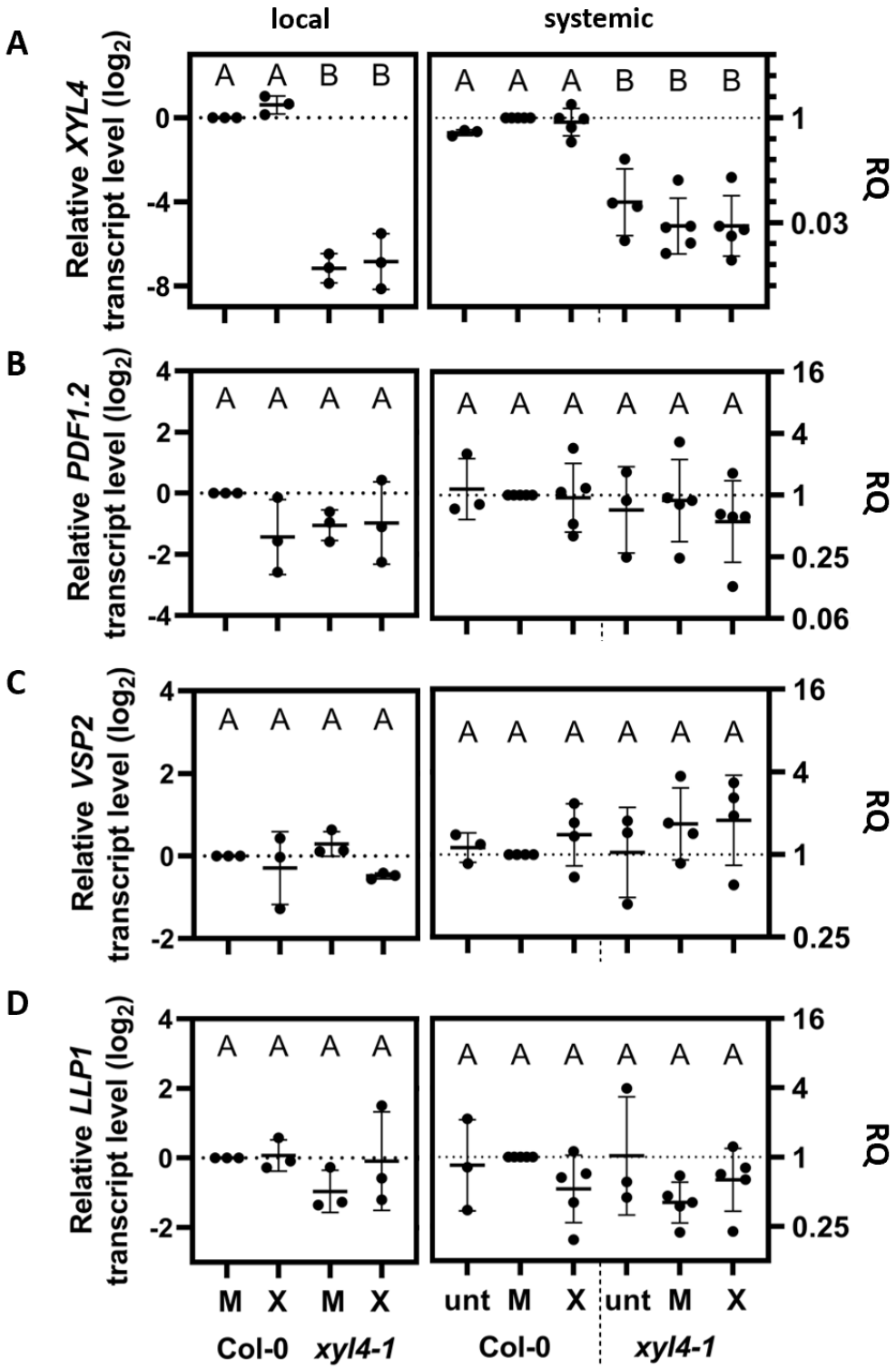

Figure S42. Late local and systemic responses after exogenous xylose are not dependent on XYL4, LLP1, or JA signaling.

Plants of the genotypes Col-0, and *xyl4-1* were inoculated with either 10 µM of D-/L-xylose (X), with a corresponding mock (M) solution, or were kept untreated (unt). Three days after, local and systemic leaves were determined for gene expression. The transcript accumulation was analyzed by qRT-PCR, normalized to that of *UBIQUITIN,* and is shown relative to the normalized transcript levels of the appropriate Col-0 mock (M) controls.

Black dots represent three to five biologically independent data points, and lines indicate the respective mean values ± SD. The letters above the scatter dot plots indicate statistically significant differences (one-Way ANOVA and Tukey test, P=<0.05, for (A, *XYL4* local): n=3, F(3, 8)=88.69; for (A, *XYL4* systemic): n=4-5, F(5, 21)=24.87; for (B, *PDF1.2* local): n=3, F(3, 8)=1.675; for (B, *PDF1.2* systemic): n=3-5, F(5, 20)=0.4918; for (C, *VSP2* local): n=3, F(3, 8)=1.656; for (C, *VSP2* systemic): n=3-4, F(5, 16)=0.7541; for (D, *LLP1* local): n=3, F(3, 8)=1.078; for (D, *LLP1* systemic): n=3-5, F(5, 20)=1.457)

8. Acknowledgements

I would like to thank here all the people who made the PhD thesis possible for me.

First of all, I would like to express my sincere thanks to Prof. Dr. Jörg Durner for allowing me to work at the Institute of Biochemical Plant Pathology and to conduct research for the purpose of my PhD thesis. His immense knowledge and ever-present helpfulness, interest and also criticism of my work including results and proposed signaling pathways illuminated the relevance of issues and background to my research topic. Through his support, I was able to advance my work in a more focused manner.

Furthermore, I am very grateful to Prof. Dr. Corinna Dawid for her professional and also idealistic support within my thesis committee. I benefited greatly from her expertise and queries on biochemical topics, her knowledge of metabolites and the assessment of the significance of my own results. Through them, I was shown important key points of my research topic including possibilities and limitations, as well as clarified the direction, priority and meaningfulness of results.

In addition, I am very grateful for Prof. Dr. Brigitte Poppenberger and Prof. Dr. Wilfried Schwab having agreed to be my chairman or second examiner in my defense.

I would like to express special thanks to Prof. Dr. Corina Vlot-Schuster for her supervision of my thesis, support in planning experiments, her patience, and the opportunity to contribute my own ideas to the research project. Through her belief in the meaningfulness of my project, her constant feedback, and discussions around topics of her expertise in the field of inducible resistance, SAR signals and her connection to collaborative partners, it was possible that I received a wide range of results on the very interesting research topic. Corina's honest and critical questions regarding the results helped me to find coherent correlations and then to put them down on paper in a motivated way.

I would like to thank Birgit Lange for the time-consuming measurements and analyses of my metabolites measured by LC-MS and her assessment of my results regarding topics of Pip, NHP and SAG. For this, I would also like to thank Anton Schäffner for making it possible for me to generate valuable metabolite data for my work through the collaboration of Birgit from his team.

I would like to thank Martin Lehman and Peter Geigenberger for the numerous plant samples measured via GC-MS. In particular, I would like to thank Martin and his laboratory team for performing the measurements and subsequent analysis, including editing the extensive list of metabolites.

A big thank you also goes to Jeanette Hansen and Bodil Jørgensen who actively supported me in the analyses by CoMPP, the evaluation as well as the interpretation of the data.

I pass many thanks to Marion Wenig (and also to her extension interns and trainees) for her ever-present support, for repeatedly performing experiments to confirm my own results, and for providing further ideas based on Marion's previous work experience with *Arabidopsis* and inducible resistance. It was a pleasure to work together with her!

Furthermore, I would like to especially thank Claudia Knappe for taking care of my plants whenever it was necessary, organizing enough supplies and materials for the lab work and for keeping the equipment for qRT-PCR analysis up and running. I really appreciated having Claudia as an always friendly contact person for any lab issues as a PhD student.

I would also like to thank my former student Shahran Nayem. Nayem was a great help with lab work, which he reliably completed. I was able to learn a lot while supervising his progress and having extensive discussions – it was very insightful. I hope that Nayem also benefited from my support and enjoyed his time as a master student in our lab.

Since Jennifer Sales and I had worked on very similar topics during our PhD, I was very grateful to discuss and get feedback on topics such as LLPs, XYL4 and abiotic stress. Also, written work improved greatly with the help of Jennys native language. I was grateful to have her as travel companion for a trip to China and the ICAR conference and for having lot of nice conversations during breaks.

I would also like to thank my colleagues, who created a pleasant and cheerful atmosphere in and outside the lab such as common gaming nights, pub quizzes and so on, and with whom I had nice conversations and made me laugh over a cup of tea during the breaks: Dr. Inonge Gross, Dr. Sanjukta Dey-Irmler, Dr. Sibylle Bauer, Dr. Miriam Lenk (thank you for always having an open ear and offering help with any topic), Yuanyuan Chen (thank you for introducing us to your Asian traditions and bringing Chinese food), Alessandro Brambilla, Anna Sommer, Laura Eccleston, Gabi Bartel, Elisabeth Georgii, Diana Lochner. I would also like to thank my 'cycling buddies' Elke Mattes and Lucia Gößl for being my office neighbors. I really appreciated that they always offered help with administrative topics or any tasks in the lab such as keeping my baby plantlets alive while I was out of the lab.

Zudem möchte ich meiner Familie und Freunden Danken, die mich während der Zeit durchgehend unterstützt haben.

Speziell bei Lena, Michi und Karin bedanke ich mich für die aufmunternden Worte, emotionale Unterstützung und offenen Gespräche, die wir zu jeder Tages- und Nachtzeit führen konnten. Es war unglaublich schön, während der doch sehr stressigen Zeit mit ihnen Freizeiten und gesellige Koch- und Spieleabende zu verbringen und sich währender intensiv auszutauschen. Ich hoffe diese Freundschaften auch in Zukunft weiter pflegen zu können. Ihr seid großartig - bin wahnsinnig stolz, dass ihr mich während der Zeit der Promotion immer für mich da wart!
Mit weiterem Dank an die liebe Karin: ihre immerwährenden, positiven Aussichten auf das Leben, ihre Stärke, Leidenschaft zum Sport und Frohmut schätze ich sehr und haben mir geholfen, mich auf die wirklich wichtigen Dinge im Leben zu konzentrieren. Karin, du wirst uns weiterhin auf all unseren Wegen begleiten und Vorbild sein als Mensch, dem ein glückliches Leben, das Wohlergehen anderer Mitmenschen, und das Verfolgen eigener Träume im Vordergrund stand – deine Mädels mit Chris und Familie vermissen dich sehr. <3

Meiner Familie mit Matthias, Mama, Oma, Alex, Agi und Tobi möchte ich zudem ein riesengroßes Dankeschön dafür aussprechen, dass sie während dem Zeitraum der Promotion durchgehend für mich da waren, meine Redeflüsse über Pflanzen & Co. und stressige Situationen mit mir ausgehalten haben. Vielen Dank, dass ihr meine Mühen für diese Arbeit wertschätzt und mich bei notwendigen Tätigkeiten im Haus und Garten unterstützt habt.

Zuletzt möchte ich mich bei meinem liebevollen Lebenspartner Andreas bedanken. Ich bin sehr froh, dass er meine Leidenschaft als interessierter und wissbegieriger „Hobby-Biologe zu Pflanzen und der Wissenschaft teilt. Während meiner finalen Phase der Doktorarbeit hat er mich immer wieder unterstützt, aufgemuntert und such angespornt, um an meinen Texten zu feilen. Durch ihn wurde ich während her mit leckeren Mahlzeiten (ob vorm PC oder zu Tisch) versorgt und an die oftmals dringend notwendigen Denkpausen erinnert. Zudem konnte ich durch sein detailliertes Feedback meine Thesis noch weiter verbessern. Vielen, vielen Dank daher für die tolle Zeit mit dir und deine immerwährende Unterstützung, Andi!